INVESTIGATIONS OF THE PHYSICO-CHEMICAL BEHAVIOUR OF STARCH-WATER SYSTEMS

A thesis presented in partial fulfilment

of the requirements for the degree

of Doctor of Philosophy

in Food Technology at

Massey University

RICHARD BEK KIONG WONG

1981

MASSEY UNIVERSITY

1. * (a) I give permission for my thesis, entitled

INVESTIGATIONS OF THE PHYSICO-CHEMICAL BEHAVIOUR OF STARCH-WATER SYSTEMS.

to be made available to readers in the Library under the conditions determined by the Librarian.

(b) I agree to my thesis, if asked for by another institution, being sent away on temporary loan under conditions determined by the Librarian.

(c) I also agree that my thesis may be copied for Library use.

2. * ~~I do not wish my thesis, entitled~~

~~to be made available to readers or to be sent to other institutions without my written consent within the next two years.~~

Signed B K W Carey

Date 6/11/81

* Strike out the sentence or phrase which does not apply.

The Library
Massey University
Palmerston North, N.Z.

The copyright of this thesis belongs to the author. Readers must sign their name in the space below to show that they recognise this. They are asked to add their permanent address.

Name and Address **Date**

A B S T R A C T

Starch is a major component of many of the world's food supplies. In order to utilise these supplies effectively the properties of starch must be fully understood. Although starch systems have been investigated quite extensively, there is relatively little information concerning the physico-chemical behaviour of starch under conditions relevant to food processing.

The texture of many fabricated foodstuffs is regulated by adding starch. In many cases the addition of starch causes food systems to behave as viscoelastic pastes. In Australasia, wheat starches are generally used to control texture. However starches from some wheat cultivars do not impart the desired rheological characteristics to foodstuffs and this thesis concerns an investigation into this phenomenon which was investigated in three sections.

In section I, a fundamental study of the rheological properties of wheat starch pastes was performed. Measurements were made of the flow behaviour of pastes under both oscillatory and steady shear conditions. Pastes formed under a range of experimental conditions from various wheat varieties were studied. Both wheat varieties and paste preparation conditions were found to influence rheological behaviour. The results show that differences in the pasting properties of starch pastes may be attributed to two factors, namely the swelling capacity of the starch (the volume which the starch gel particles would occupy when close packed if excess solvent were present) and the size distribution of the granules.

The rheological properties depend on the source of starch since this effects particle swelling capacities and size distributions. Paste preparation conditions influence rheological properties since they alter the volume occupied by gelatinised granules.

The rheological behaviour of starch pastes changes with time when the pastes are stored. The effect of storage on dynamic rigidity was investigated and the results suggested that a crystallisation process is responsible for the increase in dynamic rigidity with time. The results were therefore evaluated using the Avrami equation.

In section II, an investigation was made of the degree of crystallinity, that is the proportion of polymer chains that are in an ordered state, in a number of wheat starch varieties that have different swelling capacities. Measurements of the X-ray crystallinity index, enthalpy change and specific volume were used to investigate crystallinity. The results show that higher swelling capacities are associated with relatively disordered arrangements of polymer chains within granules. The crystallinity results for the various starch fractions with narrow size ranges confirm previous studies showing that small granules tend to be more crystalline. However small granules were found to have higher swelling capacities than large granules. In this instance the increased swelling capacity of small granules as compared to large is probably due to the decreased amount of lipid per unit area at the surface of the small particles.

In section III, Proton (^{1}H) and Carbon-13 (^{13}C) NMR were used to investigate starch pastes made from different wheat varieties that have different pasting properties. ^{1}H spin-lattice (T_1) relaxation times, ^{1}H spin-spin (T_2) relaxation times, polymer hydration coefficients (h) and ^{1}H diffusion coefficients (D) of starch-water systems were determined. Line-widths at half-heights ($\Delta\nu_{1/2}$) of peak intensities at various carbon positions and total ^{13}C liquid signals were also obtained.

In all cases the NMR parameters were not found to be dependent on wheat variety.

The polymer hydration coefficient, that is the amount of water molecules that are in the bound state, was estimated from the ratio of the amplitude of the ^{1}H signal due to unfrozen water at 258K to the amplitude of the ^{1}H signal at 303K. A value of 0.34 gH2O/g dry starch was obtained.

The T_1 and T_2 magnetisation recovery curves for starch pastes were found to be single exponential functions. This suggests a fast molecular exchange of water molecules between different sites in the system. A two-state model based on exchange between bulk and bound water was shown to be adequate in describing the relaxation behaviour of water protons in the system.

Diffusion measurements of water molecules show that there is no restricted or barrier limited diffusion occuring in starch pastes. The diffusion coefficients were interpreted

using various models. The best model was found to be one which takes into account both the obstruction and hydration effects. This gives a shape factor for the suspended gel particles which indicates that water is diffusing through oblate ellipsoids. These are probably amylopectin molecules present in the starch pastes. In an attempt to confirm this possibility, ^{1}H NMR measurements were repeated on a pure amylopectin-water system. The diffusion coefficients of the amylopectin-water system were interpreted using the same model and similar result was obtained for the shape factor of amylopectin molecules.

The ^{13}C liquid signal results confirm that sharp resonances, which correspond to liquid-like behaviour on the NMR time-scale of the polysaccharide chains, are only observed when the starch is gelatinised. The decrease in the line-widths at half heights of the peak resonances at various carbon positions when the pasting temperature is increased is probably due to an increase in mobility of the polymer chains. In the various wheat starch pastes studied, a loss of about one-third of the total ^{13}C liquid signal was observed. This was attributed to the crystallisation of polymeric material, lipid-amylose complexes and remnants of ordered structures in the starch pastes.

ACKNOWLEDGEMENTS

The author expresses his sincere thanks to the following persons who assisted him in the many facets of this thesis.

His supervisors, Dr J. Lelievre (Department of Food Technology, Massey University) and Dr P.T. Callaghan and Dr K.W. Jolley (Department of Chemistry, Biochemistry and Biophysics, Massey University), for their enthusiasm and encouragement throughout this study and help in the manuscript.

Professor E.L. Richards (Department of Food Technology, Massey University) for his advice.

Dr P. Meredith (Wheat Research Institute, Christchurch) for his help and encouragement.

My wife Connie for her continual support during my years of study.

Mr G. Burton (Department of Food Technology, Massey University) for the building of the co-axial viscometer.

Wheat Research Institute, Christchurch, for financial support.

Mrs L. Baptist for typing this thesis.

Table of Contents

Page

Page

Page

List of Tables

List of Figures

Section I.

GENERAL LITERATURE REVIEW

A.1 Statement

The information considered in this review relates to all three sections of this thesis.

A.2 Introduction

A number of textbooks and articles are available in which the chemical properties and technological behaviour of starch are described in detail (1-10). The objective of the current review is to focus attention on those aspects of the literature that may be of relevance to an understanding of the topic being investigated, namely the factors that influence the rheological behaviour of starch pastes. The review therefore seeks to present information concerning the occurrence, composition and structure of intact starch granules, the gelatinisation process and the structure of pastes. Unless otherwise stated, the information discussed relates to wheat starch.

A.3 The occurrence, composition and structure of intact starch granules

A.3.1 Occurrence

Starch isolated from plant tissues occurs in the form of discrete particles which are known as granules. Microscopic examination suggests that in samples of wheat starch two types of granules are present, namely large lenticular granules with diameters of about 15 to 25 μm and small spherical granules with diameters primarily in the range of 2 to 10 μm (11, 12). Although there is still some uncertainty as to whether spherical and lenticular granules represent two distinct populations, recent work

suggests that this is the case (13, 14). Detailed investigations of the particle size distributions of wheat starches have been carried out using sedimentation balances (15), air classifiers (16), micro-sieves (11) and Coulter-counters (17). The contribution of different size fractions to the total volume, number and weight of starch particles has been calculated (18-20). Results from such investigations suggest that small granules (<10 μm) comprise about 80% of the total number of granules and about 4% of the total weight of granules. More recent work indicates that the small particles make up about 30% of the total weight of starch (11).

The number of granules per gram of starch and the size distribution of particles are known to depend on wheat variety, so that the proportion of small and large granules may vary from one cultivar to another (21). There is also evidence that within a single cultivar of wheat, the larger the kernel the greater is the proportion by weight and by number of small granules (22). The size distribution of granules is further affected by the stage of kernel development (23), the number of small granules per gram of starch increases as the kernel matures.

A.3.2. Composition

Samples of wheat starch normally contain about 90% polysaccharide and 10% water (4). Part of the water forms an integral part of the granule structure (24, 25). Trace amounts of non-carbohydrate materials such as lipids (26) and proteins (27) are also present. These are incorporated in the granule during its botanical development, though some may be absorbed during extraction procedures.

The polysaccharide component of granules has been the subject of considerable research interest. Two main polysaccharides have been identified; viz. amylose and amylopectin. Amylose and amylopectin normally constitute about 25% and 75% respectively of total polysaccharides present in wheat starches.

Amylose is essentially a linear molecule consisting of (1→4')-linked α-D-gluco-pyranose units (28). Branch points are present in the molecule in about one per five hundred glucose units and appear to be α-(1→6')-linkages (29). Amylose is characterised by a range of molecular weights; the average degree of polymerisation is typically of the order of 10^3 (29).

Amylopectin is a highly branched molecule consisting of (1→4)-linked α-D-gluco-pyranose units (28). About one in every twenty five monomer units forms a α-(1→6') branch point. The shape of molecule that results from this branching is uncertain, some investigatiors consider the molecule to have a planar structure (30, 31). The molecular weight of amylopectin varies but is generally of the order of 10^8 Daltons (32).

The starch granule also contains about 3% of other polysaccharide material which is intermediate between amylose and amylopectin, however its exact structure is currently not known (8).

The lipid content of granules has been investigated extensively (21, 33-37). Two main types of starch lipids have been reported, namely non-polar (neutral) lipids which are mostly free fatty acids and phospholipids which are mainly lysophosphatidyl choline. These are distributed throughout the granule (33, 38) and constitue about 1.0% of wheat starch. Much less attention has been directed towards the protein component which constitutes only about 0.3% (39).

A number of investigators have shown that the variety and maturity of wheat influence granule composition (40). The average external chain length of amylopectin and the degree of polymerisation of both amylose and amylopectin increase with maturity. The composition of the granule also depends on the size of the particle (16, 21, 41). There is general agreement that small granules contain less amylose and are usually associated with more lipid and protein.

A.3.3. Structure

The precise structure of the starch granule is uncertain (42, 43). Considerable evidence suggests that the structure of the starch particle is similar to that of a polymer spherulite (31, 44). Thus both crystalline and amorphous arrangements of the polymers occur. Relatively little is known about the conformation of the starch chains in the granule. It has been suggested that the crystalline regions are made up of oriented helixes of starch chains (44). The water which forms an integral part of granule appears to be involved in these areas (24, 45). The estimate for the proportion of α-D-glucopyranose units in the crystalline assembly varies, results depend on the measuring techniques used (46) and conditions of the

starch granule (47). Thus a range of crystallinities has been reported, varying from a very low quantity to sixty percent (46). There is some evidence that amylopectin is the principal component of the crystalline regions (48) and that amylose adds little to the crystalline nature of the granule (49). The form in which amylose is present in the granule is still uncertain, however one suggestion is that it forms an inclusion complex with the starch lipids present (33, 50).

The surface structure of intact granules has been studied by a number of investigators (20, 51-55). It has been suggested that the intact granule is surrounded by a membrane which may be composed of remnants of amyloplast membrane (51), of protein (52), or of lipid (53). The interpretation of these results is complicated by the fact that different extraction methods have been used where differential absorption of these materials onto the surface of starch granule is likely to happen. Other reports indicate that the surface structure is a consequence of the molecular arrangement of polysaccharide (54, 55) and have discounted a membrane system. Others suggest that large granules have an outer shell, containing a higher proportion of amylose-lysophospholipid complexes with amylopectin (21). Clearly the surface structure of the starch granule is incompletely understood.

The structure of the starch granule may be influenced by composition and hence may vary with wheat variety and the size and maturity of kernel, however this has yet to be established. Granule structure also depends on particle size, but there is very little information available on this subject. Nonetheless it has been suggested that the polymer chains in small granules occur in a more ordered arrangement than in large granules (56).

A.4. The gelatinisation process

When intact starch granules are suspended in aqueous solution at room temperature, a limited amount of water absorption occurs. The uptake of this water is regulated by the crystalline domains of the starch granule. The absorption that does occur is an exothermic process, with water penetrating only the amorphous zones of the starch particle (57). However, on heating to 60°C a large amount of swelling takes place in an endothermic transition (58). At this temperature there are a number of other changes, including:

(i) the loss of the birefringence that characterises the intact granules (59);
(ii) the development of a diffused V-type X-ray pattern due to the formation of lipid and amylose complexes as opposed to the original crystalline A-type pattern (60);
(iii) an increase in hydration and fluidity of polymer chains (61) and
(iv) an increase in suspension viscosity.

On continued heating, the granule swells further and partly disintegrates, some polymeric material is released, this process results in the formation of a starch paste. This further heating has a profound effect on the rheological properties of starch-water systems (62). The conversion of an aqueous suspension of starch granules to a viscous paste is known as gelatinisation.

Since in the process of gelatinisation the crystalline order of the granule is destroyed, an analogy can be made between polymer melting and gelatinisation. Thus gelatinisation can be viewed as crystalline - amorphous phase transition (59). In the intact granule starch polymers are present in helical forms whereas in solution it has been suggested that a random coil configuration occurs (44, 63). This indicates that gelatinisation can also be described in terms of the helix-coil transformation of the polymer chains.

The transition temperature of the crystallites is depressed by the presence of water as in the classical polymer-diluent melting (64). A number of mechanisms for the crystalline-amorphous phase transition have been proposed (9). The fact that a given starch granule gelatinises over a narrow temperature range (1-2^{o}C) may indicate that the crystallites therein have similar energy characteristics. The range of gelatinisation temperatures of a whole population reflects therefore, the different energy characteristics of different granules (65). Another possibility is that the crystallites within the granule have slightly different energy characteristics so that upon gelatinisation the crystallites with lower energy thresholds melt first, subsequent reorganisation of these polymer chains modifies the adjacent crystallites and brings about their transformation in a semi-co-operative manner (65). While these explanations are plausible, no conclusive evidence has been established at the present time even though there is some data which points to the latter explanation as being more satisfactory (9).

The influence of lipids on gelatinisation has been studied by a number of investigators (35, 37, 66). Results suggest that defatted starch gelatinises at lower temperatures and the paste so formed has higher viscosity. However, since lipid on the surface is removed preferentially by such defatting procedures, these results may only reflect modifications to the surface of the starch granule. Firmly bound lipid is retained in the interior, thus the role of lipid within the starch granule is still not clear.

The effect of granule size distribution on gelatinisation has also been examined (16). Small granules of wheat starch have higher gelatinisation temperatures than large granules. This has been attributed to the differences in their structure described in A.3.3.

A.5 The structure of pastes

Starch pastes are disperse systems. At the temperature of their formation the main components of the disperse phase are swollen granule fragments and lipid-amylose complexes. The swollen granules are in effect viscoelastic gel particles (67). The continuous phase consists of an aqueous solution of polymeric material that has exuded from the granules. On cooling amylose crystallises out rapidly in both phases of the starch dispersion. The continuous phase then contains a colloidal dispersion of polymeric material from the gelatinised granules. Thus starch pastes are in many respects similar to polymeric microgels, that is systems containing a dispersion of gel particles in a solvent.

In the range of starch concentrations in which pastes are formed in industry, swollen granules are close packed throughout the volume of the paste. The close packed gel particles form a weak network structure (103). The volume of void in this case can be of the order of 70% of the total volume of the system (68). When the concentration of gel particles is increased, more rigid networks occur and eventually self-supporting gels are formed. It has been suggested that interparticle forces such as entanglements between the surface molecules of adjacent swollen granules play an important role in the network structure (68). The nature of the interactive forces between the instititial fluid and the swollen gel particles is uncertain (67).

SECTION I

RHEOLOGICAL PROPERTIES OF STARCH PASTES

I.I Introduction

Recent investigations by Loney et al. (41) have shown that there are significant differences in the pasting behaviour of different varieties of wheat starch. These differences were investigated using an empirical testing instrument (69). The precise behaviour of pastes also depends on the experimental conditions used during their preparation (70). An explanation of the above differences in paste properties would be of interest to the food industry. Despite the commercial significance of starch pastes there is relatively little fundamental information concerning their rheological properties. The present section describes a fundamental investigation of the rheological properties of pastes.

I.2 Literature review

Comprehensive reviews of the rheological properties of starch pastes are available (7, 62, 67). The objective of the present review is to focus attention on those areas of the literature that are most relevant to the subject under investigation. The information is considered in two categories, these are measurements obtained by empirical methods and measurements obtained by fundamental techniques. Both methods of investigation have been used to study the relationship between the structure and properties of starch pastes.

I.2.1 Empirical measurements

A wide range of empirical testing devices are available that have been used to measure the rheological properties of starch pastes. Perhaps the most commonly used of these is the Brabender Amylograph. This basically consists

of a rotating metal beaker fitted with baffles plus a stationary stirring system which is made of a set of vertical rods. The starch-water system to be studied is placed in the beaker which is then heated and cooled under controlled conditions (usually at a heating and cooling rate of 1.5^{0}C/minute). During this process the beaker is rotated about its vertical axis. The resultant torque on the stirring rods is registered by a dynanometer, so that a curve is obtained in which torque, and so consistency, is plotted against time. Since a controlled rate of heating and cooling is used the time axis fixes the temperature. Consistency is measured in the arbitrary units of Brabender units (B.U.). The height of the peak obtained during the heating part of the cycle is used to characterise the pasting behaviour of starch paste. Other information can also be obtained from the curve (7). Using this empirical measuring technique, the contrasting rheological characteristics of Australian and New Zealand wheat starches have been demonstrated (41).

Various other empirical instruments have also been used in industry to characterise the properties of starch, including Corn Industries viscometers, Stormer viscometers, MacMichael viscometers, Brook field viscometers and falling sphere viscometers (67). These viscometers give information about pastes that is similar to that obtained from the Amylograph and in most cases the viscosity results obtained have no fundamental significance.

Many attempts have been made to investigate factors that influence starch paste behaviour as measured by empirical methods. The interpretation of the results so obtained

is complicated by the arbitrary and undefined nature of the testing instruments. However, these works do suggest factors that may affect the rheological properties of starch pastes.

All methods of paste measurement show that a marked increase in viscosity occurs during paste formation and that the temperature/time treatment used in pasting influences the peak viscosity reached. The peak Amylograph viscosity depends on paste composition and is proportional to the cube of the starch concentration (69). Qualitative explanations for the increase in consistency that occurs during pasting have been suggested. Many investigators consider the increase in paste viscosity results from the increase in the hydrodynamic volume of starch granules, i.e., the swelling, that occurs during gelatinisation. In this case paste viscosity is considered to represent the work required to move the expanded granules past each other (71). On the other hand, a group of investigators have shown that the peak viscosity reached by a starch-water system during gelatinisation occurs after most of the granule swelling ceases (72). Polymeric material is released from gelatinised granules at this stage, and electron-microscopic examination suggests this forms a filamentous network structure in the paste. In this case the viscosity is thought to arise from the presence of this network.

The peak viscosity reached during gelatinisation depends on the variety of starch. Thus, Loney et al. (41) have shown that some starches form more viscous pastes than others under comparable conditions. The cause of this difference is uncertain, however Meredith et al. suggest that it arises from a variation in the physical organisation of the granule structure (21).

Measurements of Amylograph viscosities of pastes made from small granules have demonstrated differences in pasting properties compared with the unfractionated parent starch (16). The consistencies of cold pastes made from small granules are always less than those for the unfractionated starch. This difference has been attributed to the fact that small granules tend to disintegrate more on pasting.

The trace amounts of lipids in starch granules have a marked effect on pasting properties (16, 35, 37). For example, defatted wheat starches give pastes with higher viscosities than controls (35). The addition to pastes of extra lipids, of the type normally present in granules, decreases viscosities (37). However evidence suggests that neither the differences in the viscosities of pastes made from starches from various sources, nor the differences in the viscosities of pastes made from starches with controlled size ranges, can be directly attributed to lipids (16). Thus the variation in paste viscosity with source of starch and size of starch granule still holds for defatted starch.

I.2.2. Fundamental measurements

I.2.2.1. Steady shear conditions

A wide variety of rotational viscometers employing uniform shear rates are available for steady shear measurements (73). The virtually uniform shear encountered throughout the sample arises from the design of the testing system in the form of a co-axial cylinder or a cone-and-plate.

A number of investigators have studied the steady shear behaviour of pastes (68, 74-76). Earlier measurements obtained using co-axial cylinder viscometers (74-76) showed that gelatinised starch-water systems exhibit shear thinning properties. Power law equations of the form

$$\eta_{app} = K\dot{\gamma}^{m} \qquad [I.16]$$

describe their non-Newtonian flow properties, where K and m are constants, η_{app} is the apparent viscosity and $\dot{\gamma}$ is the shear rate. The results of these investigations indicated the absence of yield stress in starch pastes, suggesting that adjacent gel particles are not permanently bonded to each other in any way. Hence it was concluded that swollen starch granules were responsible for paste behaviour rather than a permanent gel network. These studies did not lead to a quantitative expression relating the structure and rheological properties of pastes.

Since the completion of the present study, Evans and Haisman (68) have reported the steady shear properties of pastes made from starches from a variety of plant species, namely corn, potato and tapioca. In addition wheat flour was studied. The results of this investigation also demonstrated that pastes obey Equation [I.16] at high shear rates. However the presence of yield stress was detected at low shear rates. The yield stress was found to be governed by the equation

$$\Gamma = \Gamma_0 + K\dot{\gamma}^{n} \qquad [I.18]$$

where K and n are constants, Γ is the shear stress and Γ_0 is the yield stress. Evans and Haisman also developed empirial equations to describe the concentration dependence of both the apparent viscosity at a given shear rate and the yield stress. However no attempt was made to reconcile the differences in rheological properties of various starch pastes.

I.2.2.2. Oscillatory shear conditions

The structure of pastes suggests they are likely to be viscoelastic fluids or weak gels. In this case, steady shear measurements reveal only part of the information required for rigorous characterisation of pastes. Viscoelastic fluids and weak gels may be fully characterised by measurements of dynamic viscosity and rigidity as a function of frequency (77). These measurements in some instances can give information about the structure of the system under test. The measurements of dynamic viscosity and rigidity may be made using co-axial cylinder or cone-and-plate viscometers.

Two approaches have been used to study the dynamic rheology of starch pastes. In the first approach, the frequency dependence of dynamic viscosity and rigidity is used to characterise rheological behaviour (78). Nakagaki and Muragishi (79) used this approach to obtain dynamic parameters of pastes made from potato, sweet potato and rice starches. Their results show that the precise behaviour of these pastes depends on concentration, type of starch and method of paste preparation. The frequency response of these pastes suggest they exhibit the viscoelastic behaviour characteristic of weak gels. Attempts to account for paste behaviour using mechanical models were unsuccessful and the authors suggested that this may indicate the fact that structural changes in the pastes occur as frequency changes.

Since the completion of the present study, Evans and Haisman (68) reported dynamic measurements on corn, potato and tapioca starches and on wheat flour. The frequency dependence of dynamic parameters again suggests that these pastes exhibit characteristcs of weak gels. Empirical equations were established that describe the concentration dependence of dynamic rigidity for a given paste.

In the second approach, a single value of dynamic viscosity and rigidity is obtained from measured parameters at the observed resonant frequency of the starch-water system, that is the frequency where maximum amplitude is observed (80). This approach has been applied to studies of modified starches of white milo starch and corn starch (70). Characteristics of gel were clearly evident from the dynamic response of these pastes. Although this method is simpler, it is less rigorous as a viscoelastic model must be assumed to represent the mechanical behaviour of pastes in order to calculate the dynamic parameters.

I.3 Scope of the present investigation

Consideration of the structure of pastes suggests factors that may account for their rheological behaviour. Starch pastes are disperse systems (81) and the main components of the disperse phase are swollen gel particles of varying sizes, lipid-amylose complexes and crystallised amylose. The continuous phase consists of dissolved polysaccharides predominantly amylose and some amylopectin. Some investigators consider that swollen granule fragments are responsible for the rheological characteristics of pastes (71), though others have suggested that the starch exuding from gelatinised granules is significant in this respect (72). In both cases a quantitative explanation is lacking. If starch pastes behave like disperse systems in general, then their properties are likely to be related to the volume fraction, number and size distribution of the swollen particles they contain. These various possibilities were therefore investigated.

The information so obtained was used in an attempt to establish reasons for differences in the rheological properties of pastes made from various wheat sources and for the variation in paste behaviour with sample preparation conditions.

It is well known that properties of gelatinised starch-water systems change with time on storage. The change in characteristics may be followed by measuring the variation in their rheological behaviour. This possibility was therefore investigated in the present study.

I.4. Experimental approach

Industry routinely monitors the rheological behaviour of starch pastes using empirical instruments in which undefined non-uniform shear conditions exist (67). This allows the determination of a viscosity-based number that is used to characterise the flow behaviour of the pastes. While techniques of this kind may be useful in predicting the properties of pastes in particular applications, they are not designed to give information of a fundamental nature. The rheological behaviour of starch pastes may be more vigorously characterised by steady or oscillatory shear methods that employ well defined shear conditions. This approach was therefore used in the present study.

The volume occupied by a bed of swollen granules was determined by swelling capacity measurements. Two approaches have been used, namely gravitational (82) and centrifugation (83) settling. Syneresis normally occurs during the course of settling in the gravitational technique. In the present investigation, swelling capacities of starches were determined by a centrifugation settling method. The amount of polymeric material released from gelatinised granules was determined by drying an aliquot of supernatant of a centrifuged sample. Microscopic observation confirms that it is not possible to measure the size distribution of gelatinised starch granules directly (84). The numbers and size distributions of particles were therefore examined prior to pasting on the assumption that they bear some relationship to the corresponding figures for swollen granules.

I.5. Experimental

I.5.1. Materials

I.5.1.1. Origin and variety of wheat

Six different varieties of wheat were used in this research; the New Zealand cultivars Karamu, Hilgendorf and Aotea and the Australian cultivars Gamenya, Raven and Gamut. All these cultivars were grown commercially throughout New Zealand. The samples of Karamu, Hilgendorf, Aotea and Gamenya wheats were grown in 1977. Raven was harvested in 1973 and Gamut in 1976. These wheats were stored at -20.0^{0}C before used.

I.5.1.2. Isolation of wheat starch

Starch was isolated according to the method of Meredith et al. (21), air-dried at ambient temperature to a moisture content (85) of about 10% and stored at 5^{0}C (86). Air-drying conditions were standardised as they can influence granule structure (47). The moisture content of starch was determined by an oven-drying method (85). The protein (87) and lipid contents (88) were measured by standard methods.

I.5.1.3. Size fractionation

Fractions of wheat starch with narrow size ranges were obtained by the sedimentation technique described by Meredith et al. (21). The range of particle sizes within each fraction was checked by microscopic observations.

I.5.1.4. Damaged starch

Commercial wheat starches normally contain small percentages of 'damaged' granules. These are starch particles that have been modified by mechanical forces entailed in milling (89). Starch samples containing such granules were obtained by ball-milling. The percentage of 'damaged' granules in a sample was determined by microscopic observations (90).

I.5.2. Method of paste preparation

Unless otherwise stated, the following procedure was used as the standard method for preparing pastes.

A starch suspension (4-16g starch/200g water), contained in a conical flask (250ml) fitted with collapsible link stirrer operating sufficiently fast to prevent the suspension settling out, was placed in a water-bath at $95.0^0 \pm 0.5^0$C for 1 hour. The weight of the paste so formed was checked and water added if required. The paste was then transferred to a water bath at 30.0^0C and equilibrated at this temperature for 0.5 hour. Thiomersal (0.01mM) was incorporated into pastes to inhibit microbial growth.

In experiments in which paste preparation conditions were varied, temperatures ranging from 70.0 - 95.0^0C and times ranging from 5 to 60 minutes were employed. These conditions are in accord with those used in industry to form pastes (91).

Some pastes were formed in a typical commercial test instrument, the Amylograph, for comparative purposes.

I.5.3. Measurement of the viscoelastic behaviour of wheat starch pastes

I.5.3.1. Introduction

The study of viscoelastic behaviour requires the determination of the relations among stress, strain and time for a particular type of deformation and a particular loading pattern (77). In so far as the viscoelastic behaviour is linear, this reduces to determining the time dependence of the shear modulus. The desired simplification of linear behaviour can be achieved by keeping the stresses sufficiently small. To find the time dependence of the shear modulus, the stress is usually varied in a sinusoidal manner at an angular frequency ($rads^{-1}$). The relationship between the stress and strain which is used to establish viscoelastic behaviour may be states as follows (77):-

$$G^* = G' + G'' \qquad [I.1]$$

or

$$G^* = G' + i\omega\eta' \qquad [I.2]$$

G'' is the loss modulus

where G* is the complex rigidity, G' is the dynamic rigidity, η' is the dynamic viscosity and ω is the angular frequency. For linear viscoelastic systems, the response to sinusoidal stress is depicted in Figure I.1 as a function of time.

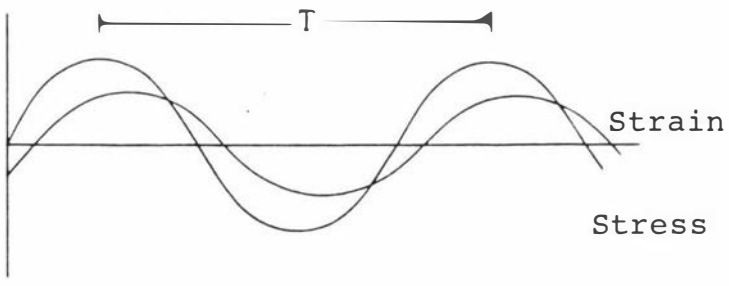

Figure I.1 Sinusoidally varying stress and strain for periodic deformation of a linear viscoelastic system.

The ratio of peak stress to peak strain is the amplitude ratio (m). The distance between these peaks in the time scale, multiplied by the frequency (ω) is the phase angle ($\emptyset$) in radians. Oka (92) has devised equations to describe the response of a linear viscoelastic system to the shear conditions encountered in a coaxial cylinder viscometer. In the present case, these simplify into the following forms:-

$$\eta' = \frac{1}{4\Pi L}\left[\frac{1}{r_1^2} - \frac{1}{r_2^2}\right]\left(\frac{k \sin \emptyset}{m \omega}\right) \qquad [I.3]$$

$$G' = \frac{1}{4\Pi L}\left[\frac{1}{r_1^2} - \frac{1}{r_2^2}\right]\left(k\left(\frac{\cos \emptyset}{m} - 1\right) + I\omega^2\right) \qquad [I.4]$$

where

r_1, r_2 = radius of inner and outer cylinders respectively
I = moment of inertia of inner cylinder.
L = immersion depth of inner cylinder
k = torsional constant of wire

The assumption made in deriving the simplified equations contribute less than 1% error (see Table I.1). Since the derivation of Equations [I.3] and [I.4] has not been documented elsewhere, a treatment is given in Appendix Ia.

Table I.1 Sample calculations of the percentage error in determining η' and G' using Equations [I.3] and [I.4]

ω	ϕ	m	Equation [I.5]		Equations [I.3] and [I.4]		% error	
			η'	G'	η'	G'	η'	G'
0.037	11.40	0.586	16.05	1.184	15.94	1.175	0.7	0.8
0.115	14.77	0.515	7.58	1.544	7.52	1.535	0.8	0.6
0.319	20.00	0.434	4.35	2.070	4.32	2.054	0.7	0.8
0.890	28.00	0.348	2.673	2.857	2.648	2.831	0.9	0.9
1.974	37.52	0.265	2.053	4.236	2.034	4.197	0.9	0.9

Equation [I.5] see page 161

I.5.3.2. Apparatus

A top-drive oscillatory co-axial cylinder viscometer was used to measure the dynamic visceolastic properties of starch pastes. The design of the instrument was based on that of Nakagawa and Seno (78). The instrument was constructed in the Food Technology Department Workshops, Massey University. A description of the apparatus is given in Appendix Ib since it is a non-standard piece of equipment.

The instrumental parameters of the viscometer are as follows:

Radius of the inner cylinder, r_1 = 0.0207 m
Radius of the outer cylinder, r_2 = 0.0265 m
Moment of inertia of inner cylinder, I = 4.015×10^{-4} kg.m^2
Thickness of suspending wire, d = 0.0007 and 0.001m
Immersion depth of inner cylinder, L = 0.157 m
Amplitude of driving ascillation, θ_0 = 0.0434-0.0576 rad
Torsional constant of wires, k = 0.136×10^{-2} and 0.382×10^{-2} Nm
Range of angular frequency, ω = 0.02 - 5 rads^{-1}

I.5.3.3. Experimental procedure

When measuring the frequency dependence of the dynamic viscosities and rigidities of wheat starch pastes, measurements were made at the lowest frequency first. Measurements were completed within 2 hours of paste formation, this time scale assured that results were not influenced by the crystallisation of polymer that occurs on paste storage. A very thin film of oil was placed on top of the paste to prevent evaporation (68), a check was made to show that this did not influence results through oil-paste interaction. Determinations were made at 30.0^{0}C.

The variation of dynamic viscosities and rigidities during paste storage was measured using a single frequency (ω = 0.02 rads $^{-1}$) and a range of ageing temperatures (10.0^{0} to 30.0^{0}C) and ageing times of up to 150h. During the course of these experiments, the pastes were stored in the viscometer.

I.5.3.4. Treatment of data

All recorded traces of input and output signals were analysed by the method described by Walters (93). Dynamic viscosity and rigidity were then calculated according to Equations [I.3] and [I.4] respectively.

I.5.4. Measurement of the rheological properties of wheat starch pastes under steady shear conditions

I.5.4.1. Apparatus

A Ferranti-Shirley cone-and-plate viscometer was used to measure the flow behaviour of starch pastes under steady shear conditions. The theoretical principles underlying the measurements of shear stress and apparent viscosity using a cone-and-plate geometry have been described in a number of texts (73, 95). The cone used in the present study was designed to make measurements of systems containing a disperse phase with particle sizes similar to those found in starch pastes. The instrumental parameters used were:-

Cone angle, Ψ	=	0.02618 rad
Radius of cone, R	=	0.035 m
Torque spring constant, T	=	2.453 Nm/Division
Shear stress constant	=	$^{3T}/2\pi R^3 = 27.32$
Shear rate constant	=	$\frac{2\pi}{60} \times \frac{1}{\Psi} = 4.0$

I.5.4.2. Experimental procedure

In experiments in which the shear rates were varied, measurements were made at the lowest shear rate first. A range of rates of shear from 0.4 to $4000S^{-1}$ was employed. All measurements were made at $30.0^{0}C$.

I.5.4.3. Treatment of data

Shear stress and apparent viscosity were calculated as a function of shear rate according to standard methods (96).

I.5.5 Determination of the number of particles per gram of sample and the size distribution of starch granules

Particle size distributions of starch granules were determined using the Coulter-Counter Model B with a 100 μm orifice tube attachment. The apparatus was calibrated using mono-sized polystyrene latex (diameter = 12.45 μm) according to the standard procedure described in the Coulter-Counter manual. During a routine counting, corrections were made for the coincidence loss by using the Coulter-Counter coincidence correction chart and corrections for background particles were also carried out but neglected if counts were less than 100. The raw data obtained from the Coulter-Counter was in the form of total number of particles greater than a given particle volume against particle volume. Particles less than 12 μm^3 in volume could not be counted accurately due to a significant noise level.

The raw data from the Coulter-Counter was transformed to give the relative distribution of weight or number against the particle diameter. Several assumptions were made in the transformation; firstly, all particles were considered to be spherical and secondly, all particles were considered to be of uniform density. These assumptions have been used elsewhere (17). The steps involved in transforming the Coulter-Counter raw data into relative weight or number against particle diameter are demonstrated for one starch in Appendix Ic. In all cases triplicate determinations were made for the various wheat starches and a mean value obtained after transformation of the raw data.

I.5.6 Determination of the swelling capacity of, and the exudate from, gelatinised granules

Preliminary measurements of swelling capacities were made using the standard procedure of Schoch (83). This entails centrifuging a paste at high speed and measuring the weight of the bed of particles so formed. However it was found that the results obtained by this method were influenced by the centrifugal conditions and hence the procedure is unsatisfactory for the present purposes. The possibility of using a gravitational settling technique (82) was therefore investigated. In this method, a paste is allowed to settle to a constant value. However, as wheat starches contain small granules, it takes about a week for particles to settle. During this period, syneresis and compression of the particle bed would occur and hence the results obtained would not refer to the original condition of the paste. A centrifugation settling technique was therefore developed to measure the swelling capacity without the effect of syneresis and with a correction for the particle bed compression.

In this centrifugation settling technique, 10.0g aliquots of a dilute paste in graduated centrifuging tubes were centrifuged for different times (in minutes) and speeds (×g) to give volumes of sedimented particles at 30.0°C. Extrapolation techniques were then used to obtain the volume of sediment at zero time and at zero speed. The steps involved in the extrapolation technique to obtain the swelling capacity of a starch sample are demonstrated for one case (Appendix Id).

I.6 Results

I.6.1. Viscoelastic behaviour of wheat starch pastes

I.6.1.1 Linear viscoelastic behaviour

The procedure for analysing the observed quantities of Equations [I.3] and [I.4] is based on the assumption that linear viscoelastic behaviour is occurring, and so the shear stress Γ and the shear strain γ satisfy the relationship:-

$$\Gamma = G^* \gamma \qquad [I.15]$$

in which complex rigidity G* should not depend upon Γ and γ but it is a function of frequency ω. Linear viscoelastic behaviour was demonstrated for the range of conditions examined by varying the shear amplitude in the standard manner as shown in Table I.2. The results in this table show that, as required, the magnitude of the shear amplitude has no significant effect on the dynamic viscosity and rigidity. Similar results were found at other frequencies.

Table I.2 Representative measurements of dynamic viscosity η' and rigidity G' as a function of the shear amplitude at an angular frequency of 0.1 rads $^{-1}$ for pastes made from Aotea wheat starch.

Shear amplitude rad	Dynamic viscosity η' Nsm^{-2}	Dynamic rigidity G' Nm^{-2}
0.0576	4.40	2.10
0.0499	4.30	1.95
0.0476	4.60	2.25
0.0433	4.20	2.05

I.6.1.2. Frequency dependence of dynamic viscosity and rigidity

The frequency dependence of the dynamic viscosity and rigidity of pastes formed from various wheat starches under a variety of conditions was determined. Figure I.3 shows plots of dynamic viscosity and rigidity as a function of angular frequency for pastes containing different concentrations of Aotea starch. Similar plots were obtained for starch pastes made from the other wheat varieties. The decrease in dynamic viscosity and increase in dynamic rigidity as the angular frequency increases is the characteristic viscoelastic behaviour shown by both concentrated solutions of polymers of high relative molar masses and of weak gels (77). A similar frequency dependence was obtained by Nakagaki and Maragishi (79) for dynamic viscoelastic behaviour for potato, sweet potato and rice starch pastes.

I.6.1.3. Effect of starch concentration

The effect of starch concentration on the frequency dependence of dynamic viscosity and rigidity is evident in Figure I.3. This can also be illustrated by plotting the variation of dynamic viscosity and rigidity at representative frequencies as a function of starch concentration as shown in Figures I.4 and I.5 respectively. A similar concentration dependence was observed by Nakagaki and Muragishi (79). The results in Figures I.4 and I.5 show that the dynamic viscosities and rigidities of starch pastes made from the Gamenya wheat variety are much higher than from the Aotea variety at any given starch concentration. According to Amylograph tests, Gamenya starches have much more desirable pasting characteristics than Aotea (41). The oscillatory measurements demonstrate the same trend.

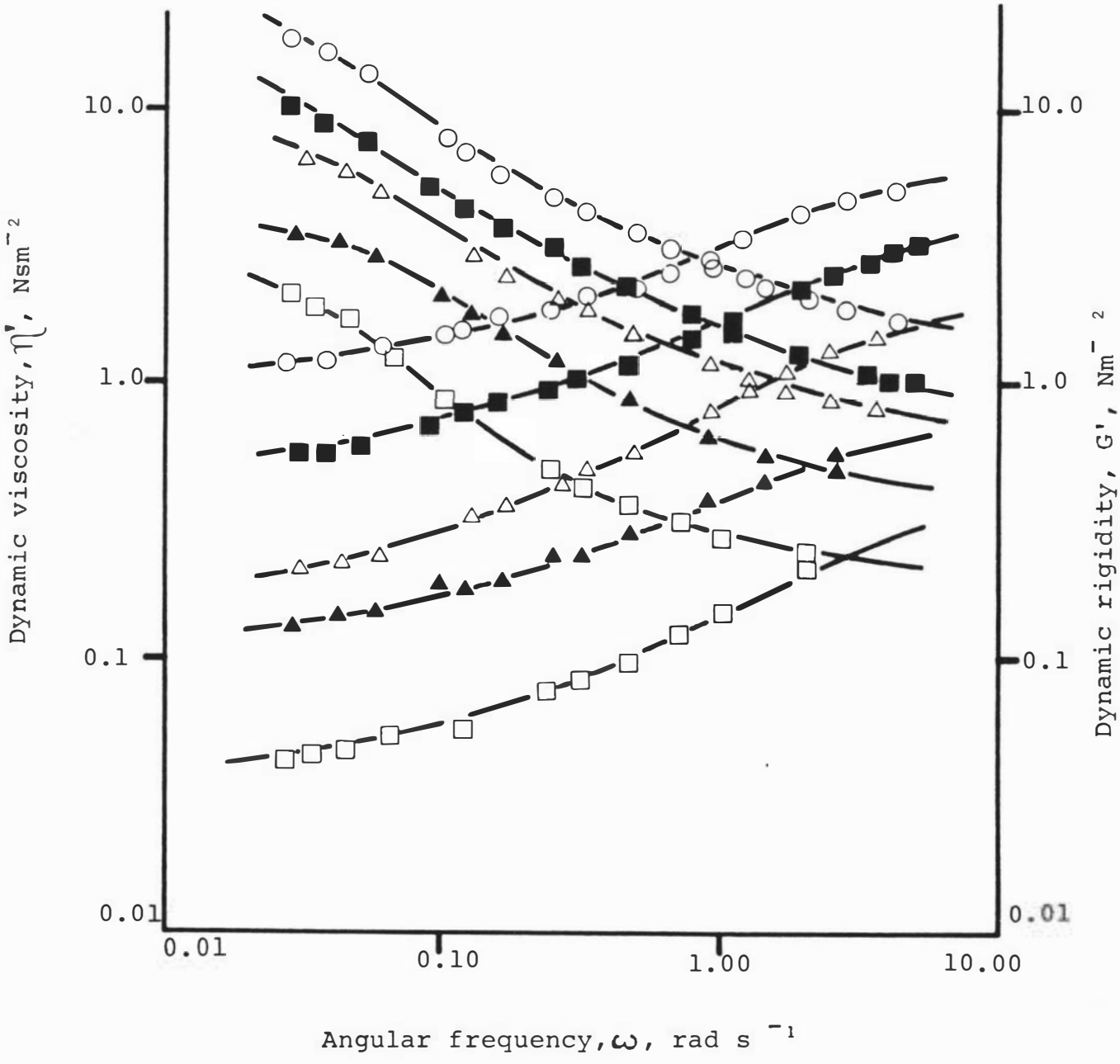

Figure 1.3 Plots of the log of the dynamic viscosity and rigidity as a function of the log of the angular frequency for pastes containing different concentrations of Aotea wheat starch.

□ 4.50% ▲ 5.00% △ 5.50% ■ 6.00%
○ 6.50%

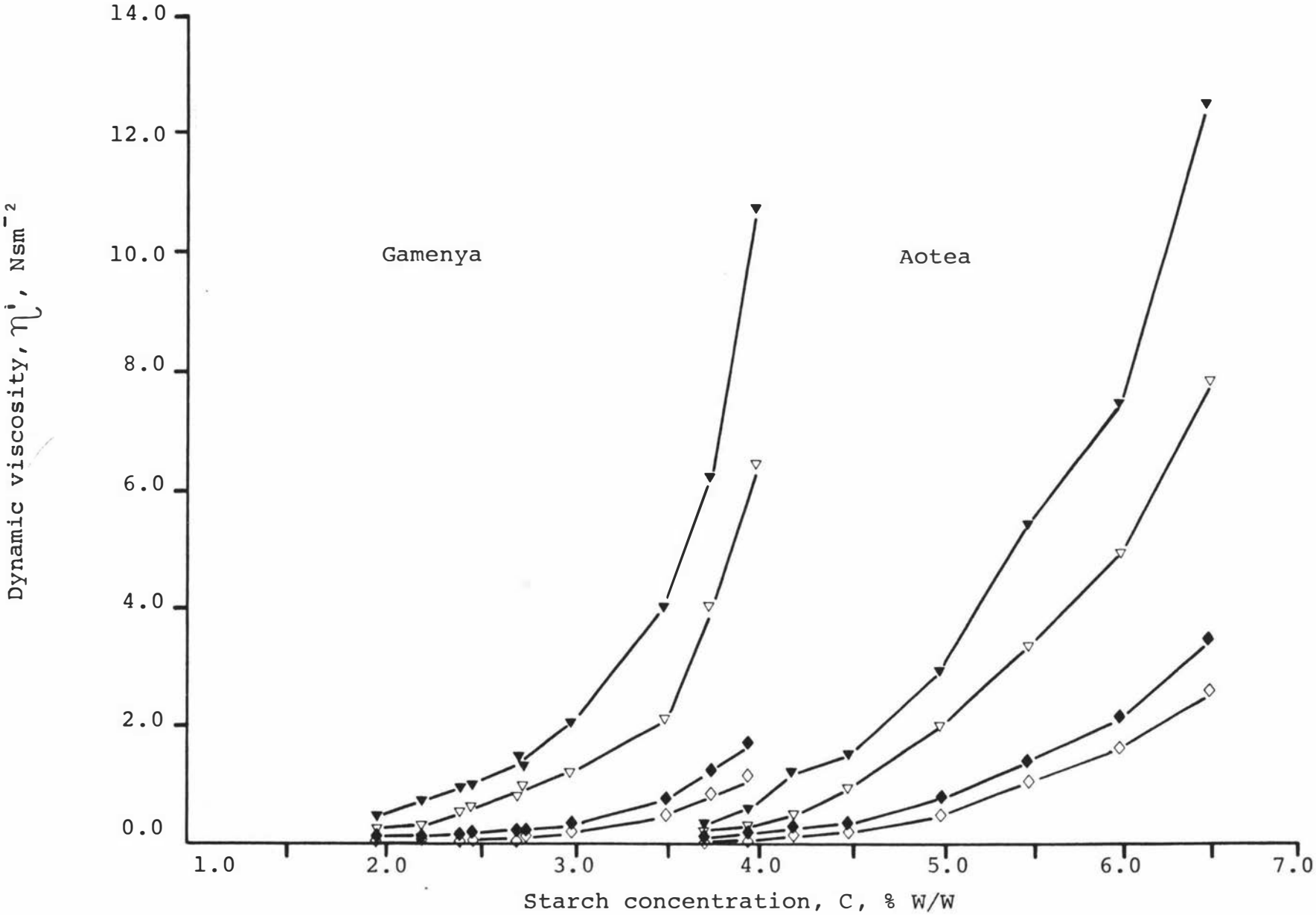

Figure 1.4 Plots of the dynamic viscosity of Gamenya and Aotea pastes as a function of the starch concentration at several frequencies.

▼ 0.05 $rads^{-1}$ ▽ 0.10 $rads^{-1}$ ◆ 0.05 $rads^{-1}$ ◇ 1.00 $rads^{-1}$

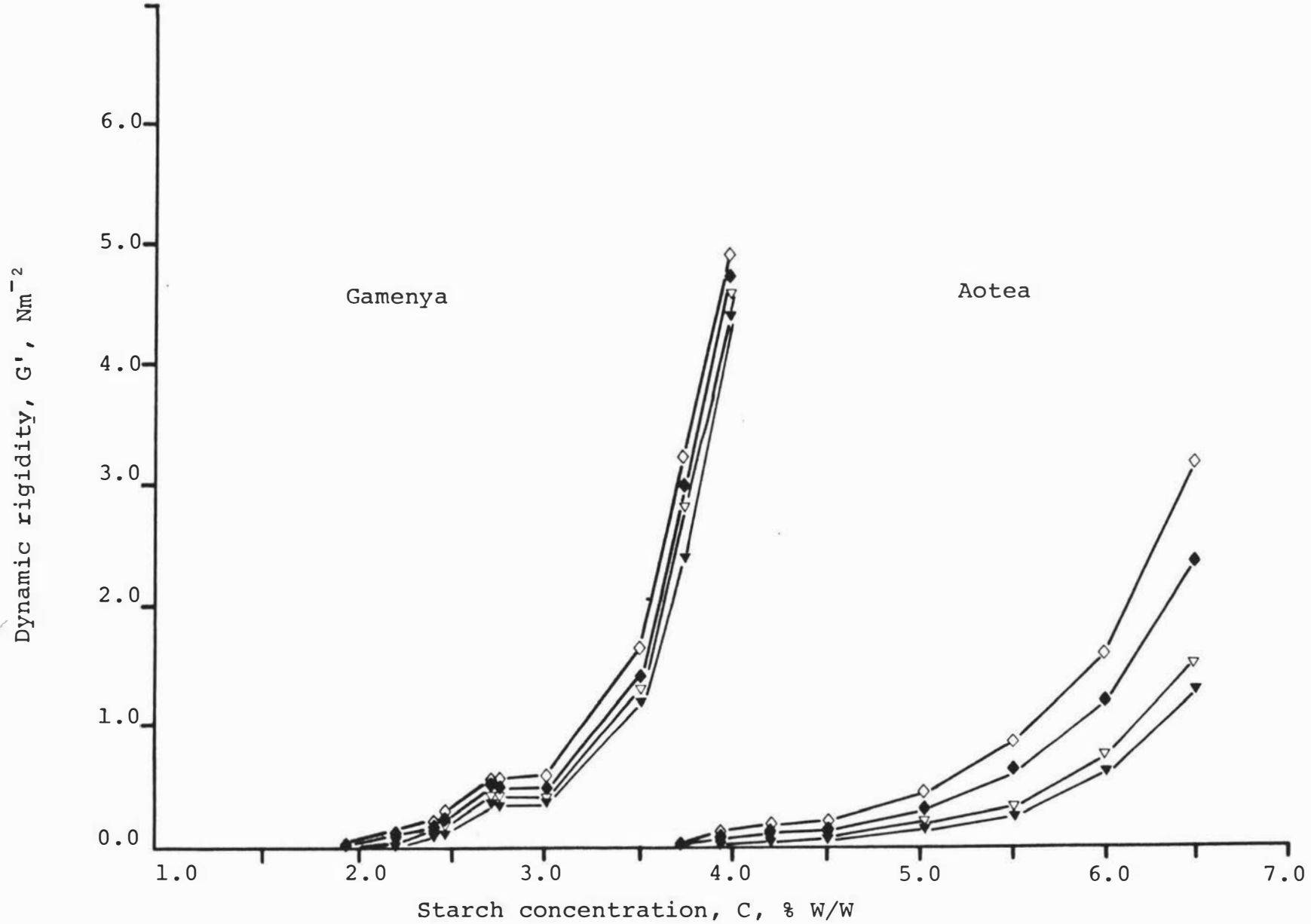

Figure 1.5 Plots of the dynamic rigidity of Gamenya and Aotea pastes as a function of the starch concentration at several frequencies.

▼ 0.05 rads $^{-1}$ ▽ 0.10 rads $^{-1}$ ◆ 0.5 rads $^{-1}$ ◇ 1.00 rads $^{-1}$

The results in Figures I.4 and I.5 suggest that gelatinised starch-water systems are characterised by three different modes of behaviour. At lower concentration of starch, the dynamic viscosity has a comparatively small value while the dynamic rigidity tends to zero. A certain minimum concentration of starch is needed before rigidity is apparent. The second type of behaviour occurs at intermediate concentrations, where both dynamic viscosity and rigidity are readily detected. These concentration ranges are of most interest in the present study as they give pastes whose rheological properties are similar to those formed in the Amylograph under standard conditions. Above the upper limits of these ranges the starch-water systems change from viscoelastic fluids to viscoelastic solids and self-supporting gels are formed. Both dynamic viscosity and rigidity then increase markedly.

I.6.1.4. Effect of paste preparation condition and starch damage

Figure I.6 shows the frequency dependence of dynamic viscosity and rigidity for pastes formed from Gamenya wheat starch under different temperature/time treatments. The dynamic viscosities and rigidities at any given frequency are reduced as a result of decreases in pasting temperature or time. Other wheat varieties studied follow the same trend. Figure I.7 shows the frequency dependence of dynamic viscosity and rigidity for pastes made from Aotea wheat starch that has been damaged to different extents. The dynamic viscosities and rigidities at any given frequency decrease with increasing starch damage. Other wheat varieties studied give similar results. Figure I.8 shows the frequency dependence of dynamic viscosity and rigidity for pastes formed from Aotea wheat variety prepared in the Amylograph. The results show that pastes formed in the Amylograph have reduced dynamic viscosities and rigidities compared with controls. Other wheat varieties studied show similar variations.

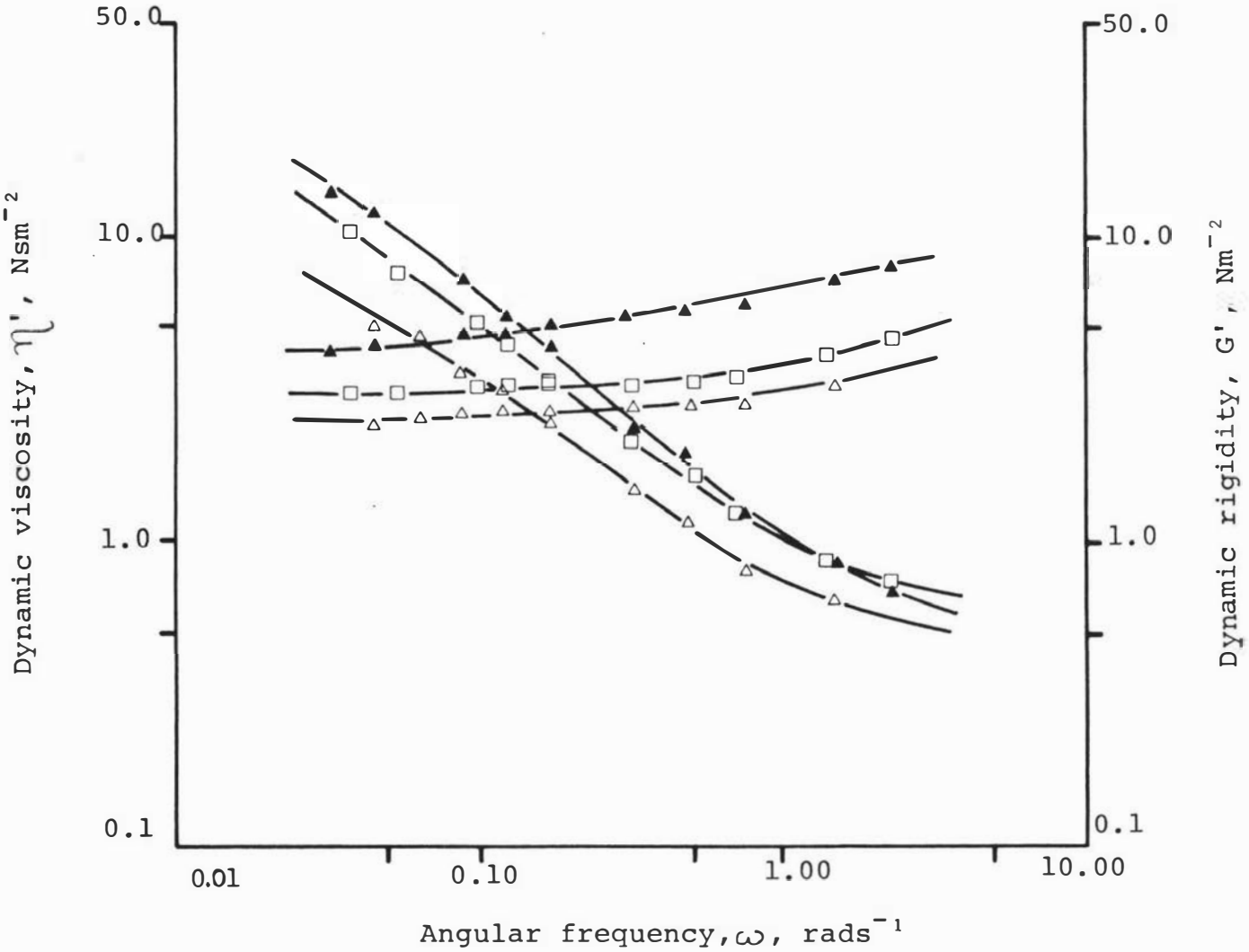

Figure 1.6 Plots of the log of the dynamic viscosity and rigidity as a function of the log of the angular frequency for pastes made from Gamenya wheat starch (3.75%) under different temperature/time treatments.

▲ 95.0°C/1.0h □ 95.0°C/0.5h △ 92.5°C/1.0h

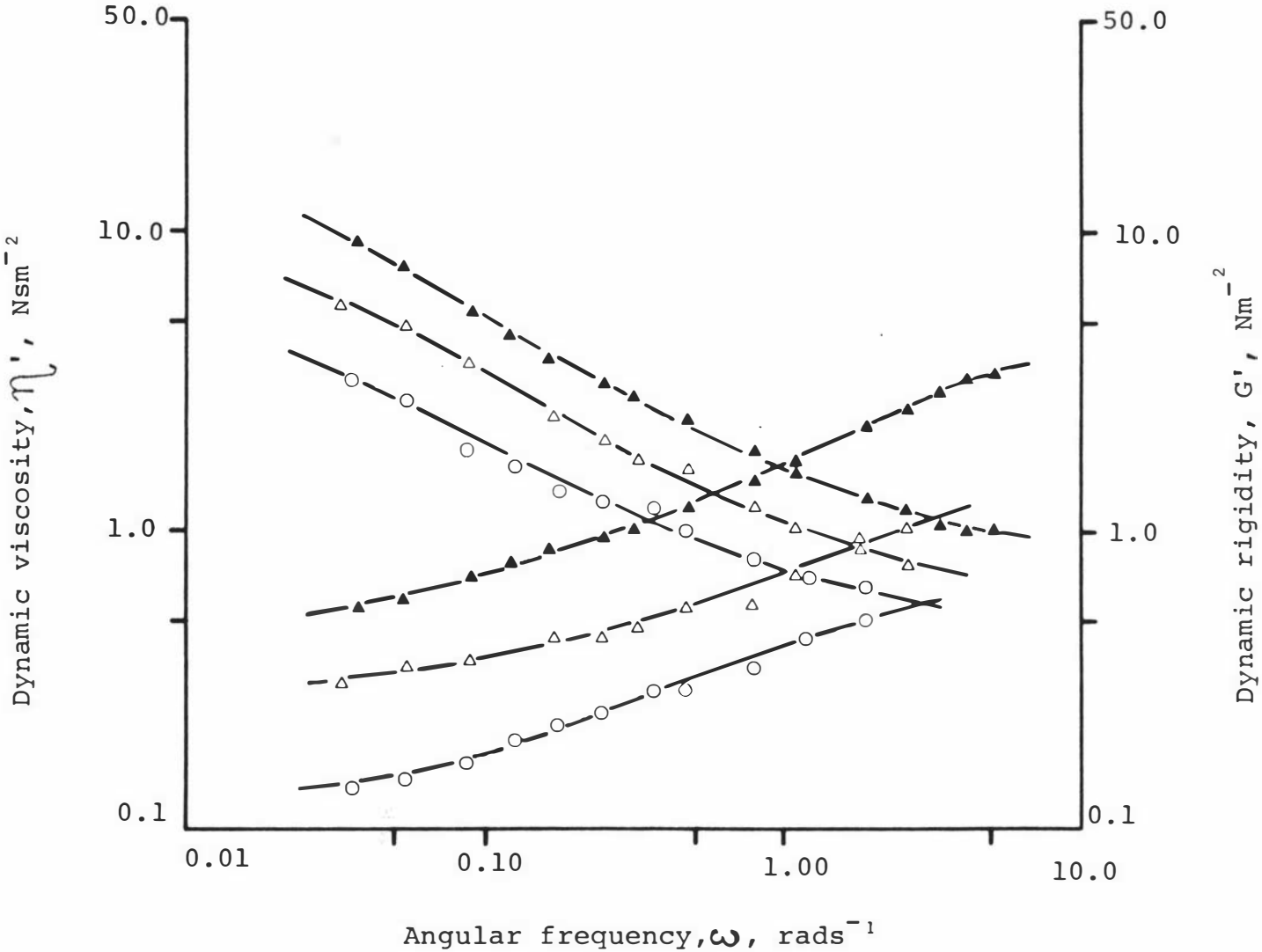

Figure 1.7 Plots of the log of the dynamic viscosity and rigidity as a function of the log of the frequency for pastes made from Aotea wheat starch (6.00%) at several damaged levels.

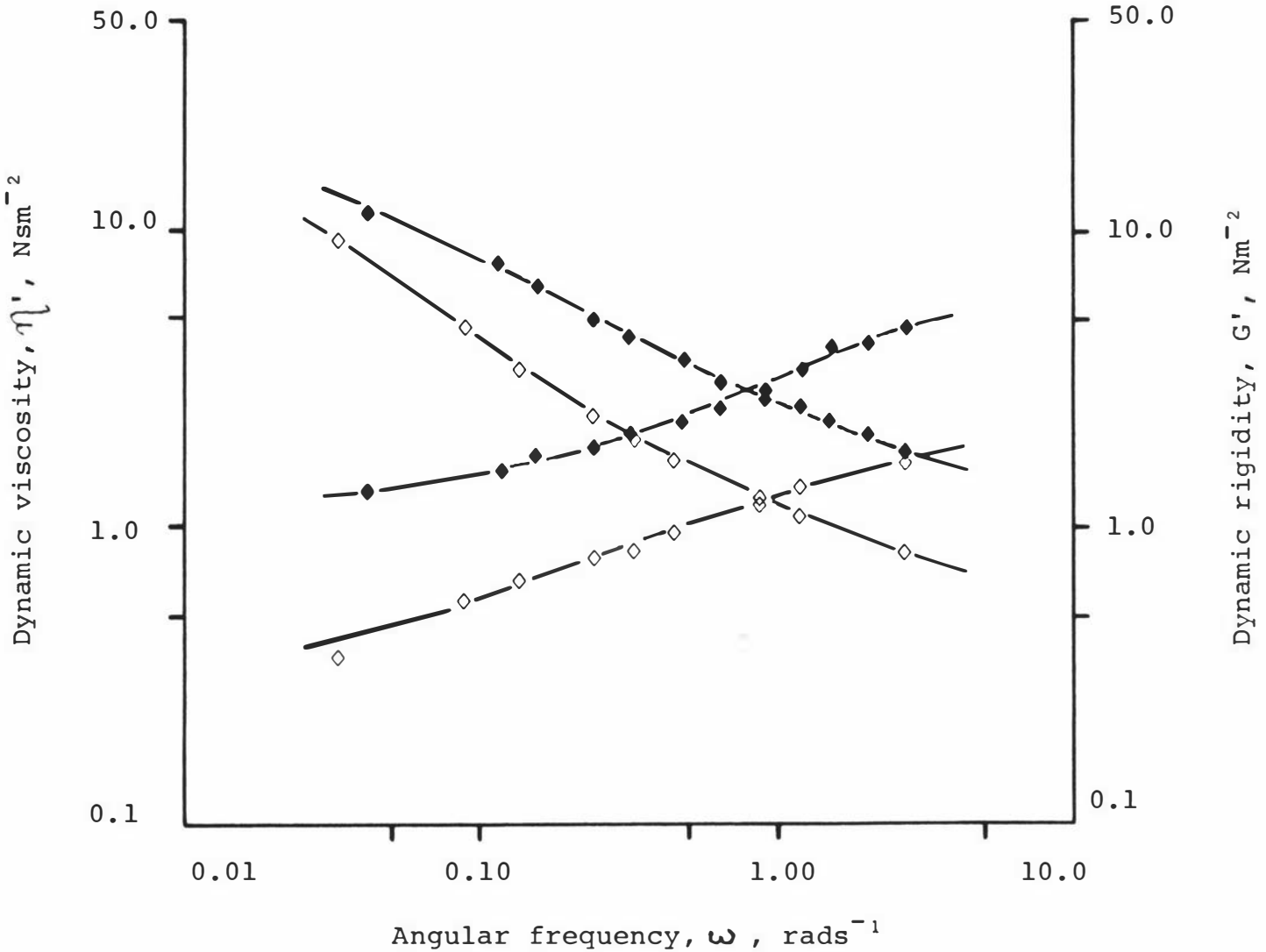

Figure 1.8 Plots of the log of the dynamic viscosity and rigidity as a function of the log of the angular frequency for pastes formed from Aotea wheat starch (6.50%)

◆ formed by the standard methods
◇ formed in the Amylograph

I.6.2 Rheological properties of wheat starch pastes under steady shear conditions

I.6.2.1. High shear rate (10-4000S^{-1})

Figure I.9 shows typical log-log plots of apparent viscosity against shear rate for various starch pastes. Clearly the pastes are shear thinning fluids that obey the law

$$\eta_{app} = K\dot{\gamma}^{m} \qquad [I.16]$$

where η_{app} is the apparent viscosity, $\dot{\gamma}$ is the shear rate and K and m are constants. K and m are a function of the concentration and variety of starch and of the temperature/time treatment used during paste preparation. These results are consistent with those reported for starches from other plant species (68).

I.6.2.1.1. Effect of starch concentration

Figure I.10 shows the apparent viscosity of pastes as a function of the shear rate for given concentrations of Gamut wheat starch. Other wheat varieties studied follow the same trend. The slopes of the log-log plots are strongly dependent on starch concentration. A plot of the pseudoplasticity constant (-m) against the starch concentration, as shown in Figure I.11, indicates that it increases to a constant value as the concentration is increased. In the lower concentration range, it decreases sharply extrapolating back to zero at some finite concentration (C_0) characteristic of each veriety of wheat starch. A linear relationship between the pseudoplasticity constant and the starch concentration can be obtained using the following standard equation (68):-

$$-\frac{1}{m} = -\frac{1}{m_{\infty}} + \frac{K_1}{C-C_0} \qquad [I.17]$$

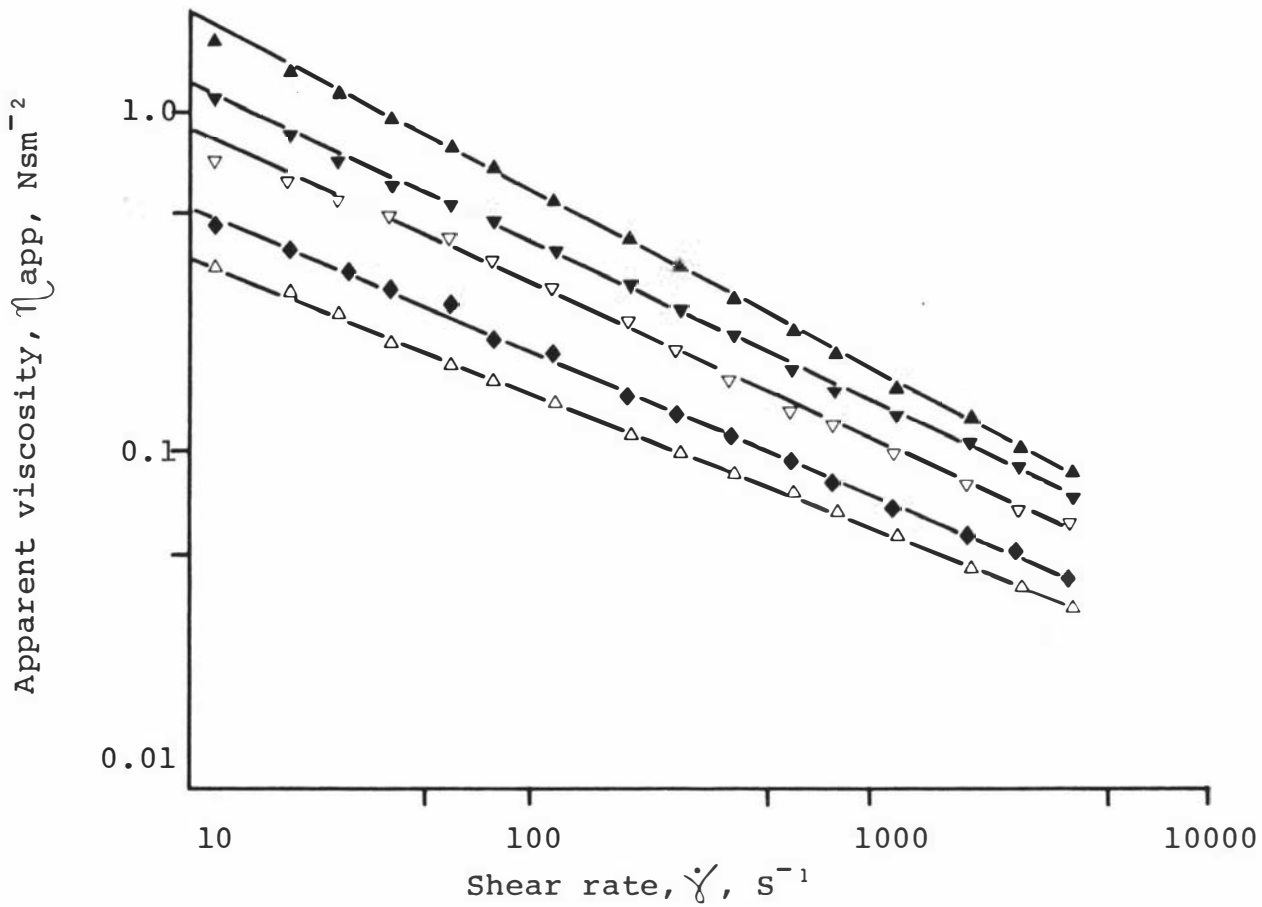

Figure I.9 Plots of the log of the apparent viscosity as a function of the log of the shear rate for various starch pastes.

▲ Gamut (6.14%) △ Hilgendorf (4.56%) ▼ Raven (5.56%)
▽ Karamu (6.49%) ◆ Aotea (5.40%)

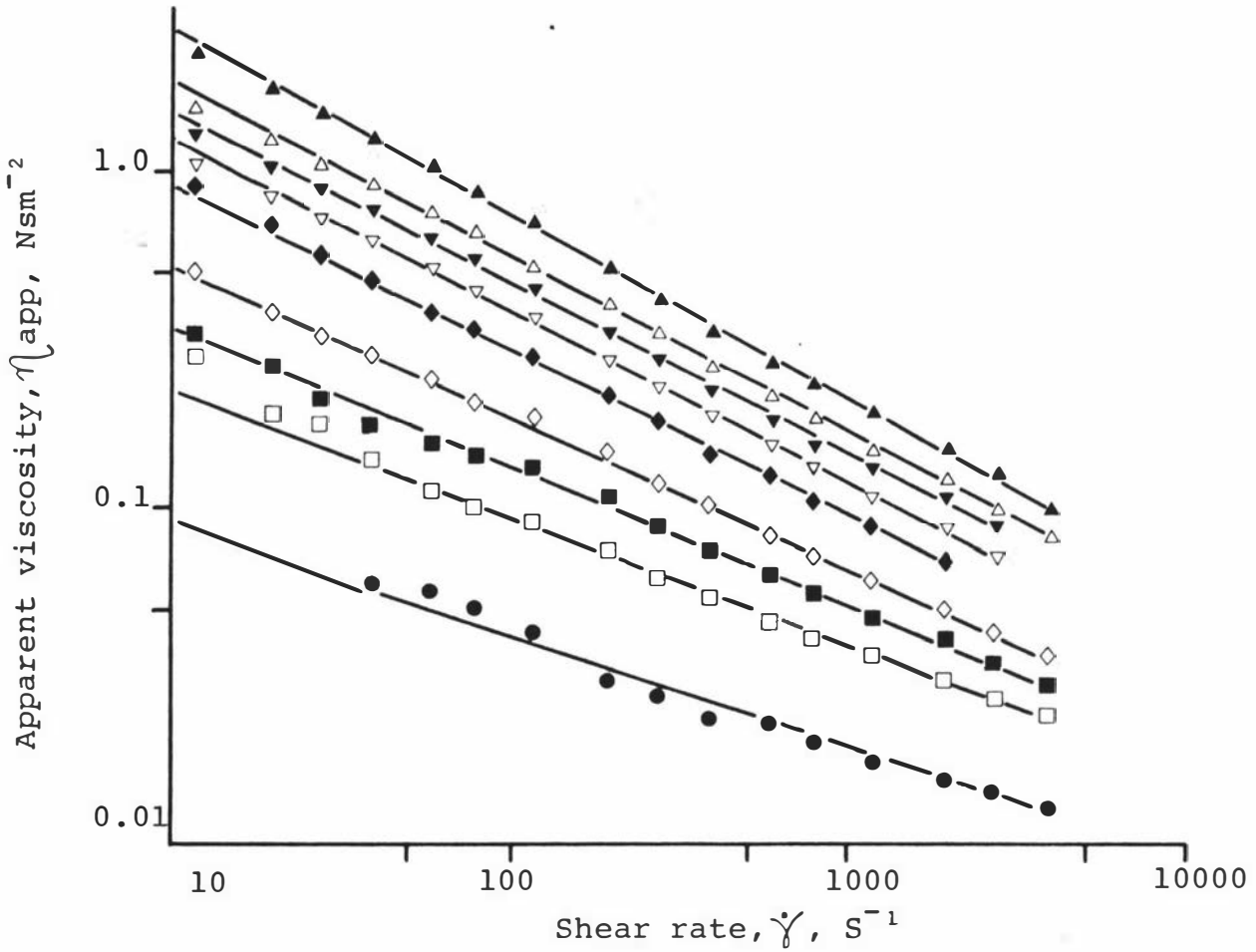

Figure I.10 Plots of the log of the apparent viscosity as a function of the log of the shear rate for pastes containing different concentrations of Gamut wheat starch.

▲ 7.10 % △ 6.40% ▼ 6.14% ▽ 5.49% ◆ 5.00% ◇ 4.34% ■ 4.08% □ 3.48% ● 2.76%

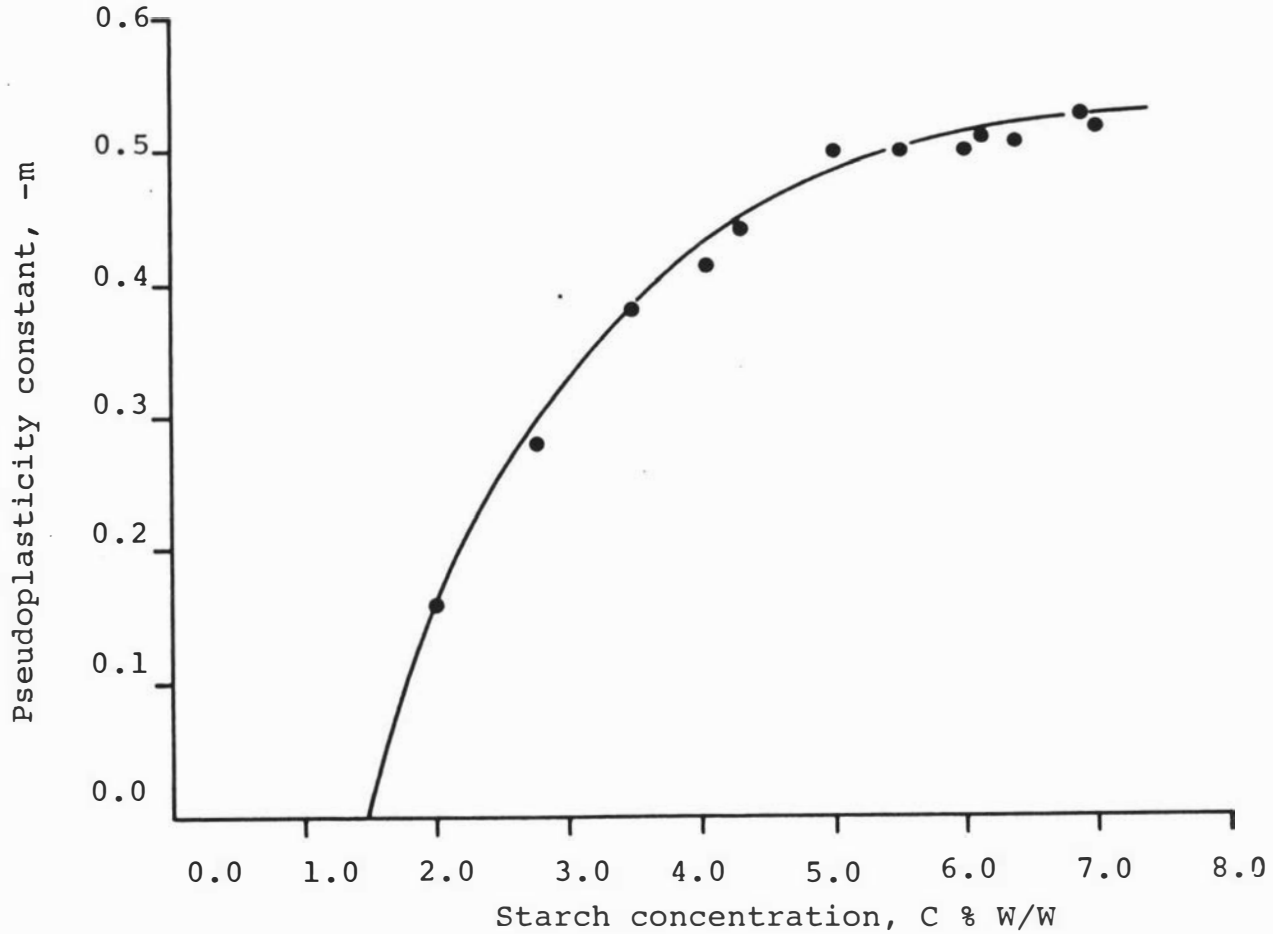

Figure I.11 Plots of the pseudoplasticity constant of Raven starch pastes as a function of the starch concentration.

The concentration at which the pseudoplasticity constant equals to zero can be calculated according to Equation [I.17] by a trial and error procedure so that the best least squares fit of the data is obtained. The results of using this procedure for data such as that in Figure I.11 are shown in Table I.3.

Table I.3 Values of C_0 , $-m_\infty$, K_1 and correlation coefficient of the least squares fits to Equation [I.17] for various starch pastes.

Wheat variety used to prepare starch	C_0 %	$-m_\infty$	K_1	Correlation coefficient
Karamu	3.20	0.51	0.60	0.998
Aotea	3.10	0.71	2.52	0.998
Hilgendorf	2.00	0.93	3.10	0.998
Gamut	2.40	0.86	3.77	0.994
Raven	1.40	0.77	3.01	0.998

The variation of the apparent viscosity of pastes at a given shear rate, $\eta_{\dot{\gamma}}$, with starch concentration is shown in Figure I.12 for Karamu and Raven wheat varieties. The same trend was obtained at other shear rates and with the other starch varieties. The results show that there is an abrupt change in apparent viscosity at a certain starch concentration characteristic of each wheat variety. The results in Figure I.12 also show that the apparent viscosity of starch pastes formed from the Raven wheat variety are much higher than from the Karamu wheat variety at any given starch concentration, this is consistent with Amylograph measurements (41).

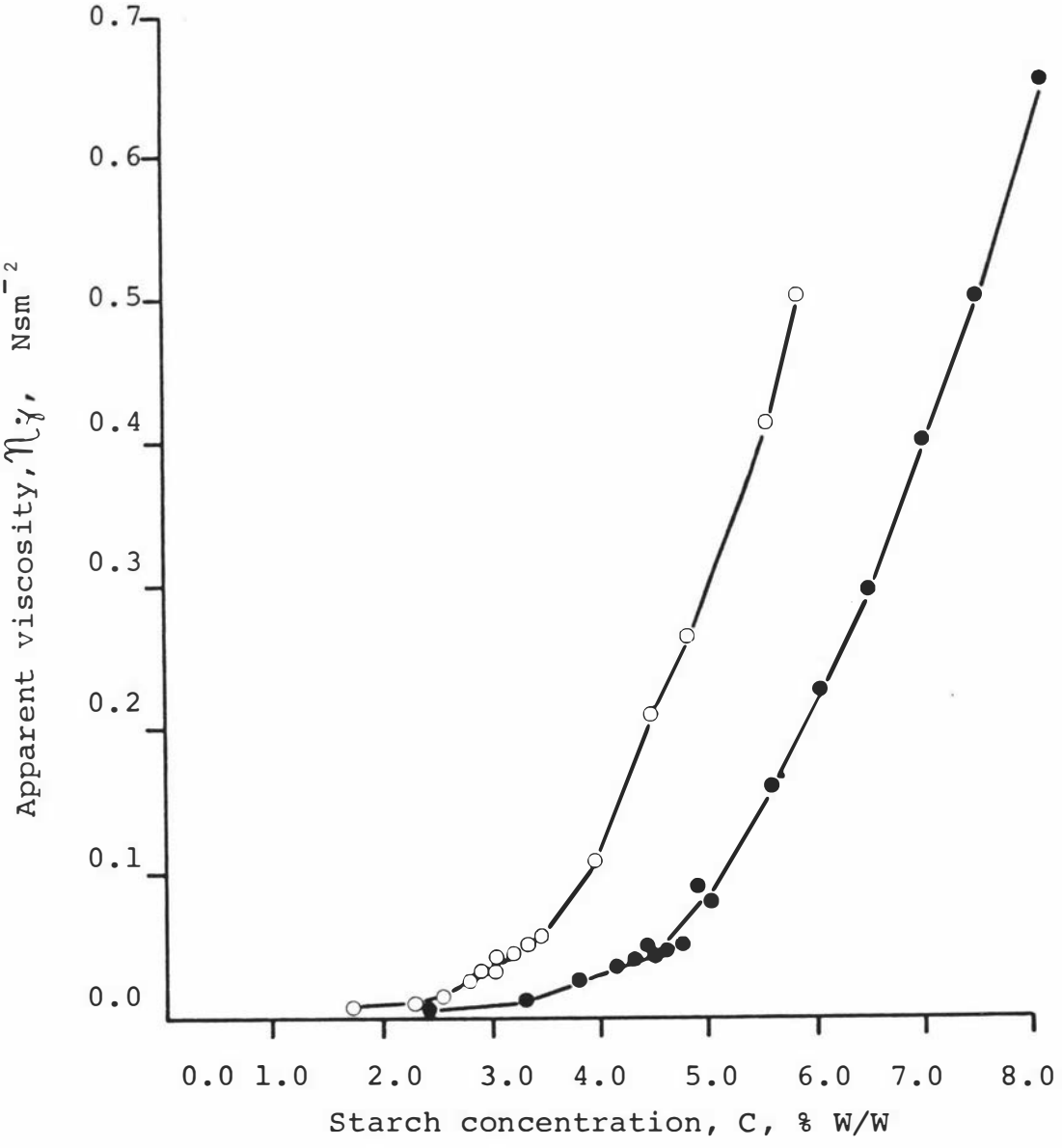

Figure I.12 Plots of the apparent viscosity at a shear rate of $120s^{-1}$ of Raven (○) and Karamu (●) starch pastes as a function of the starch concentration.

I.6.2.1.2. Effect of paste preparation condition

The effect of varying pasting temperature, with a constant heating time of 1 hour, on the apparent viscosity of pastes is demonstrated in Figure I.13 for Gamut wheat variety. The slopes of the log-log plots are dependent on the pasting temperature. Plots of the pseudoplasticity constant of the pastes against the pasting temperature for several starch concentrations (Figure I.14) shows that the pseudoplasticity constant decreases constantly when the pasting temperature is reduced. Plots of the apparent viscosity of the pastes at a given shear rate as a function of the pasting temperature (Figure I.15) show that the apparent viscosity decreases markedly when the pasting temperature is decreased. Other wheat varieties studied give similar pattern of variation.

Figure I.16 shows the effect of varying pasting time, at a constant temperature of 95.0^{0}C, on the apparent viscosity of pastes made from the Hilgendorf wheat starch. It can be seen that the slopes of the log-log plots are dependent on the pasting time. The pseudoplasticity constant of the pastes drops sharply when the pasting time is less than 10 minutes as shown in Figure I.17. Plots of the apparent viscosity of the pastes at a given shear rate as a function of the pasting time (Figure I.18) show that the apparent viscosity decreases slightly when the pasting time is reduced from 60 minutes to 15 minutes and drops sharply thereafter. A similar pattern of variation was obtained with other wheat varieties examined.

I.6.2.2. Low shear rate (0.4 -10S $^{-1}$)

Figure I.19 shows typical log-log plots of shear stress against shear rate for various wheat starch pastes. Clearly the flow curves are non-linear on the logarithmic scale and

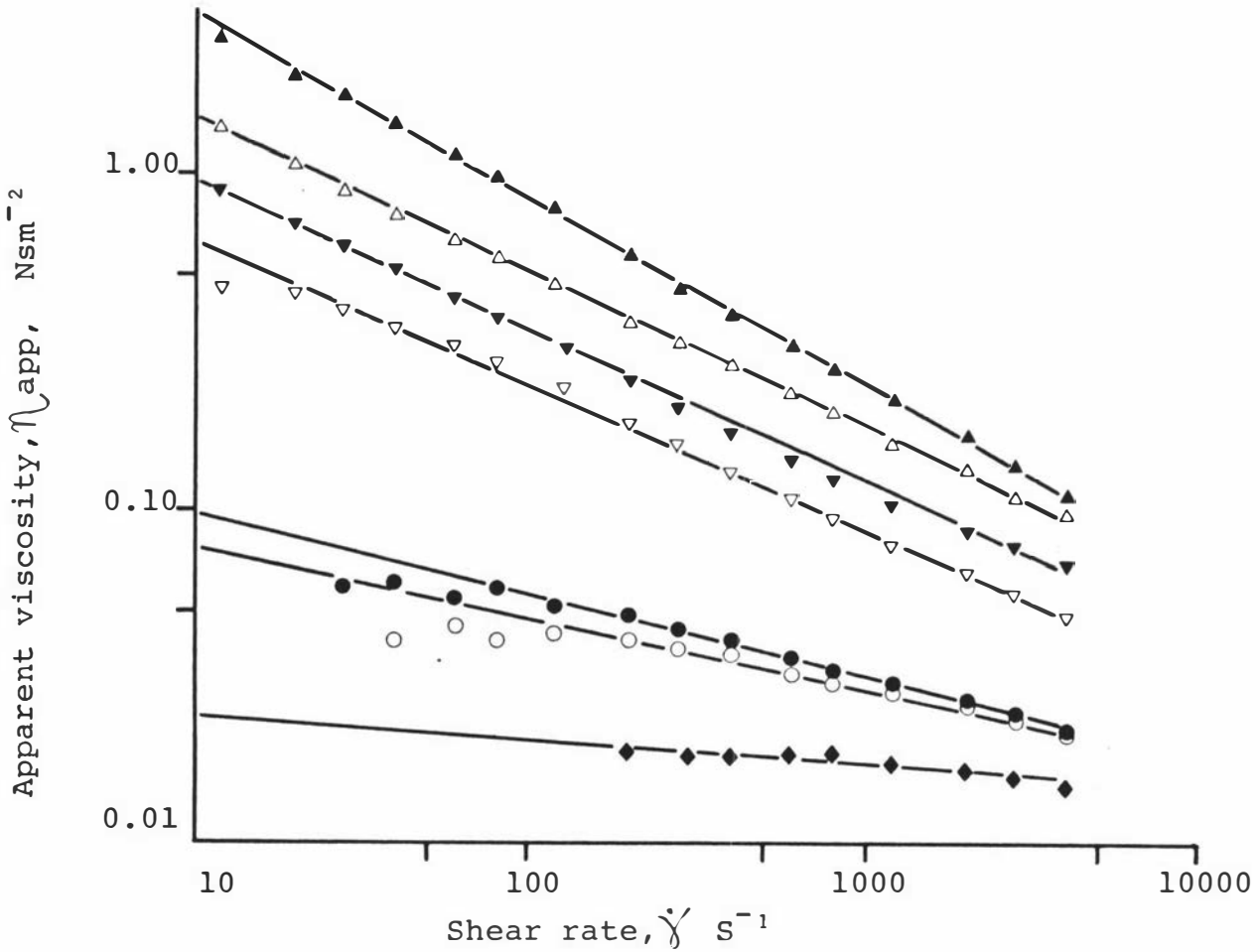

Figure I.13 Plots of the log of the apparent viscosity as a function of the log of the shear rate for Gamut starch pastes (7.00%) prepared by varying pasting temperature, at a constant heating time of 1h.

▲ 95.0°C △ 92.5°C ▼ 90.0°C ▽ 87.5°C ● 85.0°C ○ 80.0°C ◆ 75.0°C

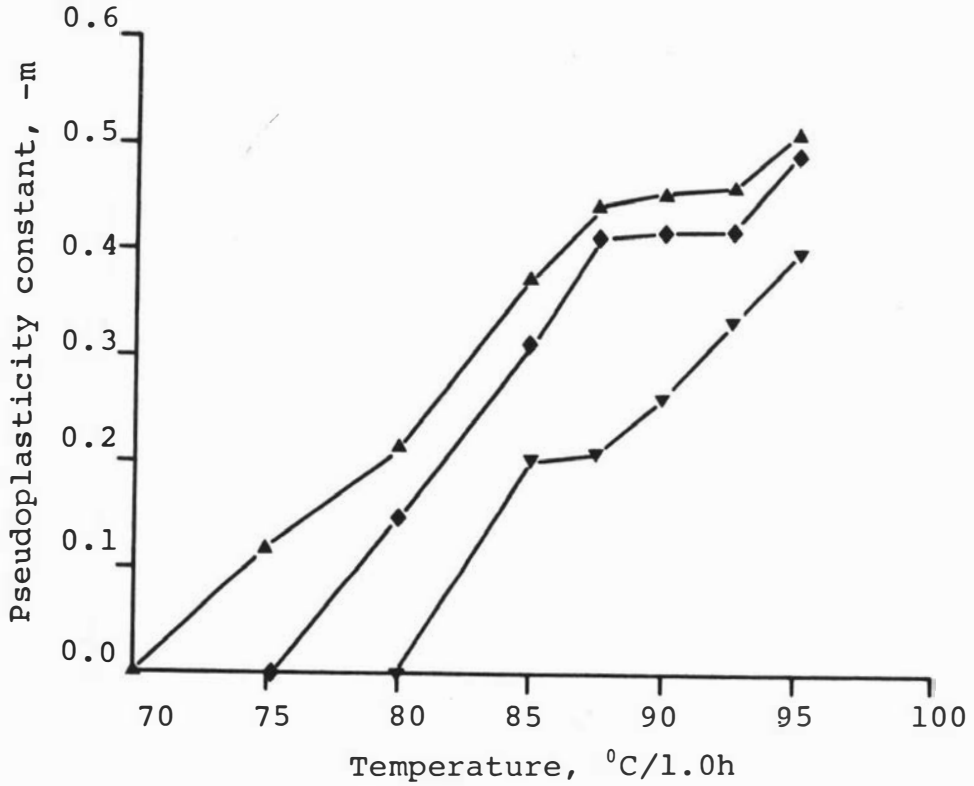

Figure I.14 Plots of the pseudoplasticity constant of Gamut starch pastes as a function of the pasting temperature for several starch concentrations.

▲ 7.00% ◆ 6.00% ▼ 5.00%

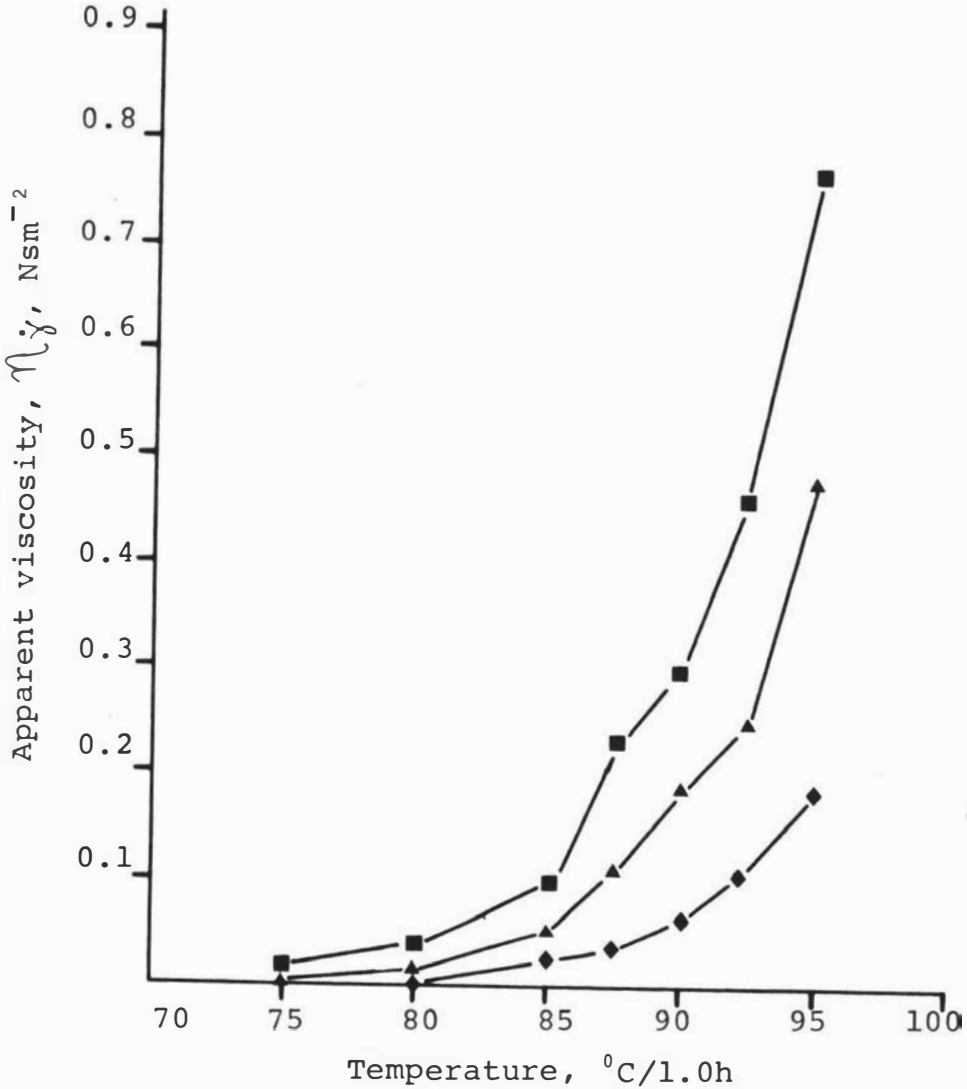

Figure I.15 Plots of the apparent viscosity at a shear rate of $120s^{-1}$ of Gamut starch pastes as a function of the pasting temperature.

■ 7.00% ▲ 6.00% ◆ 5.00%

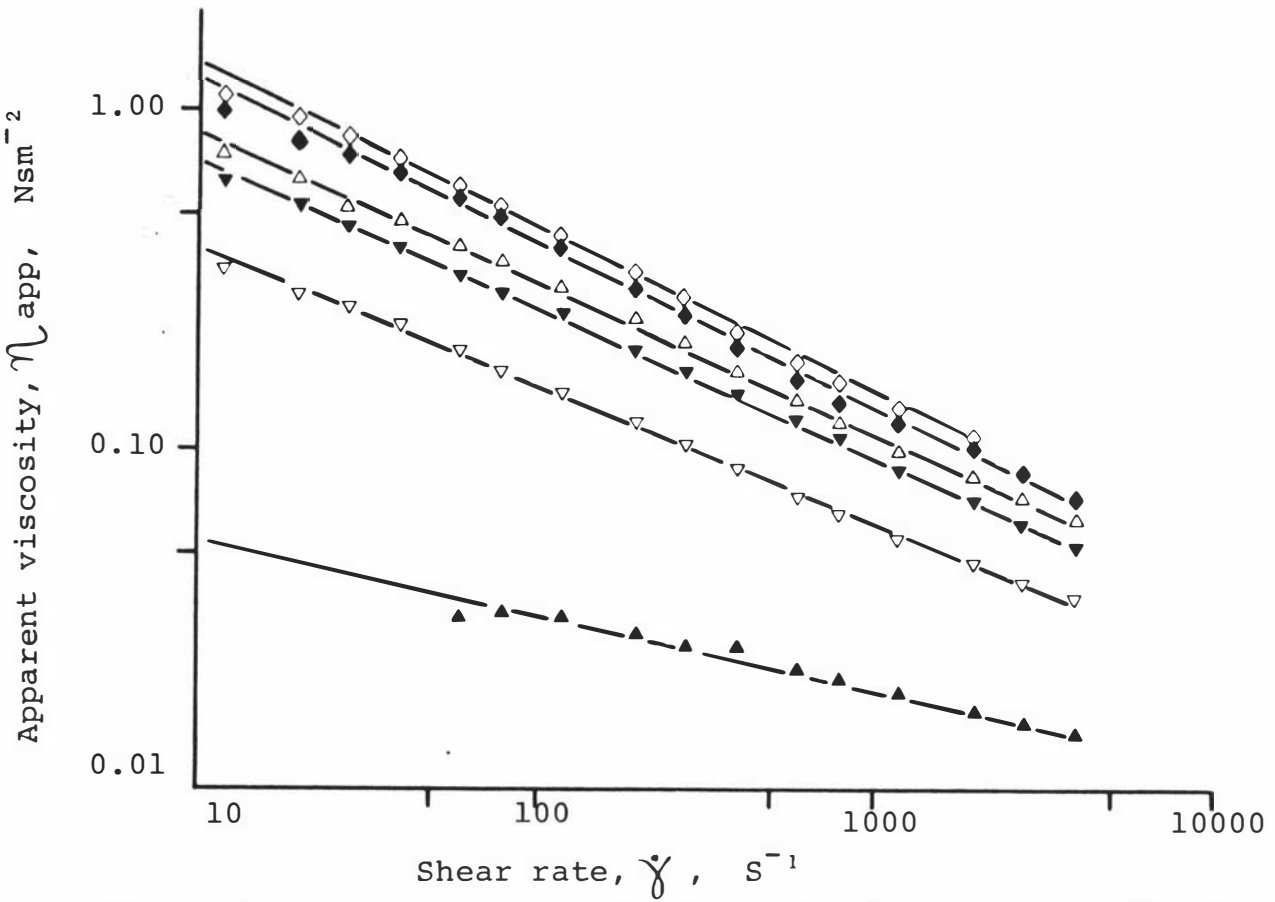

Figure I.16 Plots of the log of the apparent viscosity as a function of the log of the shear rate for Hilgendorf starch pastes (5.77%) prepared by varying pasting time, at a constant pasting temperature of 95.0°C.

◇ 60 min ◆ 30 min △ 20 min ▼ 15 min ▽ 10 min ▲ 5 min

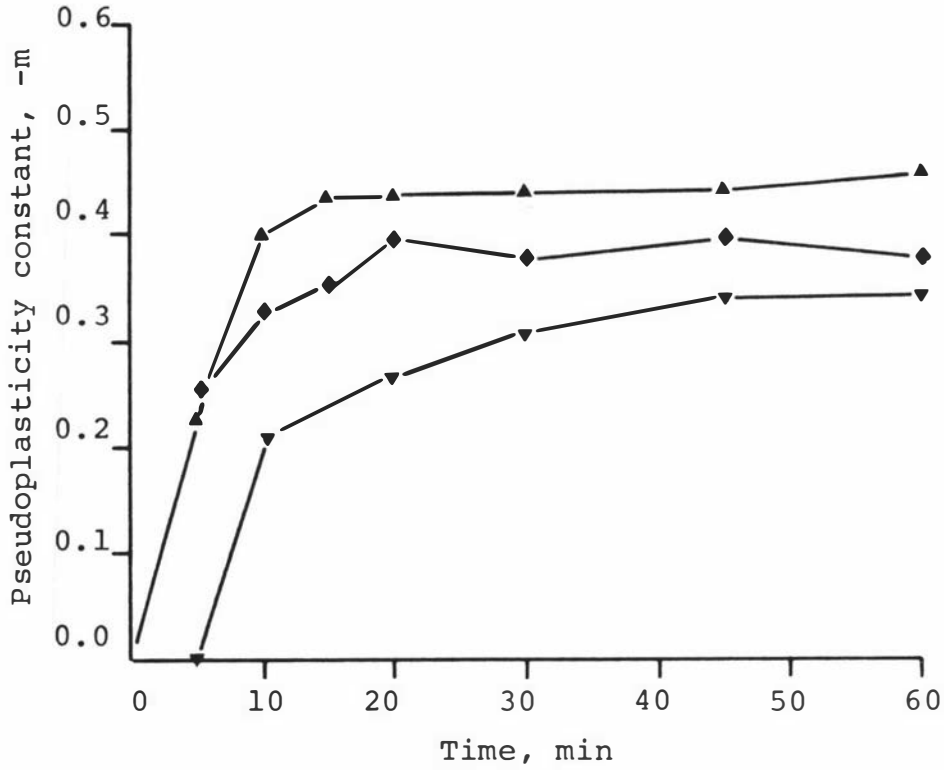

Figure I.17 Plots of the pseudoplasticity constant of Hilgendorf starch pastes as a function of the pasting time for several starch concentrations.

▲ 5.77% ◆ 5.00% ▼ 4.00%

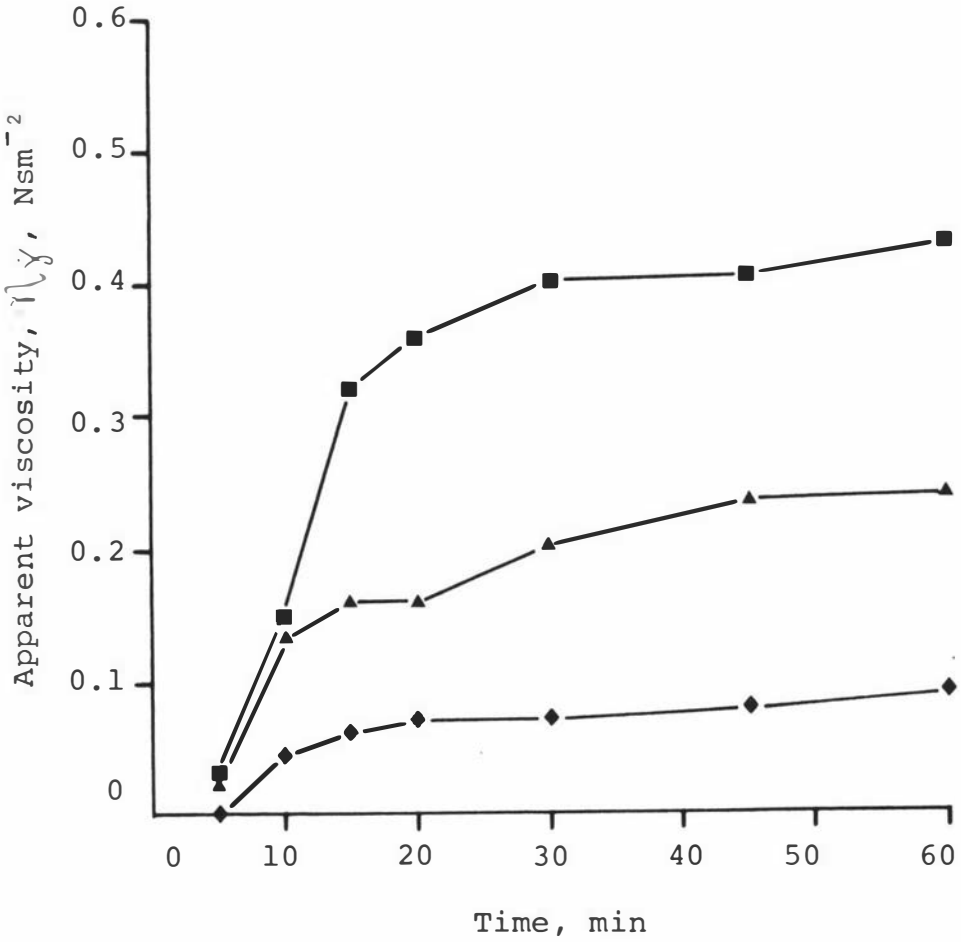

Figure I.18 Plots of the apparent viscosity at a shear rate of $120S^{-1}$ of Hilgendorf starch pastes as a function of the pasting time.

■ 5.77% ▲ 5.00% ◆ 4.00%

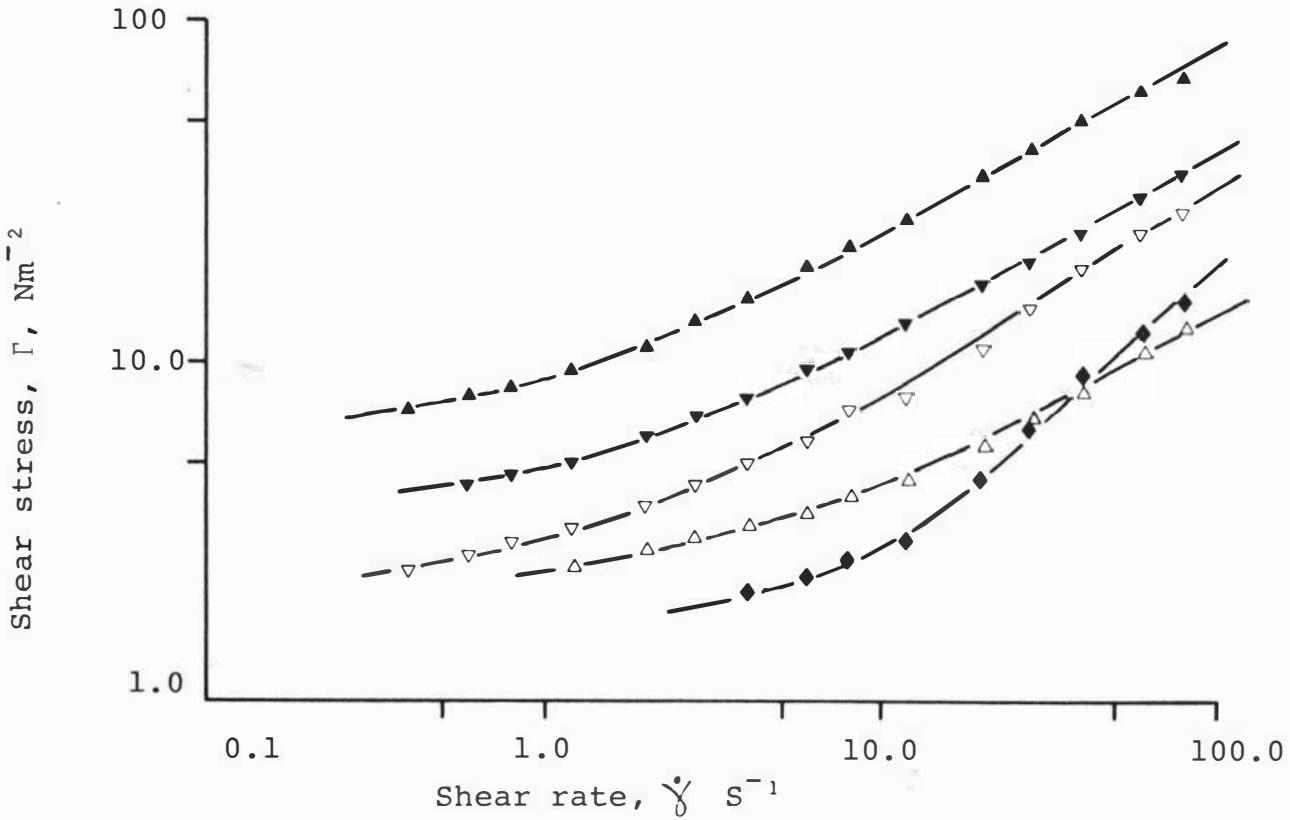

Figure I.19 Plots of the log of the shear stress as a function of the log of the shear rate for various starch pastes.

▲ Gamut (6.14%) ▼ Raven (5.56%) ▽ Karamu (6.49%)
◆ Aotea (5.40%) △ Hilgendorf (4.56%)

approach finite values at very low shear rates, suggesting that yield stresses are present. This behaviour can be described by the following equation (73)

$$\Gamma = \Gamma_0 + K_3 \dot{\gamma}^n \qquad [I.18]$$

where K_3 and n are constants and Γ_0 is the yield stress. The values of Γ_0 are determined by extrapolation.

The values of Γ_0, K_3 and n depend on the concentration and variety of starch and on paste preparation conditions. The results are consistent with those reported for starches from other plant species. Equation [I.18] applies to starch pastes which are above certain minimum concentrations and have received sufficient heat treatment, otherwise yield stresses are not apparent.

I.6.2.2.1. Effect of starch concentration

Figure I.20 shows the flow curves of pastes for given concentrations of Gamut wheat pastes. Other wheat varieties studied follow the same trend. The variation of the yield stress values of pastes with starch concentration for Karamu and Raven wheat varieties is shown in Figure I.21. The results show that the yield stresses of starch pastes made from the Raven wheat variety are higher than from the Karamu wheat variety at any given concentration. In all cases it was found that the higher is the value of the yield stress the higher is the Amylograph viscosity. When the starch concentration is too low, a stage is reached where either the yield stresses are too low to be detected by the viscometer or no yield stresses occur as an insufficient quantity of swollen gel particles is present to be packed throughout the paste volume.

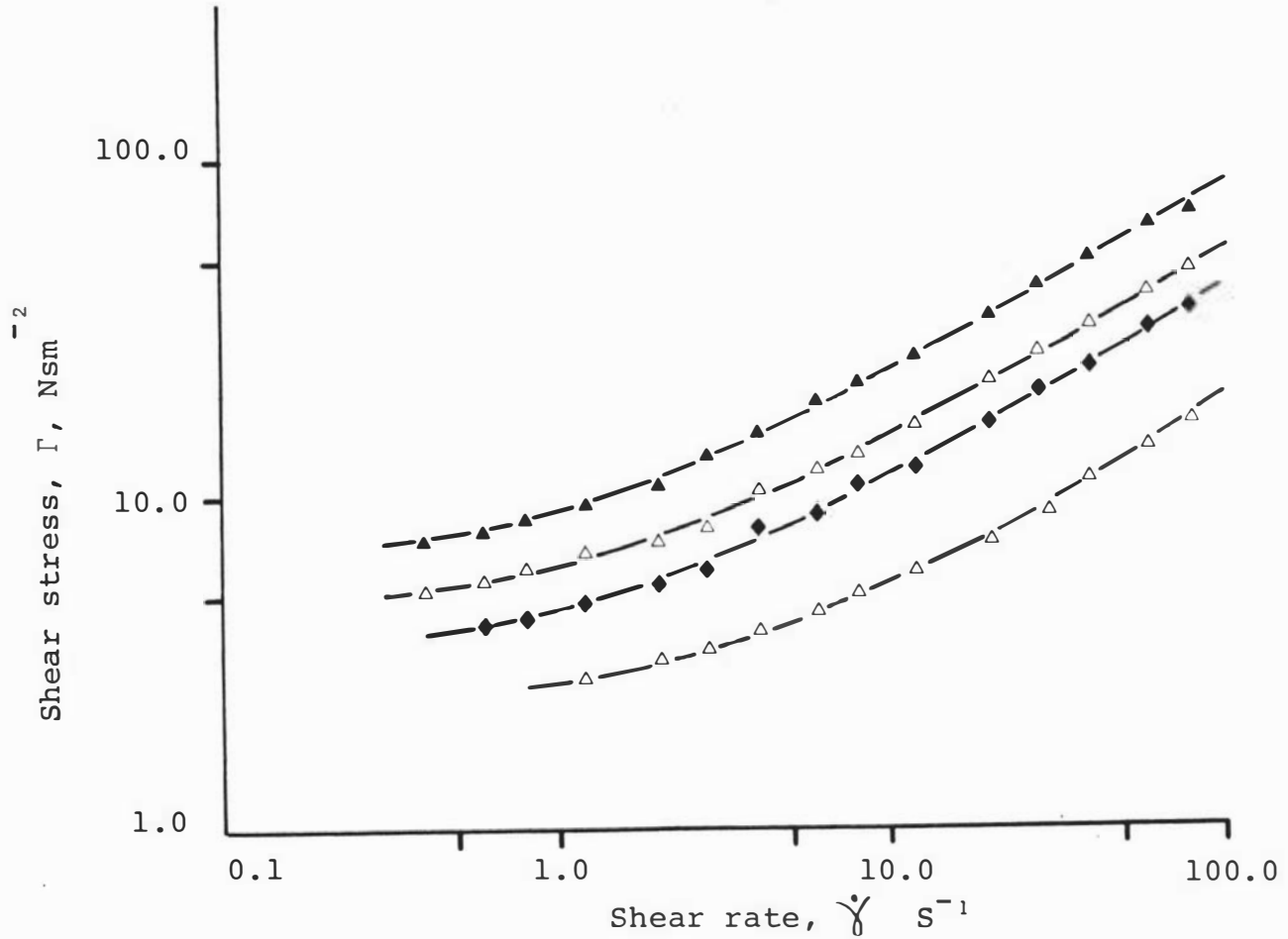

Figure I.20 Plots of the log of the shear stress as a function of the log of the shear rate for given concentrations of Gamut starch pastes.

▲ 7.12% △ 6.4% ◆ 6.14% ◇ 5.49%

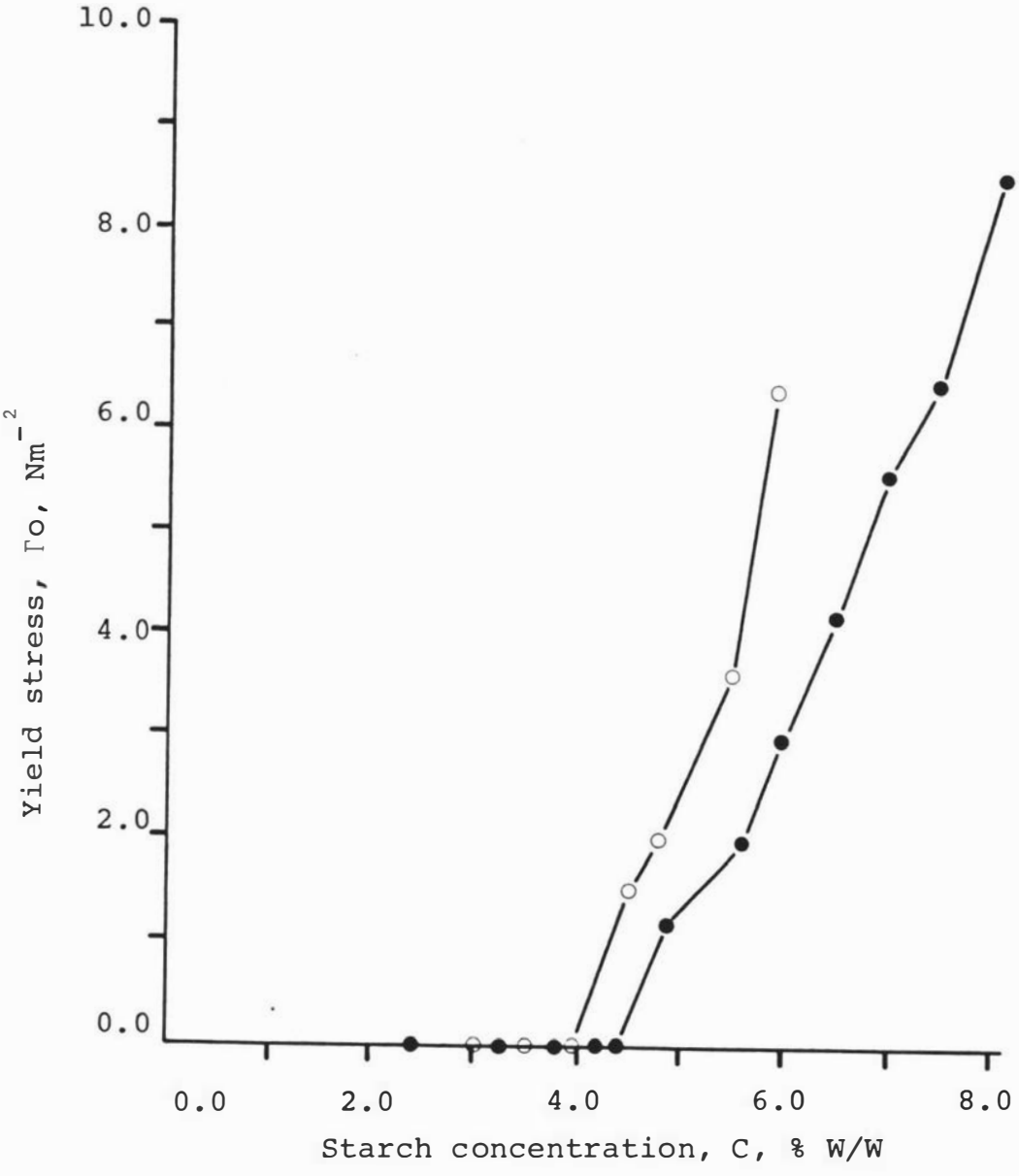

Figure I.21 Plots of the yield stress of pastes prepared from Raven (○) and Karamu (●) wheat starches against the starch concentration.

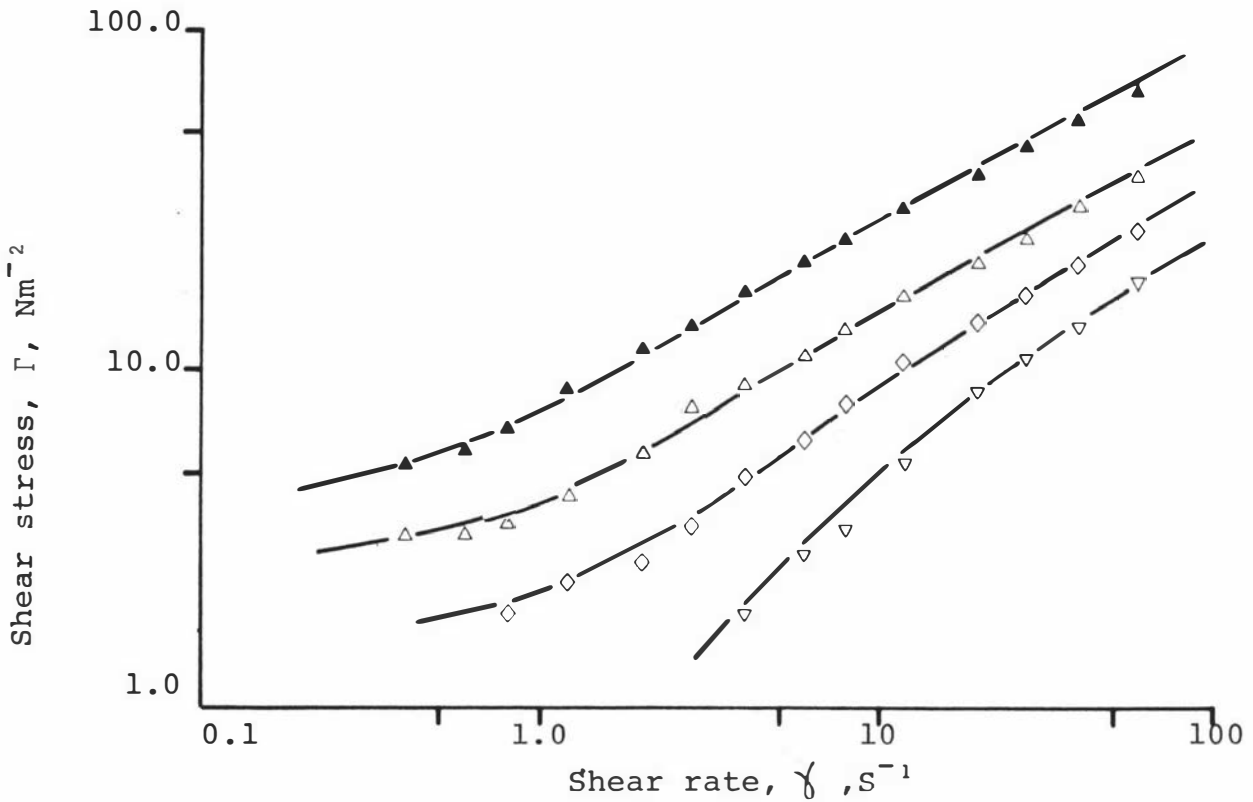

Figure I.22 Plots of the log of the shear stress as a function of the shear rate for Gamut starch pastes (7.0%) prepared by varying pasting temperature, at a constant heating time of 1h.

▲ 95.0°C △ 92.5°C ◇ 90.0°C ▽ 87.5°C

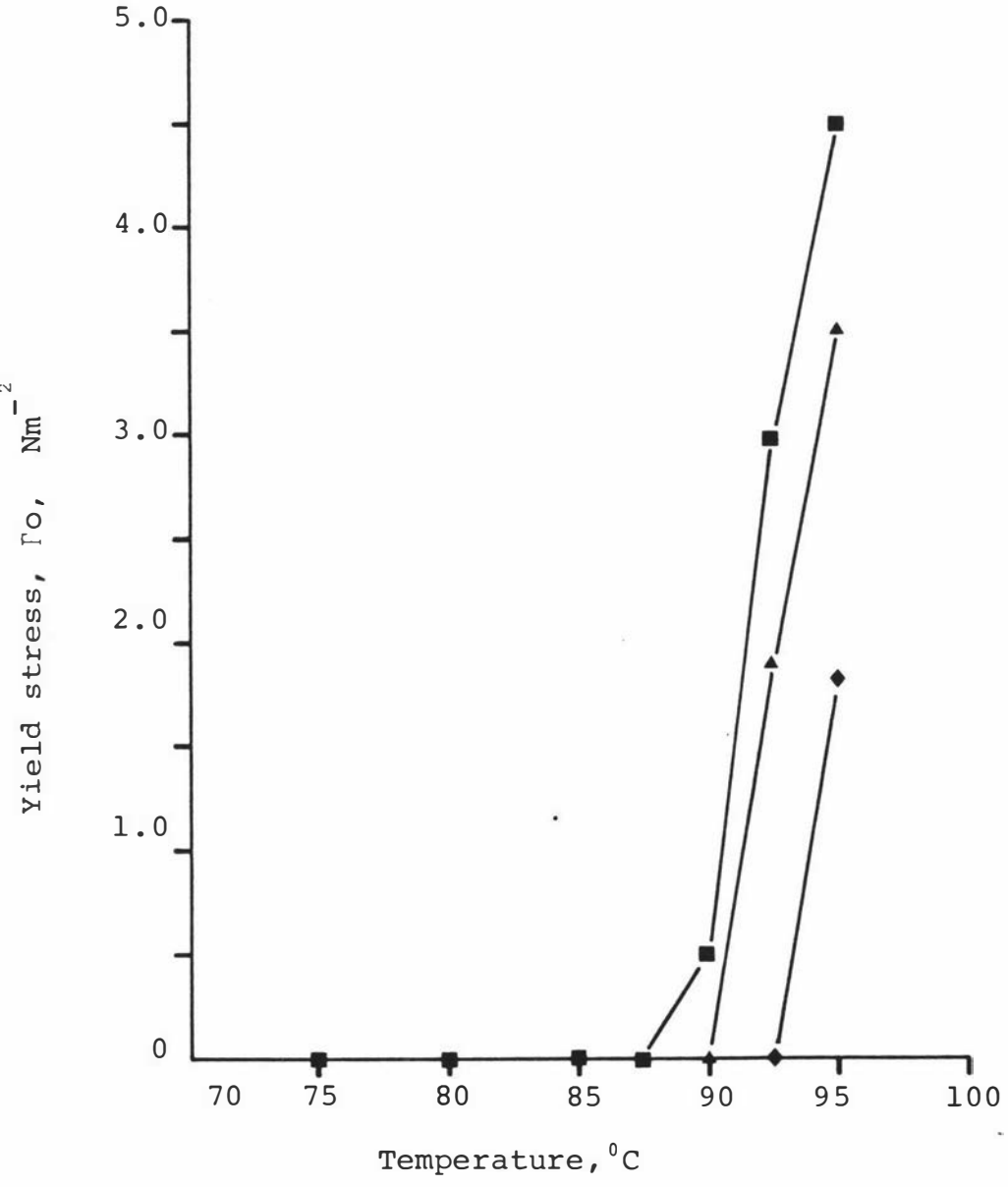

Figure I.23 Plots of the yield stress of pastes prepared from Gamut wheat starch as a function of the pasting temperature.

■ 7.00% ▲ 6.0% ◆ 5.0%

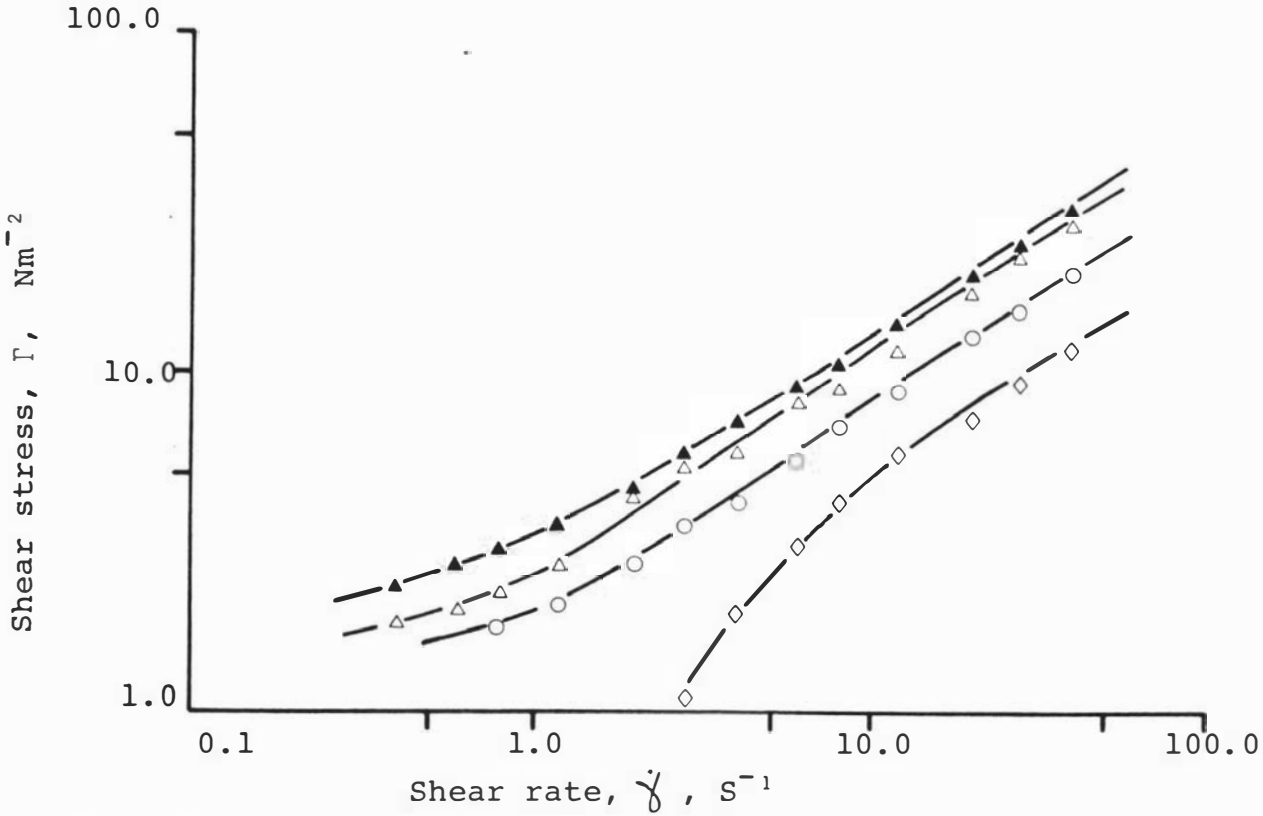

Figure I.24 Plots of the shear stress as a function of the log of the shear rate for Hilgendorf starch pastes (5.00%) prepared by varying pasting time at a constant pasting temperature of 95.0°C.

▲ 60 min △ 30 min ○ 20 min ◇ 10 min

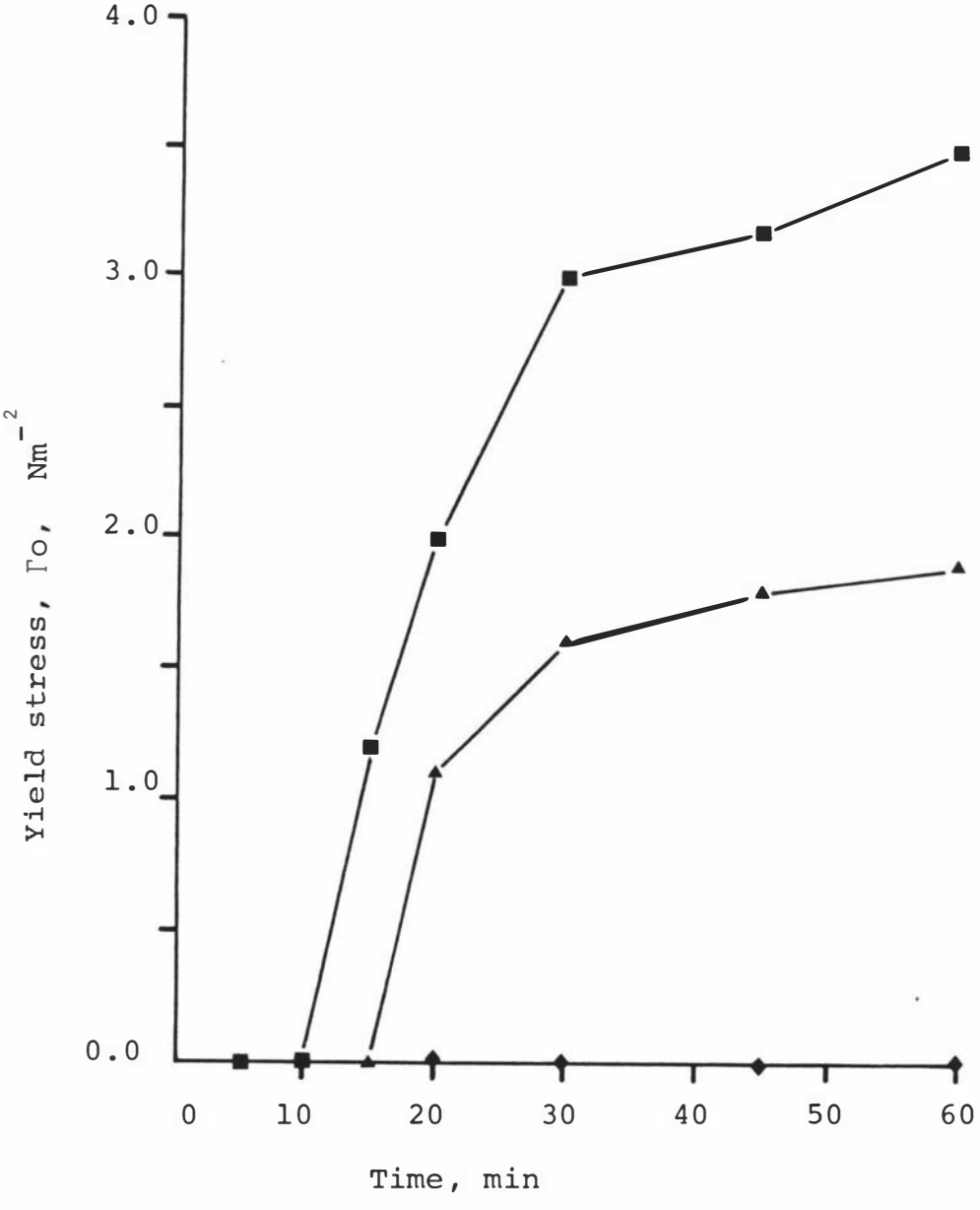

Figure I.25 Plots of the yield stress of pastes prepared from Hilgendorf wheat starch as a function of the pasting time.

■ 5.77% ▲ 5.00% ◆ 4.00%

I.6.2.2.2. Effect of paste preparation condition

The effect of varying pasting temperature, at a constant heating time of 1 hour, on the flow curves of pastes is demonstrated in Figure I.22 for Gamut wheat variety. The variation in the yield stress values with pasting temperature is shown in Figure I.23 for several concentrations of the Gamut wheat starch. The results show that the yield stress value decreases when the pasting temperature is reduced. When the pasting temperature is less than 90 ^{0}C, a stage is reached where yield stresses are no longer apparent (see Figure I.22). A similar pattern of results was obtained for all the other wheat starches examined. Figure I.24 shows the effect of varying pasting time, at a constant temperature of 95.0 ^{0}C, on the flow curves of pastes made from the Hilgendorf wheat starch. The variation in the yield stress values of pastes with pasting time is shown in Figure I.25 for several concentrations of the Hilgendorf wheat starch. The results show that the yield stress is about constant after a pasting time of 20 minutes. When the pasting time is less than 10 minutes, a point is reached where yield stresses are no longer apparent. Similar results were obtained with other wheat varieties.

I.6.3. Total number of particles per gram of sample and the size distribution of starch granules

Figures I.26a-f show plots of relative weight-diameter distribution curves for the various wheat starches studied. The bimodal size distributions described by other investigators (13, 14) are clearly evident. The corresponding graphs of cumulative mass fractions for granules less than a given hydrated particle diameter are shown in Appendix Ie. The results in Figures I.26a-f (and in Appendix Ie) indicate there are few granules with diameters between 9 and 13 μm, the minimum number generally

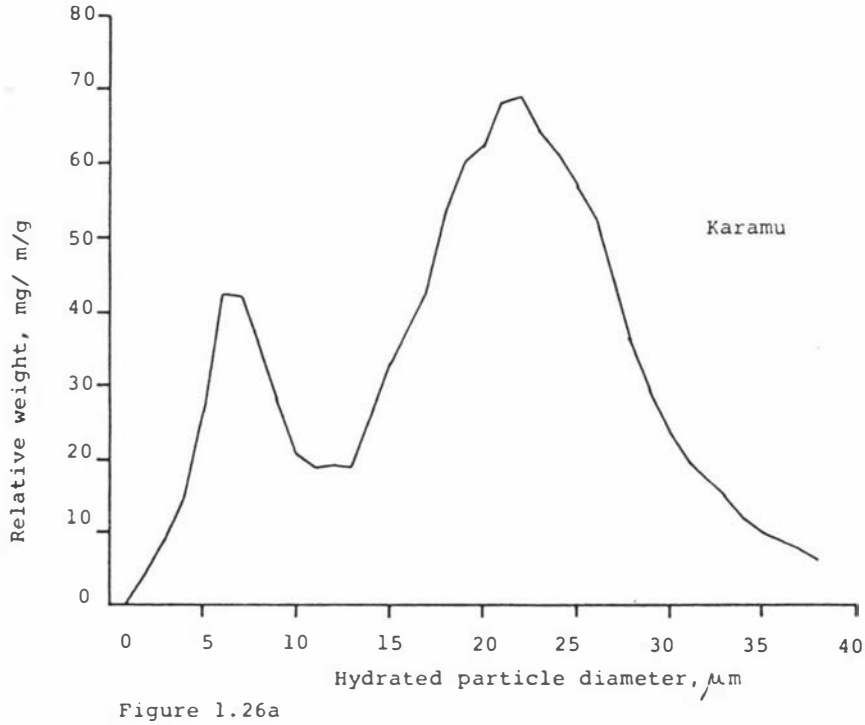

Figure 1.26a

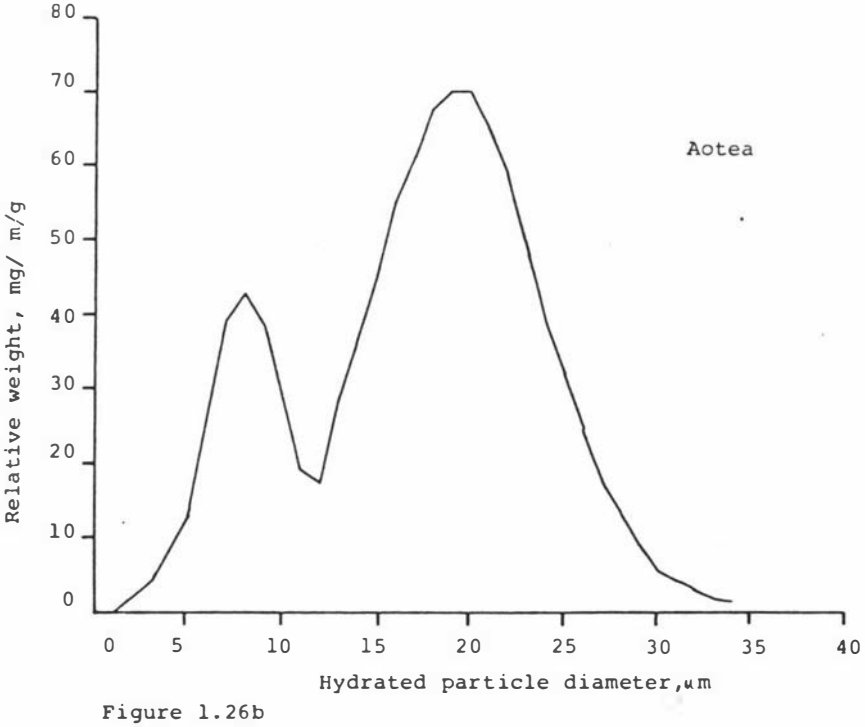

Figure 1.26b

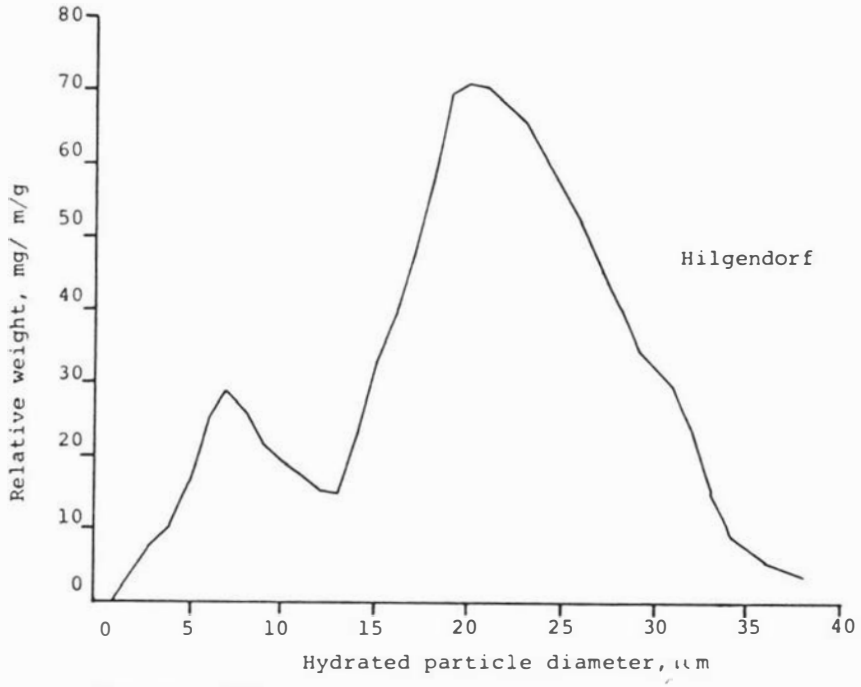

Figure 1.26c

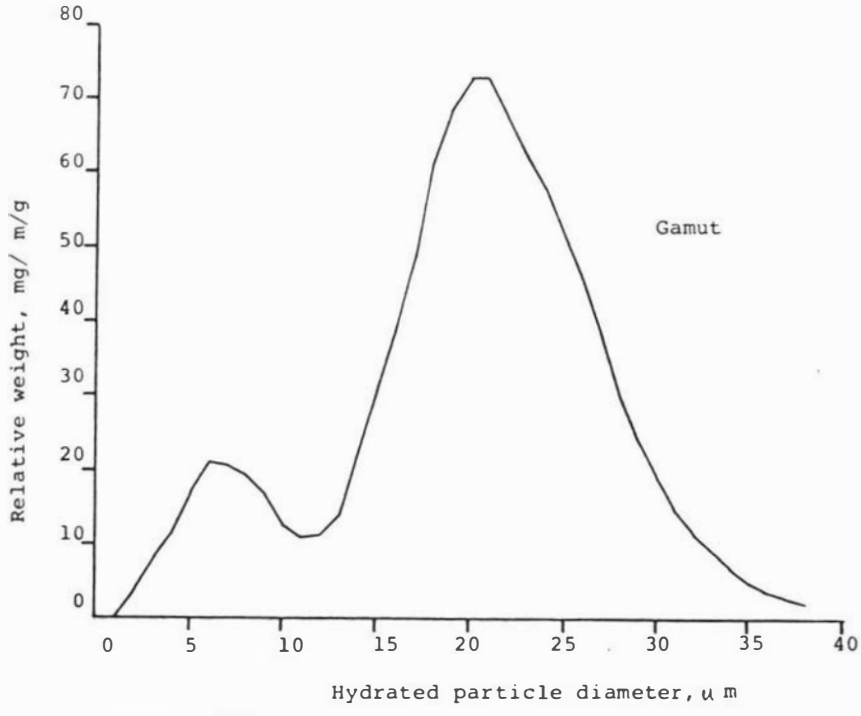

Figure 1.26d

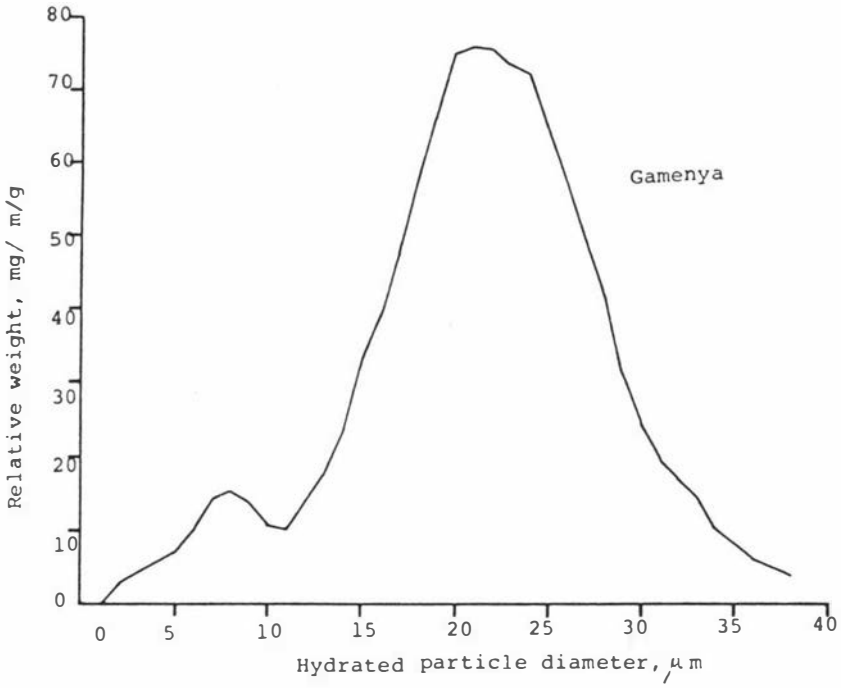

Figure 1.26e

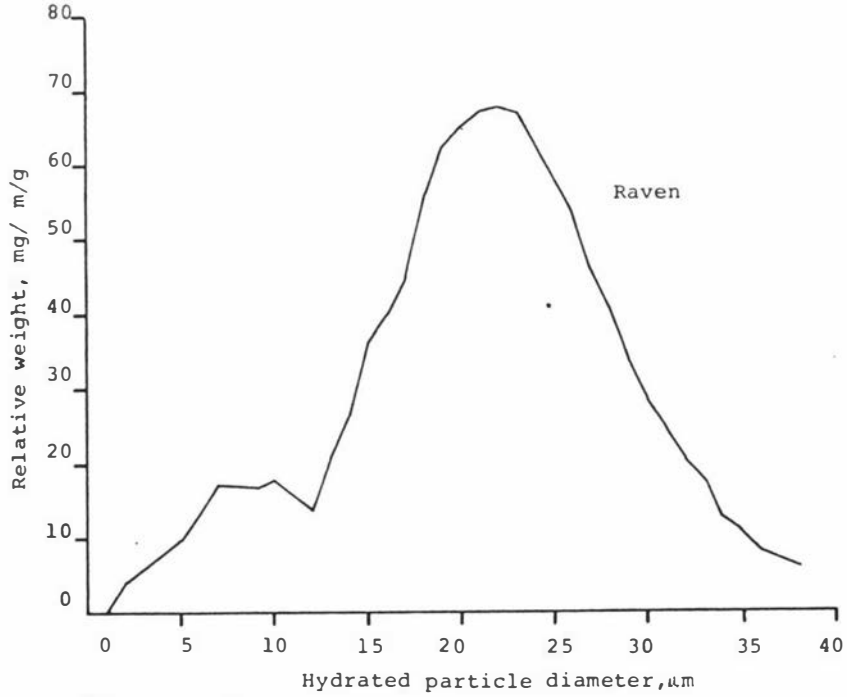

Figure 1.26f

occurs at 12 μm. Hence the figure of 12 μm hydrated diameter has been used to classify granules as either small or large. The percentages by weight of granules under 12 μm hydrated diameter for various wheat starches are tabulated in Table I.4. This percentage varies quite considerably between the various starches examined. These results are in general in agreement with other recent data (11, 20) giving the percentage by weight of small granules in a starch sample. The Australian wheat starches have consistently lower percentages by weight of small granules than New Zealand starches, this is in accordance with the results of Meredith et al (13). The total number of granules per gram of starch and the number of large granules per gram of starch, both determined from the relative number per gram - diameter distribution curves (Figures I.27 a-f) are presented in Table I.5. The values for total number of granules per gram of starch are in the range reported by other investigators (23). The results in Table I.5 show that the total number of granules differ considerably between the Australian and New Zealand wheat starches. Australian wheat starches contain higher number fraction of large granules.

Table I.4 Percentage by weight of small granules in the various wheat starches.

Wheat variety used to prepare starch	% weight (<12 μm)
Karamu	26.0
Aotea	24.4
Hilgendorf	16.9
Gamut	15.0
Gamenya	10.0
Raven	12.8

Table I.5 Total number of granules per gram of sample and number of large granules per gram of sample in the various wheat starches.

Wheat variety used to prepare starch	Number of large granules >12 μm per gram of sample	Total number of granules per gram of sample	Number fraction of large granules P
Karamu	2.49×10^8	3.32×10^9	0.075
Aotea	2.87×10^8	3.01×10^9	0.095
Hilgendorf	2.64×10^8	2.52×10^9	0.105
Gamut	2.77×10^8	2.41×10^9	0.115
Gamenya	3.04×10^8	1.44×10^9	0.211
Raven	2.78×10^8	1.86×10^9	0.145

I.6.4 Swelling capacity of, and the exudate from, gelatinised granules

I.6.4.1 Swelling capacity

I.6.4.1.1. Effect of wheat variety

Table I.6 give results showing that the Australian wheat starches have consistently higher swelling capacities than the New Zealand varieties. All the results are about 20% higher than the values obtained using the standard procedure of Schoch (83). Evans and Haisman (68) have described an alternative method of obtaining the swelling capacities of starches. In their method, different concentrations of starch pastes are allowed to settle out under gravity and the levels of the sedimenting interface are recorded at given time intervals using a TV camera.

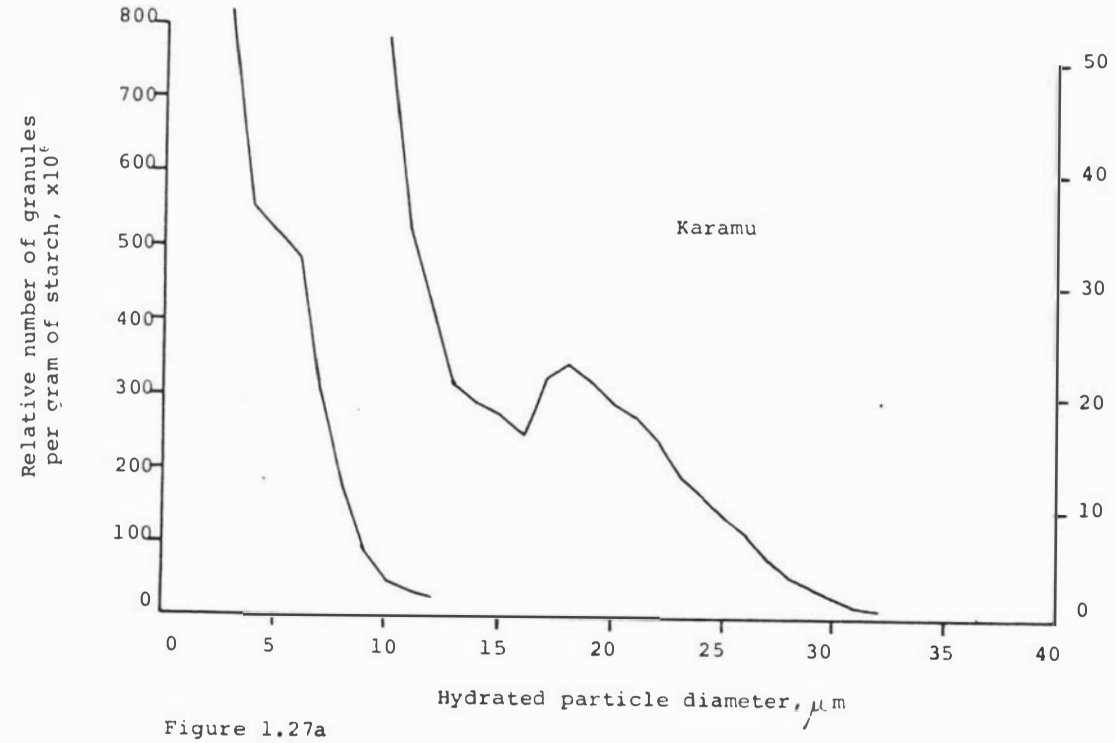

Figure 1.27a

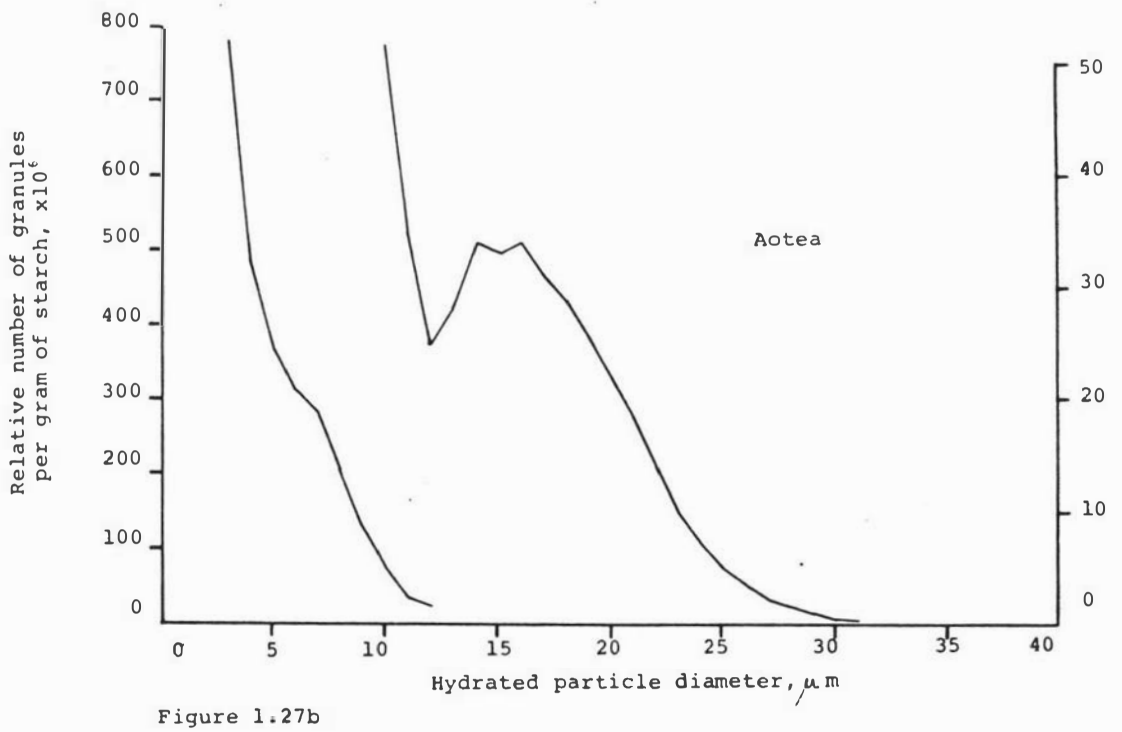

Figure 1.27b

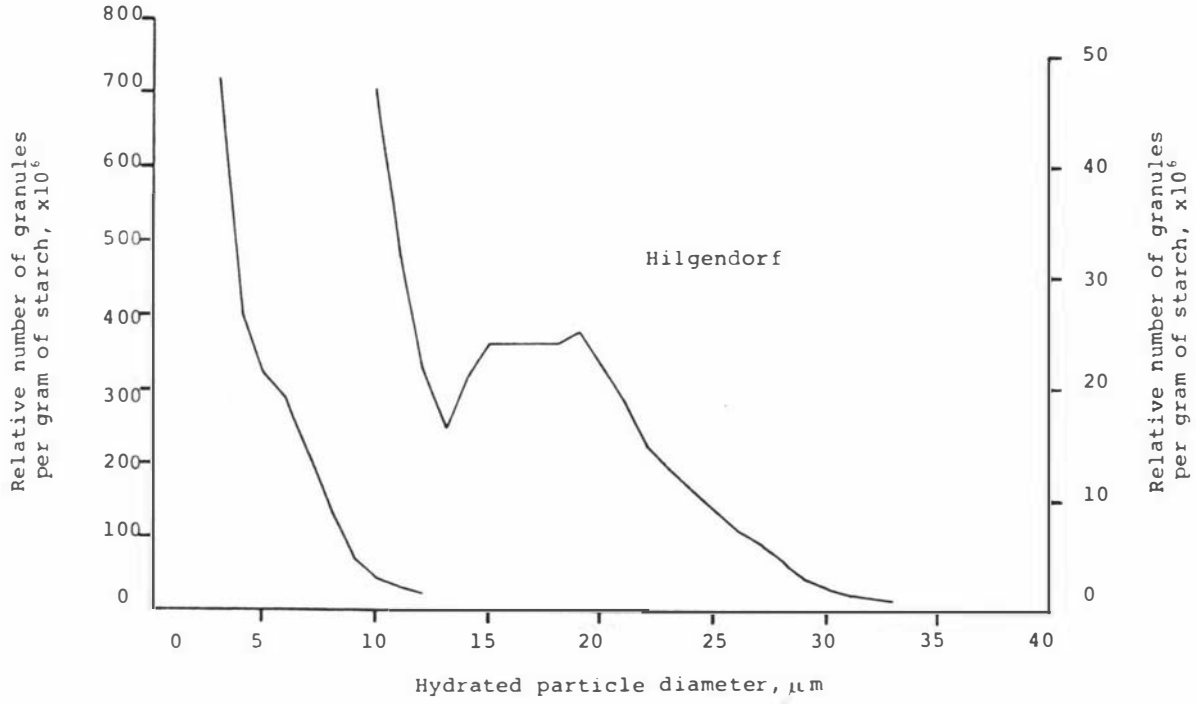

Figure 1.27c

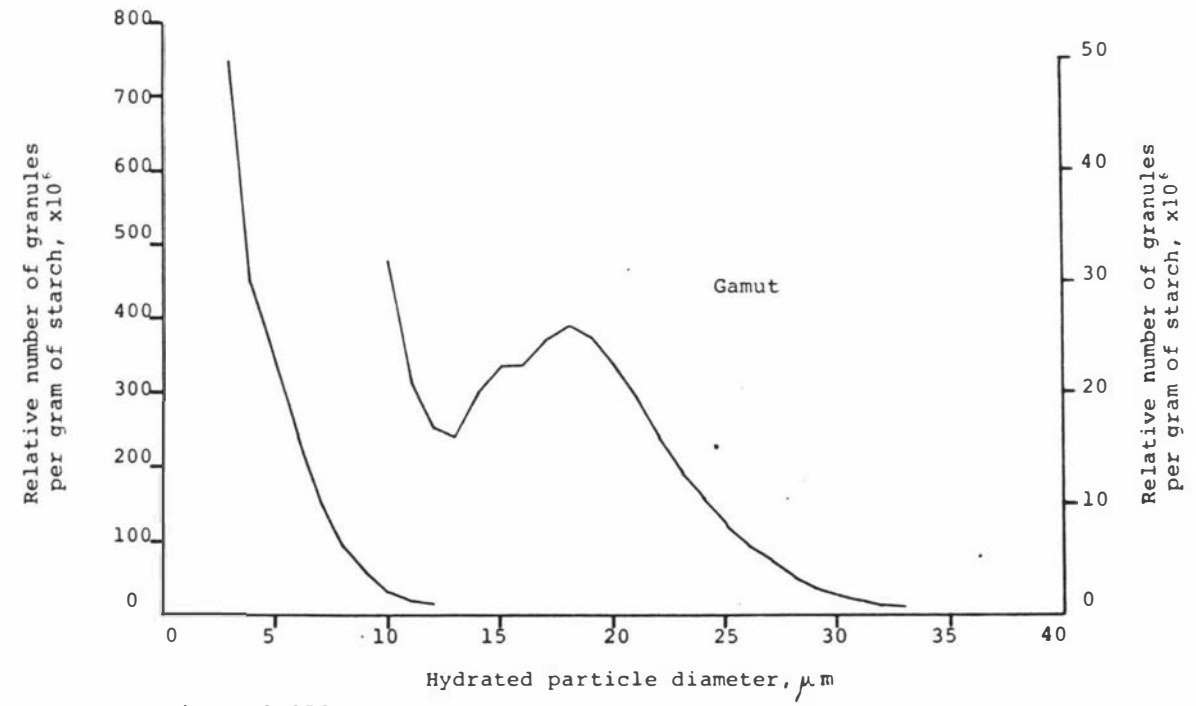

Figure 1.27d

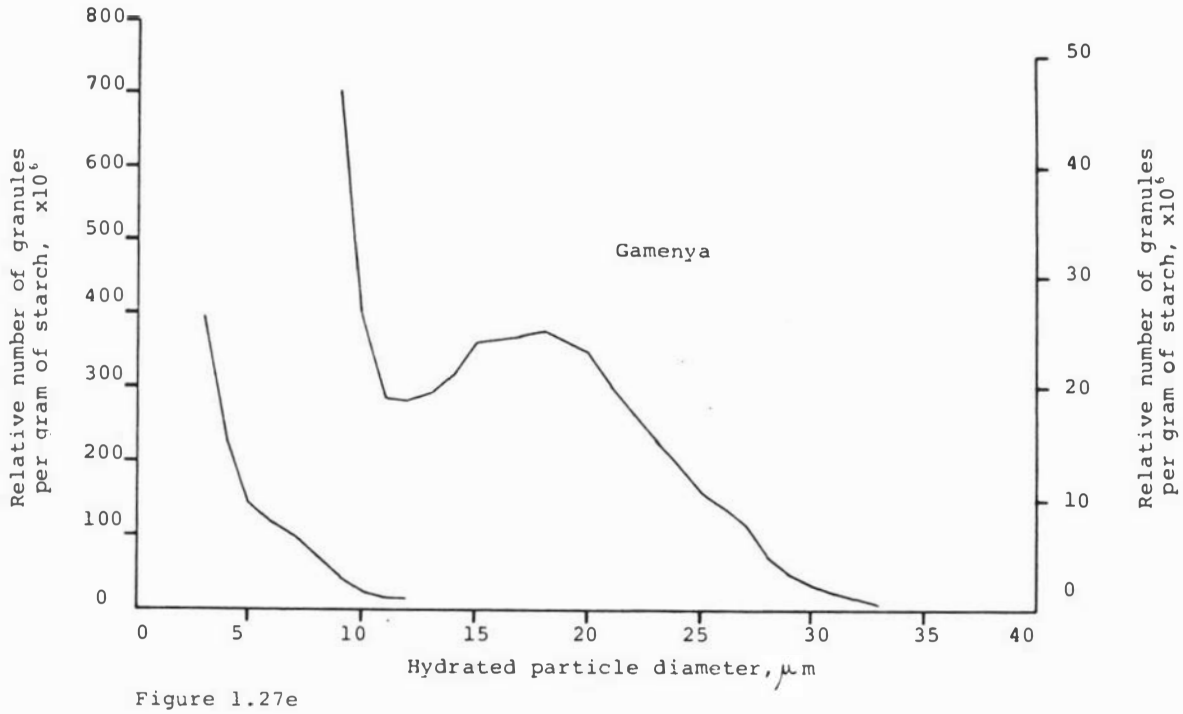

Figure 1.27e

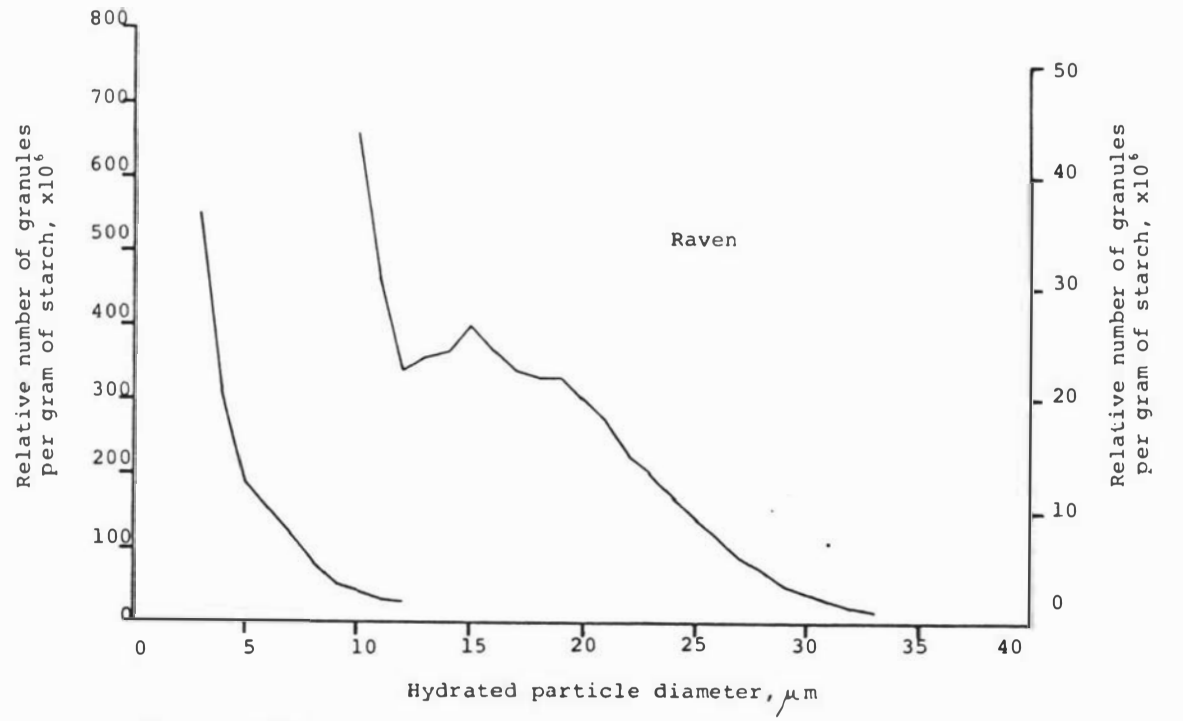

Figure 1.27f

The minimum concentration of starch at which the initial rate of sedimentation is less than $0.1 mm hr^{-1}$ is found, and so the swelling capacity. Since wheat starches contain small granules, the method is unsuitable for the present study. However the fact is stressed that an absolute method of determining the swelling capacity of wheat starch is not available, and different procedures will give different results.

Table I.6 Swelling capacities of the various wheat starches at $95.0^{0}C/1h$.

Wheat variety used to prepare starch	Swelling capacity ml/g $\pm$ 5%
Karamu	25.50
Aotea	26.25
Hilgendorf	27.30
Gamut	28.00
Gamenya	34.30
Raven	35.50

I.6.4.1.2. Effect of paste preparation condition

Figure I.28 shows the variation in the swelling capacity of Gamut wheat starch as a function of the pasting temperature. The swelling capacity increases rapidly above $85.0^{0}C$. The other wheat starches studied show the same trend. Figure I.29 shows the swelling capacity of Hilgendorf wheat starch as a function of the pasting time. The swelling capacity increases markedly for the first 10 minutes and then remains about constant thereafter. A

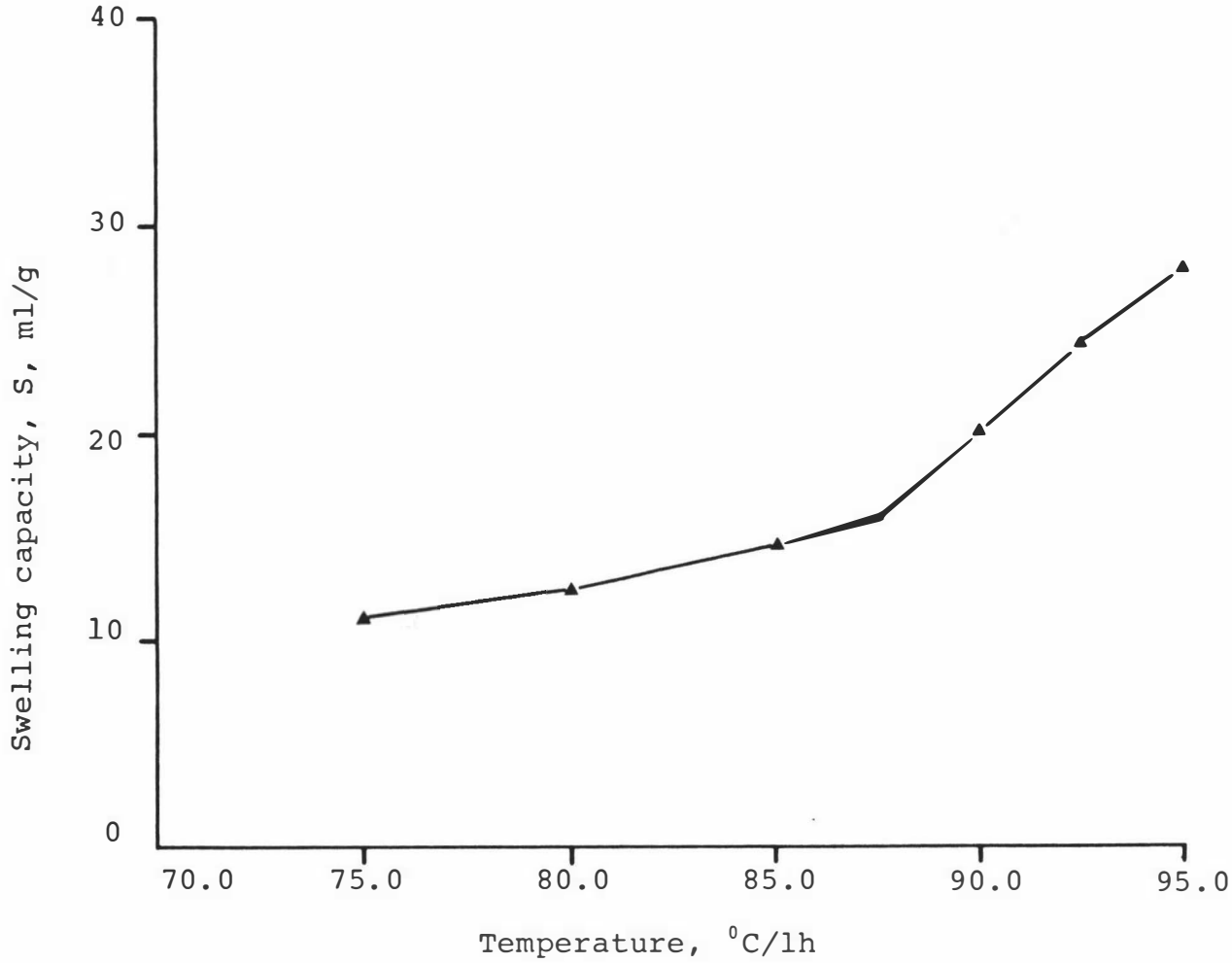

Figure I.28 Plot of the swelling capacity of Gamut wheat starch as a function of the pasting temperature, at a constant pasting time of 1h.

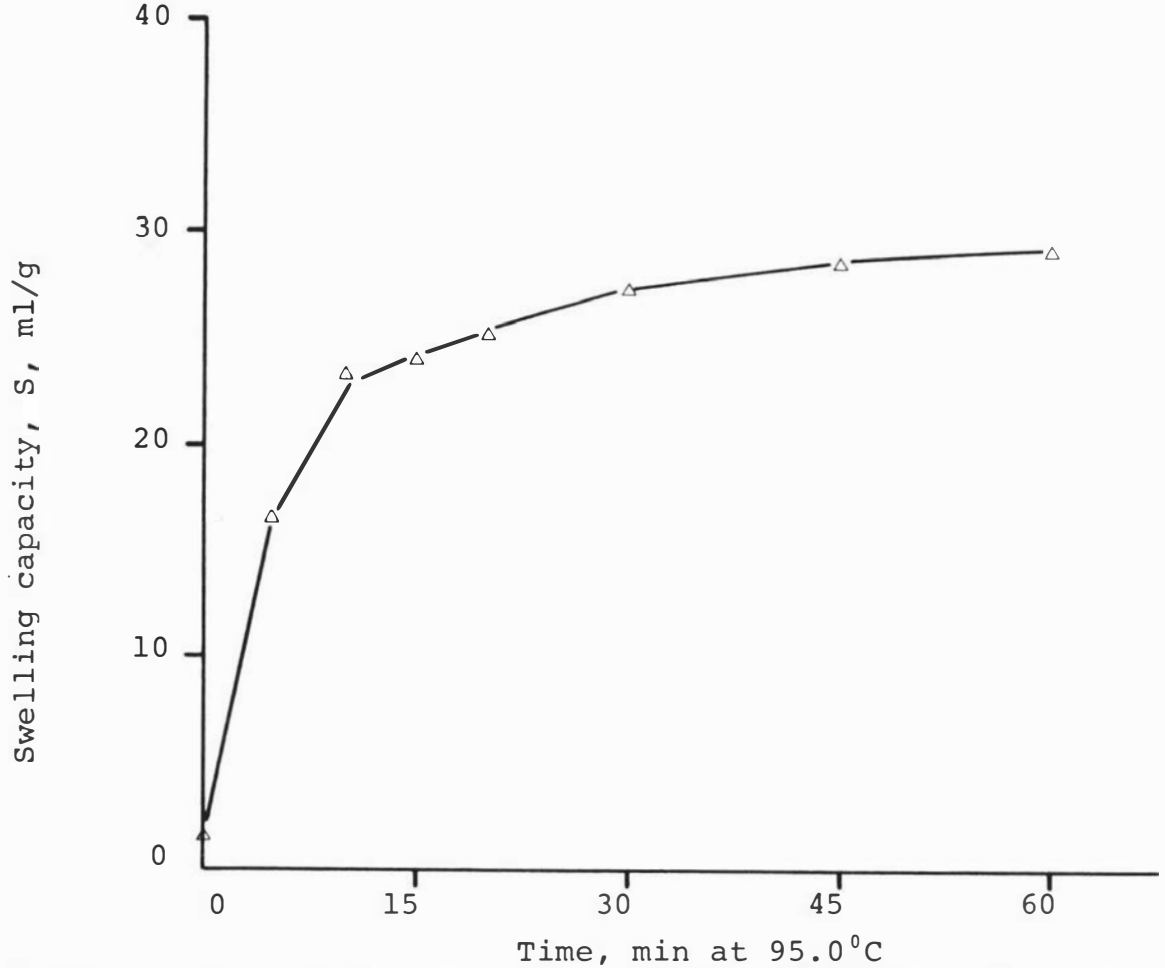

Figure I.29 Plot of the swelling capacity of Hilgendorf wheat starch as a function of the pasting time, at a constant pasting temperature of 95.0°C.

similar pattern of variation was observed for the other wheat starches examined. The influence of the extent of starch damage on the swelling capacity of starch is demonstrated in Table I.7. As the extent of starch damage increases, swelling capacity decreases appreciably. Table I.7 also shows that formation of pastes in the Amylograph reduces the value of the swelling capacity. Pastes formed in the Amylograph receive a slightly greater heat treatment than pastes formed by the standard procedure described herein, but the reduction in swelling capacity would not be expected on the basis of this difference. The Amylograph also subjects samples to high shearing forces, this results in granule disintegration (16) and hence is probably the cause of the reduction in swelling capacity shown in Table I.7.

Table I.7 Swelling capacities of various wheat starches formed in the Amylograph and of samples containing damaged granules.

Wheat variety used to prepare starch	Swelling capacity ml/g
Karamu[1]	25.50
Karamu[2]	16.50
Aotea[1]	26.25
Aotea[2]	17.65
Gamenya[1]	34.30
Gamenya[2]	21.26
Raven[1]	35.50
Raven[2]	22.85
Aotea (10% damaged)[1]	24.00
Aotea (25% damaged)[1]	18.50
Gamenya (10% damaged)[1]	30.80

[1]) the paste was formed by standard method
[2]) the paste was formed in the Amylograph

I.6.4.1.3. Effect of fractionation of starch particles according to size

Table I.8 gives the swelling capacities of fractions of Karamu and Raven wheat starches with narrow particle size ranges. The swelling capacities of unfractionated starch samples of Karamu and Raven wheat varieties are included for comparison. The values for the swelling capacity of the unfractionated starch are similar to the values for the large granules; this would be expected since large granules comprise the bulk of the weight of the sample (see Table I.4). However, the swelling capacities of pastes does not simply obey the following relationship:-

$$S = \sum_{i=1}^{i} W_i \, S_i$$

where S is the swelling capacity of a starch sample, W_i is the weight fraction of size fraction i and S_i is the swelling capacity of size fraction i . This is because in an unfractionated starch sample,the large granules pack so as to give a significant void volume (68). The voids can be occupied by small particles without markedly increasing the volume occupied by the total bed of granules. Thus the swelling capacities of starches reflect granule size distributions and samples with greater fractions of small granules swell less. However Table I.8 also shows that within the same size range, the swelling capacities of Raven wheat starch fractions are always higher than Karamu, hence factors other than size distribution influence results.

Table I.8 Swelling capacities of the various starch fraction with narrow size ranges of Karamu and Raven wheat starches.

Starch	Particle diameter μm	Swelling capacity ml/g	
		Karamu	Raven
Unfractionated		25.50	35.50
Fractionated	19.5	23.65	30.55
	14.7	23.90	31.60
	7.1	28.00	35.40
	4.3	34.40	41.55
	3.1	40.90	56.70

I.6.4.2. Exudate

I.6.4.2.1. Effect of wheat variety

Table I.9 gives the percentage of starch exuding from gelatinised granules of the various wheat starches studied. The results show that there is no definite trend in the variation between the Australian and New Zealand wheat starches.

I.6.4.2.2. Effect of paste preparation condition

Figure I.30 shows the variation in the percentage of starch released from gelatinised granules of Gamut wheat variety as a function of the pasting temperature. The polymeric material exuding from gelatinised granules increases markedly above 87.5^{0}C. The other wheat varieties studied

Table I.9 Percentages of exudate from gelatinised granules of the various wheat starches.

Wheat variety used to prepare starch	Percentage exudate, % ± 5%
Karamu	37.20
Aotea	35.20
Hilgendorf	30.78
Gamut	35.24
Gamenya	35.80
Raven	42.61

Table I.10 Percentages of exudate from gelatinised granules of various wheat starches formed in the Amylograph and of samples containing damaged particles.

Wheat variety used to prepare starch	Percentage exudate, % ± 5%
Karamu[1]	37.20
Karamu[2]	42.26
Aotea [1]	35.20
Aotea [2]	44.97
Gamenya[1]	35.80
Gamenya[2]	32.87
Raven[1]	42.61
Raven[2]	48.75
Aotea (10% starch damage)[1]	45.90
Aotea (25% starch damage)[1]	60.20
Gamenya (10% starch damage)[1]	46.50

[1]) pastes were formed by the standard method.

[2]) pastes were formed in the Amylograph.

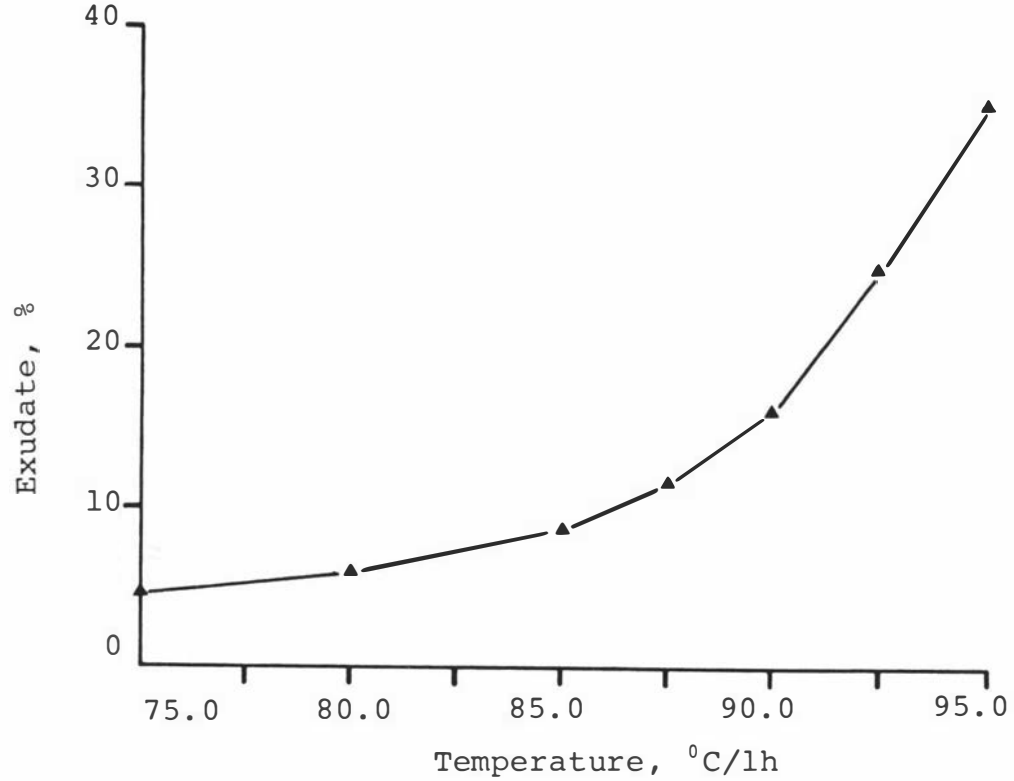

Figure I.30 Plot of the percentage of exudate from gelatinised granules of Gamut wheat starch as a function of the pasting temperature, at a constant heating time of 1h.

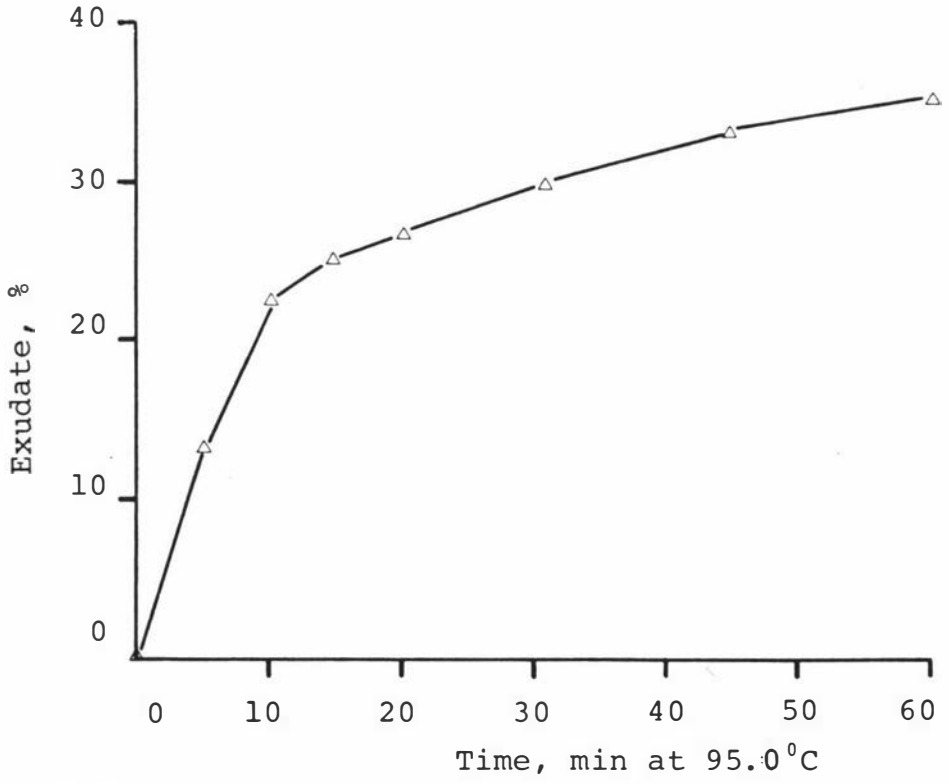

Figure I.31 Plot of the percentage of exudate from gelatinised granules of Hilgendorf wheat starch as a function of the pasting time, at a constant pasting temperature of 95.0°C.

show the same trend. Figure I.31 shows the variation in the percentage of starch released from gelatinised granules of Hilgendorf wheat variety as a function of the pasting time. The polymeric material exuding from gelatinised granules increases for the first 10 minutes and then remains about constant thereafter. A similar pattern of variation was observed for the other wheat starches examined.

The influence of the extent of starch damage on the quantity of starch exuding from gelatinised granules is demonstrated in Table I.10. As the extent of starch damage increases, the percentage of starch released from gelatinised granules increases appreciably. Table I.10 also shows that the formation of pastes in the Amylograph increases the amount of polymeric material released with the aqueous medium. This may possibly be due to the high shearing forces encountered in the Amylograph causing granule disintegration.

I.6.4.2.3. Effect of fractionation of starch particles according to size

Table I.11 shows that the percentages of exudate from unfractionated Karamu and Raven samples are similar to the corresponding values for large granules, this would be expected since large granules comprise the major weight fraction of starch. The results also show that the amount of starch released from small granules is consistently higher than from large granules, this is contrary to results obtained by some other investigators (16, 98). One factor which may account for this discrepancy is the amount of damaged granules present in starch samples. This damage normally occurs to large granules (89). In the present study, the extraction procedure used does not cause starch damage. If the samples studied by other investigators contained damaged granules, this would explain the difference.

Another possible reason for the discrepancy between results relates to the fact that small granules are more prone to disintegration than large granules above about 90^{0}C (16), and hence yield higher percentage of exudate in this range. The results in Table I.11 apply to pastes that have been formed at 95.0^{0}C/1h, this has a greater heat treatment than that used by investigators who found large granules to release more exudate. Table I.11 also shows that within the same particle size range, the exudate from Raven wheat starch fractions is greater than from Karamu starch fractions.

All the results obtained in this section of the present study show that the more a starch sample swells, the more polymeric material is released from the gelatinised granules.

Table I.11 Percentage of starch exuding from gelatinised granules of the various starch fractions with narrow size ranges of Karamu and Raven wheat starches.

Starch	Particle diameter µm	Starch exuding from gelatinised granules % g/g	
		Karamu	Raven
Unfractionated		37.20	42.60
Fractionated	19.5	36.20	38.40
	14.7	39.10	41.60
	7.1	44.70	45.70
	4.3	44.90	53.70
	3.1	43.20	52.90

I.6.5. Structural features of starch pastes characterised by different dynamic viscosities and rigidities

Table I.12 gives the characteristics of pastes formed from the various wheat starches that may be related to their varying rheological behaviour. The data suggests that pastes with relatively high dynamic viscosities and rigidities are formed from starches with higher swelling capacities and number fractions of large granules. Table I.12 also gives the characteristics of pastes as influenced by preparation conditions and the presence of 'damaged'granules. The results indicate that decreases in swelling capacities are associated with reductions in dynamic viscosity and rigidity and vice versa, this is consistent with the trend in the variation of rheological measurements with starch source. The data in Table I.12 suggests that variations in the quantity of starch exuding from swollen granules do not account for variations in paste behaviour under the conditions reported in this table.

I.6.6. Structural features of starch pastes characterised by different steady shear properties

Table I.13 gives the characteristics of pastes from the various wheat starches that may account for their varying steady shear properties. The data suggests that pastes with relatively high apparent viscosities and yield stresses are formed from starches with higher swelling capacities. Table I.13 also gives the characteristics of pastes as influenced by the different temperature/time treatments during paste preparation. The results indicate that decreases in swelling capacity are associated with reduction in both the apparent viscosity and the yield stress and vice versa, this is consistent with the trend in the variation of steady slow property with source of starch.

Table I.12 Dynamic viscosities and rigidities at representative frequencies and other characteristics of pastes made from different wheat starches under a range of conditions.

Wheat Variety Used to Prepare Starch	Starch conc. g/ml	Temp time Treat-ment °C/h	Swelling Capacity ml/g	Number Fraction of Large Granules	Starch Exu-date %g/g	$\omega = 0.05$ rads^{-1}		$\omega = 0.10$ rads^{-1}		$\omega = 0.50$ rads^{-1}		$\omega = 1.00$ rads^{-1}	
						η' Nsm^{-2}	G' Nm^{-2}	η' Nsm^{-2}	G' Nm^{-2}	η' Nsm^{-2}	G' Nm^{-2}	η' Nsm^{-2}	G' Nm^{-2}
Karamu	0.0480	95.0/1.0	25.50	0.0750	37.20	2.12	0.10	1.42	0.12	0.64	0.19	0.50	0.30
	0.0525	95.0/1.0	25.50	0.0750	37.20	4.70	0.39	3.30	0.48	1.35	0.72	1.00	0.87
	0.0571	95.0/1.0	25.50	0.0750	37.20	9.00	0.70	5.80	0.87	2.50	1.40	1.90	1.70
	0.0616	95.0/1.0	25.50	0.0750	37.20	18.00	2.00	11.20	2.47	5.00	3.90	3.80	4.90
	0.0641	95.0/1.0[1]	16.50	0.0750	42.26	3.30	0.30	1.90	0.33	0.73	0.48	0.54	0.62
Aotea	0.0433	95.0/1.0	26.25	0.0953	35.50	1.44	0.04	0.87	0.05	0.33	0.10	0.27	0.14
	0.0480	95.0/1.0	26.25	0.0953	35.50	2.85	0.14	2.00	0.16	0.80	0.28	0.74	0.38
	0.0525	95.0/1.0	26.25	0.0953	35.50	5.40	0.23	3.35	0.28	1.42	0.60	1.10	0.85
	0.0571	95.0/1.0	26.25	0.0953	35.50	7.40	0.58	4.85	0.72	2.17	1.20	1.62	1.60
	0.0616	95.0/1.0	26.25	0.0953	35.50	12.50	1.30	7.80	1.52	3.50	2.35	2.62	3.15
	0.0480	95.0/0.5	23.21	0.0953	26.50	1.90	0.07	1.25	0.09	0.50	0.12	0.35	0.15
	0.0525	97.5/0.5	29.16	0.0593	45.00	12.50	1.90	7.80	2.10	2.75	2.85	1.85	3.40
	0.0681	95.0/1.0[1]	17.63	0.0953	44.97	7.00	0.44	4.15	0.56	1.55	1.02	1.15	1.29
	0.0723	95.0/1.0[1]	17.65	0.0953	44.97	8.40	0.75	5.02	0.96	1.75	1.88	1.28	2.35
	0.0571	95.0/1.0	23.96	0.0953	45.90	4.25	0.30	3.20	0.40	1.65	0.57	1.25	0.74
	0.0616	95.0/1.0	23.96	0.0953	45.90	0.80	0.68	5.30	0.78	2.55	1.10	1.85	1.35

cont/...

Hilgen-dorf	0.0387	95.0/1.0	27.32	0.1048	30.78	3.80	0.95	2.45	0.96	0.95	1.22	0.76	1.43
	0.0433	95.0/1.0	27.32	0.1048	30.78	7.00	1.55	4.00	1.60	1.80	2.04	1.50	2.40
	0.0480	95.0/1.0	27.32	0.1048	30.78	10.00	2.50	6.70	2.55	2.30	3.70	1.70	4.70
Gamut	0.0387	95.0/1.0	28.02	0.1017	35.23	1.30	0.08	0.79	0.10	0.30	0.15	0.23	0.19
	0.0433	95.0/1.0	28.02	0.1017	35.23	4.90	0.44	2.80	0.52	1.13	0.77	0.86	1.00
	0.0457	95.0/1.0	28.02	0.1017	35.23	7.70	1.00	4.70	1.13	2.10	1.80	1.60	2.40
	0.0480	95.0/1.0	28.02	0.1017	35.23	14.00	1.70	8.50	2.20	3.00	3.30	2.25	0.50
Gamenya	0.0293	95.0/1.0	34.30	0.2111	37.50	2.00	3.60	1.10	0.38	0.40	0.47	0.29	0.55
	0.0340	95.0/1.0	34.30	0.2111	37.50	4.00	1.20	2.10	1.30	0.80	1.40	0.47	1.63
	0.0363	95.0/1.0	34.30	0.2111	37.50	6.20	2.40	3.95	2.80	1.23	3.00	0.82	3.20
	0.0387	95.0/1.0	34.30	0.2111	37.50	10.70	4.40	6.40	4.60	1.70	4.70	1.10	4.90
	0.0277	95.0/0.5	32.34	0.2111	33.85	1.10	0.12	0.70	0.20	0.38	0.28	0.20	0.31
	0.0293	95.0/0.5	32.34	0.2111	32.85	1.15	0.19	0.73	0.21	0.40	0.30	0.23	0.37
	0.0343	95.0/0.5	32.34	0.2111	33.85	4.17	1.15	2.30	1.17	0.80	1.20	0.70	1.22
	0.0387	92.5/0.5	32.32	0.2111	26.55	8.50	3.05	5.00	3.20	1.60	3.30	1.00	3.60
	0.0375	95.0/0.5	32.34	0.2111	33.85	4.70	2.50	3.40	2.55	1.40	2.70	1.00	2.90
	0.0480	92.5/1.0	32.33	0.2111	26.55	25.00	8.50	14.50	9.70	5.60	13.0	4.00	16.00
	0.0480	95.0/0.5	28.11	0.2111	21.35	21.00	7.00	11.00	8.80	4.20	11.50	3.60	14.00
	0.0520	95.0/1.0[1]	21.26	0.2111	32.87	10.00	3.50	5.70	3.66	1.94	4.20	1.40	4.60
	0.0576	95.0/1.0[1]	21.26	0.2111	32.87	15.20	4.18	9.70	4.60	3.26	5.80	2.23	6.40
	0.0363[2]	95.0/1.0	30.80	0.2111	46.50	3.80	1.60	2.10	2.10	0.85	2.50	0.60	2.85
	0.0387[2]	95.0/1.0	30.80	0.2111	46.50	6.40	2.50	4.85	2.60	1.50	3.05	0.84	3.40
Raven	0.0293	95.0/1.0	35.50	0.1495	42.61	1.50	0.40	0.92	0.43	0.27	0.48	0.20	0.50
	0.0340	95.0/1.0	35.50	0.1495	42.61	5.00	1.40	3.10	1.48	0.90	1.70	0.60	1.90
	0.0387	95.0/1.0	35.50	0.1495	42.61	13.50	3.70	8.50	4.10	2.20	4.80	1.30	5.60

[1] the paste was formed in the Brabender Amylograph

[2] the sample contained 10% 'damaged' starch

Table I.13 Apparent viscosities at specified shear rates, yield stresses and other characteristics of pastes made from different wheat starches under a range of conditions.

Wheat Variety To Prepare Starch	Starch conc. g/ml	Temp/Time Treatment $^0C/h$	Swelling Capacity ml/g	Number Fraction of Large Granules	Apparent Viscosity $\dot{\gamma}=20s^{-1}$	$\dot{\gamma}=120s^{-1}$	$\dot{\gamma}=1200s^{-1}$	Yield Stress τ_0 Nm^{-2}
Karamu	0.0427	95.0/1.0	25.50	0.0750	0.07	0.05	0.03	-
	0.0471	95.0/1.0	25.50	0.0750	0.17	0.09	0.04	1.20
	0.0535	95.0/1.0	25.50	0.0750	0.31	0.17	0.06	2.00
	0.0575	95.0/1.0	25.50	0.0750	0.46	0.21	0.08	3.00
	0.0615	95.0/1.0	25.50	0.0750	0.60	0.26	0.10	4.20
	0.0661	95.0/1.0	25.50	0.0750	0.73	0.31	0.11	5.60
	0.0704	95.0/1.0	25.50	0.0750	1.20	0.36	0.15	6.50
	0.0760	95.0/1.0	25.50	0.0750	1.30	0.42	0.18	8.30
Aotea	0.0380	95.0/1.0	26.25	0.0953	0.06	0.04	0.02	-
	0.0432	95.0/1.0	26.25	0.0953	0.16	0.08	0.04	-
	0.0487	95.0/1.0	26.25	0.0953	0.22	0.13	0.06	1.10
	0.0517	95.0/1.0	26.25	0.0953	0.37	0.17	0.07	2.00
	0.0574	95.0/1.0	26.25	0.0953	0.61	0.27	0.09	3.50
	0.0958	95.0/1.0	26.25	0.0953	0.83	0.34	0.12	5.40
	0.0649	95.0/1.0	26.25	0.0953	1.05	0.50	0.16	7.00
Raven	0.0309	95.0/1.0	35.50	0.1495	0.05	0.04	0.02	0.00
	0.0324	95.0/1.0	35.50	0.1495	0.05	0.05	0.02	0.00
	0.0340	95.0/1.0	35.50	0.1495	0.07	0.06	0.03	0.00
	0.0384	95.0/1.0	35.50	0.1495	0.20	0.12	0.05	0.00
	0.0433	95.0/1.0	35.50	0.1495	0.44	0.21	0.08	0.90
	0.0464	95.0/1.0	35.50	0.1495	0.57	0.26	0.10	2.00

cont/...

Raven	0.0531	95.0/1.0	35.50	0.1495	0.82	0.41	0.13	3.60
	0.0558	95.0/1.0	35.50	0.1495	1.13	0.55	0.20	6.40
Gamut	0.0338	95.0/1.0	28.02	0.1017	0.17	0.05	0.04	0.00
	0.0390	95.0/1.0	28.02	0.1017	0.27	0.10	0.05	1.50
	0.0419	95.0/1.0	28.02	0.1017	0.38	0.15	0.06	2.00
	0.0480	95.0/1.0	28.02	0.1017	0.69	0.26	0.09	3.40
	0.0525	95.0/1.0	28.02	0.1017	0.85	0.35	0.11	4.80
	0.0584	95.0/1.0	28.02	0.1017	1.11	0.48	0.13	6.40
	0.0607	95.0/1.0	28.02	0.1017	1.40	0.55	0.15	8.20
	0.0670	95.0/1.0	28.02	0.1017	1.67	0.69	0.19	10.00
	0.0480	92.5/1.0	24.00	0.1017	0.20	0.11	0.05	0.26
	0.0480	90.0/1.0	19.30	0.1017	0.11	0.06	0.03	0.00
	0.0571	95.0/1.0	28.02	0.1017	0.78	0.48	0.13	3.50
	0.0571	92.5/1.0	24.00	0.1017	0.55	0.25	0.10	1.85
	0.0571	90.0/1.0	19.30	0.1017	0.38	0.19	0.07	0.05
	0.0610	95.0/1.0	28.03	0.1017	1.93	0.77	0.16	4.50
	0.0610	92.5/1.0	24.00	0.1017	1.04	0.46	0.15	3.00
	0.0610	90.0/1.0	19.30	0.1017	0.70	0.30	0.10	0.50
Hilgendorf	0.0398	95.0/1.0	29.00	0.1048	0.17	0.09	0.04	0.00
	0.0439	95.0/1.0	29.00	0.1048	0.28	0.14	0.06	0.82
	0.0462	95.0/1.0	29.00	0.1048	0.41	0.19	0.08	1.65
	0.0526	95.0/1.0	29.00	0.1048	0.07	0.27	0.08	2.80
	0.0569	95.0/1.0	29.00	0.1048	0.99	0.43	0.12	4.00
	0.0623	95.0/1.0	29.00	0.1048	1.50	0.56	0.12	5.30
	0.0387	95.0/1.0	29.00	0.1048	-	0.11	0.06	0.00
	0.0387	95.0/0.75	28.30	0.1048	-	0.10	0.05	0.00
	0.0480	95.0/1.0	29.00	0.1048	0.38	0.24	0.08	1.80
	0.0480	95.0/0.75	28.30	0.1048	0.35	0.20	0.07	1.60
	0.0480	95.0/0.5	27.50	0.1048	0.35	0.20	0.06	1.60
	0.0480	95.0/0.33	25.60	0.1048	0.30	0.16	0.05	1.10
	0.0550	95.0/1.0	29.00	0.1048	0.96	0.43	0.13	3.50
	0.0550	95.0/0.75	28.30	0.1048	0.86	0.41	0.12	3.20
	0.0550	95.0/0.50	27.10	0.1048	0.82	0.41	0.11	3.00
	0.0550	95.0/0.33	25.60	0.1048	0.64	0.31	0.08	2.00
	0.0550	95.0/0.25	24.20	0.1048	0.59	0.26	0.05	1.30

I.6.7. Effect of paste storage on dynamic viscosity and rigidity

Figures I.32 and I.33 show the development of dynamic rigidity at various ageing temperatures as a function of time for pastes made from Gamenya and Aotea wheat starches respectively. Figures I.34 and I.35 give the corresponding dynamic viscosity data. These results show that as temperature increases the equilibrium values reached when ageing is completed increase for dynamic viscosity but decrease for dynamic rigidity. In general, the change in the rheological properties of pastes with time is similar to that recorded for concentrated wheat starch gels (99). However there are certain differences between the ageing processes of starch pastes and gels. For example the former has a period of slow development in dynamic viscosity or rigidity which is dependent on ageing temperature, giving a sigmoidal curve.

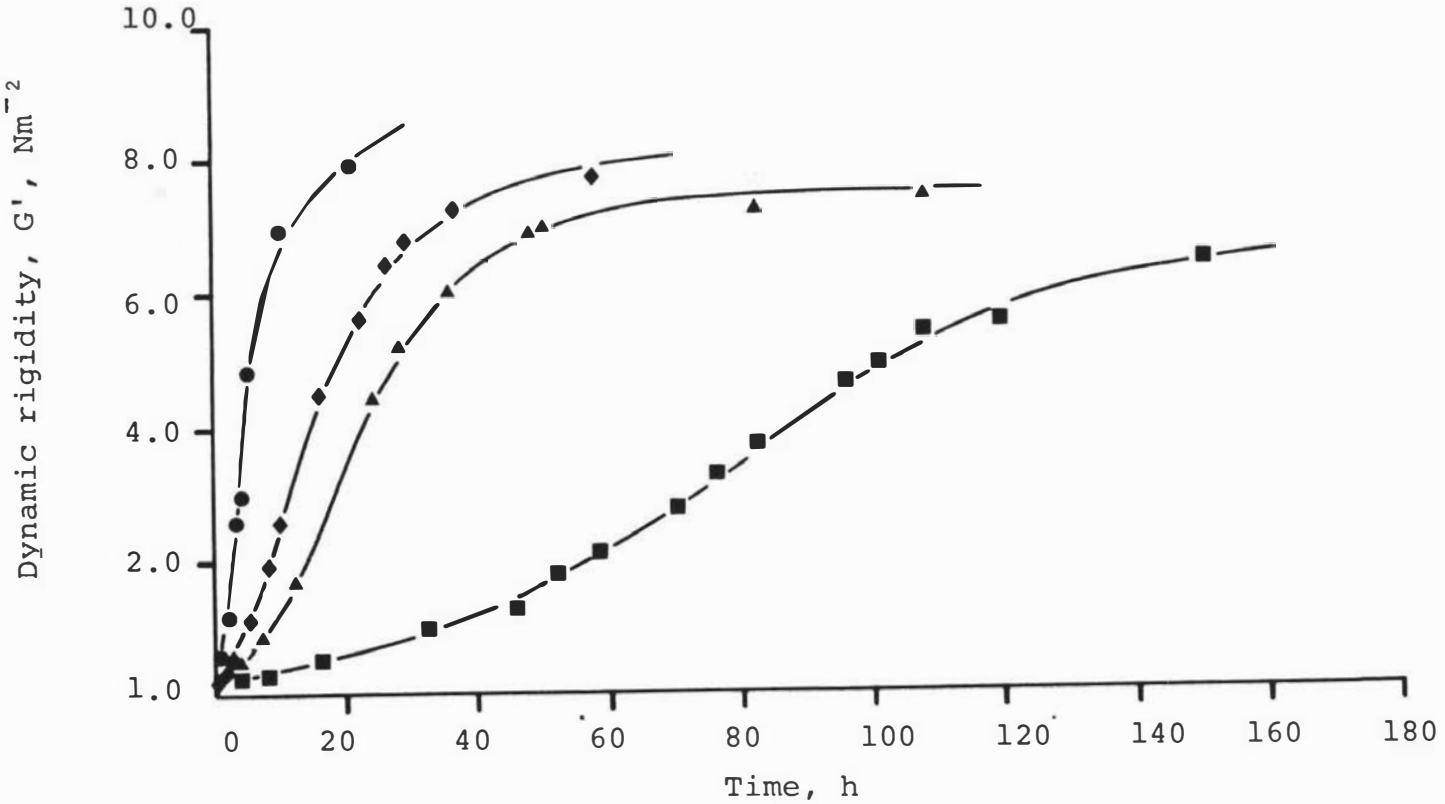

Figure 1.32 The development of dynamic rigidity at various ageing temperatures as a function of time for Gamenya starch pastes.

● 10.0°C ◆ 15.0°C ▲ 20.0°C ■ 30.0°C

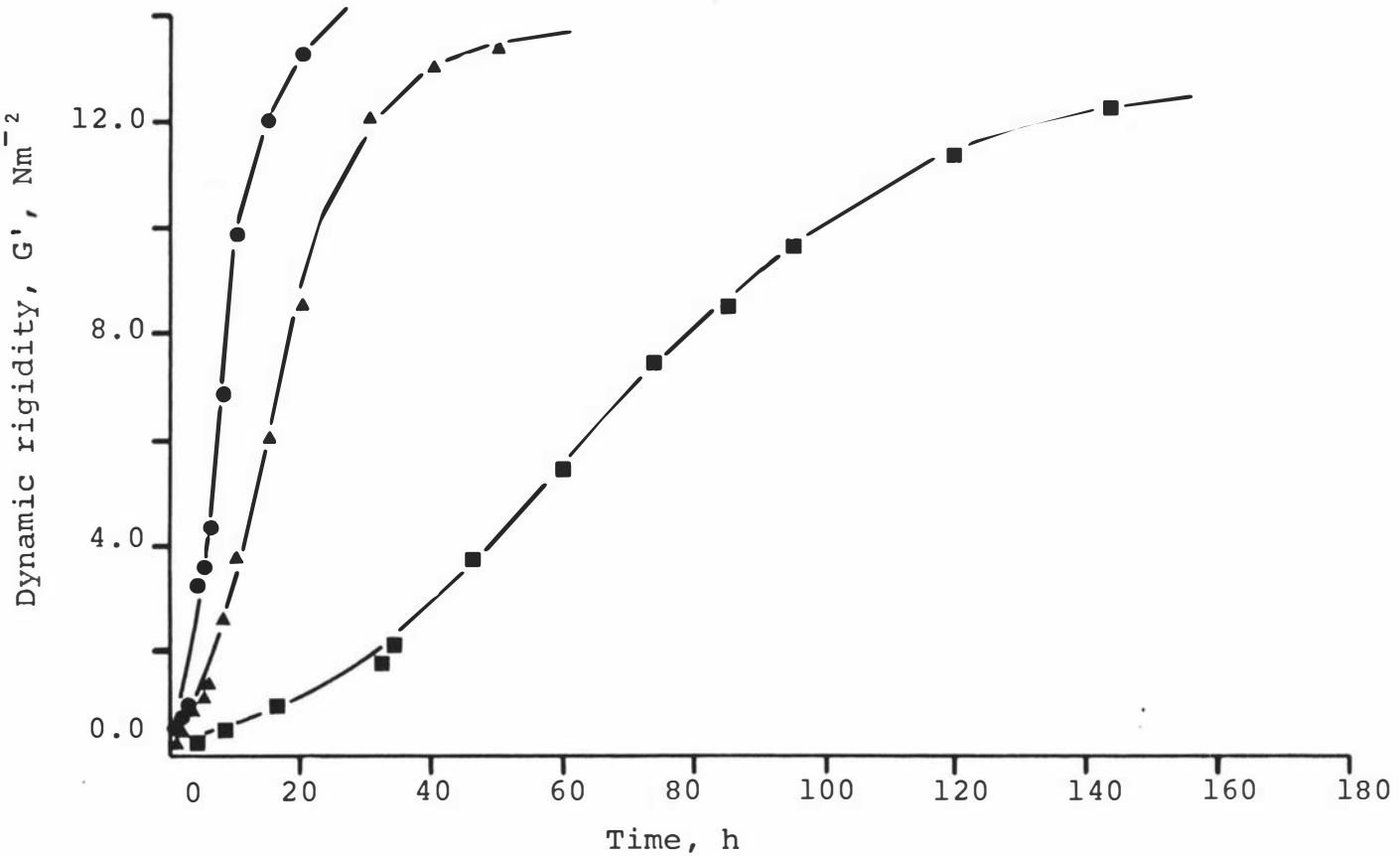

Figure 1.33 The development of dynamic rigidity at various ageing temperatures as a function of time for Aotea starch pastes.

● 10.0°C ▲ 20.0°C ■ 30.0°C

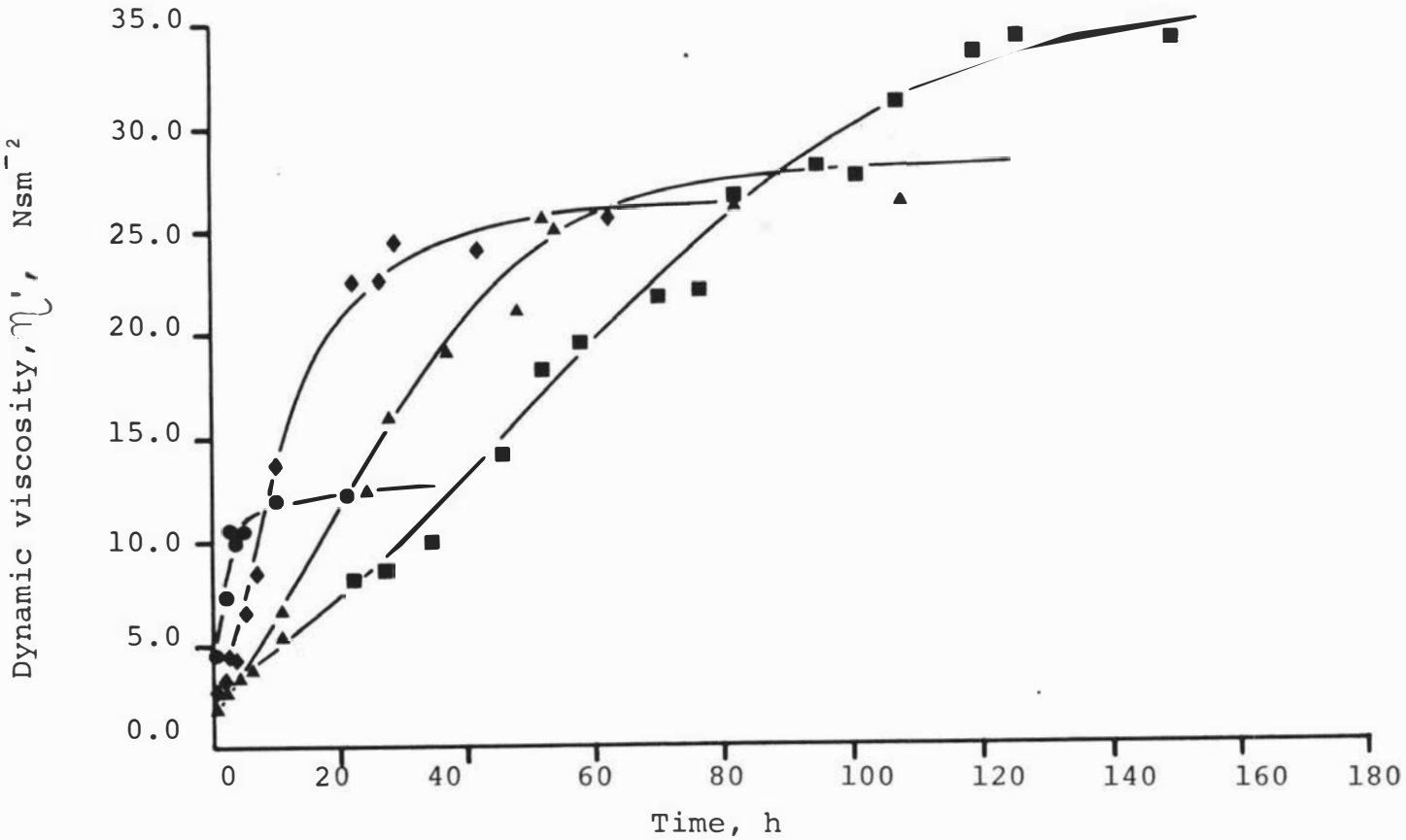

Figure 1.34 The development of dynamic viscosity at various ageing temperatures as a function of time for Gamenya starch pastes.

● 10.0°C ◆ 15.0°C ▲ 20.0°C ■ 30.0°C

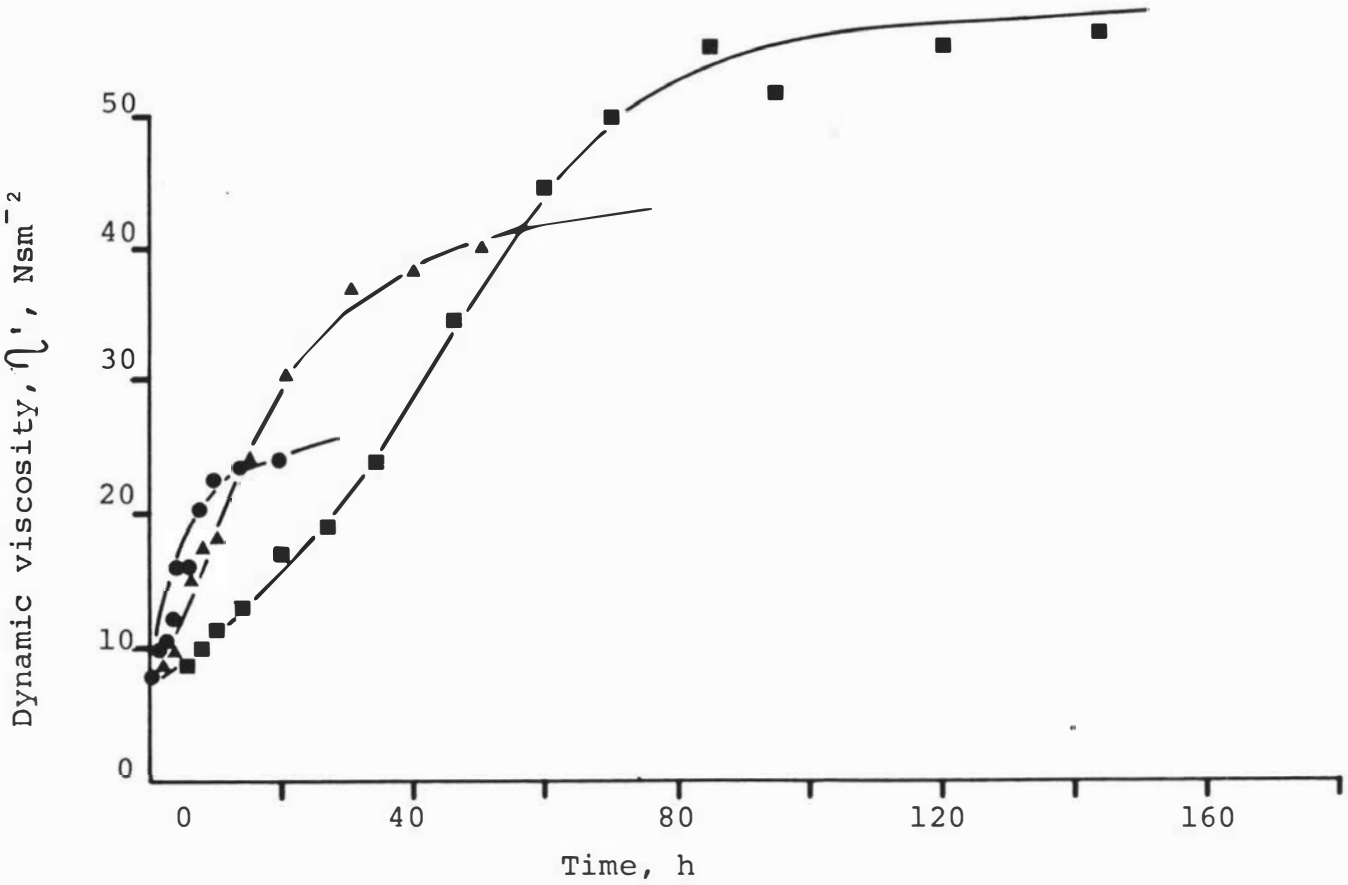

Figure I.35 The development of dynamic viscosity at various ageing temperatures as a function of time for Aotea starch pastes.

● 10.0°C ▲ 20.0°C ■ 30.0°C

1.7. Discussion

I.7.1. Viscoelastic behaviour under oscillatory shear conditions

The relationship between dynamic rigidity G' and starch concentration C as shown in Figure I.5 is, in some respects, similar to the effect of cellulose concentration on the viscoelastic properties of dilute suspensions of cellulose fibres. For the latter system Steenberg, Thalen and Wahren (100) established the following empirical relationship governing the concentration dependence of dynamic rigidity:-

$$G' = G_0' \, (C - C_s)^{K_G} \quad \text{for } C > C_s \qquad [I.19]$$

$$G' = 0 \quad \text{for } C < C_s \qquad [I.20]$$

where C is starch concentration (. %) and G_0' and K_G are constants at any given frequency characteristic of each fibre suspension. Equation [I.19] is analogous to that used to describe the steady shear properties of microgels (101). Values of C_s, G_0' and K_G can be established so that Equation [I.19] fits the data in Figure I.5 closely when $C \geqslant 1.1C_s$. Figure I.36 shows plots of log G' against log $(C - C_s)$ for two varieties of wheat starch pastes. The corresponding correlation coefficients are 0.97 and 0.98 for Gamenya and Aotea respectively. The other varieties in Table I.12 give similar results, in all cases C_s, G_0' and K_G vary from sample to sample. Figure I.36 shows that there is a discontinuity in the variation of dynamic rigidity with concentration which occurs when $C = 1.1\ C_s$, below this point dynamic rigidity declines less rapidly with decreasing concentration. When $C \leqslant 0.9\ C_s$ the dynamic rigidity is zero.

An equation of similar form fits the dynamic viscosity measurements in Figure I.4 when the C_s values established in Equation [I.19] are used,

$$\eta' = \eta_0' (C-C_s)^K \quad \text{for } C \geq 1.1C_s \qquad [I.21]$$

where K_n and η_0' are frequency dependent constants that have different magnitudes for different starches. In this case, the correlation coefficients are 0.98 and 0.99 for Gamenya and Aotea respectively, the other varieties give similar results. Figure I.37 shows the discontinuity in dynamic measurements at $C = 1.1C_s$, below this value the decrease in dynamic viscosity with concentration is less marked. In contrast to the dynamic rigidity, dynamic viscosity still has a finite value when $C \leq 0.9C_s$.

Suspensions of cellulose fibres undergo an elastic response on deformation when a three dimensional network of suspended material is present. In these conditions the term C_s has been shown to correspond to the minimum concentration of fibres needed to form this structure (102). It has been suggested that as swollen granules are in effect gels that exhibit viscoelastic behaviour, a network with elastic properties could be formed in a paste by random packing of such particles throughout the volume of the system (103). C_s would then be the concentration of starch needed to do this. In all cases C_s was found to be equal to the minimum concentration at which gelatinised granules would be expected to form a close packed network on the basis of swelling capacity measurements. The observation of an inflexion point when the concentration level is approached, at which the continuous phase is in excess, has also been shown in steady shear measurements of microgels (101). The fact that dynamic rigidity tends to zero when $C = 0.9C_s$ rather than $C = C_s$ and that

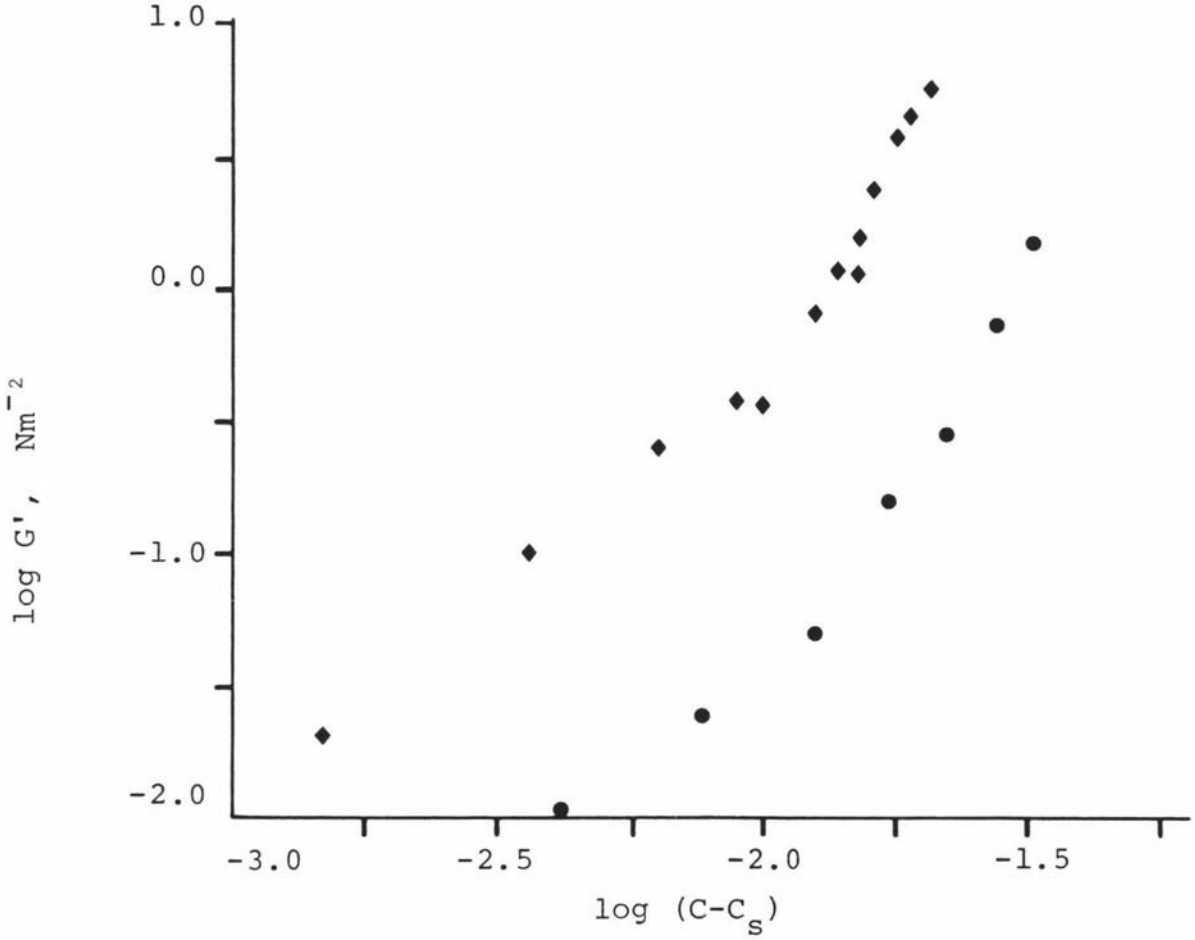

Figure 1.36 Plots of the log of the dynamic rigidity at a frequency of 0.05 $rads^{-1}$ versus log (C-C_s) for pastes made from Gamenya (◆) and Aotea (●) wheat starches.

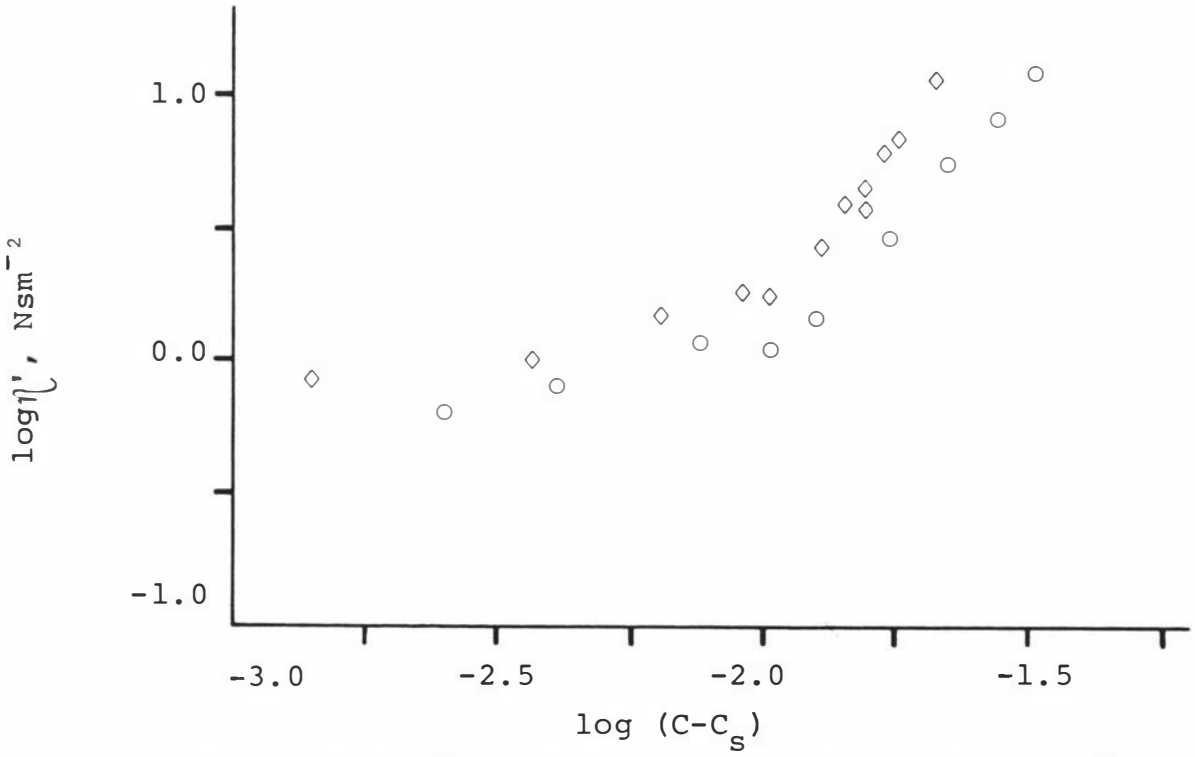

Figure 1.37 Plots of the log of the dynamic viscosity at a frequency of 0.05 $rads^{-1}$ versus log (C-C_s) for pastes made from Gamenya (◇) and Aotea (○) wheat starches.

there is a discontinuity in viscoelastic behaviour when $C = 1.1C_s$, suggests that in this range networks can exist that are more porous than the close packed assembly of particles occurring when $C > 1.1C_s$. The porosity of networks could increase as a result of the system dilating at lower starch concentrations in the presence of shear (104).

Since the completion of the present study, a similar empirical equation has been used to describe the concentration dependence of dynamic rigidity of pastes made from tapioca, corn, potato starches and wheat flour (68).

While Equations [I.19] and [I.21] account for the variation of dynamic rigidity and viscosity with concentration for any given starch, the values of the parameters, G_0', K_G, η_0' and K_n vary from sample to sample. Hence these expressions were modified in an attempt to obtain more general relationships. Gelatinised starch-water systems are dispersions that are, in many respects, analogous to microgels (101, 105). The rheological properties of such systems are known to depend on the volume fraction, number and size distribution of dispersed particles (106). These factors were therefore built into Equation [I.19] and [I.21] in a number of different forms of which the following are most successful in describing the experimental data.

$$G' = G_0' \left[(C-C_s)S \right]^{K_G} \left[P \right]^{M_G} \text{ for } C > 1.1C_s \qquad [I.22]$$

$$\eta' = \eta_0' \left[(C-C_s)S \right]^{K_n} \left[P \right]^{M_n} \text{ for } C > 1.1C_s \qquad [I.23]$$

where S is the swelling capacity of starch, this also gives C_s which is now expressed in units of g/ml, P is the number

fraction of large granules (>12 μm hydrated diameter) and M_G and M_n are constants whose values depend on frequency. The results of the statistical analysis of the application of Equations [I.22] and [I.23] to the relevant data in Tables I.12 are given in Table I.14. The correlation coefficients in Table I.14 demonstrate that these empirical expressions can account for much of the variation in the experimental data using single value of G_0' , η_0', K_G and K_n . Hence the differences in the dynamic mechanical properties from a number of wheat cultivars may be attributed to variations in both their swelling capacities and the number fractions of large granules they contain. The results also indicate that the behaviour of pastes depends on the conditions employed during their preparation as these conditions influence the volume of swollen particles occurring after gelatinisation.

The general relationship derived to predict the rheological behaviour of wheat starch pastes in terms of swelling capacity and size distribution of starch granules only applied to the range of experimental conditions detailed in Table I.12. Cases were found where experimental results did not conform to Equations [I.22] and [I.23] , these are shown in Table I.15. There are several factors that may account for these variations. In these cases the results show clearly that less swelling of granules occurs when compared to the values obtained using standard pasting conditions. Thus to obtain the same volume fraction as in controls, the starch concentration is increased. Hence the increase in the number of swollen gel particles may explain the increase in dynamic viscosity. During the pasting of starch - water system, it has been shown that granule disintegration is reduced as a result of less heat treatment (84), this effect may also contribute to the increase in dynamic viscosity. On the other hand, the decrease in dynamic rigidity of pastes may be attributed to the nature of the network structure formed in the system when the temperature/time

treatment is reduced. A weakening in the inter-particle forces such as entanglements between the surface molecules of adjacent swollen granules may results from a reduced heat treatment leading to a decrease in dynamic rigidity. Another possible reason may be the reduced synergistic interactions between the swollen granules and the polymeric material in the continuous phase as less starch is released.

Table I.14 Values of regression coefficients and correlation coefficients for the fits of Equations [I.22] and [I.23] at specified frequencies to the results in Table I.12.

	$\omega = 0.05$ rads^{-1}	$\omega = 0.1$ rads^{-1}	$\omega = 0.5$ rads^{-1}	$\omega = 1.0$ rads^{-1}
$\log \eta_0'$	3.00	2.70	2.09	1.83
K_n	1.20	1.19	1.21	1.17
M_n	0.564	0.469	0.250	0.145
Correlation Coefficient	0.894	0.904	0.907	0.889
$\log G_0'$	3.89	3.88	3.68	1.49
K_G	1.44	1.45	1.44	1.49
M_G	2.29	2.20	1.82	1.69
Correlation Coefficient	0.885	0.885	0.870	0.877

Table I.15 Dynamic viscosities and rigidities at a representative frequency and other characteristics of pastes formed from various wheat starches outside the range of experimental conditions in Table I.12.

Wheat Variety Used to Prepare Starch	Starch conc. g/ml	Temperature/ Time Treatment $^0C/h$	Swelling Capacity ml/g	$\omega = 0.1$ rads^{-1} η' Nsm^{-2}	G' Nm^{-2}
Gamenya	0.0480	89.5/1.0	23.83	8.98	0.85
		95.0/1.0	34.30	(2.20)	(1.25)
	0.0525	87.5/1.0	20.93	4.53	0.12
		95.0/1.0	34.30	(2.00)	(1.25)
	0.0571	88.5/1.0	21.63	6.04	0.20
		95.0/1.0	34.30	(2.20)	(1.25)
Aotea	0.0661	89.5/1.0	17.07	4.20	0.05
		95.0/1.0	26.25	(1.52)	(0.15)
	0.0705	89.5/1.0	17.07	5.40	0.08
		95.0/1.0	26.25	(2.00)	(0.20)

Figures in parenthesis indicate values for pastes containing the equivalent volume fractions of gelatinised granules formed by the standard pasting conditions.

I.7.2. Rheological properties under steady shear conditions

An expression of a similar form to that used in the analysis of dynamic viscoelastic data may be useful in explaining the variation in apparent viscosity between various starch pastes measured under steady shear conditions. Thus

$$\eta_s = \eta_0 (C-C_s)^{K_1} \qquad [I.24]$$

where η_0 and K_1 are constants at any given shear rate whose magnitudes depend on wheat variety and paste preparation conditions. A similar equation has been used to describe the steady shear behaviour of some microgels (101). Figure I.38 shows the results in Figure I.12 conform to this expression where $C \geqslant 1.1\ C_s$, or $\log (C - C_s) \geqslant -2.5$ and -2.4 for Karamu and Raven wheat starches respectively. The discontinuity in the results when $C = 1.1C_s$ also occurs. This may possibly be due to the fact that below this concentration paste structure changes and more porous arrangements of packed starch particles can exist, perhaps as a result of system dilating.

Although Equation [I.24] accounts for the variation in the apparent viscosity of any given paste with starch concentration, the parameters K_1 and η_0 depend on starch variety and sample preparation conditions. This equation was therefore modified in an attempt to establish a more general relationship. A number of investigators have suggested methods of unifying rheological data from steady shear measurements for systems consisting of dispersed gel particles (101, 107, 108). These methods relate rheological measurements to the volume that the bed of gel particles would occupy when close paced if excess was present. In the present study, this is determined by the swelling capacity of the starch and therefore depends on sample variety and paste preparation conditions. The work on the dynamic rheological behaviour of wheat starch pastes

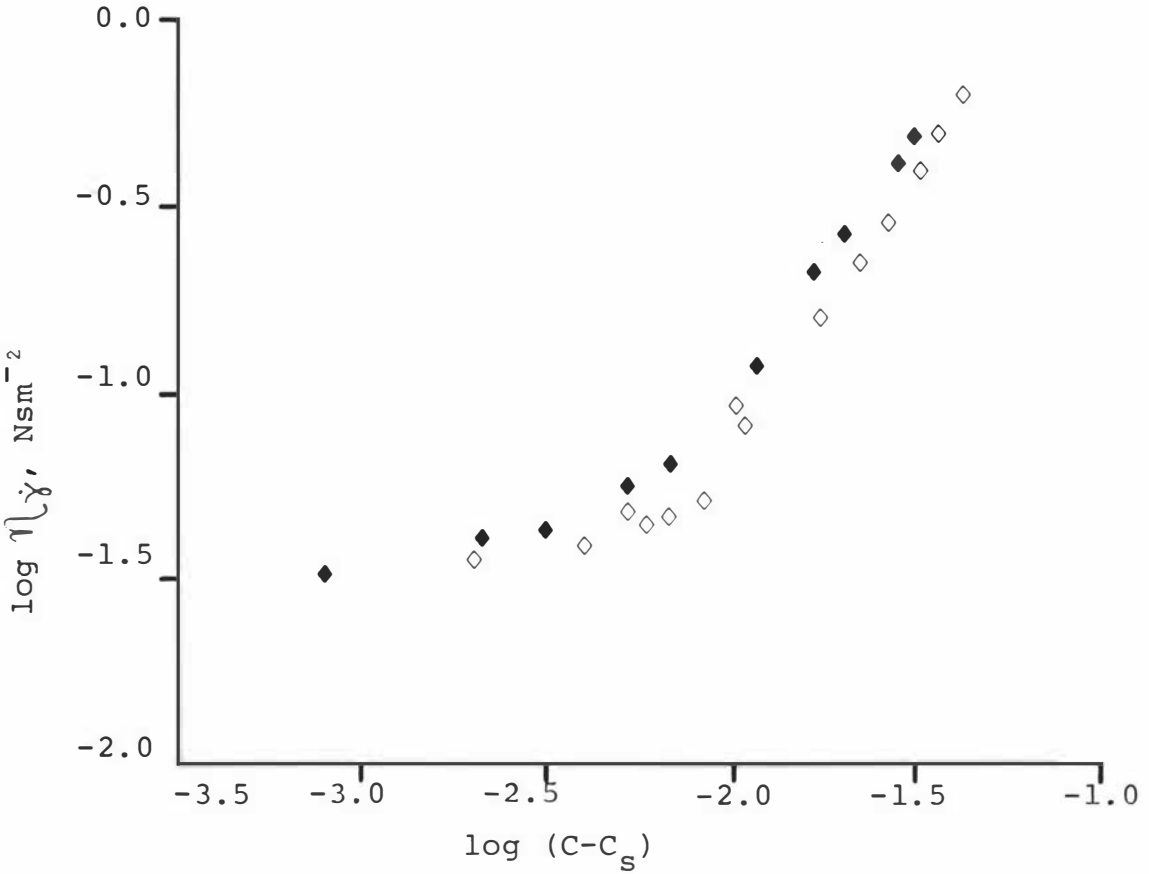

Figure I.38 Plots of the log of the apparent viscosity at a shear rate of $120s^{-1}$ of Raven (◆) and Karamu (◇) starch pastes versus log (C-C_s).

reported herein suggest that it may also be necessary to make reference to the size distribution of particles to unify results. With the present viscosity data, see Table I.13, a general relationship was found without including a term for the particle size distribution

$$\eta_{\dot{\gamma}} = \eta_{c} \left[(C - C_s) S \right]^{K_1} \qquad C \geq 1.1 C_s \qquad [I.25]$$

η_c and K_1 are constants at any given shear rate. The regression coefficients of the fits of the logarithmic form of Equation [I.25] at given shear rates to the experimental data in Table I.13 are given in Table I.16. A term for the particle size distribution was not included in Equation [I.25] as this increased the correlation coefficient by only about 0.02, and this is not statistically significant at the 5% level.

Taylor and Bagley (101) suggest a different method of unifying steady shear data such as that in Figure I.12, namely by relating viscosity values to the viscosity at the point at which the disperse particles are just close packed throughout the entire system. In the present context this leads to an equation of the form

$$\frac{\eta_{\dot{\gamma}}}{\eta_{cs}} = K_2 \left(\frac{C}{C_s} \right)^{M} \qquad [I.26]$$

where η_{cs} is the apparent viscosity at a shear rate $\dot{\gamma}$ and concentration C_s, K_2 and M are constants. The fit of the logarithmic form of this expression to the results in Table I.13 at a shear rate of $120 s^{-1}$ gives a correlation coefficient of 0.99, similar values of the correlation coefficient were obtained at other shear rates. Although Equation [I.26] unifies paste viscosity data more successfully than Equation [I.25], the relationship is less general as it requires knowledge of η_{cs} for each starch variety used and for each set of paste preparation conditions.

Table I.16 Values of regression coefficients and correlation coefficients for the fits of Equation [I.25] at specified shear rate.

	$\dot{\gamma} = 20S^{-1}$	$\dot{\gamma} = 120S^{-1}$	$\dot{\gamma} = 1200S^{-1}$
$\log \eta_0$	0.03	-0.313	-0.885
K_1	1.33	1.18	0.80
Correlation Coefficient	0.95	0.95	0.94

The variation of the yield stress with concentration and variety of starch, and paste preparation conditions, can be described by a general expression which is analogous to that established previously for the dynamic mechanical behaviour of wheat starches:

$$\Gamma_0 = \Gamma_c \left[(C-C_s)S \right]^{K_4} \left[P \right]^{N} \qquad I.27$$

where Γ_c, K_4 and N are constants and P is number fraction of large granules in the starch. Since the sensitivity of the viscometer used was such that C must be greater than $1.1C_s$ to detect a yield stress, it is not clear whether this equation applies when the starch concentration is decreased below this limit. Statistical analysis of the application of the logarithmic form of Equation [I.27] to the yield stress results in Table I.13 was found to give a correlation coefficient of 0.93, the values of Γ_c, K_4 and N being -0.05, 1.33 and -0.794 respectively. Without the term for the number fraction of large granules the correlation coefficient reduces to 0.64. The inverse relationship between yield stress and the number fraction of large granules is consistent with the variation of yield stress with particle size distribution established by Erdi et al. for certain microcrystal gels (105).

Hence the variation in the steady shear behaviour due to concentration and variety of starch and paste preparation conditions can be attributed to two parameters, namely the volume which the gel particles would occupy when close packed if excess water were present and the size distribution of dispersed particles. The values of the apparent viscosity and yield stress depend on the source of starch since this effects particle swelling volumes and size distributions. Paste preparation conditions influence rheological properties since they alter the volume occupied by gelatinised granules. The lack of theory dealing with viscoelastic particles in suspensions, combined with the fact that starch pastes have complicated structures, precludes a more fundamental interpretation of the results.

I.7.3. Effect of paste storage on dynamic viscosity and rigidity

The results in Figures I.32 - I.35 show that the rate of change of dynamic rigidity and viscosity with respect to time decreases with increasing temperature in a manner that is characteristic of crystallisation in polymer-diluent systems (109). The Avrami equation has been extensively applied to the crystallisation of polymer systems including starch gels (99). By analogy with starch gels, changes in dynamic rigidity may be assumed to be a linear measure of the extent of crystallisation. In this case the ageing of starch pastes can be described, according to the Avrami equation, as follows:

$$\frac{G_\infty - Gt}{G_\infty - Go} = \exp\ (-Kt^a) \qquad [I.28]$$

where G_∞ is the equilibrium dynamic rigidity, Gt is the dynamic rigidity at time t and Go is the dynamic rigidity at zero time. K is the rate constant and a is the Avrami exponent. The value of the Avrami exponent depends on the number of dimensions in which crystallisation takes place and the mode of nucleation (110).

Figures I.39 and I.40 show plots of log $\left[-\ln\left(\frac{G_\infty - Gt}{G_\infty - Go}\right)\right]$ against log t for Gamenya and Aotea starch pastes respectively. Two values of the Avrami exponent are obtained for each temperature, an initial slope of 1 and a final slope of 2. The 95% Confidence Interval for the slopes are shown in Table I.17.

Table I.17. 95% Confidence Intervals of the Avrami exponents from the fits of the dynamic rigidity measurements Gamenya and Aotea starch pastes to Equation [I.28].

Wheat variety used to prepare starch	Ageing temperature °C	Initial slope	Final slope
Gamenya	10.0	0.85*	1.85 ± 0.10
	15.0	1.00 ± 0.05	1.91 ± 0.10
	20.0	1.03 ± 0.03	1.98 ± 0.11
	30.0	1.03 ± 0.01	2.02 ± 0.08
Aotea	10.0	1.18 ± 0.01	1.91 ± 0.10
	20.0	1.06 ± 0.03	1.87 ± 0.04
	30.0	0.97 ± 0.02	1.98 ± 0.03

* only 2 data points

The results of the Avrami analysis can be interpreted in a number of ways. A slope of 1, as in the initial part of Figures I.39 and I.40, indicates that crystallisation is instantaneous and that the growth of crystallites is in one dimension only. The occurrence of instantaneous nucleation

is possible in starch-water systems as remnants of ordered structures are present after gelatinisation which can act as nuclei for subsequent crystal growth (125). Concentrated wheat starch gels also give a slope of 1 when crystallisation results are interpreted according to the Avrami equation (110). A change from a slope of 1 to a slope of 2, as found in the final part of Figures I.39 and I.40, suggests a change from one-dimensional to two-dimensional crystal growth. This corresponds to a change from rod-like to disc-like growth. The fact that one dimensional crystal growth occurs before two dimensional crystallisation may possibly be related to the fact that amylose crystallises faster than amylopectin (111). In this case, one-dimensional growth corresponds to amylose crystallisation and two-dimensional growth to amylopectin crystallisation.

Another interpretation for the initial slope seen in Figures I.39 and I.40 is that it represents a lag phase of the type often observed during crystallisation of polymer systems (109). If this is the case, the main crystallisation occurs when the Avrami plot has a slope of 2, the interpretation of this section of the graph would still be as before. However a value of 2 for the Avrami exponent can also indicate sporadic nucleation with crystal growth in one dimension, this possibility can not be rigorously excluded on the basis of the present results.

Although the variation in the dynamic rigidity with time obeys the Avrami equation, the mechanism of crystallisation of starch pastes remains uncertain. The Avrami plots could have no fundamental significance as empirical methods of measuring crystallisation were used. Furthermore, some evidence suggests the Avrami equation does not actually demonstrate crystallisation in polymer systems (112).

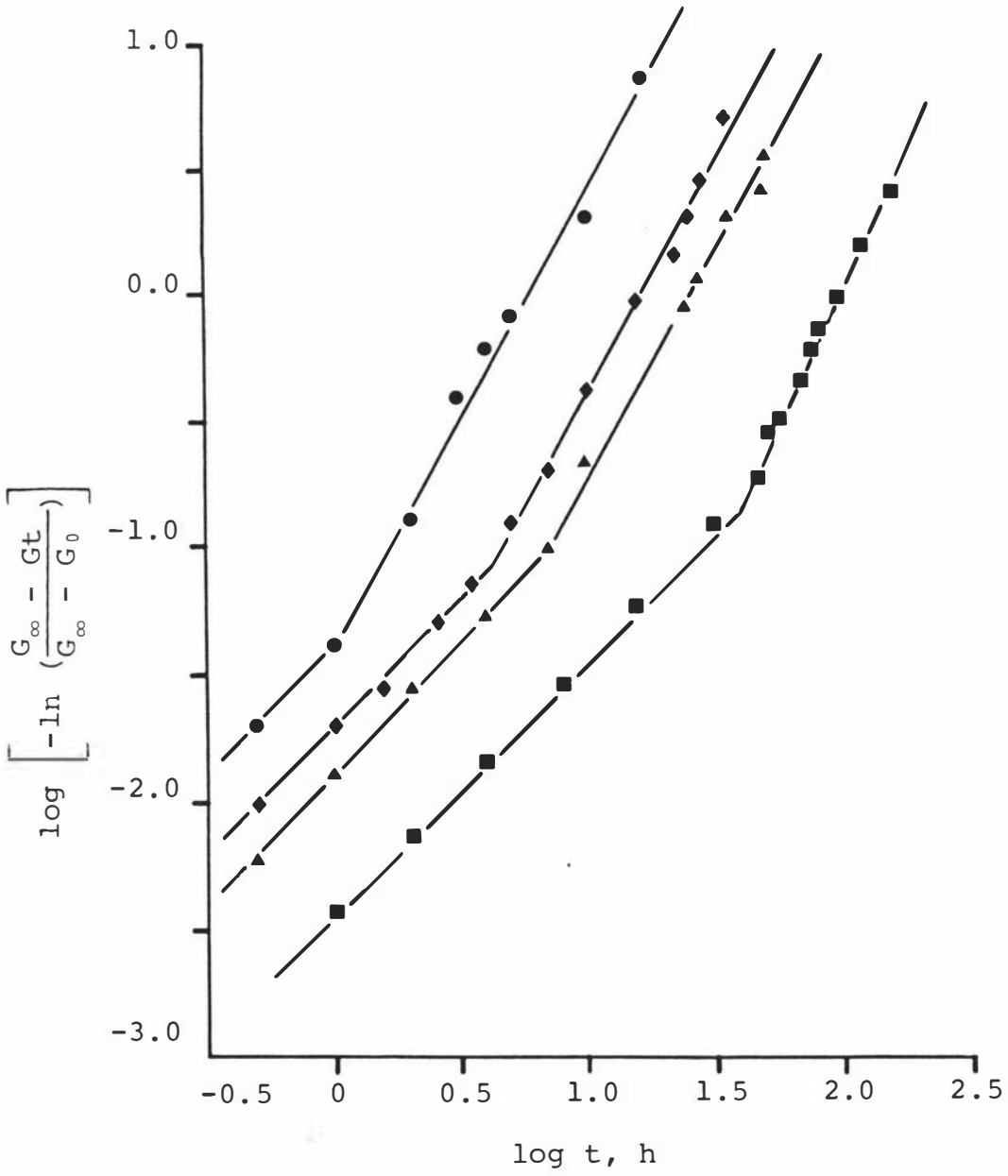

Figure 1.39 The fits of dynamic rigidity measurements for Gamenya starch pastes to Equation [I.28] at various ageing temperatures.

● 10.0°C ◆ 15.0°C ▲ 20.0°C ■ 30.0°C

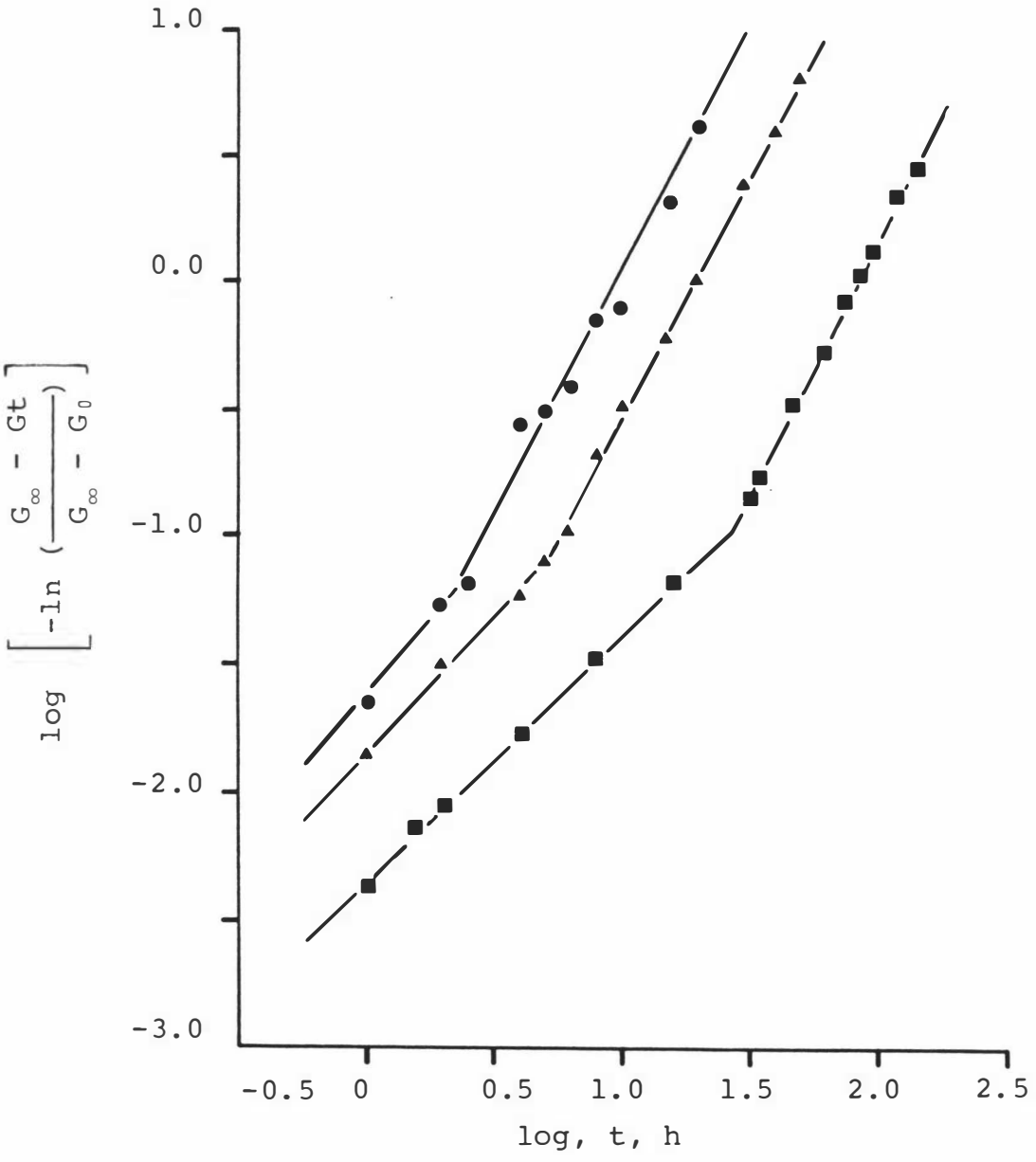

Figure 1.40 The fits of dynamic rigidity measurements for Aotea starch pastes to Equation [I.28] at various ageing temperatures.

● 10.0°C ▲ 20.0°C ■ 30.0°C

SECTION II

THE RELATIONSHIP BETWEEN THE PHYSICAL STRUCTURE AND THE SWELLING CAPACITY OF STARCH GRANULES.

II.1 Introduction and scope of the investigation

In the previous section, it was demonstrated that the flow behaviour of starch pastes depends on the volume which the gel particles would occupy when close packed if excess water were present, that is the swelling capacity of the starch. This applies to both oscillatory and steady shear conditions. It was further shown that when a range of granule sizes is present, as is the case with wheat starch, this also influences rheological behaviour. Differences in the rheological characteristics of pastes formed from starches from various wheat varieties may be attributed to differences in the volume fractions and size distributions of swollen granules they contain. The present chapter describes an investigation of physical characteristics of starch granules that may influence the swelling capacity of starch.

The volume occupied by close packed swollen granules when excess water is present is clearly influenced by the size distribution of the gelatinised particles. However, in a previous section, it was shown that the change in the swelling capacity of starch with wheat variety does not simply reflect changes in size distributions. This is because samples from different cultivars with the same narrow range of diameters still give a similar pattern of variation in swelling capacity with source. This suggests that other factors such as the composition and structure of granules must be influencing their swelling capacities. In regard to composition, differences in amylose to amylopectin ratios and in lipid components could influence granule swelling, but investigations suggest that these are not primarily responsible for the observed variations in swelling (21, 113). Some evidence suggests that the degree of physical organisation of polymer constituents within the granule, that is their crystallinity, may regulate particle swelling (114). This possibility was therefore investigated in the present section.

II.2 Experimental approach

Various methods of measuring polymer crystallinity are available and have been reviewed (115). The different methods do not necessarily give the same results because they measure different aspects of polymer structure. Therefore a combination of techniques is normally used to check results obtained.

X-ray diffraction provides a potential means of determining the absolute polymer crystallinity and starch crystallinity has been measured by this technique (46). However, theoretical difficulties are normally associated with this absolute method (116). As an alternative, polymer crystallinity can be determined by a relative crystallinity method. This method compares the crystalline content of a sample with that of crystalline and amorphous standards (116, 117). This technique has already been applied to starches (47, 118).

In some polymer systems, the enthalpy change associated with the melting of polymer can be used as a measure of crystallinity (115) and this can be determined by Differential Scanning Calorimetry (DSC) methods. In pure starch systems, the polymer decomposes before it melts (119), but it is possible to depress the melting point by addition of a diluent (59). In this case, a solvent assisted melting of crystallites occurs. The enthalpy change associated with this order-disorder phase transition has been used to give an indication of starch crystallinity (47).

Any change in the degree of physical organisation in a polymer system is associated with a change in specific volume (115), this can be determined by standard methods (120).

The above techniques were used in the present study to evaluate the crystallinities of starches with different swelling capacities.

II.3 Experimental

II.3.1 Materials

Starches were extracted from six different wheat varieties as in I.5.1.2 and fractions of defined size ranges were obtained as in I.5.1.3. As the presence of moisture in samples influences crystallinity measurements (25), the moisture contents of starches were adjusted to 12% by equilibrating at a relative humidity of 33.0% and a temperature of 20^{o}C for three weeks. This relative humidity was obtained using a saturated solution of magnesium bromide.

II.3.2 DSC Measurements

Measurements of the enthalpy changes occurring during gelatinisation of starch samples were made using a Perkin-Elmer DSC-1B.

An accurately weighed sample of wheat starch was thoroughly mixed with an known amount of distilled water in a small glass bottle with an air tight lid. Portions (15 mg) of the starch-water suspension were then transferred into previously weighed aluminium DSC pans using a micropipette. The pans were immediately sealed using a volatile sample sealer. Sample weights were then determined.

DSC traces were obtained using the following conditions: 1 minute equilibration time for the samples in the

sample holder; heating rates of 2^{o}, 4^{o} and 8^{o} min^{-1}; and dry nitrogen flushing through DSC head (30 ml min^{-1}).

At least three replicate runs were made for all samples.

By using Indium as a standard, the measurement of the area under the DSC trace could be used to provide the direct basis for calculating the enthalpy change during gelatinisation (cal/g).

II.3.3. X-ray measurements

Measurements of the relative crystallinity of starch samples were made using an X-ray diffractometer, consisting of a PW1011 X-ray generator with goniometer attachment. A starch sample that had been ball milled for 72 hours was used as the amorphous reference and a sample of Karamu starch as the crystalline standard.

X-ray diffractometer traces were obtained using the following experimental conditions: CoK_{α} radiation, voltage (40 KV), current (30 mA), scanning speed ($2\theta=2^{o}$ min^{-1}), recorder speed (1200 mmh^{-1}), range (2000 counts S^{-1}) and a time constant of 2. Diffraction angles were taken from $2\theta=12^{o}$ to 31^{o}, most of the peak intensities occur in this region (56).

Measurements were made at least in triplicate.

Diffraction patterns were analysed for discrete values of intensity at angular increments of 0.2^{o} from 12^{o} to 31^{o}.

The resultant data was then normalised by dividing the intensity at any diffraction angle by the scatter integrated over the total angular range. Crystallinities were then calculated using the correlation and integral methods (116).

II.3.4. Specific volume measurements

Specific volumes of starches were determined using standard methods (120).

Determinations were made in triplicate.

No measurements were made on fractions with narrow size ranges. However, it is known that small granules have lower specific volume than large granules (56).

II.4 Results

II.4.1 Enthalpy change during gelatinisation

Thermograms such as that shown in Figure II.1 were obtained for the order-disorder phase transition that occurs during gelatinisation. Figure II.2 shows plots of average enthalpy change as a function of water/starch ratio for two varieties of wheat starch. The DSC results show that the endotherm measured during gelatinisation at first increases as starch concentration decreases and then reaches a maximum value and remains constant thereafter. Similar results have been reported for potato starch (121). Since there is no significant variation in the enthalpy change for systems when the water to starch ratio is above 4 to 1, this data has been pooled for each individual wheat starch to obtain the maximum enthalpy change. The magnitude of the maximum enthalpy change was

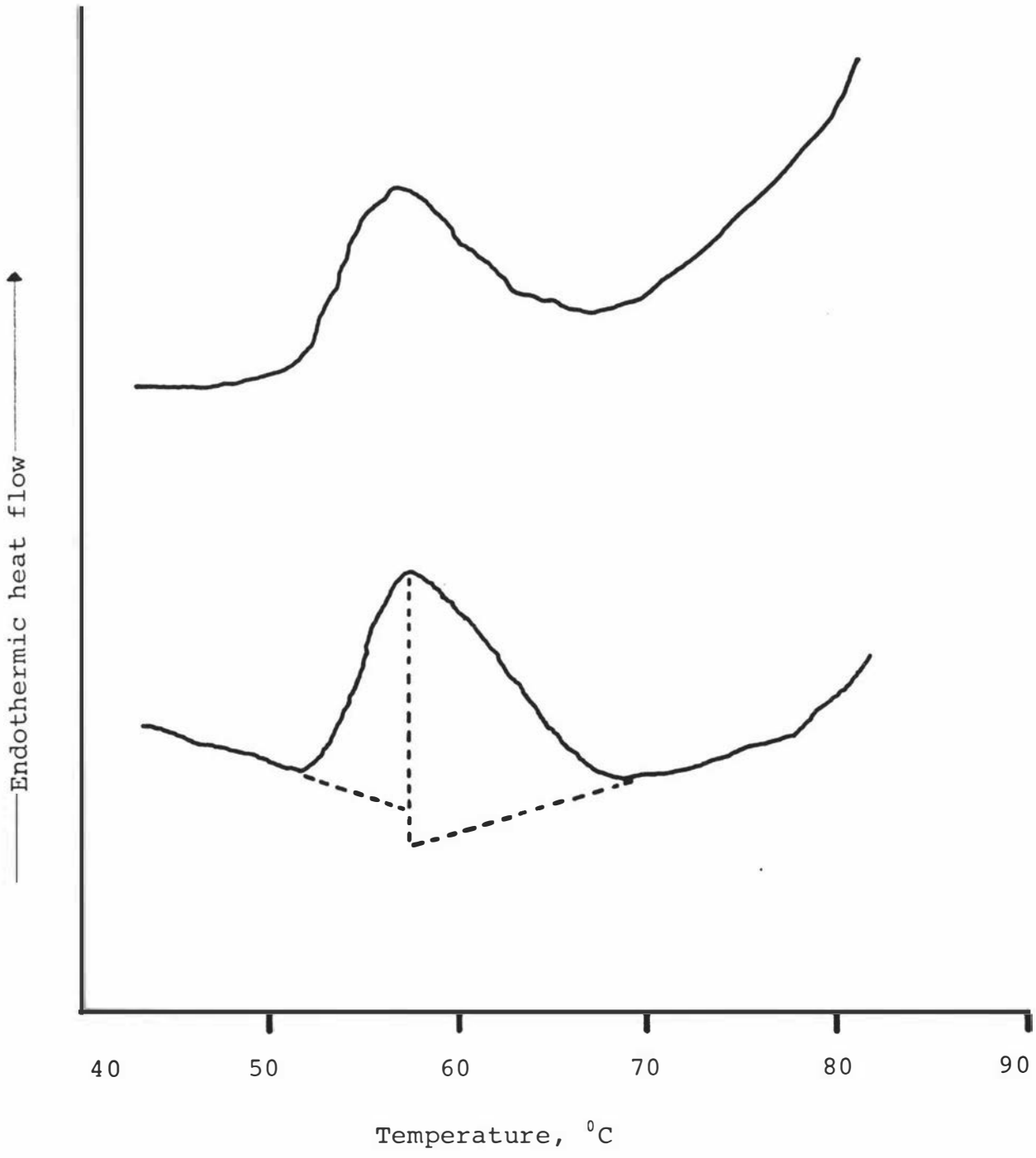

Figure II.1 Typical DSC themograms of starch samples.

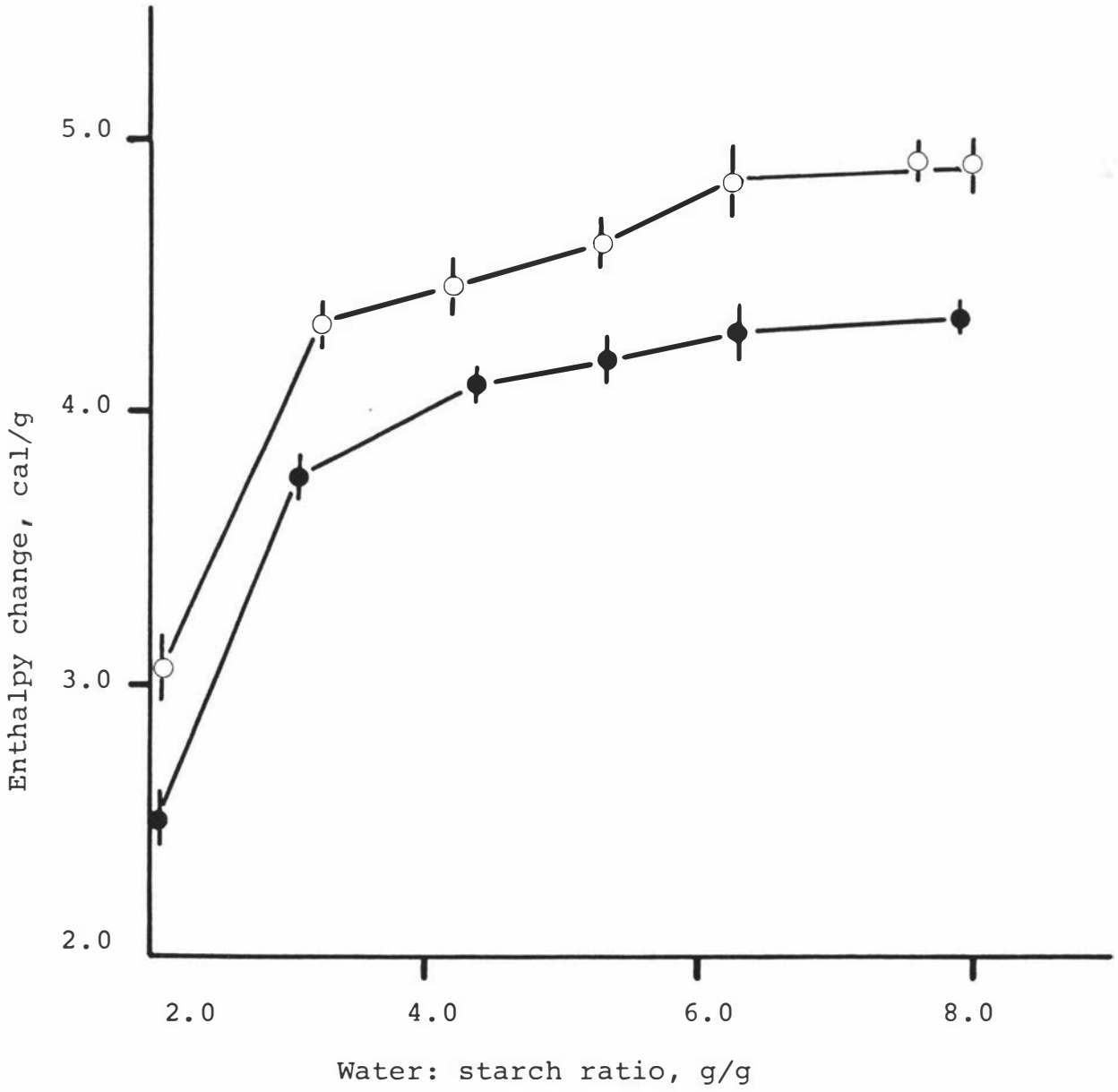

Figure II.2 Plots of the average enthalpy change as a function of the water:starch ratio for Raven (●) and Karamu (○) wheat starches.

not found to be affected by heating rate in the range of starch concentration studied, this is in contrast to results reported for higher starch concentrations (122). The explanation for the decline in enthalpy change with increase in starch concentration as shown in Figure II.2 is uncertain. The phenomenon may reflect a fundamental change in gelatinisation mechanism (121) or simply a redistribution of water (123). In any case, there is general consensus that the enthalpy change measured when excess water is present reflects starch granule crystallinity since it measures the enthalpy of melting of crystallites plus the enthalpy change accompanying hydration (56).

The combined results in Table II.1 show that significant differences exist between the maximum enthalpy change recorded for the various wheat starches. One way analysis of variance, means and 95.0% Confidence Intervals for the enthalpy change of various starches are shown in Appendix IIa. The variation in the enthalpy change with particle size shown in Table II.2 is similar to that reported previously (56), that is smaller granules have consistently higher enthalpy changes than large granules. The DSC results in Table II.2 also show that significant differences exist between the maximum enthalpy change recorded for the Karamu and Raven fractions of the same size range. The enthalpy change for the Karamu size fraction is consistently higher than the comparable Raven size fraction.

II.4.2 Relative crystallinity

All the samples studied gave the crystalline 'A' pattern characteristic of all cereal starches (124) unless crystallinity had been disrupted by ball milling. Typical normalised diffractometer traces in the 2θ range

of 12^0 to 31^0 for a starch sample and for an extensively milled amorphous sample are depicted in Figure II.3. The X-ray crystallinity values for the various wheat starches obtained from such traces are given in Table II.1. The results show that the polymer material in some wheat starch samples is in a more ordered state than in others. One way analysis of variance, means and 95.0% Confidence Intervals for the relative crystallinity index of various wheat starches are shown in Appendix II b. The X-ray results for fractions of limited size ranges shown in Table II.2 confirm earlier work (56) demonstrating that compared with large particles, polysaccharide chains in small granules are in a more crystalline arrangement. The X-ray results in Table II.2 also show that significant differences exist between the relative crystallinities for the Karamu and Raven fractions of the same size range. The relative crystallinity for the Karamu size fraction is consistently higher than the comparable Raven size fraction.

II.4.3. Specific volume

Table II.1 gives the specific volumes of various wheat starches studied. The results show that only small differences exist between the specific volumes and in most cases these differences are not significant. The amorphous reference sample gives a considerably higher value of the specific volume (0.680) than the other samples as would be expected (56).

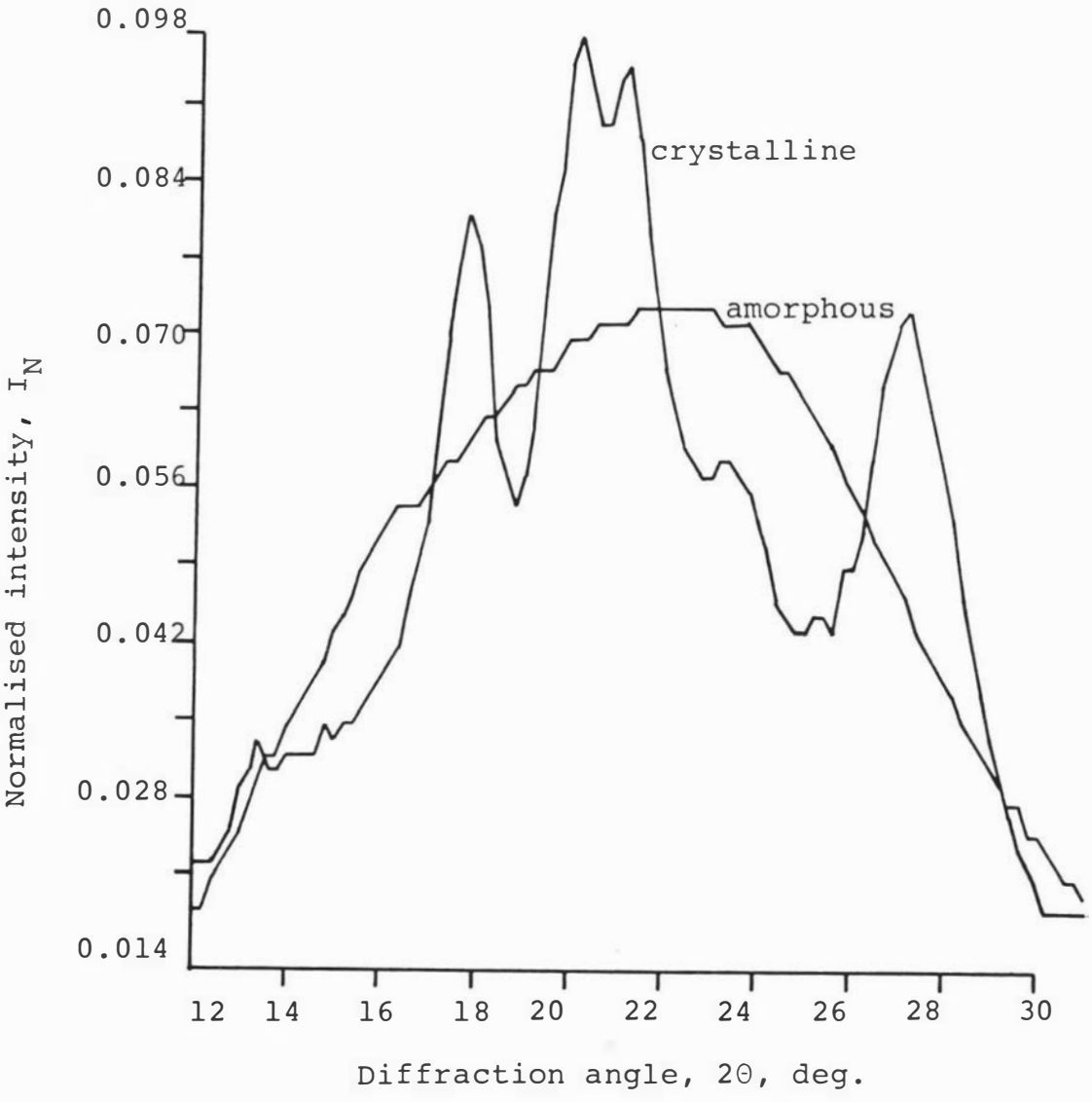

Figure II.3 Typical X-ray normalised diffractometer traces of starch samples.

Table II.1 Enthalpy change, relative crystallinity index, specific volume and number fraction of small granules for the various wheat starches.

Wheat variety used to prepare starch	DSC maximum enthalpy change, Cal/g	X-ray Crystallinity Index, % Correlation	Integral	Specific volume ml/g	Number fraction of small granules
Karamu	4.99±0.08	100.0±1.3	100.0	0.636±0.005	0.925
Aotea	4.96±0.08	97.3±3.4	97.9	0.634±0.005	0.905
Hilgendorf	4.49±0.05	91.8±1.5	92.0	0.630±0.005	0.895
Gamut	4.51±0.05	90.7±2.0	91.4	0.630±0.005	0.889
Gamenya	4.38±0.06	88.3±2.3	90.4	0.639±0.005	0.789
Raven	4.34±0.08	85.9±2.1	87.4	0.645±0.005	0.851

Table II.2 Enthalpy change, relative crystallinity index and swelling capacity for the various size fractions of Karamu and Raven wheat starches.

Wheat Variety Used to Prepare Starch	Particle Diameter μm	DSC Maximum enthalpy change cal/g	X-ray correlation Crystallinity Index, %	Swelling Capacity ml/g
Karamu	19.5	4.75±0.07	96.2±2.4	17.8
	14.7	5.24±0.02	98.2±3.1	18.8
	7.1	5.56±0.20	99.5±3.3	21.0
	4.3	6.45±0.33	100.4±1.7	25.9
	3.0	6.79±0.20	101.4±2.4	30.9
Raven	19.5	3.92±0.06	85.2±3.4	26.2
	14.7	4.22±0.15	86.7±1.9	27.0
	7.1	4.97±0.09	87.9±2.2	28.4
	4.5	5.37±0.25	89.0±3.2	35.6
	3.1	6.43±0.07	92.8±0.5	46.7

II.5 Discussion

The trend in the X-ray and DSC results is the same, thus starch samples having a greater crystallinity as measured by X-ray methods also exhibit a greater enthalpy change on gelatinisation. This is consistent with previous work (47).

The fact that only small, and in most cases insignificant, differences exist between the specific volumes of the wheat starches studied, suggests that specific volume as determined herein is a less sensitive probe of starch crystallinity than DSC or X-ray measurements. In any case, work on synthetic polymers shows that different methods of measuring crystallinity can give different results (115).

Figure II.4 shows plots of relative crystallinity as a function of swelling capacity for the various wheat starches. The results show that increases in the crystallinity of starch samples are associated with decreases in swelling capacity. This partly reflects the fact that starch samples with high swelling powers contain lower fractions of the more crystalline small granules as shown in Table II.1. Nevertheless, the results for samples containing granules with similar diameters still show a significant decrease in crystallinity with increase in swelling power (see Table II.2). This suggests that the results in Figure II.4 do not simply reflect differences in particle size distributions. However, the interpretation of the variation in swelling capacity with crystallinity is complicated since within any given starch type, small granules are more crystalline and yet have higher swelling capacities than large granules.

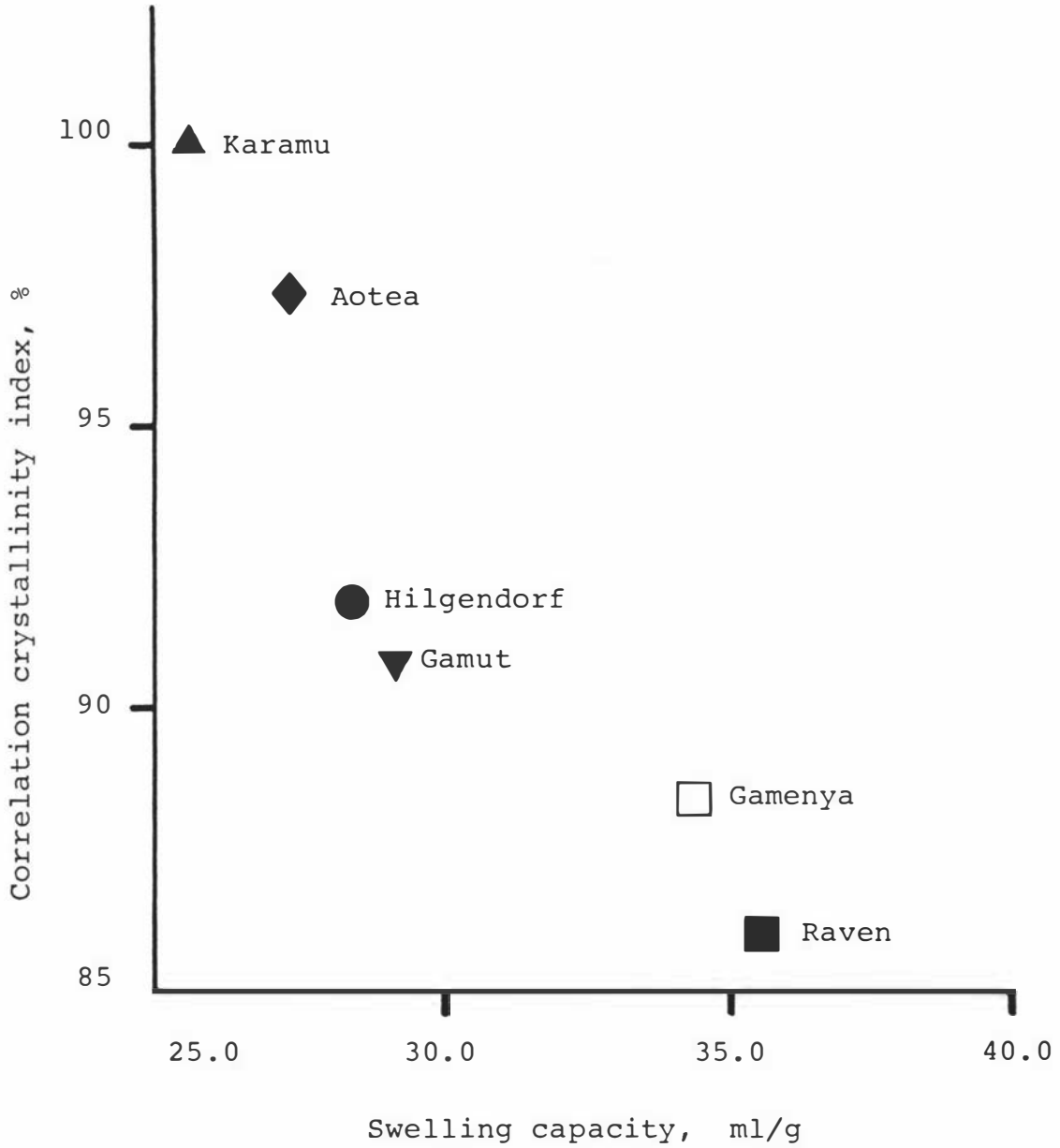

Figure II.4. Plot of the X-ray correlation crystallinity index as a function of the swelling capacity of various wheat starches.

The gelatinisation of starch entails a solvent assisted melting of polysaccharides in the crystalline domains of granules to give an essentially amorphous arrangement (59). The fact that when this crystalline-amorphous transition occurs the polysaccharides of starch granules form swollen gel particles rather than going into solution, indicates that structures must be present in the gelatinised granules that act as crosslinks, so preventing the dissolving of all the polymeric material. These structures could arise from polymer chain entanglements (64), from lipid-amylose complexes (33, 50), or from remnants of crystalline material (125). It has been shown that as the number of crosslinks increases in gel particles, swelling decreases (64). Thus one possible interpretation of the present results is that the more ordered the initial state of the starch granule, the more order remains after gelatinisation and so the less swelling occurs. This is consistent with work performed on the heat moisture treatment of starches (114). If the above explanation is correct, then small granules of any grain starch type should have lower swelling capacity than large granules. However the results obtained, as shown in Table II.2, are to the contrary. These results only apply to pastes made with the heat treatment used in the present study, at temperatures below about 90^{0}C small granules have lower swelling capacities than large granules (16). The relative increase in the swelling capacity of small granules above about 90^{0}C could arise if the packing and deformability of large and small granules changes in this range. Another possible explanation relates to the fact that small granules have a much greater surface area per gram of starch than the large granules, though the quantities of lipid in each size fraction are approximately similar (21). In this case the small granules would have less lipid per unit area at the surface, and as such lipid inhibits swelling (35), they would therefore be expected to swell more.

The results presented in this section demonstrate differences in the crystallinity of starches from different wheat varieties that have contrasting swelling capacities. While the change in crystallinity may contribute to a change in swelling capacity, other mechanisms may also be responsible for the observed effects.

SECTION III

NUCLEAR MAGNETIC RESONANCE STUDIES

OF WHEAT STARCH PASTES.

III.1 Introduction

NMR spectroscopy has been used to study polymer and biological systems at a molecular level. This section of the thesis describes ^{1}H and ^{13}C NMR investigations of starch-water systems.

III.2 Literature review

^{1}H NMR spectroscopy is a powerful technique for studying the structure, mobility and degree of ordering of water molecules in biological systems (126-131). In general, water relaxation times and diffusion coefficients are lower than those for pure water and reflect the reduced mobility of hydrated or bound water in the system. Water molecules in the bound state exhibit distinctively different properties from those observed for free or bulk water. Furthermore, the behaviour of the bound water molecules has been shown by various investigators (132, 133) to depend strongly on the structure of the hydrated species.

In order to explain ^{1}H relaxation results from ^{1}H NMR experiments, models have been developed to interpret the variations of T_{1obs} and T_{2obs} in terms of exchange between bulk and bound water (134). These models relate the observable relaxation rates and populations to those of the bound and free water molecules. In many biological systems (132, 133) at least two ordered states of water have been shown using these models. In many of these cases, a 2-state model has been shown to be successful in explaining the relaxation data. However it has been stressed that (135) due to the complicated nature of many of the biological systems, these models are inadequate to draw conclusive inferences based on the relaxation data at a single frequency and a single temperature.

^{1}H NMR relaxation studies have been carried out on starch-water systems by a number of investigators (61, 136-138). Two states of water molecules have been observed in a fried product containing a high percentage of starch, characterised by their different mobilities (136). The relaxation behaviour of water molecules absorbed on intact starch granules have also been investigated (137). The existence of two states of water with different mobilities has been shown to be clearly evident. Other researchers have studied the relaxation behaviour of water protons during the gelatinisation of starch-water systems (61, 138). A marked change in the spin-spin relaxation time (T_2) has been observed during the process. Increases in mobility and hydration of the polymer chains, associated with the melting of the crystalline ordered structure of the starch granule, have been suggested for the variation. Similar observations have been reported for water protons relaxation behaviour using steady state NMR during gelatinisation (138). The line-width of the water signal of the starch suspension decreases with increasing temperature.

Measurements of diffusion constant of water have provided information concerning the degree of ordering of water molecules in various biological systems (139,140). The diffusion coefficient of water in macromolecular systems is slower than that found in pure free water. Various diffusion models have been developed to interpret the decrease in diffusion coefficient of water. For example, a direct binding and retardation of some small fraction of water present and from the increased diffusion paths transversed by the water molecules to bypass the macromolecules has been used (140). Other investigators have considered results in terms of an infinite network obstruction model (141). Although NMR provides an elegant technique for determining diffusion coefficients, only a few studies have been made on starch-water systems (142) employing this method of measurement.

The advent of Fourier Transform techniques has made possible the use of ^{13}C NMR spectroscopy as a means of studying the mobility of macromolecules and obtain information about their architecture in the network of various types of gels, such as those of polysaccharides (143-145). Notable success has been achieved, especially in elucidating the gel structure of a number of gelling systems including carrageenan (143), alginate (143), agarose (146) and gelatin (147). It has been shown that in the ^{13}C spectra of gross plant tissues containing starch, sharp resonances are not evident until the starch has been gelatinised (148).

III.3. Scope of the investigation and experimental approach

While there have been a number of studies on starch-water systems by NMR (61, 136-138, 142, 148), starch pastes have not been investigated. It has been suggested that the exchange-averaged spin-lattice relaxation times (T_1) and spin-spin relaxation times (T_2) of water can, in some cases, be related to the rheological properties of the system (131). It has also been shown that certain information such as the structure of macromolecules (140, 141) and the occurrence of restricted or limited diffusion process (149) can be obtained from diffusion measurements. These various possibilities were therefore investigated. Measurements were made of water ^{1}H relaxation times and diffusion coefficients in starch pastes formed from various wheat varieties having different rheological properties. ^{1}H measurements were also made on a pure amylopectin-water system in an attempt to confirm some of the results obtained for starch pastes.

The polysaccharide chain mobility of starch pastes made from various wheat varieties was further investigated by the use of ^{13}C NMR.

III.4 Theoretical principles of the NMR experiment

III.4.1. Quantum mechanical description

Nuclear magnetic resonance spectroscopy is based on the fact that the nuclei of most atoms behave as though they have spin angular momentum. The angular momentum is quantised and is governed by the spin quantum number I. It can adopt (2I + 1) orientations with respect to a reference direction, i.e.

$$P_Z = \hbar m_I \qquad [III.1]$$

where m_I = (+I, +I-1, ..., -I)

P_Z = angular momentum along a reference (z) direction

$\hbar$ = Planck constant /2π

As a consequence of spin and charge, these nuclei posses a nuclear magnetic moment (μ) given by

$$\mu_z = \gamma \hbar m_I \qquad [III.2]$$

where μ_z = nuclear magnetic moment along a reference (z) direction

γ = magnetogyric ratio (ratio of magnetic moment to angular momentum)

In the presence of an external field (B_o), applied along z direction, the components of μ_z have two possible energies given by

$E = - \gamma \hbar m_I B_o$ which for nuclei of spin ½ (I=½) becomes

$$= \pm \tfrac{1}{2} \gamma \hbar B_o \qquad [III.3]$$

Both nuclei investigated in the present study, i.e., ^1H and ^{13}C have spin ½. At equilibrium, nuclei are

distributed among the energy levels according to a Boltzmann distribution given by

$$P_{(m)} = \exp(-E_{(m)}/kT) / \mathcal{Z} \qquad [III.4]$$

where $\mathcal{Z} = \Sigma_m P_{(m)}$ and $P_{(m)}$ is the population of energy state $E_{(m)}$

In the case for ^1H in 1.4T magnetic field

$$P_{(\frac{1}{2})} = 0.5 + 2.4 \times 10^{-6}$$

$$P_{(-\frac{1}{2})} = 0.5 - 2.4 \times 10^{-6}$$

In other words, there is a small excess population in the lower energy state. This population distribution can be disturbed by irradiating with electromagnetic radiation of the appropriate frequency

$$\nu_0 = \Delta E/h$$
$$= \gamma\hbar B_0/h$$
$$= \gamma B_0/2\pi \qquad [III.5]$$

or $\omega_0 = 2\pi \nu_0 = \gamma B_0$ (rad s^{-1}) [III.6]

where ω_0 = Larmor frequency

III.4.2. Classical description

This is a more useful description for explaining the phenomena associated with pulsed NMR. By classical mechanics, the torque exerted on a spinning magnetic moment by a magnetic field inclined at an angle θ relative to the moment causes the nuclear magnetic moment to precess about the direction of the field with a frequency $\omega_0 = \gamma B_0$. For a macroscopic sample some of the spins will be orientated against the field direction ($m_I = -\frac{1}{2}$) and a small excess will be orientated along the field direction

($m_I = +½$). The summation of all the nuclear magnetic moments results in a net magnetisation along the field direction.

Application of a radio frequency pulse of frequency ω_o at right angle to B_o will appear as stationary in a frame rotating at ω_o (the rotating reference frame). On absorption of energy from B_1, the magnetic moment precesses about B_1 at an angular frequency given by

$$\omega_1 = \gamma B_1 \qquad [III.7]$$

In a time t (s), the angle through which the magnetisation vector will precess is given by

$$\theta = \omega_1 \cdot t$$
$$= \gamma B_1 \cdot t \qquad [III.8]$$

For $\Pi/2$ pulse, then

$$t = \Pi/2\gamma B_1$$
$$= 20\ \mu s \text{ for } ^{13}C \ (F\lambda - 60)$$

After the $\Pi/2$ pulse, the return to equilibrium of the magnetisation is characterised by two relaxation times T_1 and T_2. T_1 is the spin-lattice or longitudinal relaxation time and is the time constant for the restoration of equilibrium magnetisation along the Z axis. T_2 is the spin-spin or transverse relaxation time and is the time constant for the restoration of equilibrium magnetisation in the X, Y plane.

Since the NMR apparatus is normally arranged to examine magnetisation following an rf pulse along an axis perpendicular to B_o direction (i.e. in XY plane), the magnitude of M_{xy} determines the strength of the observed signal. It can be shown that (150) following a $\Pi/2$ pulse along the X-axis the decay of the x and y components of the magnitisation (FID) are given by

$$M_x(t) = M_o \exp(-t/T_2) \sin \omega_o t \qquad [III.9]$$

$$M_y(t) = M_o \exp(-t/T_2) \cos \omega_o t \qquad [III.10]$$

i.e. $M_{x,y} \rightarrow 0$ at $t \rightarrow \infty$

The free induction decay for Mx (FID) is shown in Figure III.1.

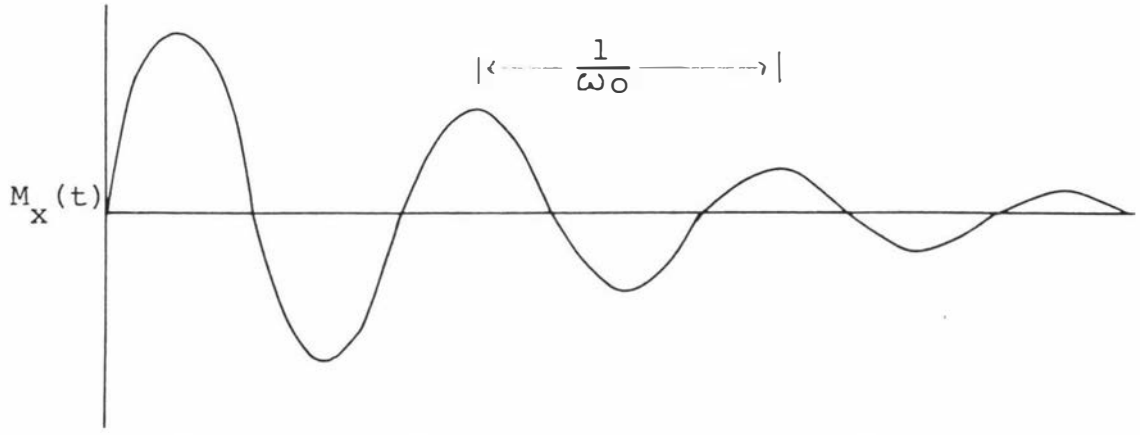

Figure III.1 Free Induction Decay (FID)

In practice the oscillation frequency of the FID is not ω_o but the difference between the r.f. irradiation frequency and the Larmor precessional frequency

i.e. $\omega = \omega_o - \omega_{rf}$. [III.11]

where ω = oscillation frequency

ω_o = Larmor frequency for nuclei under study

ω_{rf} = rf frequency (rotating frame frequency)

The time constant of the FID is T_2 if B_o is homogenous. Field inhomogeneity will cause a dephasing of $M_{x,y}$ since not all the nuclei will be precessing at ω_o. This will result in an apparent T_2^*, related to the time T_2 by

$$\frac{1}{T_2^*} = \frac{1}{T_2} + \frac{\gamma \Delta B_o}{2} \qquad [III.12]$$

where ΔB_o is the field spread over the sample volume. In order to overcome the problem of magnetic field inhomogeneity in the measurement of T_2, multipulse techniques have been evolved (151). The modified spin-echo technique by Hahn consists of the application of a 90^0_x, τ, 180^0_y sequence and the observation at a time 2τ of the

echo for a pulse separation (τ)$_{\text{this}}$ is given by

$$A \text{ (echo at } 2\tau) \propto \exp\left[-\left(\frac{2\tau}{T_2}\right) - \frac{2}{3}\gamma^2 G^2 D\tau^3\right] \qquad \text{[III.13]}$$

where G = magnetic field gradient

D = Diffusion coefficient

Provided that the second term can be ignored, a plot of lnA against 2τ will yield a straight line whose slope is $-1/T_2$. The spin-echo method is very much dependent on τ, so that the effect of diffusion becomes pronounced for large values of τ. Consequently the Carr-Purcell Meiboom-Gill technique (152) was evolved by using the pulse sequence $90^0_x - \tau - [180^0_y - \tau - \text{echo}]_n$. It can be shown that the magnitude of the echo at time t is

$$A \text{ (echo at t)} \propto \exp\left[-\left(\frac{t}{T_2}\right) - \frac{1}{3}\gamma^2 G^2 D\tau^2 t\right] \qquad \text{[III.14]}$$

It is apparent that by choosing τ short enough the diffusion term may in principle be made as small as possible, then a plot of lnA against t will give a straight line whose slope is $-1/T_2$.

The diffusion coefficients can also be determined as a special case of T_2 measurements. The magnitude of the spin-echo at 2τ in the absence of field gradient is (using Hahn echo sequence)

$$A_0 \ (2\tau) \propto \exp\left(-\frac{2\tau}{T_2}\right) \qquad \text{[III.15]}$$

In a fixed field gradient, the magnitude is given by Equation [III.13] . Thus

$$\frac{A}{A_0} \propto \exp\left[-\frac{2}{3}\gamma^2 D G^2\tau^3\right] \text{ at constant } \tau \text{ .} \qquad \text{[III.16]}$$

Provided G is known, D can be obtained from the slope of a plot of ln A/A_0 against $\gamma^2G^2\tau^3$. This is known as the steady field gradient technique and is limited in the dynamic range of D it can measure. A better technique, known as the pulse field gradient method has been developed (153). The experiment is described in Figure III.2 . It can be shown that (150) for such an experiment

$$\frac{A}{A_0} = \exp\left[-\gamma^2 G^2 \delta^2 D \left(\Delta - \frac{1}{3}\delta\right)\right] \qquad [III.17]$$

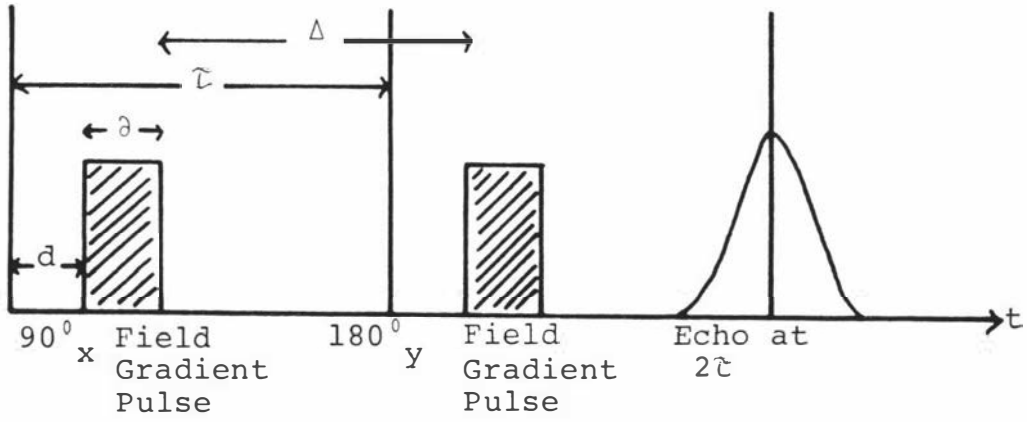

Figure III.2 Pulse Field Gradient method.

Then a plot of ln A/A_0 against $\gamma^2 G^2 \delta^2 (\Delta - \delta/3)$ will give a straight line whose slope is D. An additional advantage of pulse field gradient technique is that diffusion can be investigated over various diffusion times $(\Delta - \delta/3)$.

The evolution of M_z following a $\pi/2$ pulse is given by (150)

$$M_z(t) = M_0 \left(1 - \exp\left(-\frac{t}{T_1}\right)\right) \qquad [III.18]$$

T_1 relaxation times are usually measured by firstly applying a π pulse where

$$M_z(t) = M_0 \left(1 - 2\exp\left(-\frac{t}{T_1}\right)\right) \qquad [III.19]$$

and the evolution of M_z with time is depicted in Figure III.3

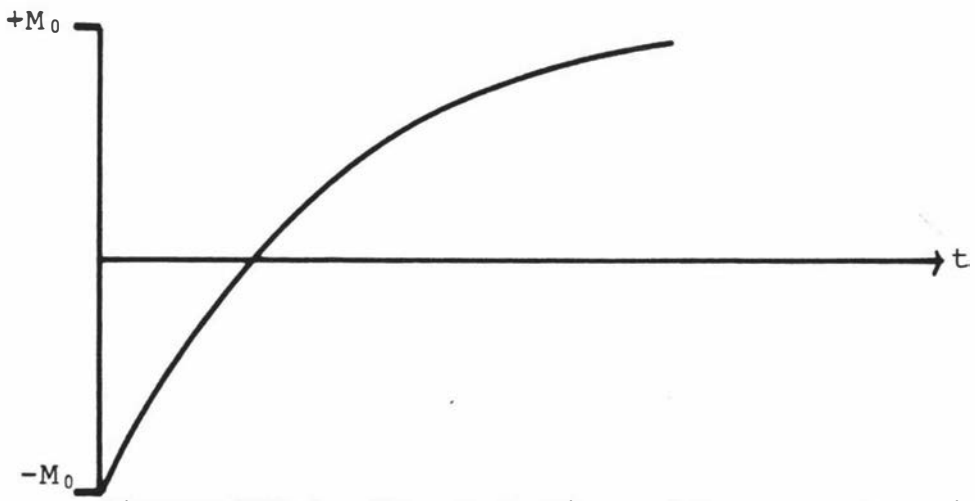

Figure III.3 The evolution of M_z as a function of time.

T_1's may be measured by the inversion recovery pulse sequence $180_x, \tau, 90_x$.

The magnitude of T_1 and T_2 depend on the mobility of the molecules which is usually measured by correlation time τ_c. τ_c can be regarded as the time interval during which fixed spatial relaxation of the nuclei can be expected. The connection between the relaxation times and the correlation time is depicted in Figure III.4. For small correlation times corresponding to high molecular mobility, T_1 and T_2 are equal. With increasing correlation time, T_1 goes through a minimum and T_2 decreases steadily and becomes constant for long τ_c.

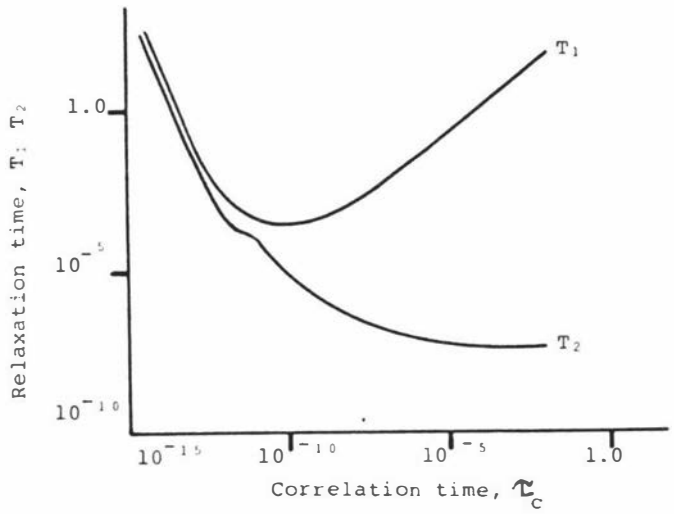

Figure III.4 The relationship between the ^1H relaxation times and the correlation time of water molecules.

In a system that contains several nuclei of the same species that differ in resonance frequencies because of chemical shifts and/or spin-spin couplings, a complex waveform called an interferogram is observed following an rf pulse. By performing a Fourier transform on the FID it is possible to separate the complex waveform into its frequency components.

The time constants (T_2) of the FID's appear as line widths at half-heights of the peaks in the frequency domain spectrum ($\Delta\nu_{\frac{1}{2}} = \frac{1}{\pi T_2}$). Similarly the initial amplitudes of the FID components which are proportional to the total number of spins are proportional to the total area under the corresponding peaks of the frequency domain spectrum.

III.5. Experimental

III.5.1. Apparatus

All measurements were made on the JEOL FX-60 spectrometer, a pulse Fourier Transform spectrometer operating at a constant field strength of 1.4 T. The pulse sequences for T_1 and T_2 were set up using the FX-60 computer software. The apparatus for pulse field gradient technique used for diffusion measurements was developed at Massey University (154). Temperature control was achieved through a thermocouple hot air feed-back system and temperatures were measured with a quartz-oscillator calibrated thermometer encased in an NMR tube. Temperatures were accurate to 0.5^0C over the sample volume.

III.5.2. Paste preparation

Pastes were formed as in I.5.2. for various wheat starches in the range of concentrations from 0.005g/g$H_2$0 to 0.08g/g$H_2$0. Samples of pastes were carefully transferred to NMR tubes and for the ^{13}C work the weights of the samples were recorded. Amylopectin samples were also prepared accordingly for a range of concentrations from 0.01g/g$H_2$0 to 0.12g/g$H_2$0.

III.5.3. Experimental procedure and treatment of data

For T_1 measurements, the spin-lattice relaxation for the ^{1}H nuclei of various starch pastes and the amylopectin-water system was observed by recording the initial height of the FID after the 90^0 pulse in a 180^0x, t, 90^0x pulse sequence as the pulse spacing (t) was varied. The amplitude (A) is directly proportional to the magnetisation (M) and from Equation [III.19] , for a 180^0x, t, 90^0x pulse sequence,

$$A = Ao\ (1 - 2 \exp - (^{t}/_{T_1})) \qquad [III.20]$$

i.e. $$A - Ao = - 2Ao \exp (-^{t}/_{T_1})$$

$$\ln (A-Ao) = - \ln 2Ao + {}^{t}/_{T_1}$$

or $$\ln (Ao-A) = - {}^{t}/_{T_1} + \ln 2Ao \qquad [III.21]$$

from which it can be seen that a plot of ln (Ao-A) against t will give a straight line of slope = $(-\frac{1}{T_1})$. Typical plots of ln (A_0-A) against t for the determination of T_1 are shown in Figure III.5.

Spin-spin relaxation times for the ^1H nuclei of various starch pastes and the amylopectin-water system were measured by the Carr-Purcell/Meiboom Gill technique (152) with 2Γ=8ms which is sufficiently small so that the second term in Equation [III.14] can be neglected. To evaluate the T_2 time constant, the intensity of the FID was plotted semi-logarithmically as a function of t and the spin-spin relaxation time was determined from the slope $(-\frac{1}{T_2})$. Typical plots of lnA against t for the determination of T_2 are shown in Figure III.6.

Diffusion coefficients of water molecules in various starch pastes and the amylopectin-water system were determined with the pulse-field gradient spin-echo technique of Stejskal and Tanner (153). It can be seen from Equation [III.17] that by keeping γ, ∂, and Δ constant, $^{A}/Ao$ will be a function of G and D only. G is proportional to the current (I) applied to the field gradient coils. A plot of ln $(^{A}/Ao)$ against I^2 gives a straight line shown in Figure III.7.

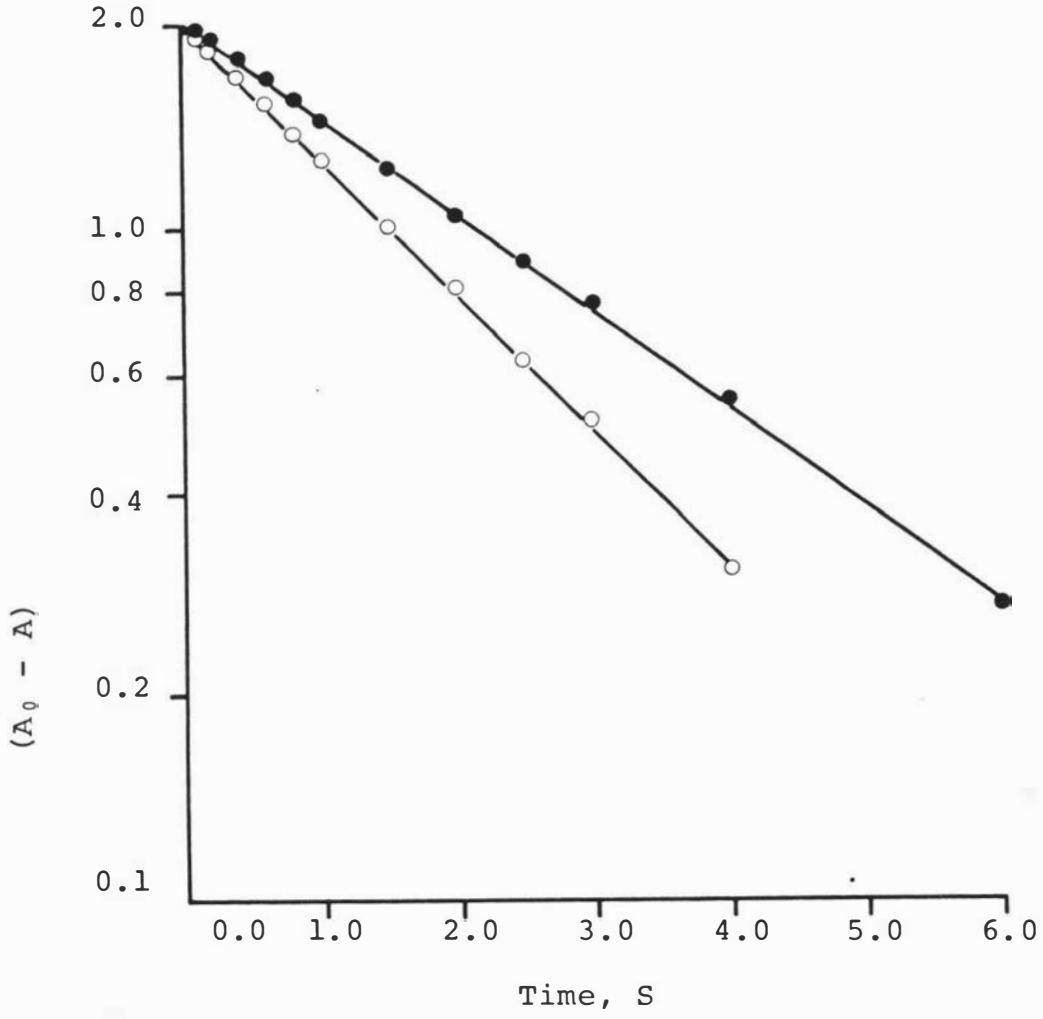

Figure III.5 Plots of ln (A_0 - A) against time for two concentrations of Gamenya starch pastes.

● 0.05g/gH_2O

○ 0.01g/gH_2O

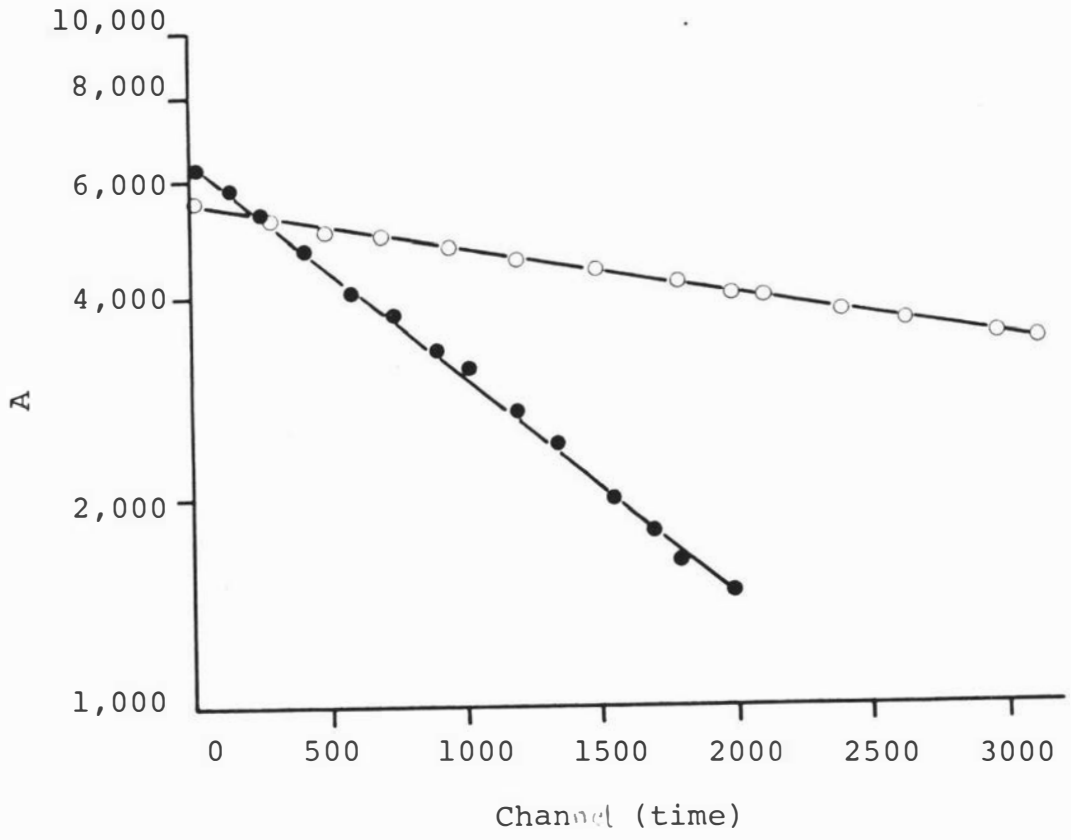

Figure III.6 Plots of ln A against time for two concentrations of Gamenya starch pastes.
● $0.01 g/gH_2O$
○ $0.075 g/gH_2O$

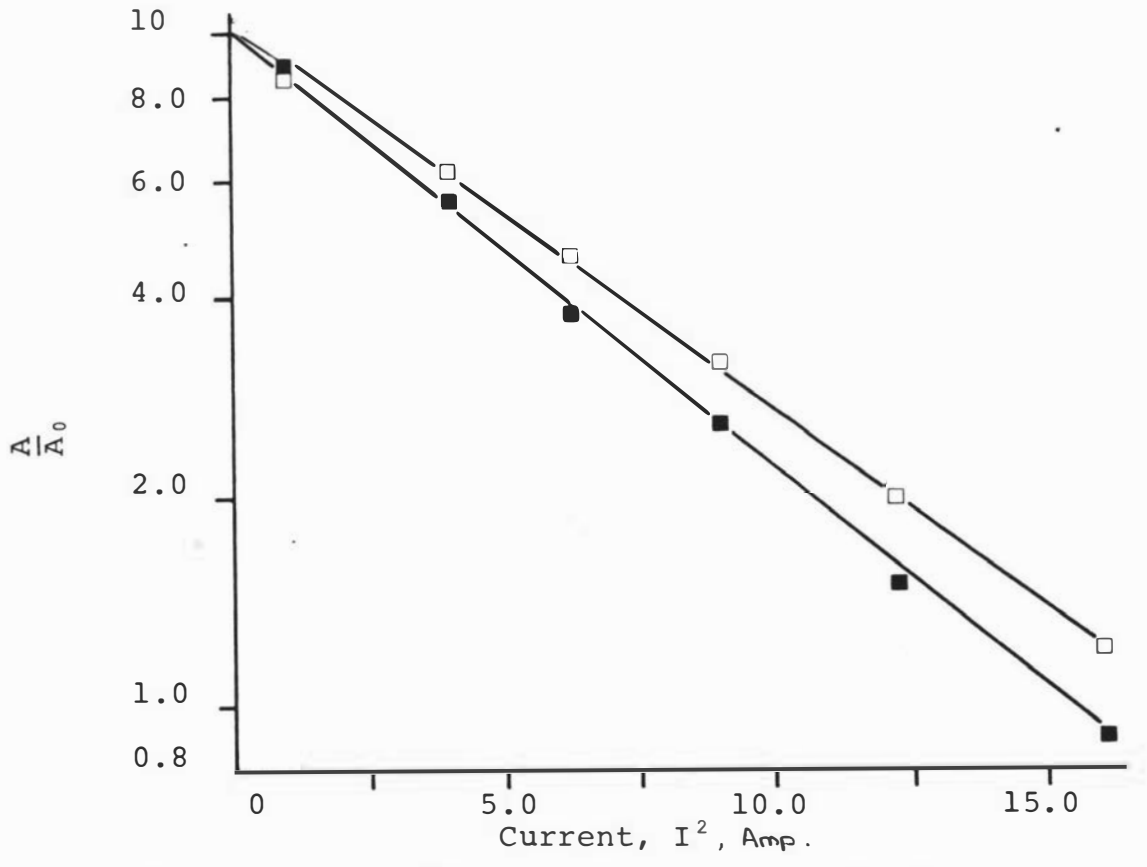

Figure III.7 Plots of ln $\frac{A}{A_0}$ against I^2 for two concentrations of Gamenya starch pastes.
□ $0.01 g/gH_2O$
■ $0.08 g/gH_2O$

The slope of this line is $-\delta^2 \gamma^2(\Delta - \frac{1}{3}\delta) D \times 1.6 \times 10^2$, where the factor 1.6×10^2 takes into account the constant of proportionality between I and G and the value of γ^2 for the proton. For δ and Δ in ms D has units of $cm^2 s^{-1}$. Hence D can be readily calculated. For determination of the concentration dependence of diffusion coefficient, Δ, δ, and repetition time were kept constant at 10 ms, 2 ms and 12 seconds respectively. By investigating the dependence of diffusion coefficient on field gradient pulse separation (Δ), it is possible to detect the occurrence, within the appropriate time scale, of restricted or barrier limited diffusion. For this determination, the field gradient pulse separation was varied from 10 ms to 560 ms, equivalent to a root mean square diffusion distance in the measuring direction from 7,000 nm to 50,000 nm.

Measurements of the signal attenuation upon freezing were made by recording the initial height of FID at temperatures of 258K and 303K. The ratio of the height at 258K to the height at 303K gave the fraction of non-freezing component.

Spectrum accumulation was necessary to observe the ^{13}C spectra of various wheat starch pastes and maltose solutions. The FID's following the 90^0 pulses (25 μs) were stored and accumulated in the computer. Repetition times greater than $5T_1$'s were used and the total number of accumulations depended on the starch concentration, as shown in Table III.1. The FID was then Fourier transformed. Typical FT ^{13}C NMR spectra for a wheat starch paste and a maltose solution are shown in Figure III.8. The total ^{13}C liquid signal was obtained by summation of all intensities under a spectrum.

Table III.1. Number of 90^0 pulses required for a satisfactory spectrum at various starch concentrations.

Starch concentration g/gH_2O	Number of accumulations
0.08	2,000
0.07	2,000
0.06	2,000
0.05	2,000
0.04	4,000
0.03	8,000
0.02	16,000
0.01	32,000

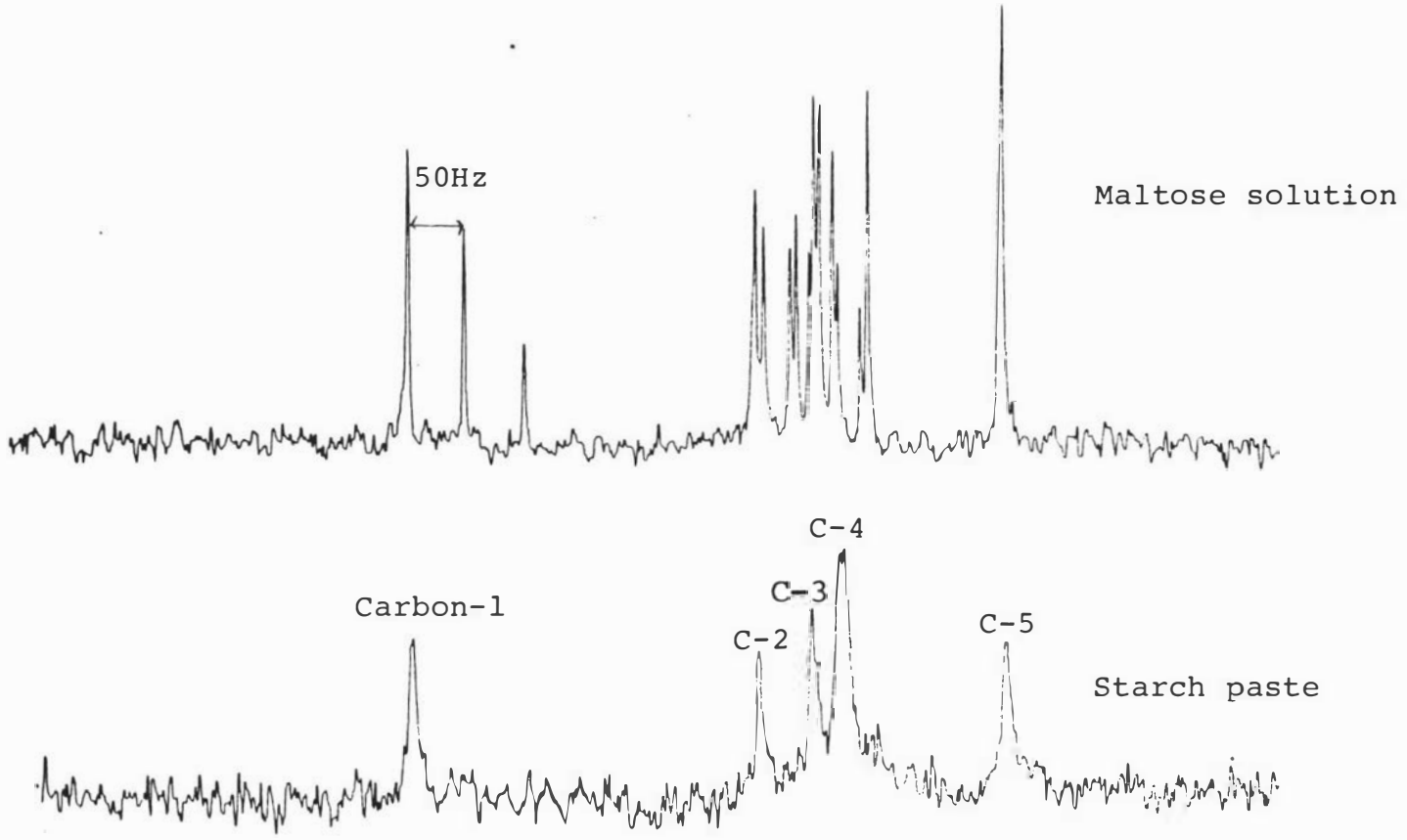

Figure III.8 Typical FT ^{13}C NMR spectra.

III.6. Results

III.6.1. FID signal attenuation upon freezing

Figure III.9 shows plots of the relative ^1H signal anplitude at 258 K against the starch concentration for Aotea and Gamenya wheat varieties. The relationship is linear (correlation coefficient = 0.979 and 0.970 for Gamenya and Aotea respectively) with zero intercepts. The gradients which correspond to the hydration coefficients (h) (130) give values of 0.347 and 0.331 g H_2O/g starch on a dry weight basis for Gamenya and Aotea wheat starches respectively. No significant differences were found for the slopes of the regression lines within the 95.0% confident limits.

Figure III.10 shows a plot of the relative ^1H signal amplitude at 258 K against the amylopectin concentration. A slope of 0.254g H_2O/g amylopectin which corresponds to the hydration coefficient of the polysaccharide is obtained. The lower extent of hydration as compared with starch molecules probably arises from an increase in the overall branching per unit mass of polymer.

The non-freezable water, observed in frozen starch pastes and amylopectin samples is attributed to water associated with the polysaccharide chains. These water molecules are unable to participate in the formation of an ice-like lattice.

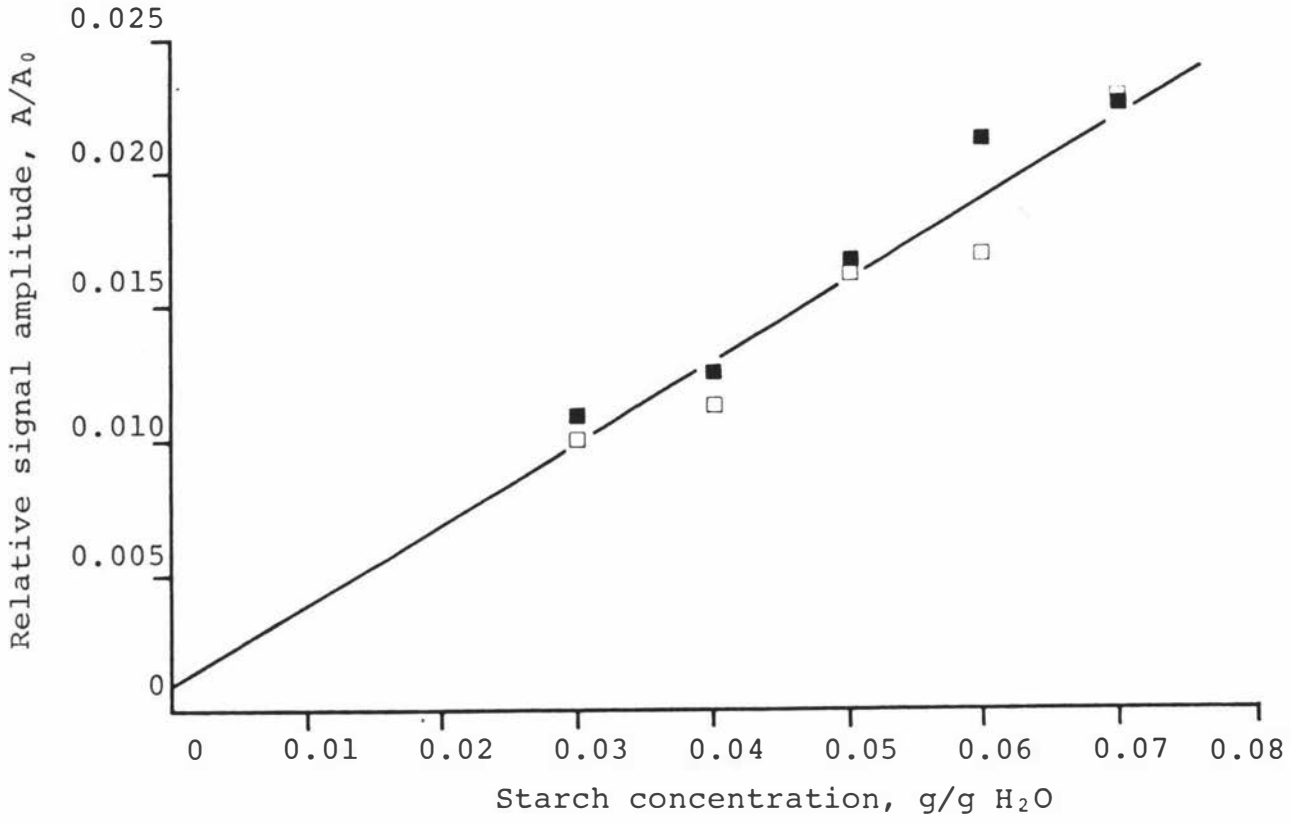

Figure III.9 Plots of the relative ^1H signal amplitude of pastes at 258K against the starch concentration for Aotea (□) and Gamenya (■) wheat varieties.

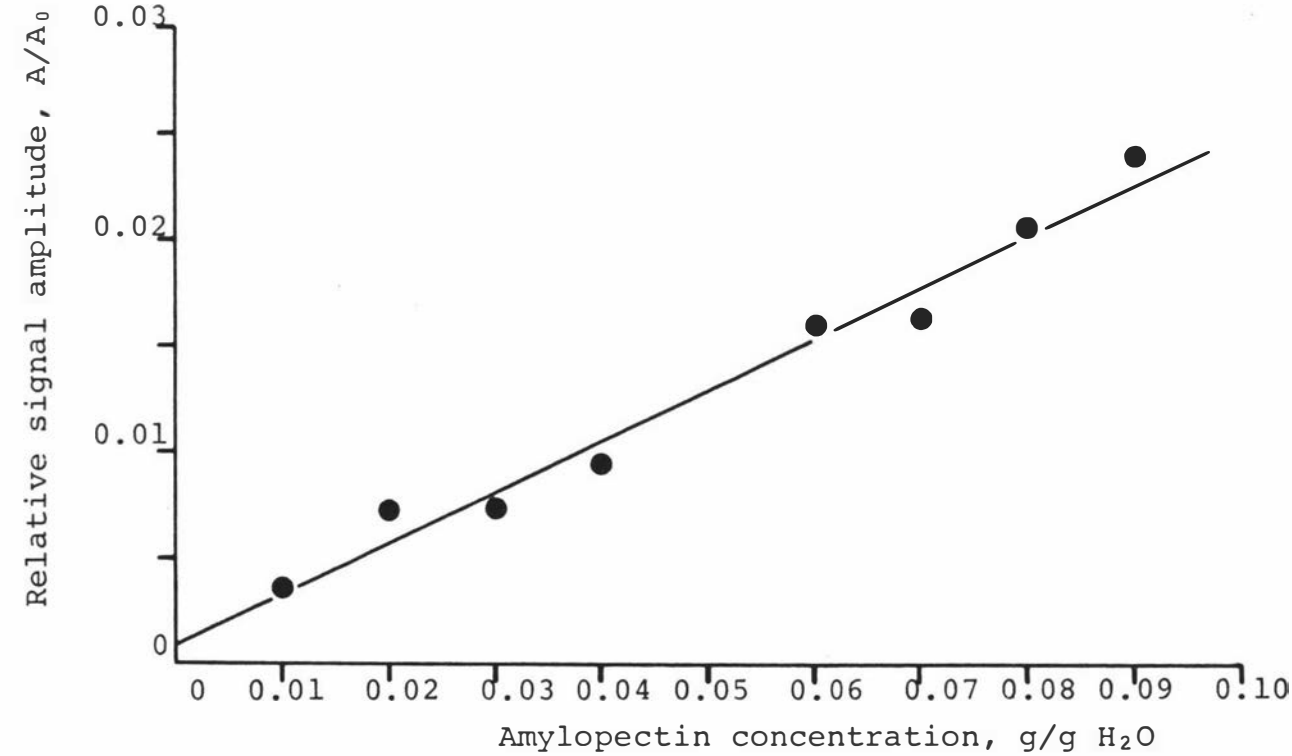

Figure III.10 Plot of the relative ^1H signal amplitude at 258K against the amylopectin concentration for the amylopectin - water system.

III.6.2. Self-diffusion

The concentration dependence of water diffusion coefficient (D) in starch pastes made from Aotea and Gamenya wheat varieties is shown in Figure III.11. Statistical analysis of the experimental results show that the differences in diffusion coefficients between the two starches are not significant within the 95.0% confidence limits. In an effort to detect the occurrence of restricted diffusion, D was measured for a range of Δ values between 10 and 560 ms. It was found that D did not change significantly up to 560 ms, equivalent to a root mean square distance travelled by water molecules of 50,000 nm, that is, water molecules diffused 50 μm without significant restriction on its patch and thus no restricted diffusion was indicated. The fact that diffusion coefficients for starch pastes are only slightly less than that for pure water for the concentration range studied indicates that a major portion of water molecules are not in the bound or modified state.

Figure III.12 shows a plot of the concentration dependence of diffusion coefficient of water in the amylopectin-water system. These experimental results are similar to those obtained for the starch-water system, indicating that diffusional processes in both systems are similar.

The problem of diffusion in a complex system has been treated quantitatively by Wang (140) and Mackie and Meares (141). Wang discussed two mechanisms that decrease the observed D below that of pure water, the "obstruction effect", which is caused by the longer path transversed by water diffusing around the macromolecules and the "direction hydration and obstruction effect", which arises because some water molecules spend part of the time in the slowly moving "hydration layer" of the macromolecules. Mackie and Meares treated the analogous problem as an infinite network of obstruction medium. Mathematically, these obstruction models are represented by the following equations:-

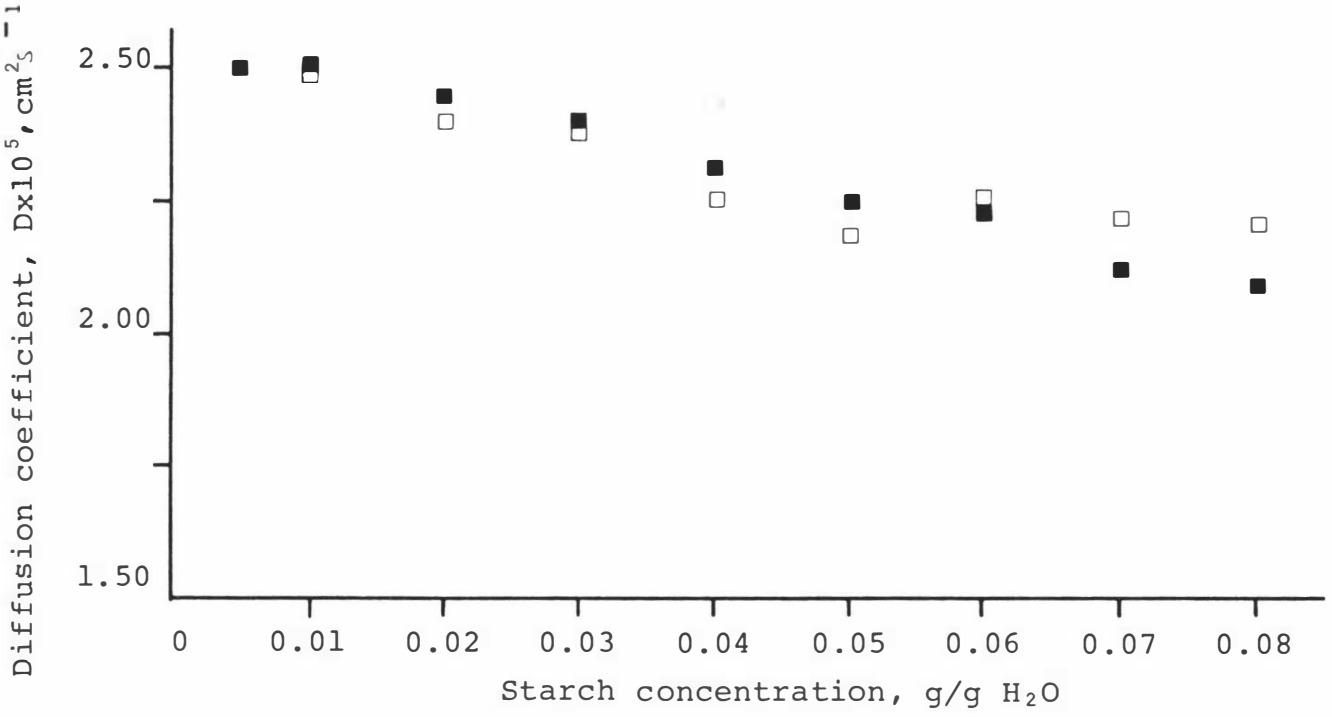

Figure III.11 Plots of the diffusion coefficient of water in pastes against the starch concentration for Aotea (□) and Gamenya (■) wheat varieties.

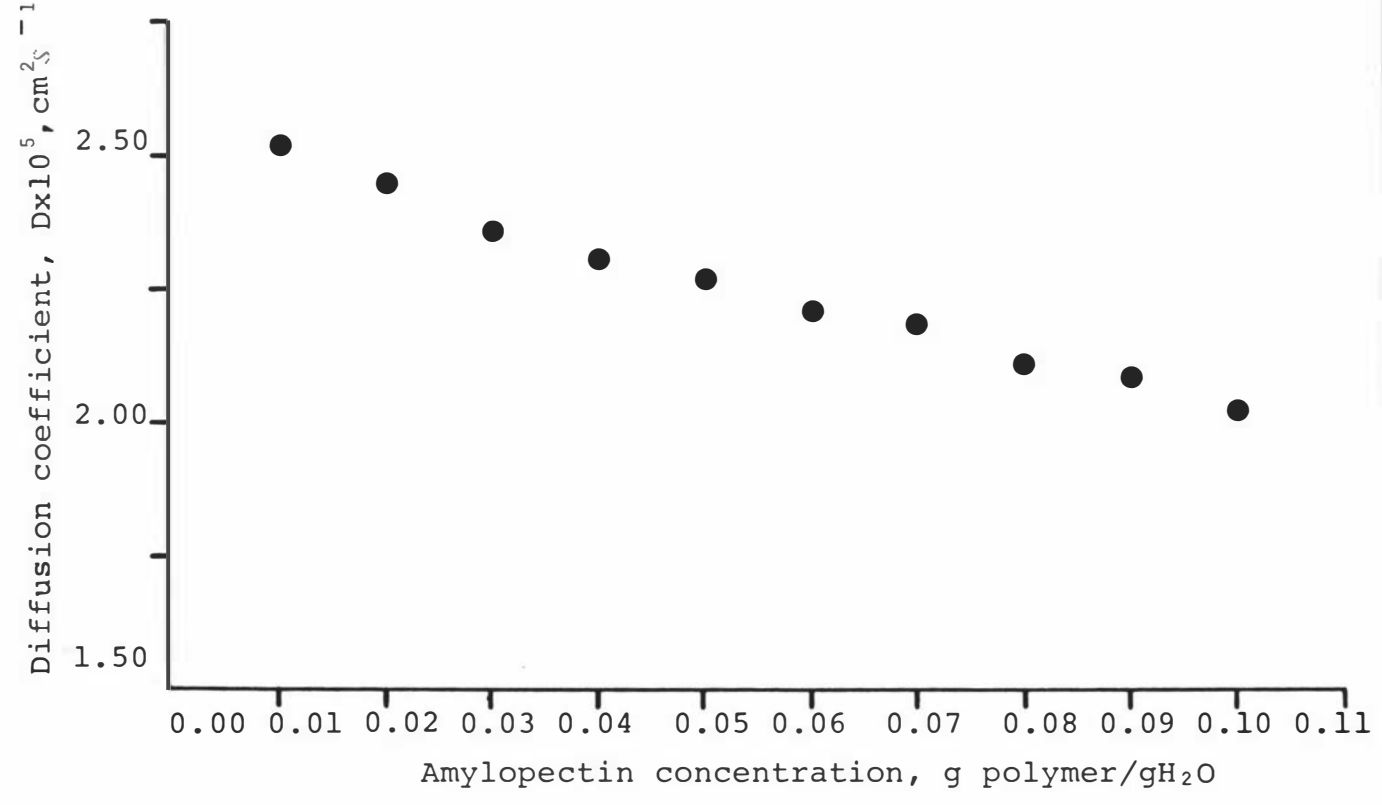

Figure III.12 Plot of the diffusion coefficient of water in the amylopectin-water system against the amylopectin concentration.

$$\frac{D}{D_0} = 1 - 1.5\,\phi \qquad \text{[III.22]}$$

Wang "obstruction effect" model.

$$\frac{D}{D_0} - \Delta_1 = 1 + \Delta_2 - \left[\bar{\mathcal{L}}(\bar{V}_\rho\, d_0 + h)\quad h\right] W \qquad \text{[III.23]}$$

Wang "direct hydration and obstruction" model

$$\frac{D}{D_0} = \left(\frac{1-\phi}{1+\phi}\right)^2 \qquad \text{[III.24]}$$

Mackie and Meares "infinite obstruction effect" model.

D_0 = Diffusion coefficient of pure water
ϕ = Volume fraction of polymer
$\bar{\mathcal{L}}$ = shape factor for polymer
$\bar{V}_\rho$ = apparent specific volume of dry polymer
= $^1/$ density of dry polymer
d_0 = density of pure water
h = hydration coefficient
W = weight fraction of dry polymer

$$\Delta_1 = \frac{\bar{\mathcal{L}}\,\bar{V}_\rho d_0\,(\bar{V}_\rho d_0 - 1)W^2}{1 + (\bar{V}_\rho\, d_0 - 1)\,W} \qquad \text{[III.25]}$$

$$\Delta_2 = \left[\frac{\bar{\mathcal{L}}h\,(\bar{V}_\rho\, d_0 - 1)}{1+(\bar{V}_\rho\, d_0 - 1)\,W} - \frac{h}{1-W} + \frac{\bar{\mathcal{L}}(\bar{V}_\rho + h)}{1 + (\bar{V}_\rho\, d_0 - 1)W(1-W)}\right] W^2 \qquad \text{[III.26]}$$

It may be noticed from Equations [III.25] and [III.26] that the magnitude of both Δ_1 and Δ_2 increase with polymer concentration. However, it can be shown that (Appendix IIIa), even for the most concentrated starch paste, the magnitudes of Δ_1 and Δ_2 are still very small as compared to the other terms in Equation [III.23] Thus over the concentration range of this study, Δ_1 and Δ_2 may be neglected, so that Equation [III.23] reduced to:

$$\frac{D}{D_0} = 1 - \left[\bar{\mathcal{L}}(\bar{V}_\rho\, d_0 + h) + h\right] W \qquad [III.27]$$

Figure III.13 shows a plot of the experimental results (D/D_0) for Gamenya starch pastes against the volume fraction of polymer ($\emptyset$). The theoretical models of Wang "obstraction effect" and Mackie and Meares "infinite obstruction effect" are shown as straight lines in Figure III.13. It can be seen that the Wang "obstruction effect" model cannot account for the observed behaviour. Neither the results can be fitted to the Wang "hydration only" model (140). For example, at a starch concentration of 8%, the experimental value of D/D_0 is 0.825 compared with the theoretical value of 0.97. Mackie and Meares "infinite obstruction effect" theoretical values give a better fit but is consistently below that of the experimentally determined values.

The experimental results were then fitted to the Wang "direct hydration and obstruction effects" model as shown in Figure III.14. The linear relationship between the experimental results and the weight fraction of dry polymer is encouraging. From Equation [III.27] it can be seen that the slope of the best fit line is $-\left[\bar{\mathcal{L}}(\bar{V}_\rho\, d_0 + h) + h\right]$ where $\bar{V}_\rho$ is 0.645 and the

hydration coefficient h is 0.34 g H_2O/g dry starch as determined by freezing experiments. Linear regression analysis of the results in the form of Equation [III.27] gives the least squares slope of -2.64 $\pm$ 0.13. This gives a best fit $\bar{\ell}$ value of 2.3 $\pm$ 0.1. This value of $\bar{\ell}$ indicates that water is diffusing through oblate ellipsoids (140) with axial ratios of 6.0 to 1.0.

Figure III.15 shows a plot D/D_0 for the amylopectin-water system as a function of the weight fraction of dry polymer. Linear regression analysis of the results gives the least squares slope of -2.5 $\pm$ 0.10. This gives a best fit $\bar{\ell}$ value of 2.6 $\pm$ using a $\bar{V}_p$ of 0.62 (155) and an h of 0.255 g/g amylopectin (freezing experiments). This value of $\bar{\ell}$ for amylopectin molecules indicates that water is diffusing through oblate ellipsoids with axial ratios of 8.0 to 1.0 (140).

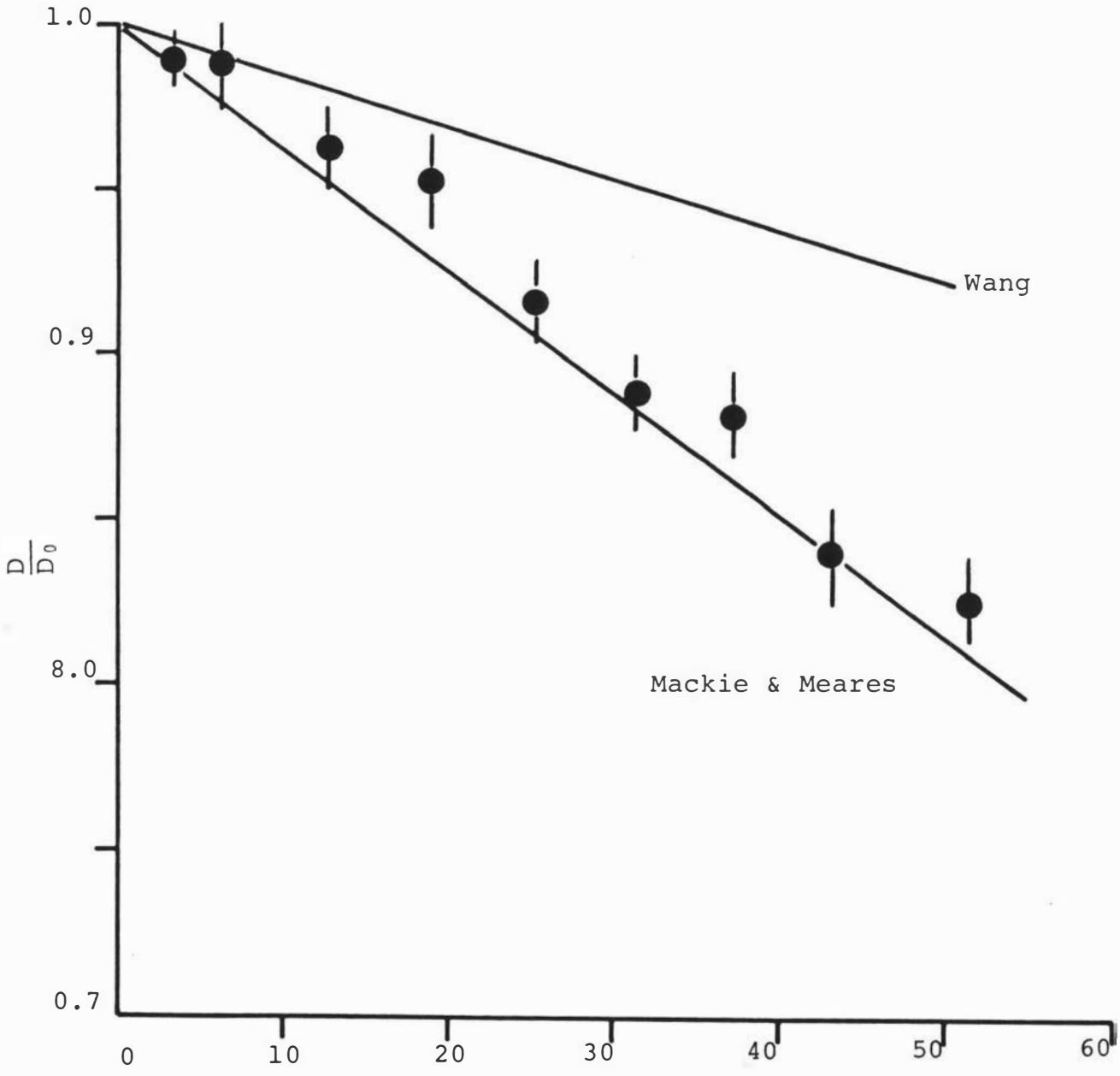

Figure III.13 Plot of $\frac{D}{D_0}$ as a function of the volume fraction of polymer (Ø) for Gamenya starch pastes.

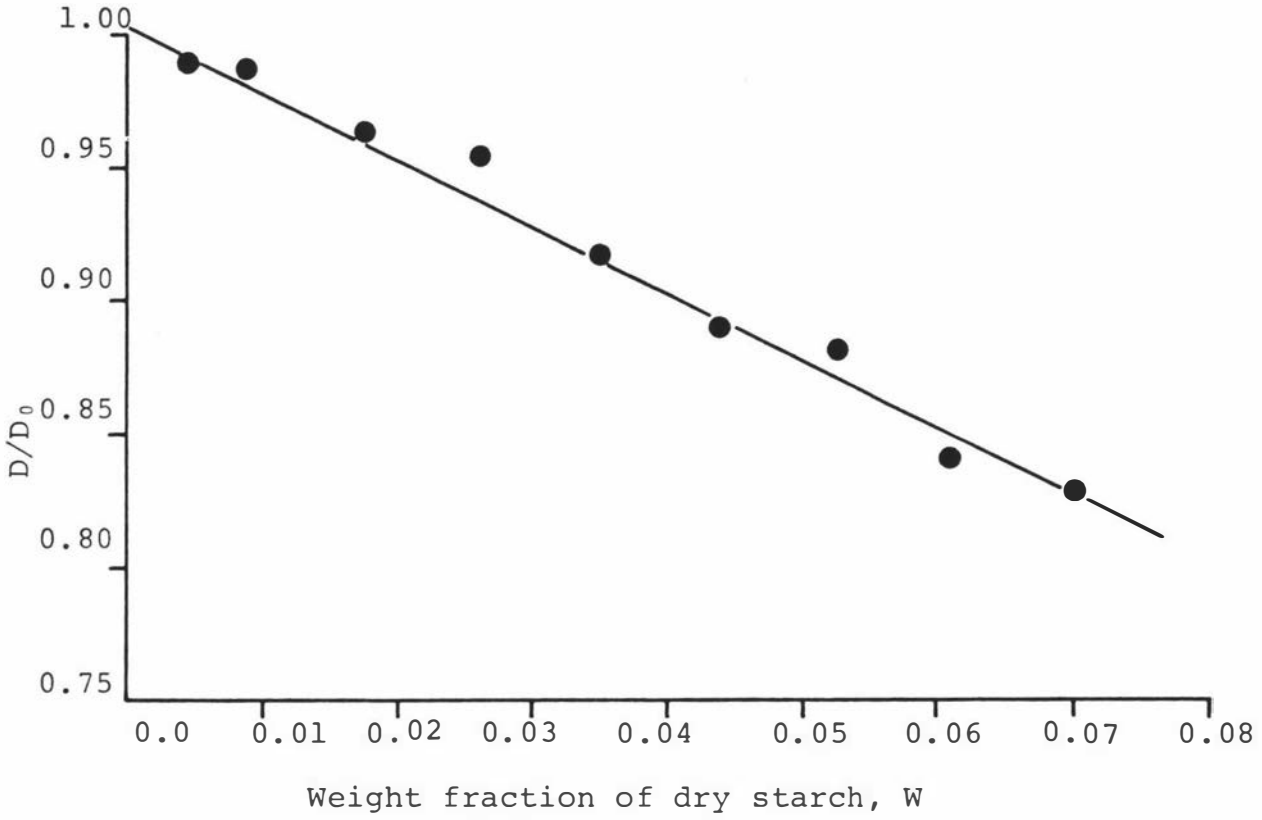

Figure III.14 Plot of D/D_0 as a function of the weight fraction of Polymer (W) for Gamenya starch pastes.

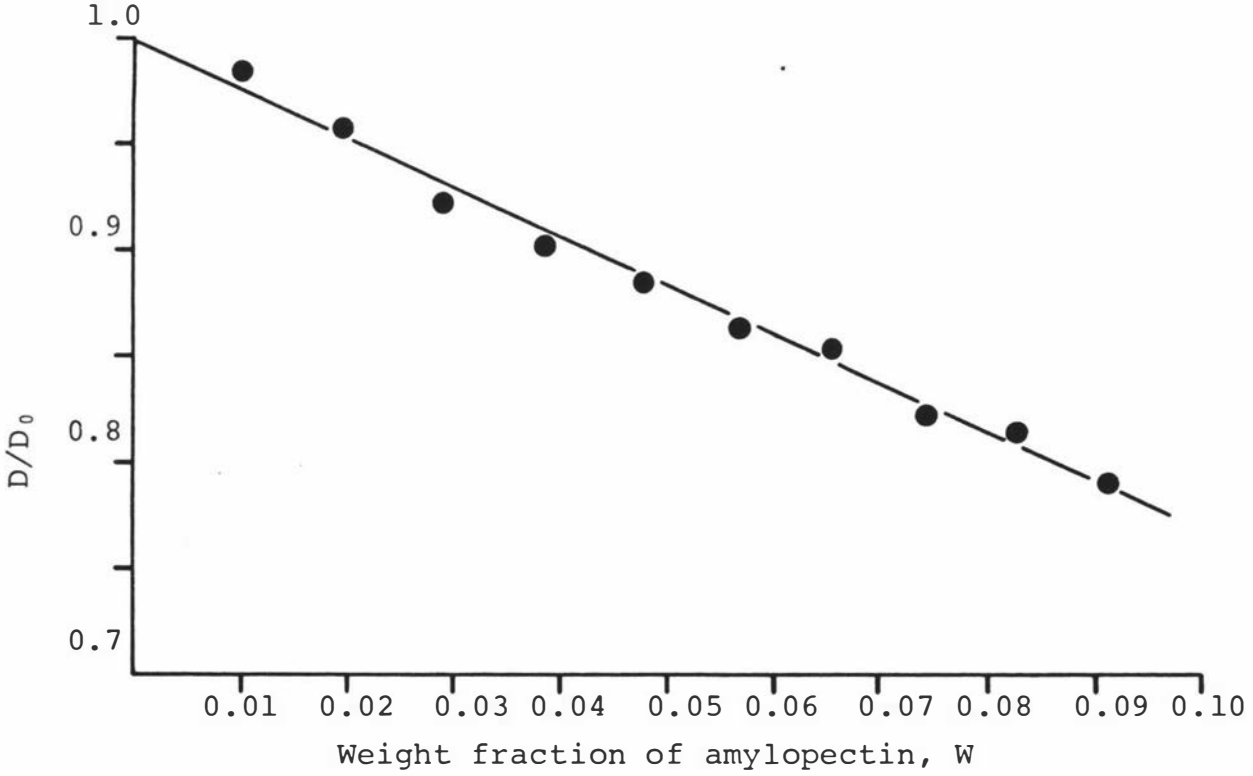

Figure III.15 Plot of D/D_0 as a function of the weight fraction of polymer (W) for the amylopectin-water system.

III.6.3. Spin-lattice and spin-spin relaxation times

Figure III.16 shows the ^1H relaxation times, T_1 and T_2 of pastes made from Aotea and Gamenya wheat varieties as a function of the starch concentration at 30.0^{0}C while Figure III.17 shows the corresponding data for the amylopectin-water system. The T_1 values of both starch pastes and amylopectin samples are slightly less than that of pure water but are still relatively long at higher concentrations, indicating only small changes from bulk water behaviour.

The contrasting shape for T_2 behaviour shows clearly that different factors are affecting the T_1 and T_2 relaxation behaviour in both starch-water and amylopectin-water systems. The T_2 values fall rapidly in the initial stages and then begin to level off. The results also show that both starch pastes and the amylopectin-water system have T_2 relaxation times of the order of 100 ms at higher concentrations. In the intermediate range, starch pastes have longer T_2 values, this is probably an effect of the presence of linear and lower molecular weight amylose fraction in the starch molecules. The characteristic T_2 relaxation behaviour exhibited by starch pastes and the amylopectin-water system has been observed for other systems such as agarose gels (129).

The minor differences in the T_1 values for pastes made from Aotea and Gamenya wheat starches are probably not real. T_1 measurements were repeated for pastes made from Karamu and Raven wheat starches, which also have contrasting rheological properties, at concentrations of 2% and 6%, but no significant variation was obtained. There are also no significant differences in the T_2 values for pastes made from Aotea and Camenya wheat starches. It is therefore evident that T_1 and T_2 are not very useful in characterising the differences in rheological behaviour of starch pastes made from various wheat sources.

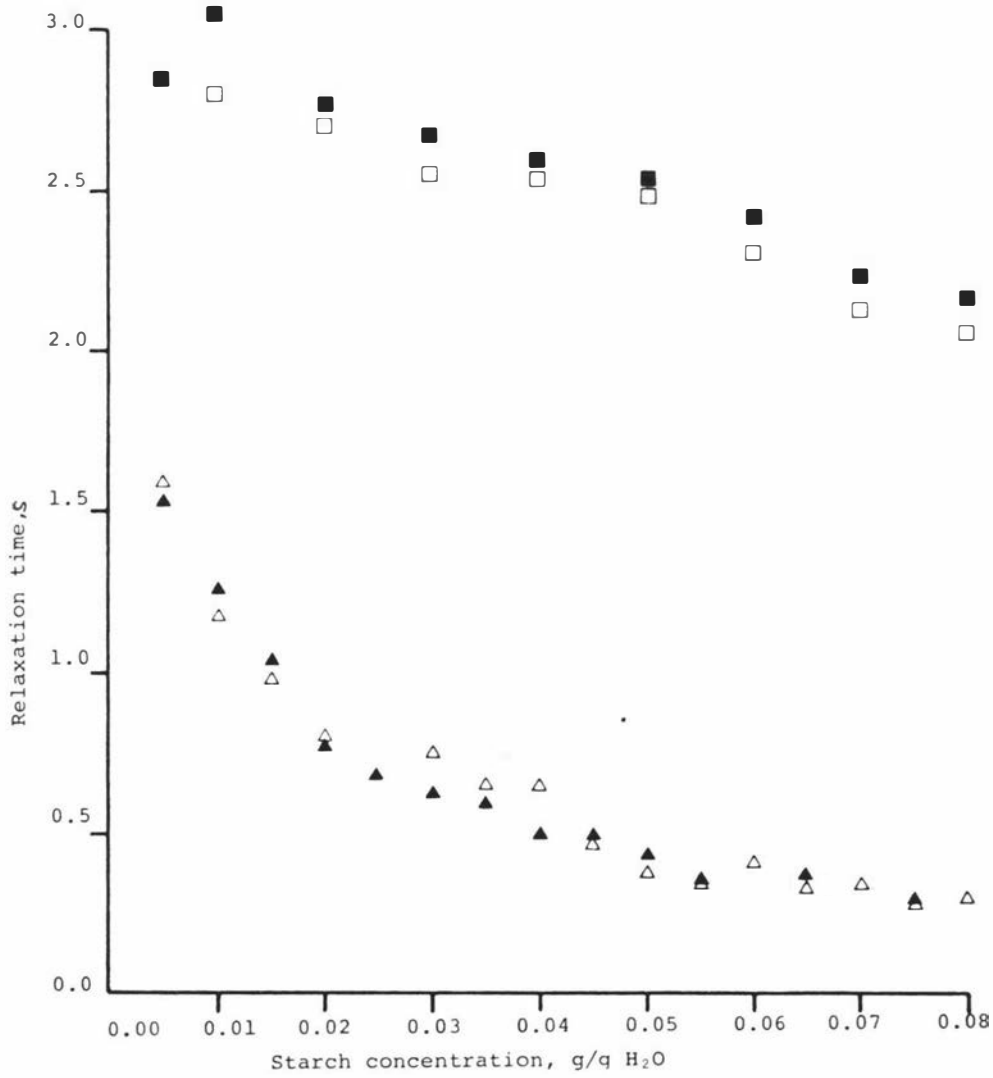

Figure III.16 Plots of T_1 and T_2 of ^1H in pastes made from Aotea (□ ,△) and Gamenya (■ ,▲) wheat varieties as a function of the starch concentration.

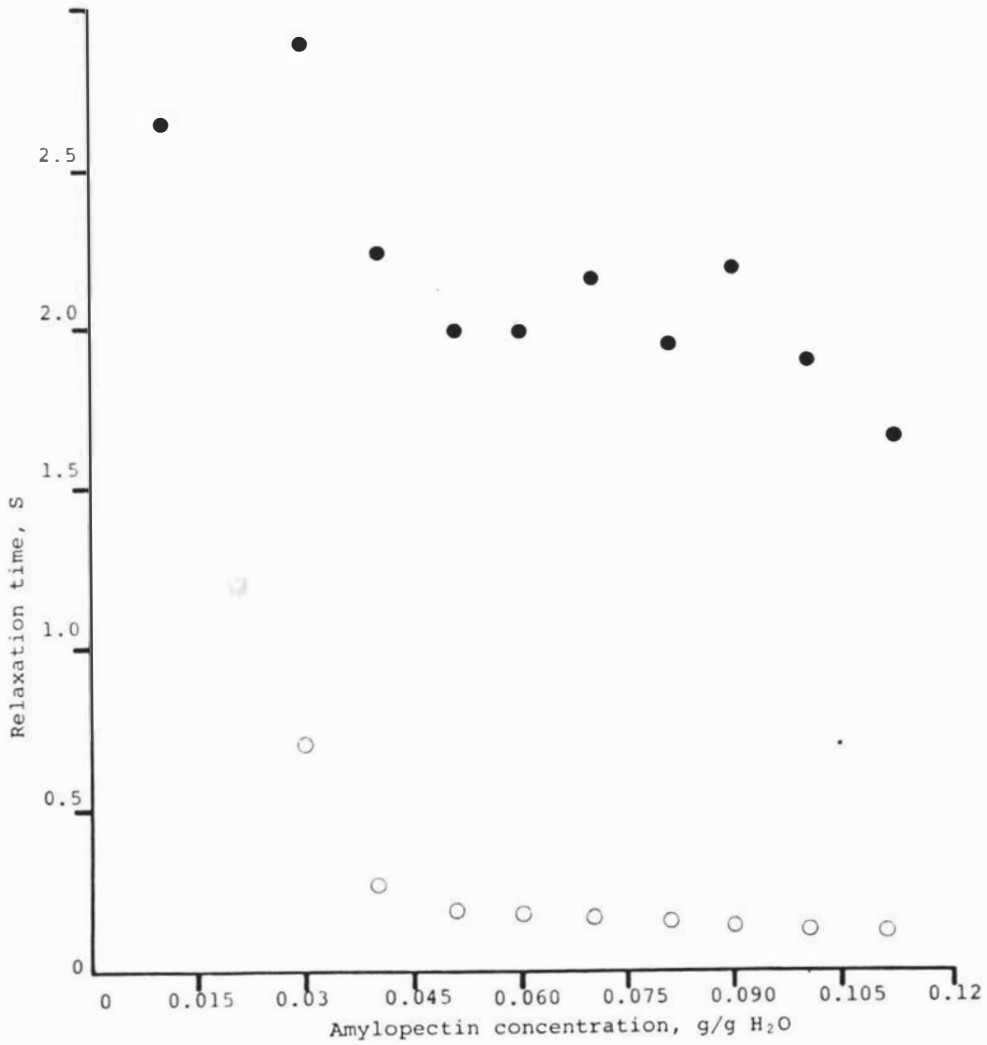

Figure III.17 Plots of T_1 (●) and T_2 (○) of ^1H in the amylopectin-water system as a function of the polymer concentration.

The T_1 and T_2 magnetisation recovery curves for both starch pastes and amylopectin samples were observed to be single exponential functions (see typical results in Figures III.5 and III.6), indicating that there is only one type of water present or that they are two or more types of water in the sample with rapid molecular exchange between different sites such that an average relaxation time is observed (129). Evidence from the FID attenuation upon freezing suggests that the latter explanation is the most probable cause. Evidence from the diffusion measurements also indicates that most of the water has a mobility equal to that of pure water and there exists only a small fraction of bound water molecules of which they may be many types, which has a much lower mobility (127). This minor fraction of water can alter molecular properties because of its strong interaction with the starch polymer and the amylopectin molecule, as has been observed to be the case with other polymer systems (127).

Expressions have been developed relating the observable relaxation rates and populations to those of the free and bound sates for all rates of exchange between different sites. If $\left(\frac{1}{T}\right)_{obs}$ were to be composed of a number of components of bound water in rapid exchange with free water, then (134)

$$\frac{1}{T_{obs}} = \frac{P_f}{T_f} + \Sigma \left(\frac{P_{bi}}{T_{bi}}\right) \qquad [III.28]$$

$$P_f + \Sigma P_{bi} = 1$$

b & f refer to bound and free species respectively
P is the mole fraction
i is the i^{th} component of the population of bound water
For a two-state model, Woesnner and Zimmerman (156) and Derbyshire and Duff (130) have shown that

$$\frac{1}{T_{obs}} = \frac{1}{T_f} + \frac{hc}{1-hc}\left(\frac{1}{T_b + \tau_c}\right) \qquad [III.29]$$

where Tb is the relaxation time of bound water molecules, τ_c is the correlation time, describing the average time that a water molecule stays in the bound phase, c is the polymer concentration and h is the hydration coefficient of polymer. T can be spin-lattice relaxation time or spin-spin relaxation time.

Plots of $\left(\frac{1}{T_1 obs}\right)$ and $\left(\frac{1}{T_2 obs}\right)$ against $hc/(1-hc)$ for pastes made from Aotea and Camenya wheat starches are shown in Figures III.18 and III.19 respectively. The excellent fits of the results of the linear regression analyses (r = 0.97, 0.97) show that the data fits the two-state model well. The straight line relationship also indicates that there is no change in hydration behaviour within the concentration range examined. Figures III.20 and III.21 give plots of $\left(\frac{1}{T_1 obs}\right)$ and $\left(\frac{1}{T_2 obs}\right)$ against $(hc/1-hc)$ for the amylopectin-water system. Linear relationships were also observed (r=0.95, 0.91). Table II.2 summarises the results of linear regression analyses of both starch pastes and the amylopectin-water system.

Table III.2 Values of regression coefficients of the fits of experimental results in Figures III.16 and III.17 to Equation [III.29]

Wheat variety used to prepare starch	T_1f s	$(T_1b+\Gamma c)$ ms	T_2f s	$(T_2b+\Gamma c)$ ms
Aotea	3.1 ± 0.3	180 ± 18	2.5 ± 0.1	8.8 ± 0.4
Gamenya	3.8 ± 0.3	216 ± 16	2.5 ± 0.1	8.9 ± 0.4
Amylopectin	2.9 ± 0.4	120 ± 15	2.7 ± 0.4	3.3 ± 0.5

From Table III.2, it can be seen that the values of T_1f and T_2f of water protons in starch pastes estimated from the intercepts of lines in Figures III.18 and III.19 are comparable to those of pure water which has a value of 2.60s and 2.60s for T_1 and T_2 respectively (157). The T_1f and T_2f values obtained for water protons in the amylopectin-water system are also similar when compared with those of pure water. The T_1b and T_2b values obtained for water protons in the amylopectin-water system are shorter than those of the starch-water system.

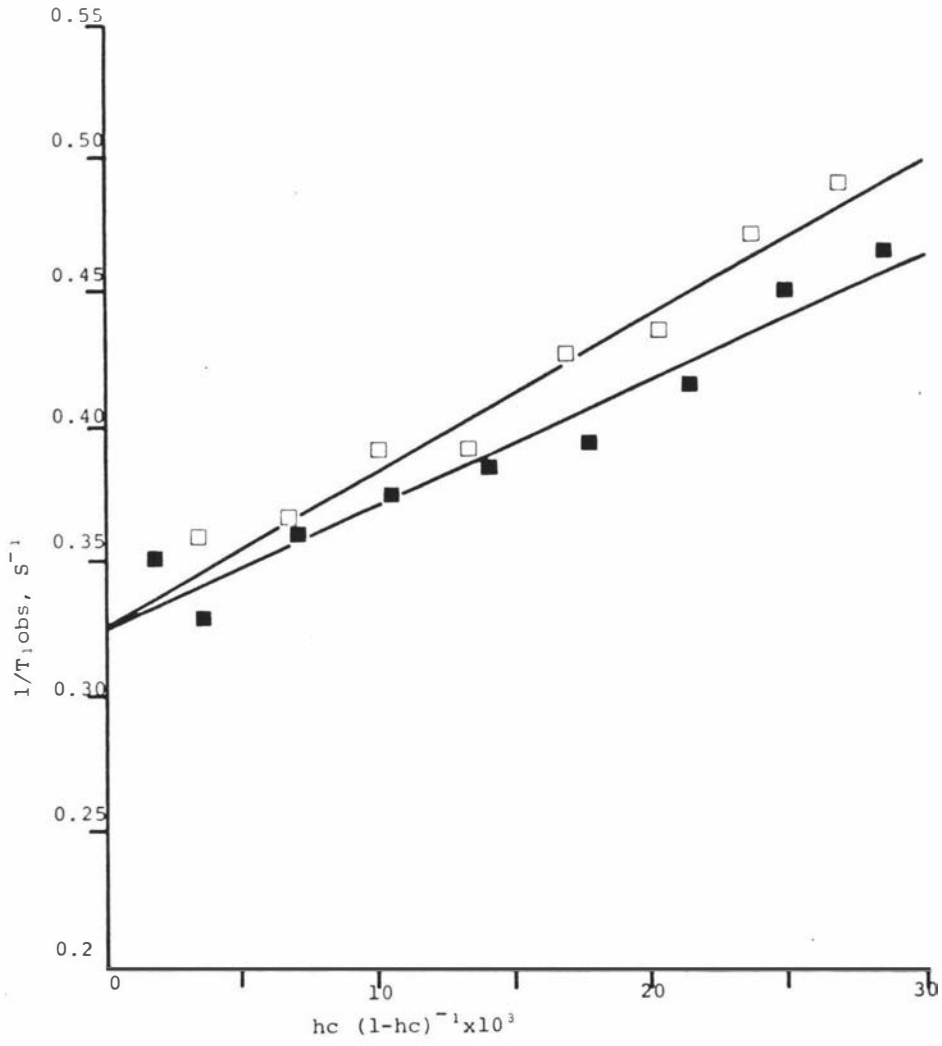

Figure III.18 Plots of $1/T_1$obs of ^1H in pastes made from Aotea (□) and Gamenya (■) wheat starches as a function of (hc/1-hc).

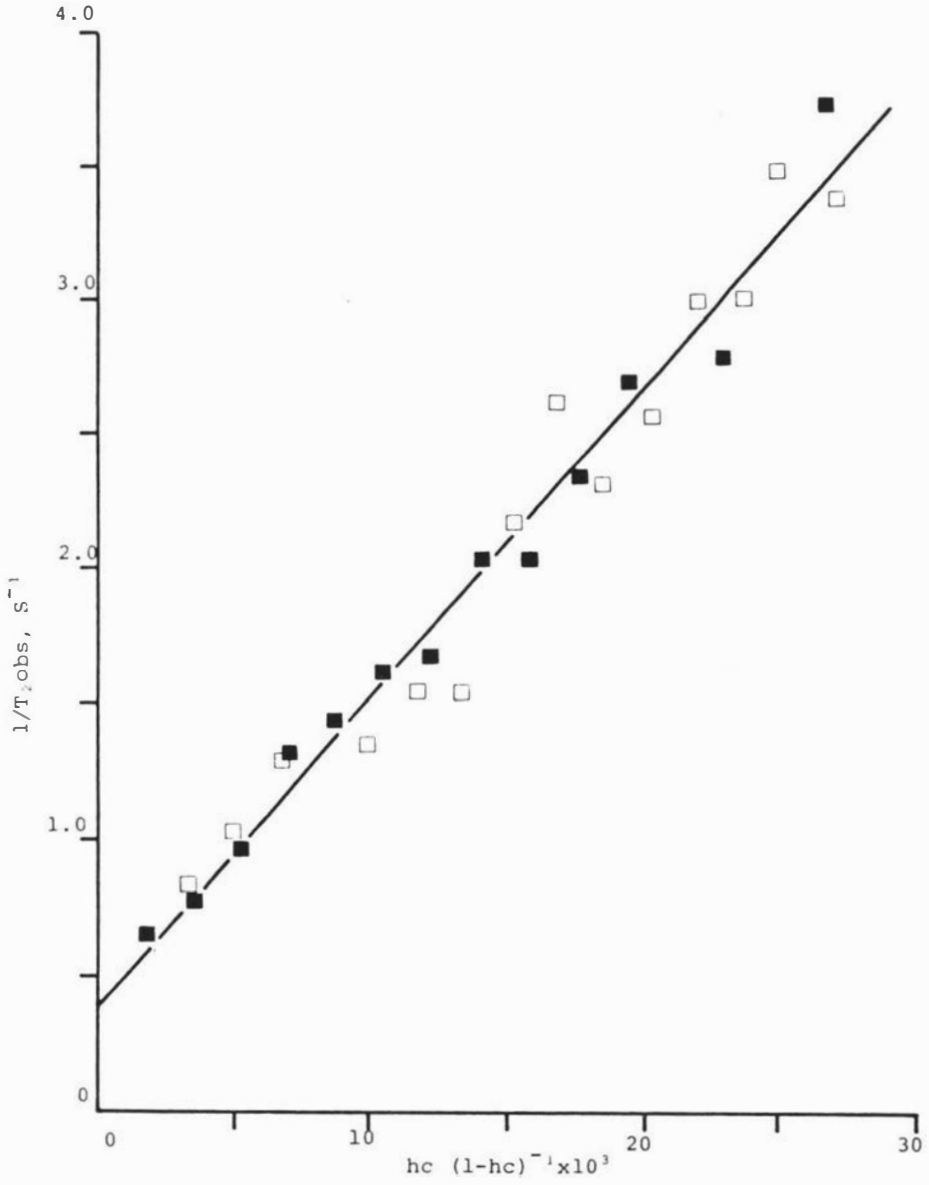

Figure III.19 Plots of $1/T_2$obs of ^1H in pastes made from Aotea (□) and Gamenya (■) wheat starches as a function of (hc/1-hc).

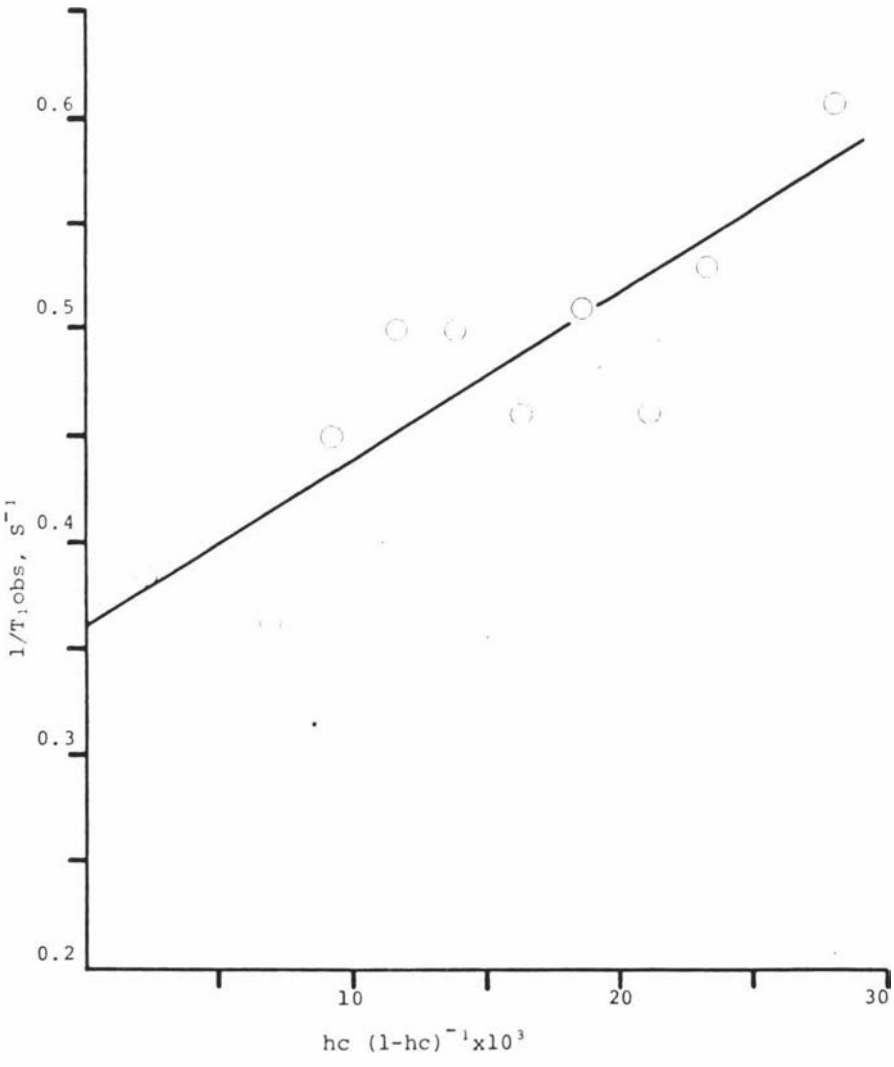

Figure III.20 Plot of $1/T_1$obs of ^1H in the amylopectin-water system as a function of (hc/1-hc).

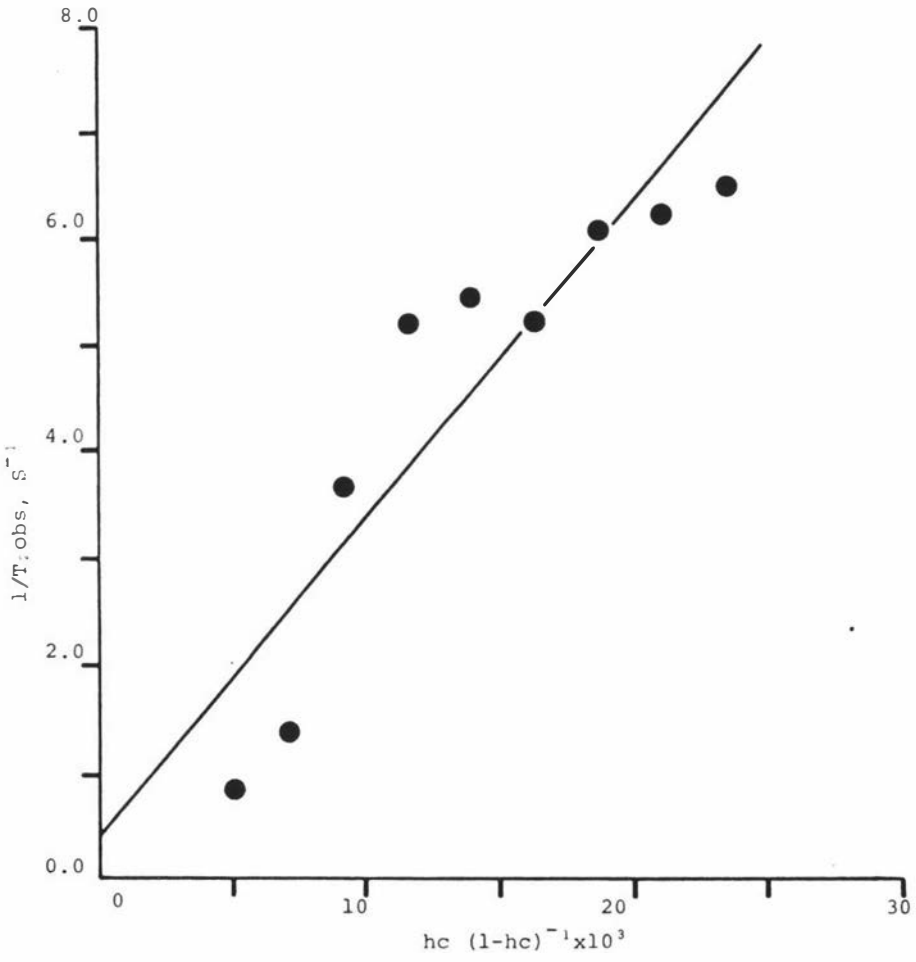

Figure III.21 Plot of $1/T_2$obs of ^1H in the amylopectin water system as a function of (hc/1-hc)

III.6.4 ^{13}C liquid signal

Figure III.22 shows plots of ^{13}C liquid signal per unit mass of starch against concentration for various starch pastes at 30.0°C. Included also is a plot of ^{13}C liquid signals of maltose solutions at various concentrations. The results show that the ^{13}C liquid signals of various starch pastes studied appears to be independent of wheat variety and concentration. It is observed that the ^{13}C liquid signal per unit mass of starch for various starch pastes is only two-thirds that of the maltose solution at equivalent solute concentration. This suggests that not all the polymer chains in starch molecules are liquid-like with short correlation times. In fact, some of the polymer chains have very long correlation times so that on the NMR time scale, they are regarded as solids and therefore give reduced peak intensities at the various carbon positions on the ^{13}C spectra. Table III.3 gives measurements of the line-widths at half height, $\Delta\nu_{\frac{1}{2}}$ of the peak intensities at various carbon positions of the ^{13}C spectra for pastes of varying starch concentrations. The results show that $\Delta\nu_{\frac{1}{2}}$ values are not dependent on starch concentration.

Table III.3 Line widths at half-height of the peak intensities at various carbon positions of ^{13}C spectra for several concentrations of Gamenya starch pastes.

Starch concentration g/g H_2O	Carbon-1	Carbon-2	Carbon-3	Carbon-4	Carbon-5
0.02	9.77	7.34	7.32	14.65	7.32
0.03	13.43	7.52	10.98	14.65	9.76
0.04	9.76	8.54	12.20	15.87	7.32
0.05	8.54	9.77	12.20	15.87	7.32
0.06	8.54	10.98	8.54	14.65	8.54
0.07	8.54	8.52	9.76	15.87	9.73

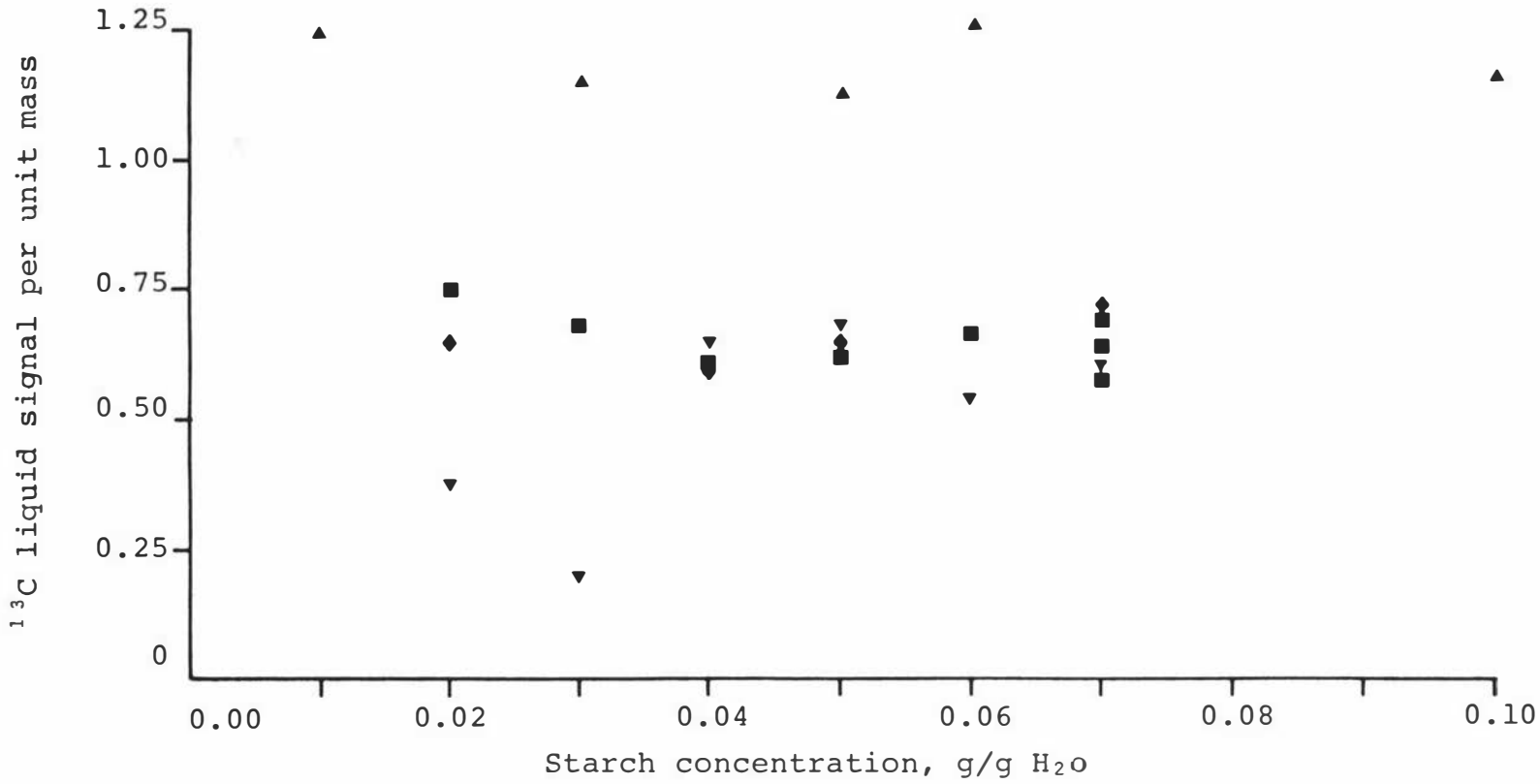

Figure III.22 Plots of the ^{13}C liquid signal per unit mass of starch as a function of the starch concentration for various pastes.

▲ Maltose ■ Karamu ◆ Gamut ▼ Raven

Figure III.23 shows plots of the total ^{13}C liquid signal for Karamu and Raven starch pastes (7.0%) as a function of the pasting temperature, at a constant heating time of one hour. The results show that in both starches there is no liquid signal (solid on NMR time-scale) observed for the starch-water system when the pasting temperature is below 50.0^{0}C. However, when the pasting temperature is increased to 55.0^{0}C, a ^{13}C liquid signal is readily observed. The ^{13}C liquid signal continues to increase until about 75.0^{0}C and remains constant thereafter. Within experimental variations, no difference is observed between the two starches examined. These results are consistent with the observations reported for starches contained in the gross plant tissues of white potato, corn kernel and chestnut. Figure III.24 shows the variation of $\Delta\nu_{1/2}$ values of the various carbons of the ^{13}C spectra of Karamu starch pastes as a function of the pasting temperature. The results show that $\Delta\nu_{1/2}$ values decrease with increasing pasting temperatures.

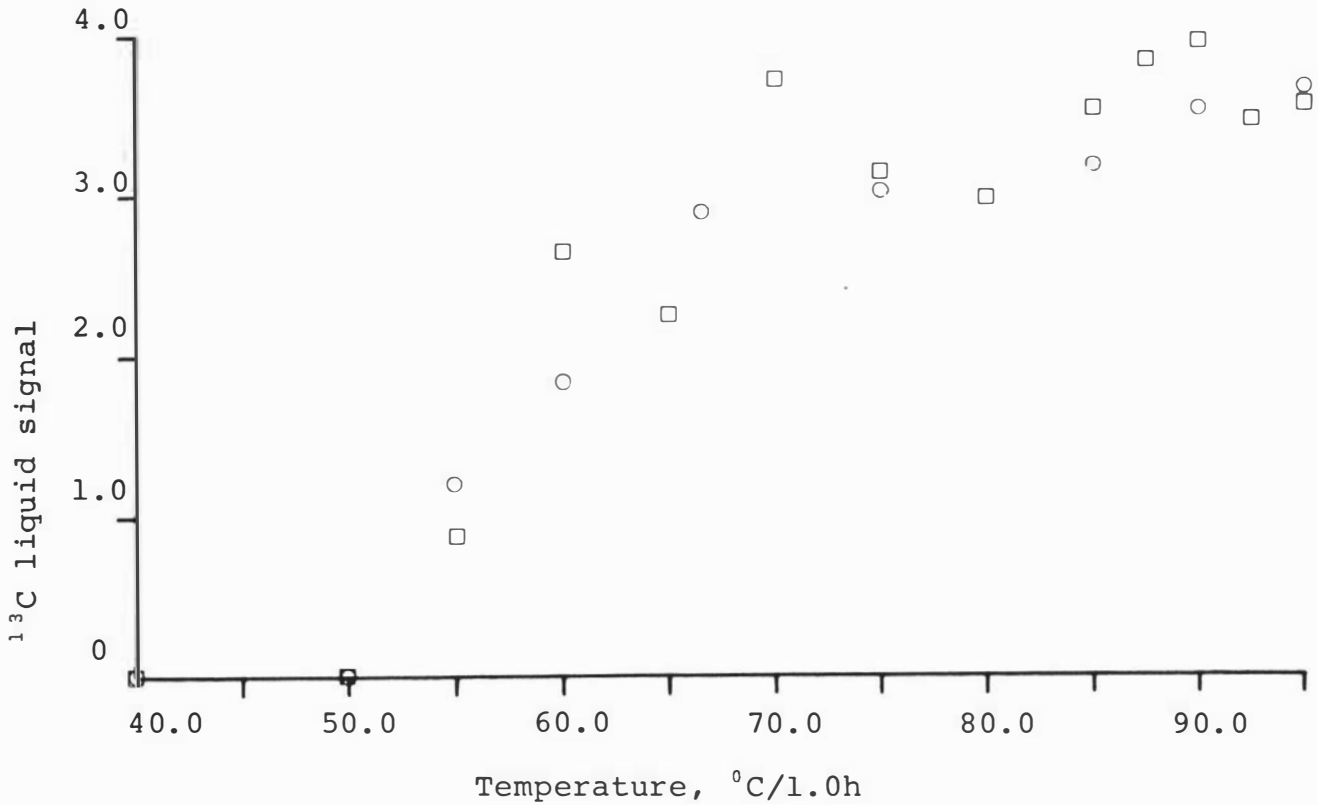

Figure III.23 Plots of the total ^{13}C liquid signal for Karamu (□) and Raven (○) starch pastes (7.0%) as a function of the pasting temperature, at a constant heating time of 1h.

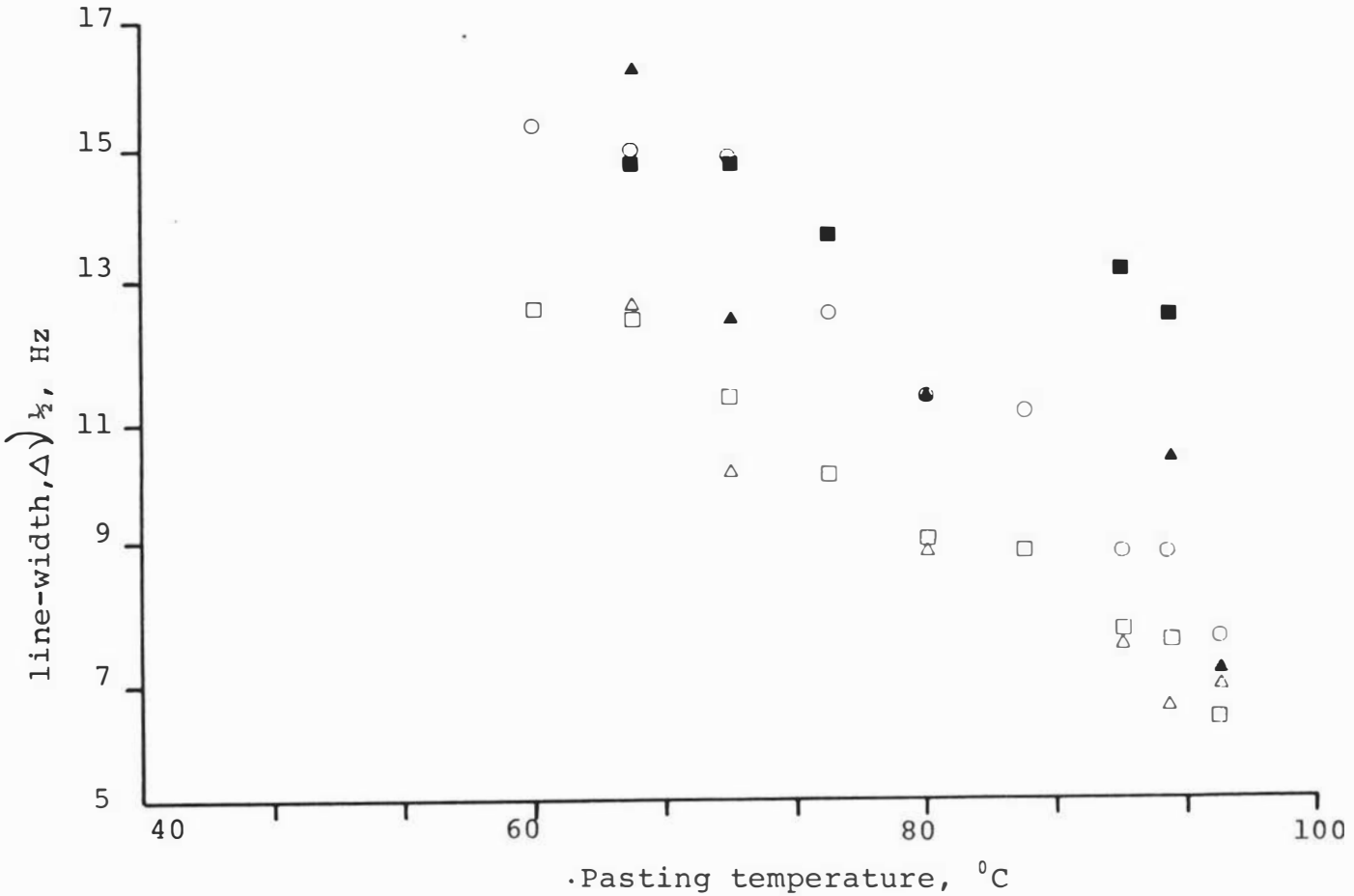

Figure III.24 Plots of the line-width at half-height of various carbons of the ^{13}C spectra of Karamu starch pastes as a function of the pasting temperature.

□ Carbon-1 ○ carbon-2 ▲ carbon-3 ▼ carbon-4 △ carbon-5

III.7. Discussion

III.7.1. Self-diffusion

The results obtained from the diffusion coefficient measurements of water molecules in starch pastes and the amylopectin-water system are interpreted using various models. The best model to describe the linear relationship between D/D_0 and the weight fraction of dry polymer is one which takes into account both the obstruction and hydration effects of the polymers in the aqueous continuous phase. As a result of this analysis, shape factors ($\bar{\lambda}$) are established for the starch molecules in the paste and for the amylopectin molecules in the amylopectin-water system. This gives $\bar{\lambda}$ values of 2.3 and 2.6 for the starch molecules and the amylopectin molecules respectively which are consistent with water diffusing through oblate ellipsoids.

The conformation of amylopectin molecules in ammonium thiosulphate solution has been reported to be prolate ellipsoids of axial ratios similar to that of globular proteins (158). This indicates that amylopectin molecules are spherical in shape. The results obtained in the present investigation thus contradict earlier reports. For some time investigators have suggested that in order to understand the behaviour of starch the amylopectin component must be planar. The concept of folded amylopectin chains (159) to form planar molecules has been suggested. However there is no firm evidence to substantiate this suggestion. The results in the present investigation provide direct experimental evidence demonstrating that molecules in gelatinised starch (which contain 75% amylopectin) and amylopectin molecules are two-dimensional.

III.7.2. Spin-lattice and spin-spin relaxation times

The results of T_1 and T_2 measurements of water protons in starch pastes and the amylopectin-water system are interpreted using a two-state fast exchange model. This model is adequate in describing the relaxation behaviour of water molecules in both systems. The T_1f values estimated from the intercepts for starch pastes and the amylopectin-water system are similar to the value obtained for agarose gels (129). However, unlike agarose gels, the T_2f values of starch pastes and the amylopectin-water system which are similar to pure water, are 3 orders of magnitude higher than the value for the agarose gel. This discrepancy has been attributed to the presence of paramagnetic impurities in the agarose samples. The T_2 values for the bound water in starch pastes and the amylopectin-water system are much higher than the values reported for agarose gels (T_2b=10μs) (129). However they are still much shorter than T_2f (400X). On the other hand, the T_1 values for the bound water in starch pastes and the amylopectin-water system are of the same order of magnitude reported for agarose gels (100ms) (129). The difference between T_1f and T_1b of starch pastes and the amylopectin-water systems is about 20X which is much less than the difference between T_2f and T_2b (400X). Any change in the amount of bound water will therefore has a much greater influence in T_2 relaxation behaviour. This explains the contrasting shape of T_1 and T_2 relaxation data obtained.

III.7.3. ^{13}C liquid signal

The results in Figure III.22 show that there is a loss of about one-third of the total ^{13}C liquid signal from pastes. This loss is probably due to crystallisation of amylose, to lipid-amylose complexes and to remnants of ordered granule structure. Figure III.22 also shows that the observed total ^{13}C liquid signals per unit mass of starch do not vary with increasing concentration. If the polysaccharide chains in the pastes are in closer proximity when the starch concentration is increased, this could lead to a greater amount of crystallisation so that the total ^{13}C liquid signals would decrease. However, this did not occur in the present case. One possible explanation for this relates to the fact that the gel particles in pastes pack so as to give a significant void volume. As the concentration increases, further granules fill these voids, hence the environment within any given gel particle is not altered by this process. For this reason the ^{13}C liquid signals of the polysaccharide chains may be unaffected. Another possible explanation could be that the mechanism of crystallisation involves a constant ratio of the polymeric components in the system, this would give a constant ^{13}C solid-liquid signal, irrespective of the starch concentration.

The ^{13}C liquid signal results observed as a function of the pasting temperature indicate that the ^{13}C liquid signal is only observed when the starch is gelatinised. This is consistent with the view that mobility of the polysaccharide chains in starch granules increases during gelatinisation so that the ^{13}C's making up the polysaccharide chains have liquid-like behaviour. The decrease in $\Delta\nu_{\frac{1}{2}}$ values with increase in the pasting temperature could be either due to an increase in T_2 relaxation times of the various carbons on the polysaccharide chains or to a decrease in

the spread of chemical shift values for the various carbon nuclei (150). If the former is regarded as the explanation, then the results are in accord with the view that an increase in mobility of the polymer chains during gelatinisation results in longer T_2 relaxation times (61).

APPENDICES

Appendix Ia Derivation of the simplified equations for the calculations of η' and G' using Oka's quadratic equations.

Oka (92) has derived quations to describe the response of a linear viscoelastic system to the shear conditions encountered in a coaxial cylinder viscometer. The equations are of the form:-

$$(B_0 + B_1)\, G^{*2} - (\mu B_1 - (B_2 + B_3)\rho\omega^2 r_1^2)\, G^* - B_3 \mu \rho \omega^2 r_1^2 = 0 \qquad [I.5]$$

where

$$\mu = \frac{1}{2\pi L r_1^2} \cdot \left(I\omega^2 - k + \frac{k}{M^*}\right) \qquad [I.6]$$

where

$$M^* = me^{-i\phi} \qquad [I.7]$$

where

ρ = density of starch paste
r_1 = radius of inner cylinder
L = length of the immersed portion of the inner cylinder
I = moment of inertia of inner cylinder
k = torsional constant of the suspending wire used
M^* = complex amplitude ratio

$$m = A/\Theta_0 \qquad [I.8]$$

where

A = amplitude of the output
Θ_0 = amplitude of the input

From Equation [I.7]

$$\frac{1}{M^*} = \frac{e^{i\phi}}{m}$$

$$= \frac{1}{m}\left[\cos\phi + i \sin\phi\right] \text{ by expansion} \qquad [I.9]$$

B_0, B_1, B_2 and B_3 are geometric factors of the coaxial cylinders.

$$B_0 = \frac{1+ (1+x)^2}{2(1+x)} \qquad [I.10]$$

$$B_1 = \frac{x\ (2+x)}{2\ (1+x)} \qquad [I.11]$$

$$B_2 = \frac{1}{16}\left[- 4\ (1+x)\ \ln\ (1+x) + 4x - 6x^2 + 2x^3 - \frac{3x^4}{1+x}\right] \qquad [I.12]$$

$$B_3 = \frac{1}{16}\left[4\ (1+x)\ \ln\ (1+x) - 4x - 2x^2 - 2x^3 + \frac{x^4}{1+x}\right] \qquad [I.13]$$

where $x = \frac{r_2 - r_1}{r_1}$ r_2 = radius of outer cylinder

Equation [5] which is of quadratic form, can be solved to obtain G*. It can be shown that the geometric factors are such that B_3 and $(B_2 + B_3)$ << $(B_0 + B_1)$, and at small frequency, can neglect higher order of ω in Equation [5]. Thus

$(B_0 + B_1)\ G^{*2} - (\mu B_1)\ G^* = 0$

solving $G^* = 0$

$$\text{or } G^* = \frac{\mu B_1}{B_0 + B_1}$$

$$\therefore G' + i\omega\eta' = \frac{B_1}{B_0 + B_1}\left[\frac{1}{2\pi L\ r_1^2}(I\omega^2 - k + \frac{k\cos\phi}{m} + \frac{ki\sin\phi}{m}\right] \qquad [I.14]$$

Equating all real terms for G'

$$G' = \frac{B_1}{B_0 + B_1}\left[\frac{1}{2\pi L r_1^2}\ (I\omega^2 - k + \frac{k\cos\phi}{m})\right]$$

$$= \frac{B_1}{B_0 + B_1}\left[\frac{1}{2\pi L r_1^2}\ (\ I\omega^2 - k\ (\frac{\cos\phi}{m} - 1)\right]$$

$$\text{but } \frac{B_1}{B_0 + B_1} = \frac{r_2^2 - r_1^2}{2r_2^2}$$

$$\therefore \quad G' = \frac{1}{4\pi L}\left[\frac{1}{r_1^{\,2}} - \frac{1}{r_2^{\,2}}\right]\left(k\left(\frac{\cos\phi}{m} - 1\right) + I\omega^2\right) \qquad [I.4]$$

Equating all imaginery terms for η'

$$\omega\eta' = \frac{B_1}{B_0+B_1}\left[\frac{1}{2\pi L r_1^{\,2}} \cdot \frac{k\sin\phi}{m}\right]$$

$$\text{i.e. } \eta' = \frac{1}{4\pi L}\left[\frac{1}{r_1^{\,2}} - \frac{1}{r_2^{\,2}}\right]\left(\frac{k\sin\phi}{m\,\omega}\right) \qquad [I.3]$$

Thus from the foregoing, rigorous evaluation of dynamic viscosity and rigidity involves the separate determination of two variables, namely the amplitude ratio m and the phase angle ø.

Appendix Ib

A description of the top-drive oscillatory coaxial viscometer.

Plate I.1 gives a picture of the instrument which consisted of three major components, the structural framework plus cylinder assembly, the driving mechanism and the sensing devices.

The structural framework of the instrument consisted of a triangular brass base plate, three vertical pillars and an aluminium top end plate. The outer cylinder was secured into a recess at the geometric centre of the base plate. The inner cylinder was suspended by a steel piano wire from the bearing ferrule situated at the top bearing assembly. The outer and inner cylinders could be aligned by means of a fine thread screw. A water jacket vessel was incorporated onto the outer cylinder to control the temperature. The driving mechanism consisted of a variable speed driving motor, three series of reduction gear train and a bearing assembly. Rotational motion from the driving wheel was changed into oscillatory motion by the eccentric coupling mechanism. This assembly made it possible to obtain the driving oscillation whose period could be changed from 1s to about 300s.

An optical system (94), coupled with a light dependent resistor (LDR) and U.V. recorder was used to monitor the input and output oscillations. The set-up of the measuring devices were such that nearly identical sinusoidal oscillations were observed for both input and output signals when there was no sample in the annular space between the inner and outer cylinders. The signal response dead time was shown to be

negligible. The input and output voltage signals which were dependent on the amount of light picked up by the LDR's were amplified through an amplifying circuit, see Figure I.2 and recorded onto U.V traces.

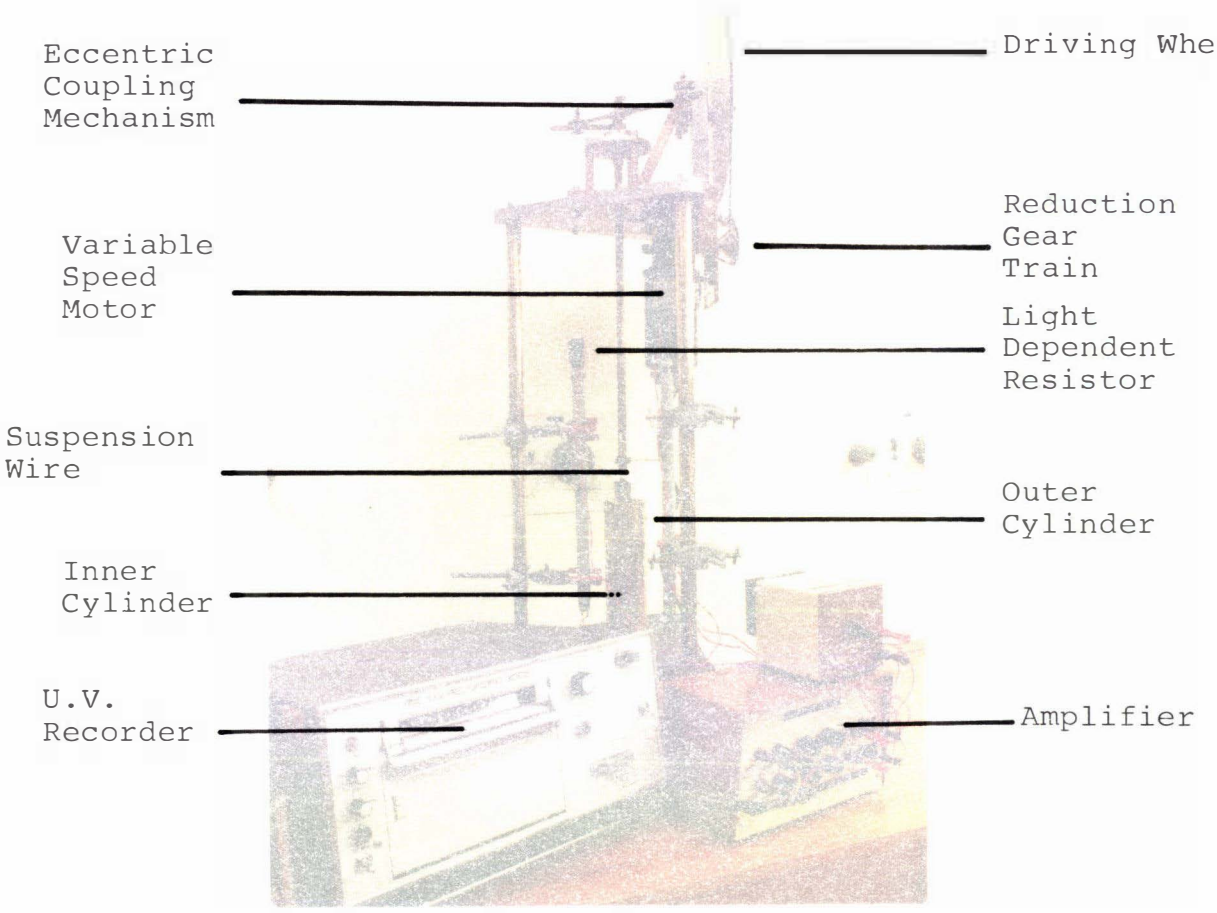

Plate I.1. The top-drive oscillatory co-axial viscometer.

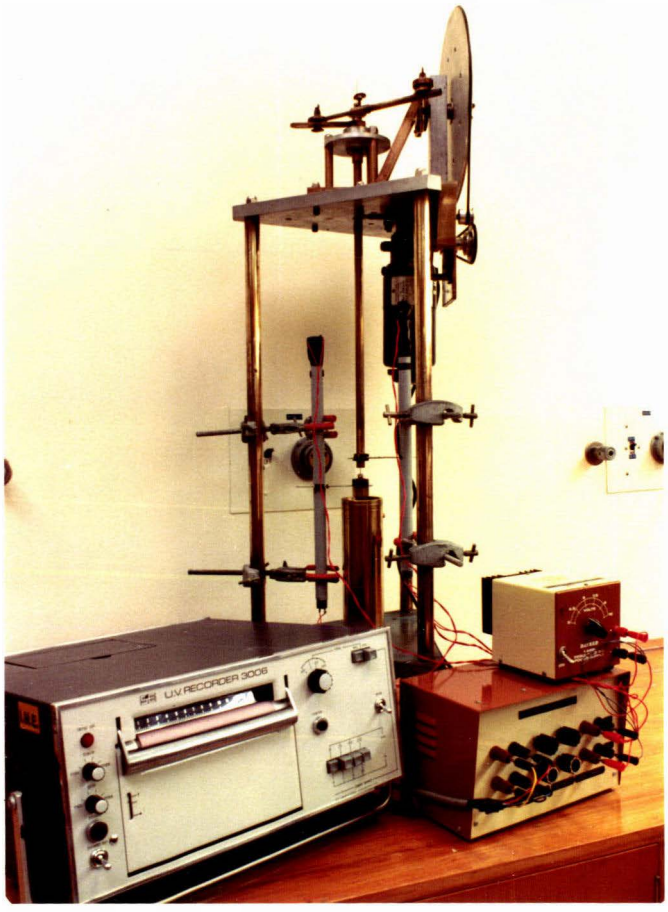
UV RECORDER 3006

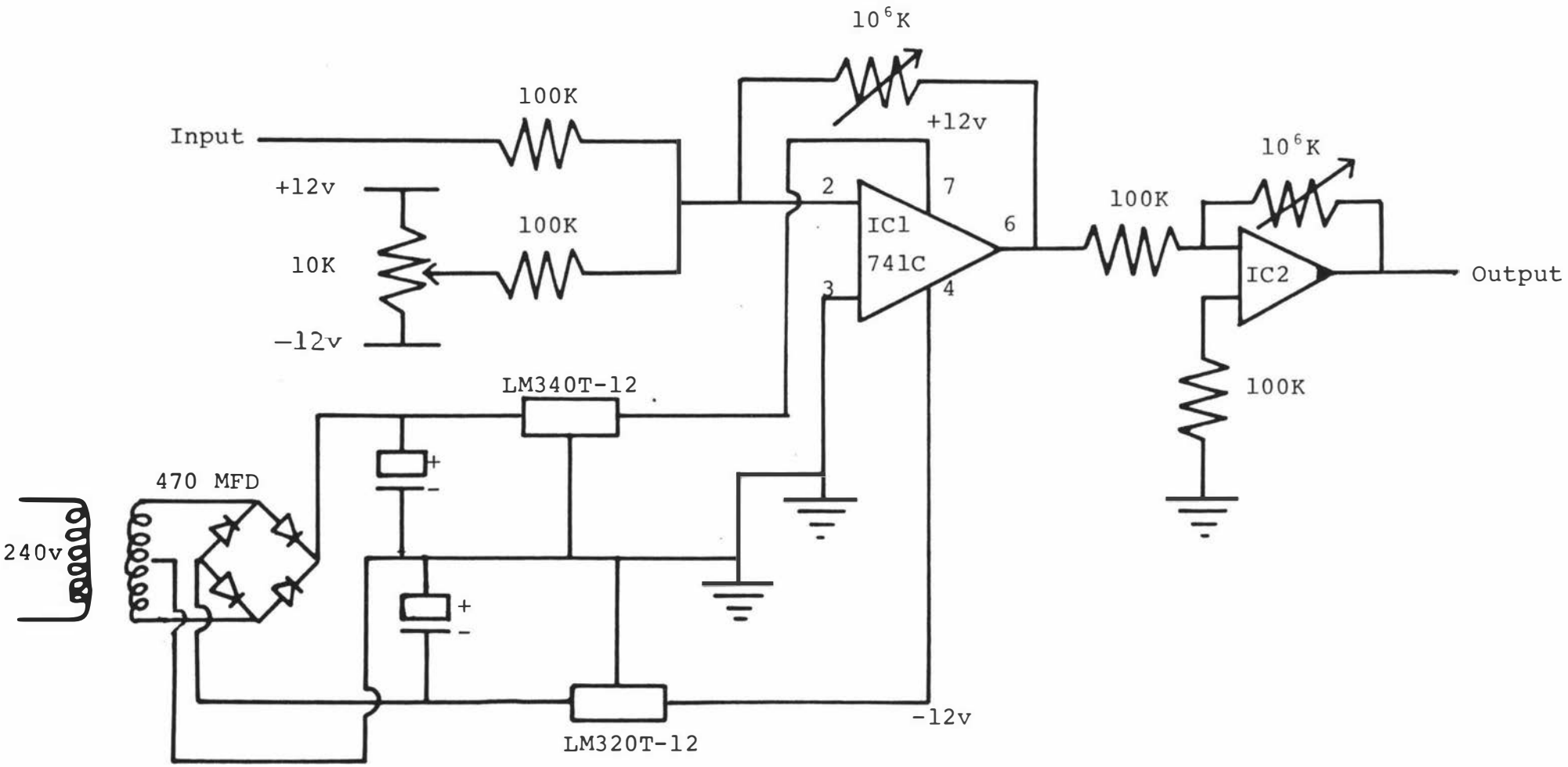

Figure 1.2 Amplifier circuit diagram for the oscillatory co-axial viscometer.

Appendix Ic. A sample calculation in determining the relative weight-size distribution curve of Gamut wheat starch from Coulter Counter raw data.

Coulter counter volume (μm)[3] (calibrated)	Diameter (μm)	ln cumulative number)	Diameter[1] (μm)	ln cumulative number)[1]	Slope by numerical differentiation	Cumulative number	Relative number	Relative number/g x10^6	Relative weight[2] (mg/μm/g)
18	3.25	10.514	2	10.95	0.390	56,950	22,210	1110.0	3.57
24	3.56	10.364	3	10.68	0.344	43,475	14,955	747.8	8.11
30	3.86	10.356	4	10.26	0.315	28,625	9,017	450.9	11.59
36	4.10	10.225	5	9.97	0.320	21,380	6,842	342.1	17.17
42	4.31	10,156	6	9.62	0.325	15,060	4,895	244.8	21.23
48	4.51	10.099	7	9.32	0.27	11,155	3,012	150.6	20.74
60	4.86	10.015	8	9.08	0.215	8,780	1,888	94.4	19.40
72	5.16	9.945	9	8.89	0.160	7,260	1,162	58.1	17.00
84	5.43	9.828	10	8.76	0.100	6,375	638	31.9	12.80
96	5.68	9.744	11	8.69	0.070	5,945	416	20.8	11.12
120	6.12	9.612	12	8.62	0.060	5,540	332	16.6	11.52
144	6.50	9.465	13	8.57	0.060	5,270	316	15.8	13.94
168	6.85	9.363	14	8.50	0.083	4,915	405	20.3	22.30
192	7.16	9.283	15	8.40	0.100	4,470	447	22.4	30.29
240	7.71	9.155	16	8.30	0.118	4,020	472	23.6	38.82
288	8.20	9.044	17	8.17	0.140	3,533	495	24.8	48.83
336	8.63	8.952	18	8.02	0.173	3,040	524	26.2	61.36
384	9.02	8.883	19	7.83	0.200	2,502	500	25.0	68.86
480	9.71	8.796	20	7.62	0.223	2,040	454	22.7	72.93
576	10.32	8.767	21	7.38	0.245	1,604	393	19.7	73.08
672	10.87	8.71	22	7.13	0.255	1,248	318	15.9	67.99
768	11.36	8.666	23	6.87	0.265	963	255	12.8	62.30
960	12.24	8.603	24	6.60	0.285	735	209	10.5	58.01
1152	13.00	8.572	25	6.30	0.300	545	164	8.2	51.45
1344	13.69	8.523	26	6.00	0.320	403	129	6.5	45.53
1536	14.32	8.474	27	5.66	0.338	287	97	4.9	38.34
1920	15.36	8.369	28	5.33	0.330	205	68	3.4	29.97
2304	16.39	8.258	29	5.00	0.338	148	50	2.5	24.49
2688	17.25	8.114	30	4.65	0.345	105	36	1.8	19.52
3672	18.04	8.020	31	4.31	0.330	75	25	1.3	14.96
3840	19.43	7.720	32	3.99	0.330	55	18	0.9	11.84
4608	20.65	7.432							
5376	21.74	7.200							
5401	21.77	7.244							
6482	23.13	6,835							
7562	24.35	6.540							
8642	25.46	6.110							
9720	26.48	5.860							
10752	27.38	5.521							
12288	28.63	5.075							
13824	29.78	4.700							
15360	30.84	4.250							
16896	31.84	3.690							

[1] From plot of ln cumulative number against diameter

[2] Relative weight = relative number/g x density of hydrated starch x particle volume x correction factor.

Appendix Id Extrapolation technique to obtain the swelling capacity of a starch sample.

Step 1 Obtain volumes of sediment at zero time from plots of the volume of sediment versus the centrifuging time for various centrifuging speeds (rpm).

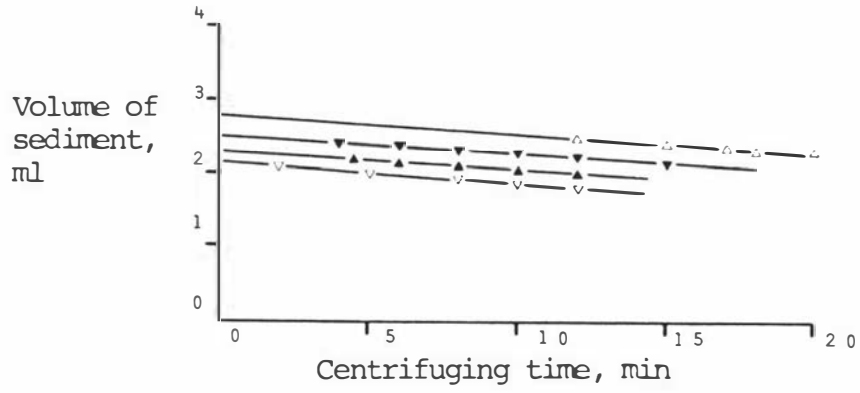

Step 2 Plot volumes of sediment at zero time versus centrifuging speeds.

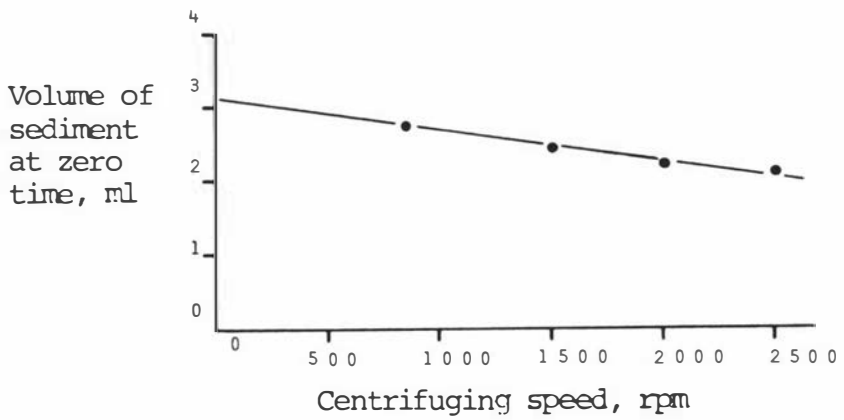

Step 3 Calculate swelling capacity.

Swelling capacity, $S = \frac{y}{x}\left[\frac{200+x}{10}\right]$ ml/g

where y = volume of sediment at zero time and at zero rpm

x = weight of starch sample

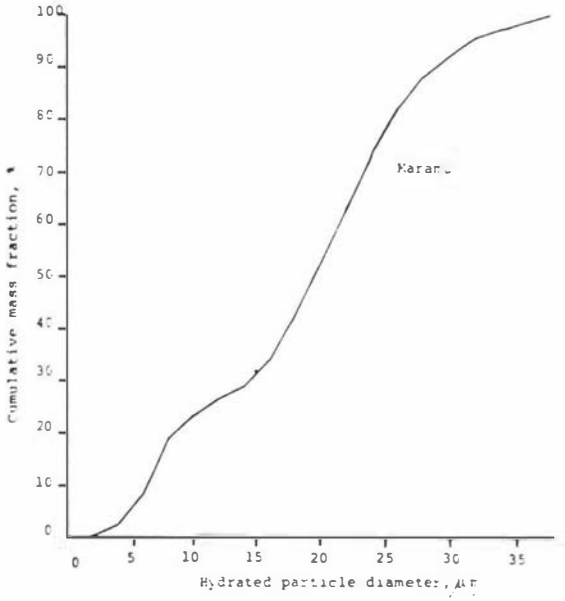
Cumulative mass fraction, %
100
90
80
70
60
50
40
30
20
10
0
0
5
10
15
20
25
30
35
Hydrated particle diameter, µm

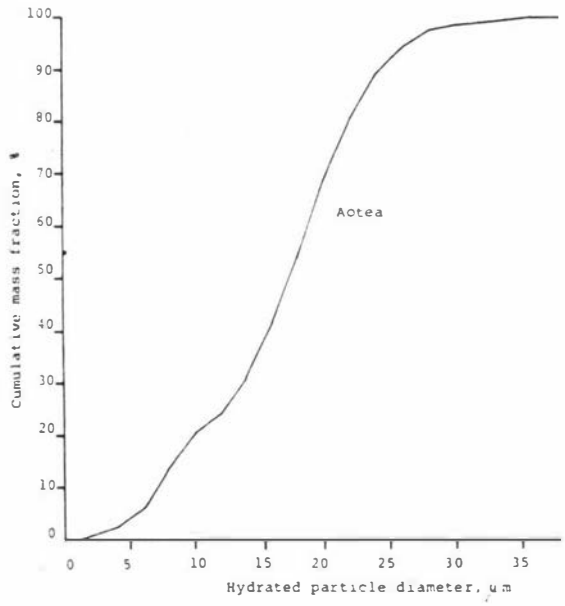
Cumulative mass fraction, %
100
90
80
70
60
50
40
30
20
10
0
Aotea
0
5
10
15
20
25
30
35
Hydrated particle diameter, µm

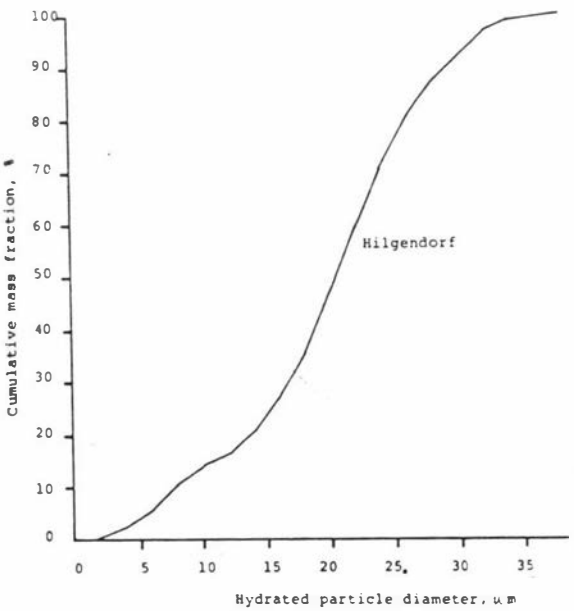
Cumulative mass fraction, %
100
90
80
70
60
50
40
30
20
10
0
Hilgendorf
0
5
10
15
20
25
30
35
Hydrated particle diameter, µm

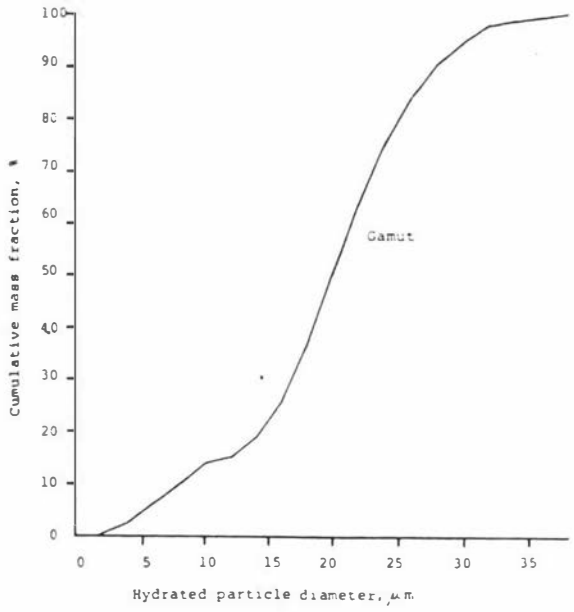
Cumulative mass fraction, %
100
90
80
70
60
50
40
30
20
10
0
Gamut
0 5 10 15 20 25 30 35
Hydrated particle diameter, μm

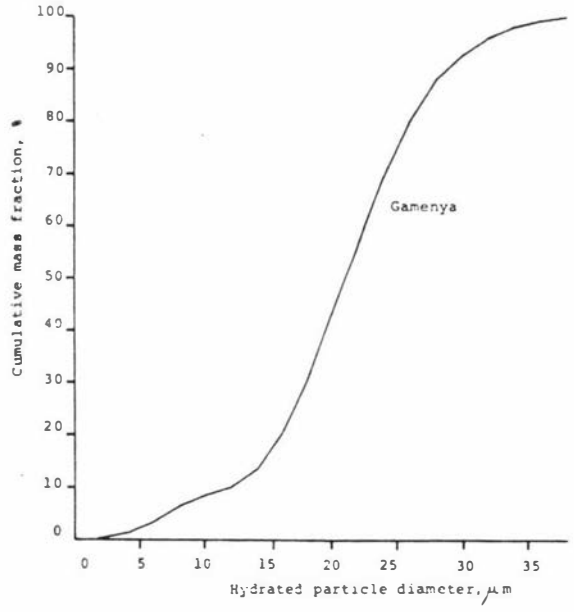
Cumulative mass fraction, %
100
90
80
70
60
50
40
30
20
10
0
Gamenya
0 5 10 15 20 25 30 35
Hydrated particle diameter, μm

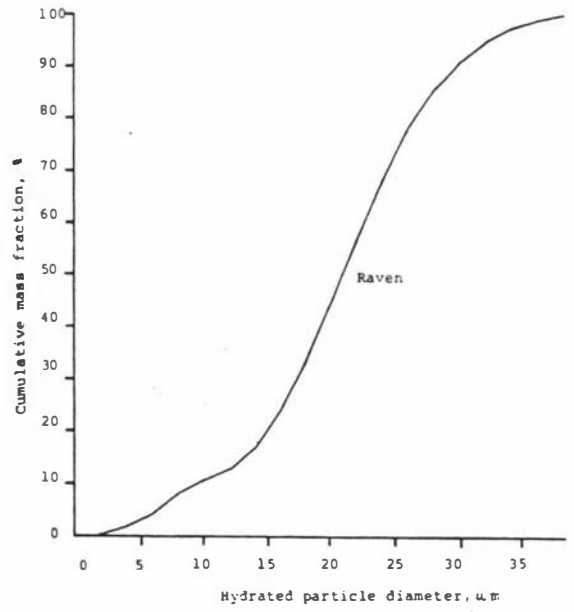
Cumulative mass fraction, %
100
90
80
70
60
50
40
30
20
10
0
Raven
0 5 10 15 20 25 30 35
Hydrated particle diameter, μm

Appendix IIa One-way analysis of variance, means and 95% Confidence Intervals for the enthalpy changes of various wheat starches.

One-way analysis of variance

Source of variance	Sum of squares	d.f.	Mean squares	F-ratio
Between starches	4.3665	5	0.8733	9.935***
Error	0.4659	53	0.0879	
Total	4.8324			

$F_{0.01,\ 5,\ 53} = 3.43$ *** 1.0% significance level

Means and 95% Confidence Intervals

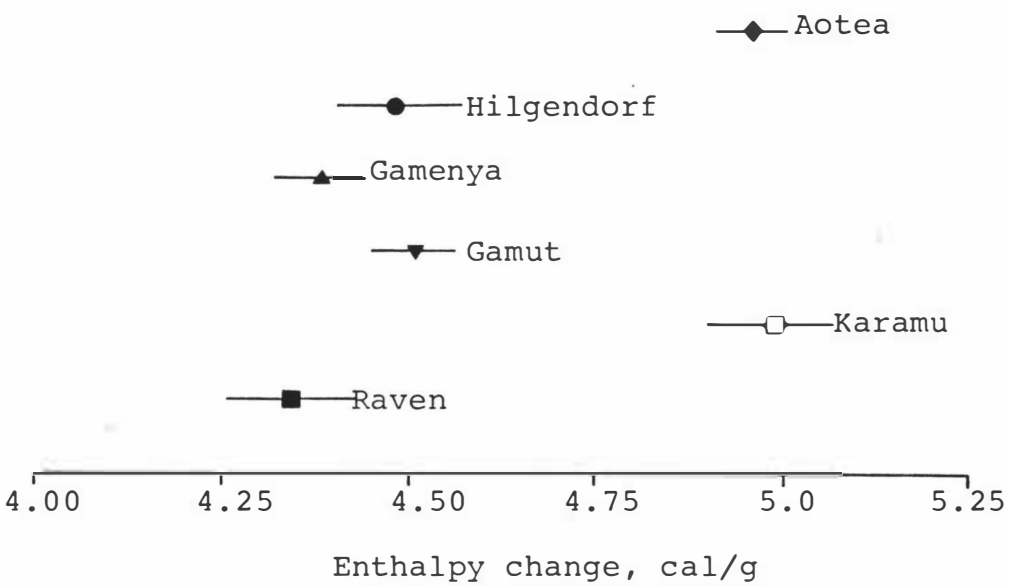

Appendix IIb One-way analysis of variance, means and 95% Confidence Intervals for the X-ray correlation crystallinity indexes of various wheat starches.

One-way analysis of variance

Source of variation	Sum of squares	d.f.	Mean squares	F-ratio
Between starches	0.075	5	0.015	14.59 ***
Error	0.031	30	0.00102	
Total	0.105	35		

$F_{0.01,5,30}$ = 3.7 *** 1.0% significance level

Means and 95% Confidence Intervals

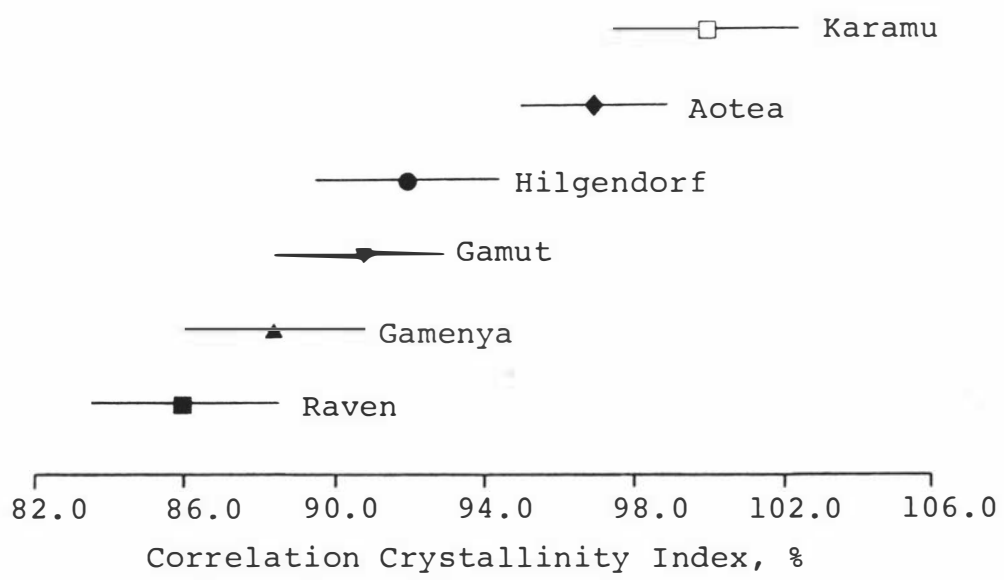

Appendix IIIa A sample calculation showing the percentage of variation in using the simplified form of Equation [III.23].

$$\frac{D}{D_0} - \Delta_1 = 1 + \Delta_2 - \left[\bar{\alpha}(\bar{V}_\rho d_0 + h) + h\right] W \qquad [III.23]$$

$$\Delta_1 = \frac{\bar{\alpha}\bar{V}_\rho d_0 (\bar{V}_\rho d_0 - 1) W^2}{1 + (\bar{V}_\rho d_0 - 1) W} \qquad [III.25]$$

$$\Delta_2 = \left[\frac{\bar{\alpha} h (\bar{V}_\rho d_0 - 1)}{1 + (\bar{V}_\rho d_0 - 1) W} - \frac{h}{1-W} + \frac{\bar{\alpha}(\bar{V}_\rho + h) h}{1 + (\bar{V}_\rho d_0 - 1) W (1-W)}\right] W^2 \qquad [III.26]$$

For $W = 0.07$

$\bar{\alpha} = 2.3$, $\bar{V}_\rho = 0.645$, $d_0 = 1$ and $h = 0.34$

W	Δ_1	$D/D_0 - \Delta_1$	D/D_0	% variation
0.07	-0.00265	0.8287	0.826	0.3

W	Δ_2	$1+\Delta_2 - \left[\bar{\alpha}(\bar{V}_\rho d_0 + h) + h\right] W$	$1 - \left[\bar{\alpha}(\bar{V}_\rho + h) + h\right] W$	% variation
0.07	0.00640	0.824	0.8176	0.73

PUBLICATIONS

The results in Section I have been reported in:-

Wong, R.B.K. and Lelievre, J. 1981. Viscoelastic behaviour of starch pastes. Rheol. Acta, 20, 299.

Wong, R.B.K. and Lelievre, J. Rheological characteristics of wheat starch pastes under steady shear conditions. J. Appl. Polym. Sci., in the press.

The results in Section II have been reported in:-

Wong, R.B.K. and Lelievre, J. A comparison of the crystallinities of wheat starch samples with different swelling capacities. Starke, in the press.

REFERENCES

1. Whistler, R.L. and Paschall, E.F. (Eds), 1967. Starch: Chemistry and Technology, Vol. I & II, Academic Press, New York.

2. Radley, J.A. 1968. Starch and its Derivatives, 4th ed., Chapman and Hall Ltd., London.

3. Knight, J.W. 1969. The Starch Industry, Pergamon Press, Oxford.

4. Banks, W. and Greenwood, C.T. 1975. Starch and its Components, Edinburgh University Press, Edinburgh.

5. Radley, J.A. (Ed). 1976. Examination and Analysis of Starch and Starch Products, Applied Science Publishers Ltd., London.

6. French, D. 1973. J. Animal Sci., 37, 1048

7. Olkku, J. and Rha, Chokyan. 1978. Food Chem., 3, 293

8. Greenwood, C.T. 1979. in J.M.V. Blanchard and J.R. Mitchell (Eds), Polysaccharides in Foods, Butterworths, London., Chap.8.

9. Blanchard, J.M.V. 1979. in J.M.V. Blanchard and J.R. Mitchell (Eds), Polysaccharides in Foods, Butterworths, London., Chap.9.

10. Banks, W., Greenwood, C.T. and Muir, D.D. 1973. in G.G.Birch and L.F.Green (Eds), Molecular Structure and Function of Food Carbohydrate, Applied Science Publishers Ltd., London., Chap. II.

11. Evers, A.D. 1973. Starke, 25, 303

12. Kerr, R.W. 1950. Chemistry and Industry of Starch, 2nd Ed., Academic Press, New York.

13. Meredith, P.1981. Starke, 33, 40

14. Evers, A.D. and Lindley, J. 1977. J.Sci.Food Agric. 28, 98.

15. Baruch, D.W. 1974. New Zealand J. of Sci., 7, 21

16. Kulp, K. 1973. Cereal Chem., 50, 666

17. Meredith, P., Baruch, D.W. and Jenkins, L.D. 1977. Starke, 29, 217

18. Stamberg, O.E. 1939. Cereal Chem., 16, 769

19. Hansen, E., Dodt. and Niemann, E. 1953. Kolloid.Z., 130, 19

20. Evers, A.D., Greenwood, C.T., Muir, D.D. and Venables.C.1974. Starke, 26, 42.

21. Meredith, P., Dengate, H.N. and Morrison, W. 1978. Starke, 30, 119.

22. Brocklehurst, P.A. and Evers, A.D. 1977. J.Sci. Food Agric., 28, 1084.

23. Baruch, D.W., Meredith, P., Jenkins, L.D., and Simmons, L.D. 1979. Cereal Chem, 56, 554

24. Guilbot, A. Charbonniere, R. and Draprom, R. 1961. Starke, 13, 204.

25. Sair, L. and Fetzer, W.R. 1944. Ind. Eng. Chem., 36, 205.

26. Taylor, T.C. and Iddles, H.A. 1926. Ind. Eng. Chem., 18, 713.

27. Stacey, M. 1943. Chem. and Ind., 62, 110.

28. Banks, W. and Greenwood, C.T. 1959. Starke, 10, 294

29. Banks, W. and Greenwood, C.T. 1967. Starke, 19, 197

30. Greenwood, C.T. 1956. Adv. Carbohydrate Chem., 11, 335

31. Geddes, R. and Greenwood, C.T. 1969. Starke, 21, 148

32. Whelan, W.J. 1971. Biochem. J., 122, 609

33. Wren, J.J. and Merryfield, Danata, S. 1970. J.Sci. Food Agric., 21, 254.

34. Morrison, W.R., Mann, D.L., Soon, W. and Coventry, Anne, M. 1975. J.Sci. Food Agric., 26, 507.

35. Melvin, Madeleine, A. 1979. J.Sci. Food Agric., 30, 731

36. Acker, L., and Schmitz, H.J. 1967. Starke, 19, 233

37. Medcalf, D.G., Youngs, V.L. and Gilles, K.A. 1968. Cereal Chem., 45, 88.

38. Schoch, T.J. 1942. J. Amer. Chem. Soc., 64, 2954

39. Mangels, C.E., and Bailey, C.H. 1933. Ind. Eng. Chem., 25, 456

40. Manners, D.J. 1962. Adv. Carbohydrate Chem., 17, 371

41. Loney, D.P., Jenkin, L.D. and Meredith, P. 1975. Starke, 27, 145

42. Bear, B.S. and French, D. 1941. J. Amer. Chem. Soc., 63, 2298.

43. Senti, F.R. and Witnauer, L.P. 1946. J. Amer. Chem. Soc., 68, 2407

44. French, D. 1972. Depun Kagaka, 19, 8

45. Leach, H.W., McCowen, L.D. and Schoch, T.J. 1959. Cereal Chem., 36, 534

46. Sterling, C. 1968. in J.A. Radley (Ed), Starch and its Derivatives, 4th ed., Chapman and Hall Ltd., London Chap. 4.

47. Ahmed, M. and Lelievre, J. 1978. Starke, 30, 78

48. Montgomery, Edna, M. and Senti, F.R. 1958. J. Polym. Sci., 28, 1.

49. French, D., Smith, E.E. and Whelan, W.J. 1972 Carbohydrate Res., 22, 123.

50. MacRitchie, F. and Alexander, A.E. 1961. J. Colloid Interface Sci., 16, 57.

51. Simmonds, D.H. 1971. Wallerstein Lab. Comm., 17, 113.

52. Czaja, A.T. 1961. Starke, 13, 357.

53. Buttrose, M.S. 1963. Austral. J. Biol. Sci., 16, 305.

54. Knight, R.A. and Wade, P. 1971. Ind. Eng. Chem., 63, 568.

55. Evers, A.D., Gough, B.M. and Pybus, J.N. 1971. Starke, 23, 16.

56. Lelievre, J. 1975. Starke, 27, 2.

57. Winkler, C.A. and Geddes, W.F. 1931. Cereal Chem., 8, 455.

58. Kuntzel, A. and Doehner, K. 1939. Kolloid-Z, 38, 209

59. Lelievre, J. 1974. J. Appl. Polym. Sci., 18, 293

60. Priestly, R.J. 1975. Starke, 27, 416.

61. Lelievre, J. and Mitchell, J. 1975. Starke, 27, 113

62. Collison, R. 1968. in J.A. Radley (Ed), Starch and its Derivatives, 4th ed., Chapman and Hall Ltd., London, chap. 3.

63. French, A.D. and Murphy, V.G. 1977. Polymer, 18, 489

64. Flory, P.J. 1953. Principles of Polymer Chemistry, Cornell University Press, Ithaca, New York.

65. Marchant, J.L. and Blanchard, J.M.V. 1978. Starke, 30, 257

66. Lorenz, K. 1976. J. Food Sci., 41, 1357

67. de Willigen, A.H.A. 1976. in J.A. Radley (Ed), Examination of Starch and Starch Products, Applied Science Publishers Ltd., London, Chap. 3.

68. Evans, I.D. and Haisman, D.R. 1979. J. Texture Studies, 10, 347.

69. Anker, C.A. and Geddes, W.F. 1944. Cereal Chem., 19, 335

70. Myers, R.R. Knauss, C.J. and Hoffman, R.D. 1962. J. Appl. Polym. Sci., 6, 659

71. Katz, J.R., Desai, M.C. and Seiberlich, J. 1938. Trans. Faraday Soc., 34, 1258.

72. Miller, R.S., Derby, R.I. and Trimbo, H.B. 1973. Cereal Chem., 50, 271.

73. Sone, T. 1972. Consistency of Foodstuffs, D.Reidel Publishing Company, Dordrecht-Holland.

74. de Willigen, A.H.A. 1953. Anal. Chem., 25, 314.

75. Schutz, R.A. and Nadonchelle, Y. 1966. Starke, 18, 180.

76. Wood, F.W. 1967. In Rheology and Texture of Foodstuffs, SCI Monograph 27.

77. Ferry, J.D. 1961. Viscoelastic Properties of Polymers, John Wiley & Sons Inc., New York and London.

78. Nakagawa, T. and Seno, M. 1956. Bull. Chem. Soc. Jap., 29, 471.

79. Nakagaki, M. and Muragishi, K. 1961. Bull. Chem. Soc. Jap., 34, 316.

80. Myers, R. and Knauss, C.J. 1964. In W.R. Whistler (Ed), Methods in Carbohydrate Chemistry, Vol. IV Academic Press, London and New York, Chap. III.

81. Sterling, C. 1978. J. Texture Studies, 9, 225.

82. Radley, J.A. 1953. Starch and its Derivatives, 3rd ed., Chapman and Hall Ltd, Chap. 3.

83. Schoch, T.J. 1964. In W.R. Whistler (Ed), Methods in Carbohydrate Chemistry, vol.IV, Academic Press, London and New York, 106.

84. Hill, R.D. and Dronzek, B.L. 1973. Starke, 25, 367.

85. Smith, R.J. 1964. In R.L. Whistler (Ed), Methods in Carbohydrate Chemistry, Vol. IV, Academic Press, London and New York, 36.

86. Loney, D.P. and Meredith, P. 1974. Cereal Chem., 51, 702.

87. Smith, R.J. 1964. In R.L. Whistler (Ed), Methods in Carbohydrate Chemistry, Vol. IV, Academic Press, London and New York, 47.

88. Schoch, T.J. 1964. In R.L. Whistler (Ed), Methods in Carbohydrate Chemistry, Vol. IV, Academic Press, London and New York, 56.

89. Kent, N.L. 1966. Technology of Cereals, Pergamon Press Ltd., U.K.

90. MacMasters, M.M. In R.L. Whistler (Ed), Methods in Carbohydrate Chemistry, Vol. IV, Academic Press, London and New York, 233.

91. Osman, E.M. In R.L. Whistler and E.F. Paschall (Eds). Starch: Chemistry and Technology, Vol. II, Academic Press, New York and London, Chap. VIII.

92. Oka, S. 1953. Bull Kobayashi Inst. Phys. Res., 3, 17.

93. Walters, K. 1975. Rheometry, Chapman and Hall Ltd, London.

94. Goldberg, H. and Sandvik, O. 1947. Anal. Chem., 19, 123.

95. Dinsdale, A. and Moore, F. 1962. Viscosity and its measurement, Chapman and Hall Ltd., London and New York.

96. Ferranti-Shirley Cone and Plate Viscometer manual.

97. deMan, J.M. 1976. In J.M. deMan, P.W. Voisey, V.F. Rasper and D.W. Stanley (Eds), Rheology and Texture in Food Quality, The AVI Publishing Co., Inc., Westport, Connecticut, Chap. 2.

98. Kulp, K. 1972. Cereal Chem., 49, 697

99. Colwell, K.H., Axford, D.W.E. Chamberlain, N. and Elton, G.A.H. 1969. J.Sci. Food Agric., 20, 550.

100. Steeberg, B., Thalen, N. and Wahren, D. 1965. In Bolam (Ed), Consolidation of Paper Web, Vol.1, Trans. Symp., Cambridge, England, 177.

101. Taylor, N.W. and Bayley, E.B. 1974. J. Appl. Polym.Sci., 18, 2274.

102. Attanasio, A., Bernini, U. and Segre, G. 1969. J. Colloid Interface Sci., 29, 81.

103. Schoch, T.J. and Elder, A.L. 1955. In American Chemical Society, Use of Sugars and Carbohydrates in the Food Industry, American Chemical Society, Washington, 21.

104. Roscoe, R. 1953. In J.J. Herman (Ed), Flow Properties of Disperse Systems, North Holland Publishing Company, Amsterdam.

105. Erdi, N.Z., Cruz, M.M. and Battista, O.A. 1968. J. Colloid Interface Sci., 28, 36.

106. Sherman, P. 1968. In P. Sherman (Ed), Emulsion Science, Academic Press, London and New York, 286.

107. Sieglaff, C.L. 1963. Polymer, 4, 281.

108. Shashoua, V.E. and Beaman, R.G. 1958. J. Polym. Sci., 33, 101.

109. Mandelkern, L. 1964. In Crystallisation of Polymers, McGraw-Hill Book Company, New York, 273.

Colwell, K.H.

110. McIver, R.G., Axford, D.W.E., and Elton, G.A.H. 1968. J. Sci. Food Agric., 19, 560.

111. Collinson, R. 1968. In J.A. Radley (Ed), Starch and its Derivatives, 4th ed., Chapman and Hall Ltd, London, chap. 6.

112. Billmeyer, F.W. 1971. Textbook of Polymer Science, John Wiley and Sons, Inc., New York, 165.

113. Medcalf, D.G. and Gilles, K.A. 1968. Cereal Chem., 45, 550.

114. Kulp, K. and Lorenz, K. 1981. Cereal Chem., 58, 46.

115. Richardson, M.J. 1969. Br. Polym. J., 1, 132.

116. Statton, W.O. 1963. J. Appl. Polym. Sci., 7, 803.

117. Wakelin, J.H., Virgin, H.S. and Crystal. E. 1959. J. Apply. Phys., 30, 1654.

118. Lelievre, J. 1974. Starke, 26, 85.

119. Wendlandt, W.M. 1974. in Thermal Methods of Analysis, 2nd ed., John Wiley & Sons Inco., New York and London, 293.

120. Schoch, T.J. and Leach, H.W. 1964. In R.L. Whistler (Ed), Methods in Carbohydrate Chemistry, Vol. IV, Academic Press, New York and London, 101.

121. Donovan, J.W. 1979. Biopolymers, 18, 263.

122. Wooton , M. and Bamunuarachchi, A. 1979. Starke, 31, 262.

123. Biliaderis, C.G., Maurice, T.J. and Vose, J.R. 1980. J. Food Sci., 45, 1669.

124. Banks, W. and Greenwood, C.T. 1975. In Starch and its Components, Edinburg University Press, Edinburgh, Chap. 6.

125. Hollinger, G., Kuniak, L. and Marchessault, R.H. 1974. Bio-polymers, 13, 879.

126. Mathur-De Vre, R. 1979. Progr. Biophys. Molec. Biol., 35, 103.

127. Cooke, R. and Kuntz, I.D. 1974. Annual Reviews of Biophysics and Bioengineering, 3, 95.

128. Woesner, D.E. and Snowden, B. S. 1972. J. Colloid Interface Sci., 34, 290.

129. Child, T.F. and Price, N.G. 1972. Biopolymers, 11, 409.

130. Derbyshire, W. and Duff, I.D. 1973. Faraday Discuss. Chem. Soc., 57, 243.

131. Oakes, J. 1976. J.Chem. Soc., Faraday, I., 72, 228.

132. Bratton, L.B., Hopkins, A.L. and Weinberg, J.W. 1965. Science, New York, 147, 738.

133. Hazlewood, C.F., Nichols, B.L. and Chamberlain, W.F., 1969. Nature, London, 222, 747.

134. Zimmerman, J.R. and Brittin, W.E. 1957. J. Phys. Chem., 61, 1328.

135. Fung, B.M., Durham, D.L. and Wasil, D.A. 1975. Biochim. Biophys. Acta, 399, 192.

136. Tait, M.J., Ablett, S. and Wood, F.W. 1972. J. Colloid Interface Sci., 41, 594.

137. Hennig, H.J. and Lechert, H. 1978, Starke, 30, 197.

138. Jaska, E. 1971. Cereal Chem., 48, 437.

139. James, T.L. and Gillen, K.T. 1972. Biochim. Biophys. Acta, 286, 10.

140. Wang, J.H. 1954. J. Amer. Chem. Soc., 76, 4755.

141. Mackie, J.S. and Meares, P. 1955. Proc. Roy. Soc., Ser. A 232, 498.

142. Lechert, H. and Hennig, H.J., in "Magnetic Resonance in Colloid and Interface Science." Ed. Resing, H.A. and Wade, C.G. ACS. Symposium Series, No. 34. Amer. Chem. Soc. 1976.

143. Bryce, T.A. McKinnon, A.A., Morris, E.R., Rees, D.A. and Thom, D. 1974. Faraday Discuss. Chem. Soc., 58, 221.

144. Saito, H., Ohki, T. and Sasaki, T. 1978. Carbohydrate Research, 74, 227.

145. Yokata, K., Abe, A., Hosaka, S., Sakai, I. and Saito, H. 1978. Macromolecules, 2, 95.

146. Dea, I.C.M. McKinnon, A.A. and Rees, D.A. 1972. J. Mol. Biol., 68, 153.

147. Traub, W. and Piez, K.A. 1971. Adv. Protein Chem., 25, 243.

148. Kainosho, M. and Ajisaka, K. 1978. Tetrahedron Letters, 18, 1563.

149. Callaghan, P.T., Jolley, K.W. and Lelievre, J. 1979. J. Biophys., 28, 133.

150. Farrar, T.C. and Becker, E.D. 1974. Pulse and Fourier Transform NMR, Academic Press, New York and London.

151. Hahn, E.L. 1959. Phys. Rev., 80, 580.

152. Meiboom, S. and Gill, D. 1958. Rev. Sci. Instrum, 29, 688.

153. Stejskal, E.O. and Tanner, J.E. 1965. J. Chem. Phys., 42, 288.

154. Callaghan, P.T., Trotter, C.M. and Jolley, K., 1980. J. Magnetic Resonance, 37, 247.

155. Banks, W., Geddes, R., Greenwood, C.T. and Jones, I.G. 1972. Starke, 24, 245.

156. Woessner, D.E. and Zimmerman, J.R. 1963. J. Phys. Chem., 67, 1590.

157. Basler, W. and Lechert, H. 1973. Starke, 25, 289.

158. Tomitta, S. and Terajima , K. and Kidu, Y. 1969. Nippon Nogel Kagaku Kaishi, 43, 638.

159. Frey-Wyssling, A. 1969. Amer. J. Bot., 56, 696.